Location Based Energy Efficient Security Mechanism in Wireless Sensor Networks using Qlearning-PSO-AES Algorithm

1st Rajashree V Biradar
Dept. Of CSE
Ballari Institute of Technology and Management
Ballari, India
rajashreebiradar@bitm.edu.in

2nd Sudhakar Avareddy
Dept. Of CSE
Ballari Institute of Technology and Management
Ballari, India
sudhakaravareddy@bitm.edu.in

3rd V.C.Patil
Dept. Of ECE
Ballari Institute of Technology and Management
Ballari, India
patilvc@bitm.edu.in

Abstract—Wireless Sensor Networks (WSNs) are gaining popularity in various applications, including environmental monitoring, healthcare, and security surveillance. However, ensuring the security of WSNs is challenging due to resource limitations and dynamic nature of WSNs. Location-based security management has emerged as an effective approach to enhance WSN security by leveraging node location information to mitigate security threats. A hybrid Qlearning-PSO-AES technique for location-based security management in WSNs has been proposed in this paper. The proposed technique incorporates location information, dynamic trust evaluation, and advanced encryption algorithms to enhance WSN security. In this proposed work, the Qlearning algorithm is applied to learn the node's current state, including position and velocity, and to estimate trust values of nodes based on their past interactions. The PSO algorithm is used to determine the optimal placement of sensor nodes within the network, optimizing network lifetime, coverage, connectivity and energy consumption. Furthermore, the optimal solution obtained from PSO, represented by the best fitness value, is utilized for selecting encryption keys in the AES algorithm. The encryption keys are dynamically updated based on node movement to enhance WSN security. Simulation results clearly demonstrate that the proposed technique not only enhances the security of WSNs but also optimizes network performance, making it well-suited for real-world applications in various domains.

Keywords—wireless sensor network(WSN), Objective Function, Localization, Security, Particle Swarm Optimization (PSO), Advanced Encryption Security Algorithm(AES), Qlearning.

I. INTRODUCTION

WSNs consist of small, low-cost, and low-power independent sensor nodes that communicate with each other to collectively gather and process data from the surrounding environment [1]. The Fig.1 dipicts the architecture of WSN.
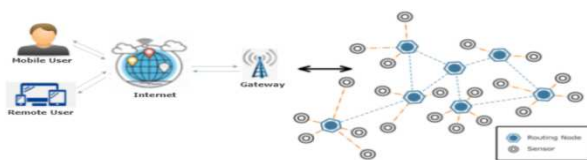

Fig. 1. Architecture of WSN

Wireless sensor networks have gained significant attention in recent years due to their wide range of applications in various domains such as environmental monitoring, surveillance, healthcare, and industrial automation. Although WSNs play a crucial role in various applications, and their distributed and resource-constrained nature poses several challenges. Challenges in WSN include: Limited resources, Energy efficiency, Scalability, Communication reliability, Data aggregation and fusion, Localization and positioning, Network dynamics, Quality of Service (QoS) and integration with other networks etc. Addressing these challenges requires innovative solutions and careful trade-offs to optimize performance, energy efficiency and security in WSNs. The proposed algorithm mainly concentrate on two main challenges of WSNs i.e. localization and security. Localization [2] is an important issue in WSN, and accurate localization is essential for many applications like target tracking, object localization, environment monitoring etc. that rely on precise location information in WSNs. Security [3] of communication in WSN is a critical issue that needs to be addressed. Due to the limited computational resources of the sensors, it is a challenging to implement robust encryption algorithm. This paper proposes a hybrid approach that combines the Qlearning-PSO-AES algorithms to achieve enhanced location based energy efficient secured communication over WSNs. The proposed work can be effectively used in certain applications within the context of Wireless Sensor Networks (WSNs) like Intrusion Detection Systems (IDS), Environmental Monitoring, Target Tracking and Localization, Traffic Monitoring and Control etc. Section II describes Related Work, section III describes Proposed Work, section IV describes Simulation Setup and Results. Followed by Conclusion, Future Scope and References at the end.

II. RELATED WORK

The relevant methods such as localization, security, and the Qlearning Algorithm are discussed in this section.

A. Localization

The Localization algorithms [4] are of great significance in WSNs as they enable node positioning, coverage optimization, efficient geographic routing etc. Localization is a key issue for WSNs as it determines the location of sensor nodes within a particular area. It is essential for many applications such as target tracking, object location, perimeter monitoring [5] [6] etc. Localization issues in WSNs arise due to limited communication range, limited computational resources, inaccurate range measurement and mobility of nodes.

TABLE I. COMPARISON OF VARIOUS LOCALIZATION TECHNIQUES USED IN SPECIFIC APPLICATION

Methods	Expenditure	Accuracy	Energy consumption	Hardware size
Include GPS	Additional amount	Max	Low	Large
Exclude GPS	Less	Avg	Medium	Small
Centralized	Based on type	Max	Low	Based on type
Decentralized	Based on type	Min	High	Based on type
AOA	Additional amount	Min	Medium	Large
TOA	Additional amount	Avg	Low	Large
RSSI	Less	Avg	High	Small
PSO	Less	Max	High	Small

Table I gives comparison of location methods that are currently used [7] and based on analysis, it is found that PSO is the best localization algorithm. PSO [8] is a metaheuristic algorithm used for optimization problems. It is used to find the optimal placement of sensor nodes in the network to achieve the required objectives.

In WSNs, the position of a particle represents the location of a sensor node, and the velocity represents the movement of the node in the network. The fitness function in PSO [10] is used as optimal solution that meets the required objectives which is defined as a combination of network lifetime, coverage, connectivity, and energy consumption. Each particle in the swarm has a position and velocity in the solution space. The position of a particle represents a potential solution to the problem, and the velocity determines the direction and magnitude of the movement of the particle in the solution space.

The PSO algorithm begins by randomly initializing each particle's position and speed in the target area. The algorithm then evaluates the fitness of each particle using the fitness function. Each particle maintains its own (Personal Best) pbest value, which represents the best objective function value or fitness achieved by that particle. PSO also determines gbest (Global Best), the location in the search space with the best objective function value or fitness among all the particles. The following equations are used to update each particle's velocity and position:

$$v\_i(t+1) = w * v\_i(t) + c1 * r1 * (pbest\_i - x\_i(t)) + c2 * r2 * (gbest - x\_i(t)) \qquad (1)$$

$$x\_i(t+1) = x\_i(t) + v\_i(t+1) \qquad (2)$$

Where $v\_i(t)$ is the velocity of particle i at time t, $x\_i(t)$ is the position of particle i at time t, $pbest\_i$ is the best-known position of particle i, gbest is the best-known position among all particles, the inertia weight w , the acceleration constants c1 and c2 , and the random numbers r1 and r2 are in between 0 and 1.

The PSO algorithm iteratively updates the position and velocity of each particle and hence pbest and gbest until the stopping criterion is met. The stopping criterion is usually based on a maximum number of iterations or a desired fitness value.

B. Security

With WSNs, it is very challenging to meet high-security requirements with constrained resources. The security issues include node authentication, data confidentiality, anti-compromise and resilience against traffic analysis, Integrity, Availability, Privacy and physical security [9]. Addressing these security issues requires the use of cryptographic algorithms, access control mechanisms, and intrusion detection systems [7] [11].

Table II gives information about the comparative analysis of existing security mechanisms in WSN. From the comparative analysis it is found that the Advanced Encryption Standard (AES) [7] [12] is the best security mechanism due to its high block length and various key lengths.

TABLE II. COMPARISON OF VARIOUS ENCRYPTION ALGORITHMS

Encryption algorithms	Release Date	Block length (bit)	Key length(bit)	N0. of cycles
XXTEA	1998	64	128	32
SAFER K-64	1993	64	64	6,10
DES	1977	64	56	16
AES	2002	128	128,192,256	10,1214

AES is a widely-used symmetric encryption algorithm that can be used in wireless sensor networks (WSNs) to provide secure communication between nodes. AES is a block cipher algorithm that operates on fixed-length blocks of data, with a block size of 128 bits. In AES, the encryption and decryption keys are the same. The key size can be 128, 192, or 256 bits. The strength of encryption increases with key size.AES is considered a secure encryption algorithm for WSNs because it provides strong encryption with a relatively low computational overhead. This is important for resource-constrained WSN nodes, which may have limited processing power, memory, and battery life.

C. Qlearning Algorithm

In this proposed work, the Qlearning is used to learn the best action (velocity) for each state (position + velocity) in the PSO algorithm and Q-learning also estimate trust values of nodes based on their past interactions. Qlearning [13] is a model-free reinforcement learning algorithm that enables an agent to learn an optimal policy in a Markov Decision Process (MDP) through trial and error. It is based on the concept of estimating the value of state-action pairs, known as Q-values, and updating the iteratively based on observed rewards [14]. In Qlearning, the agent engages with environment by taking actions & receiving rewards. The agent's goal is to learn the optimal policy that maximizes the cumulative rewards over time. The Q-values represent the expected return for taking a particular action in a specific state. The Qlearning algorithm [15] iteratively updates the Q-values using the following update rule.

$$Q(s, a) = (1 - \alpha) * Q(s, a) + \alpha * (r + \gamma * max(Q(s', a')) \qquad (3)$$

In the above equation

1. Q(s, a) represents the Q-value of taking action a in state s.
2. α (alpha) is the learning rate, which controls the weight given to the new information compared to the existing Q-values.
3. r is the immediate reward obtained after taking action a in state s.
4. γ (gamma) is the discount factor that determines the importance of future rewards compared to immediate rewards.
5. Max (Q(s', a')) denotes the maximum Q-value achievable for the action a' in the next state s'.

The Qlearning algorithm starts with initializing the Q-values arbitrarily or with some predefined values. Then, it repeatedly interacts with the environment, observes the current state, takes an action based on an exploration-exploitation strategy (e.g., epsilon-greedy), receives a reward, and transitions to the next state. After each transition, the Q-values are updated using the update rule. Over time, as the agent explores the environment and accumulates experience, the Q-values gradually converge towards the optimal Q-values, which correspond to the optimal policy. The agent learns to choose actions that maximize the expected cumulative rewards, balancing between exploration (trying new actions) and exploitation (choosing actions with high Q-values).

III. PROPOSED WORK

Lack of adaptability, insufficient exploration and exploitation, lack of security and limited trust management are some of the limitations of existing models. Majority of these limitations are addressed in this proposed work. The proposed hybrid Qlearning-PSO-AES key management technique for location-based security management in WSNs integrates the Qlearning algorithm, Particle Swarm Optimization (PSO) algorithm and Advanced Encryption Standard (AES) algorithm. The proposed work involves incremental way of development with two stages. In the first stage hybrid PSO-AES algorithm is implemented and Qlearning-PSO-AES algorithm in the second stage.

A. Hybrid PSO-AES

In the first stage, PSO mechanism is used to find the optimal placement of sensor nodes in the network to optimize the network lifetime, coverage, connectivity, and energy consumption. Additionally, the optimal solution obtained from PSO, represented by the global best fitness value (gbest), is utilized for selecting encryption keys for the AES algorithm and the key is updated dynamically as per the node movement to enhance the security of the WSN. The proposed hybrid encryption scheme provides several benefits. Firstly, the use of PSO is to generate the AES key to provide a more secure key that is harder to crack. Secondly, the PSO algorithm can optimize the key generation process, reducing the computational overhead associated with generating keys. Finally, the AES provides a

highest level of security and efficiency, ensuring that the data is securely transmitted over the network.

B. Qlearning-PSO-AES

In this stage Qlearning mechanism is applied to the above Hybrid PSO-AES algorithm. Qlearning algorithm, a reinforcement learning technique, enables sensor nodes to learn from their interactions with the environment and make informed decisions, leading to improved performance and convergence towards better solutions.

Fig.2 depicts the flowchart for implementing the proposed Qlearning-PSO-AES algorithm.
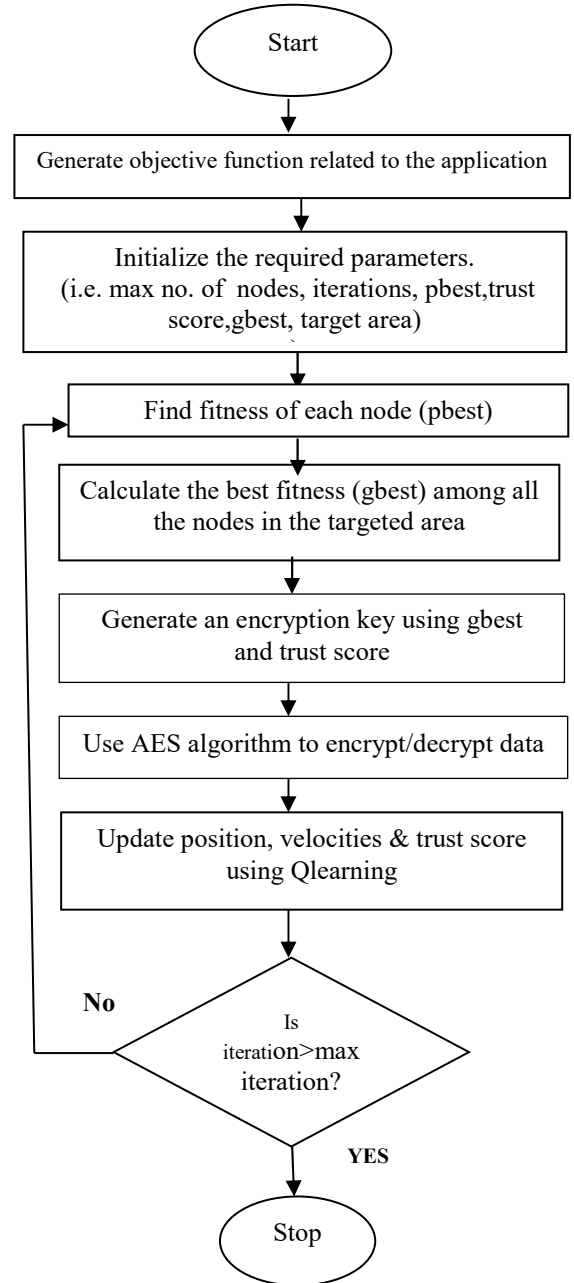

Fig.2. Flow diagram of QLearning-PSO-AES

The Qlearning-PSO-AES mechanism consists of the following steps:

i. Define the problem for the required WSN Application.

ii. Define the objective function based on problem defined keeping in view on mainly minimizing Energy Consumption and maximizing coverage area.
iii. Initialization.
   • Number of Nodes.
   • Maximum number of iterations.
   • pbest, gbest &Trust score
   • Lower bound & Upper bound of simulation area
iv. Find the fitness value(pbest) of each node using objective function
v. Calculate the gbest (position & fitness) using PSO Algorithm that gives the position in the search space that has the best objective function value among all the nodes in the targeted area
vi. Generate an encryption key using gbest and   trust score
vii. Use AES algorithm to encrypt/decrypt data using trust key.
viii. Using Q-learning mechanism, update the velocity, position and trust score of each node to move towards gbest position
   ix. Repeat steps iv to vii till the completion of all the iterations/Maximum number of Nodes.

IV. RESULTS AND DISCUSSION

Simulations were performed using python IDE (Pycharm) to evaluate the performance of the proposed algorithm .Simulations are run using different parameter settings that leads to the optimal solution. The simulation parameters provided in Table III define the specific characteristics and constraints of the wireless sensor network (WSN) for the proposed Qlearning-PSO-AES algorithm. The learning rate (Alpha) determines the impact of new information on the Q-values, the discount factor (Gamma) influences the importance of future rewards, and the exploration rate (Epsilon) controls the balance between exploration and exploitation in the Q-learning process. The cognitive constant (C1), social constant (C2), inertia weight (W), and random numbers (r1, r2) are used to influence the velocity update and exploration-exploitation trade-off during optimization. By configuring these parameters, the algorithm is evaluated under different scenarios and conditions to assess its performance and effectiveness in optimizing WSNs.

A. Simulation Parameters

TABLE III: Simulation Parameters

Target Area	100m*100m
Sensor Nodes	10,20,30,40,50,60
Maximum Iterations,	100,150,200,250,300,350
Learning Rate (Alpha)	0.1
Discount Factor (Gamma)	0.9
Exploration Rate (Epsilon)	0.1
Transmission range	10m
Energy Threshold.	5J
Data packet	1024 bits
Transmission energy	0.1J
Receiving energy	0.1J
Idle energy	0.05J
Encryption Key Size	256
C1(Cognitive constant)	1
C2(Social constant)	1
W	0.5
r1,r2	Random number between 0 to 1

In this proposed approach simulations are carried out by varying the number of nodes from 10-60 to verify the ability to handle computational complexity. In order to improve performance, simulations are also run with iterations ranging from 100 to 350.

B. Results& Analysis

Simulation results are analyzed to understand the performance of the proposed approach using the following performance metrics.

- Scalability: It refers to the ability of the proposed algorithm to handle increasing amounts of data without significant performance degradation.
- Convergence speed: It indicates how quickly the algorithm reaches a desired or optimal solution.
- Energy consumption: The total energy utilized in computational and communication process while obtaining the desired solution
- Efficiency: It is a measure of how well it balances the trade-off between solution quality, convergence speed, computational complexity, and scalability.

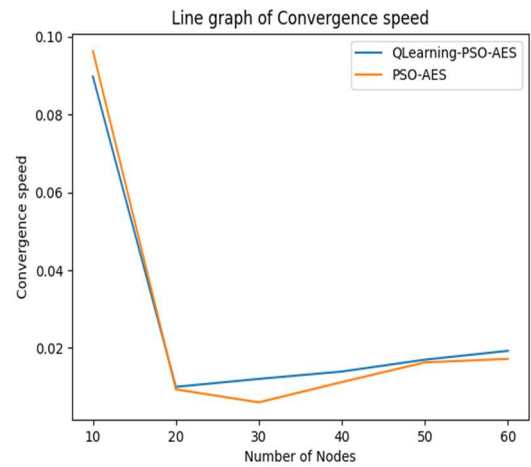The results obtained by varying number of nodes from 10 to 60 are shown in Fig 3 to Fig 6.

Fig.3. Number of Nodes v/s Convergence speed

Qlearning-PSO-AES algorithm performs better over PSO-AES in terms of efficiency, scalability and convergence speed because Qlearning enhances the optimization process by incorporating reinforcement learning techniques. Qlearning-PSO-AES consumes comparatively more energy as it involves complex computations due to the integration of PSO, AES and Qlearning techniques. As number of nodes increases efficiency, energy consumed increases where as convergence speed and scalability decreases due to several factors like increased communication overhead, resource constraints, and limited global knowledge, synchronization and coordination challenges. With increasing nodes, the Q-table that stores the Q-values may become larger and more

complex, requiring additional memory and computational resources.

The results obtained the by varying iterations from 100 to 350 are shown in Fig 7 to Fig 10.
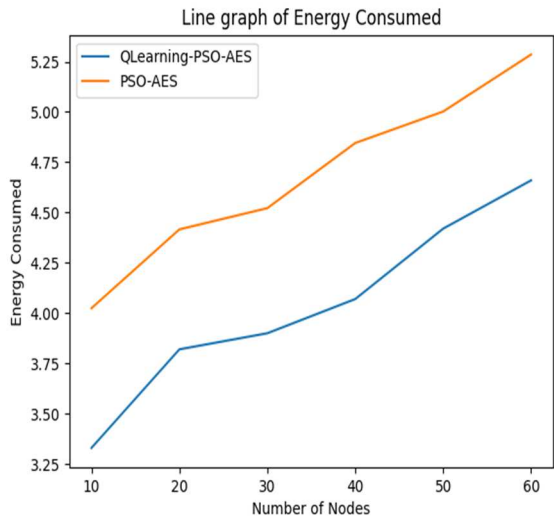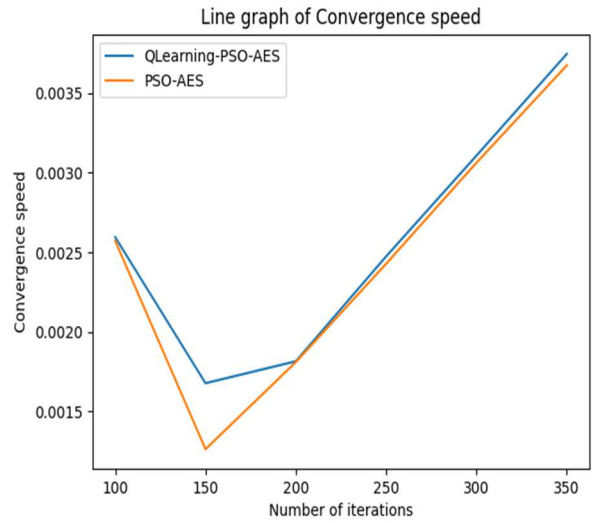

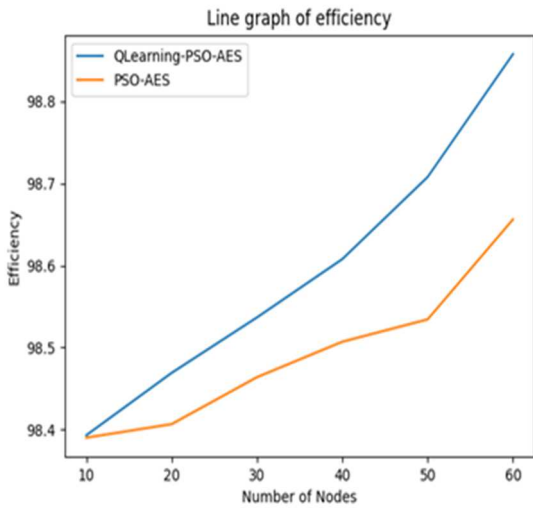Fig. 4. Number of Nodes v/s Energy consumed

Fig.5. Number of Nodes v/s Efficiency

Fig.6.Number of Nodes v/s Scalability

Fig.7. Number of Iterations v/s Convergence speed
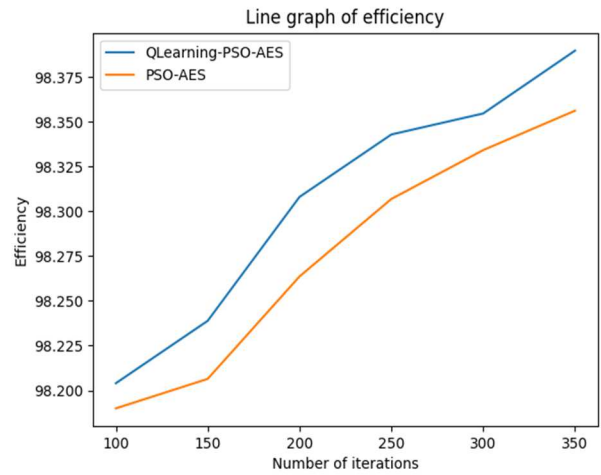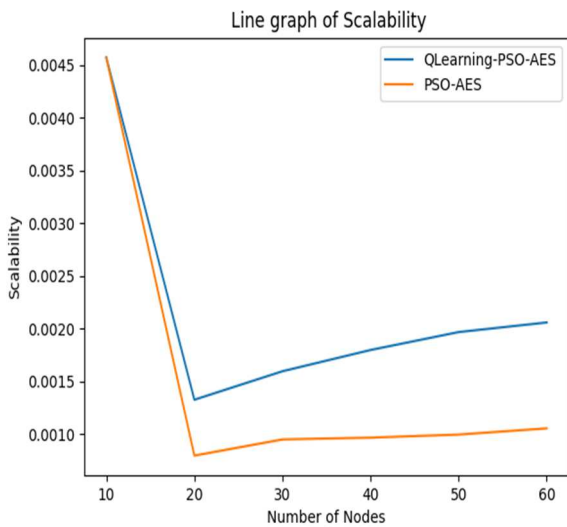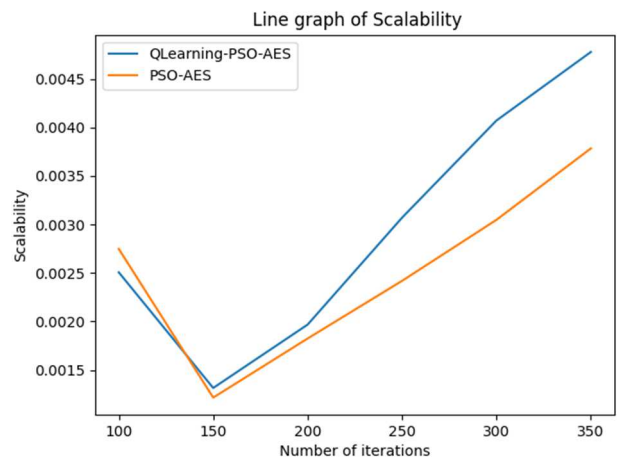

Fig.8. Number of Iterations v/s Efficiency

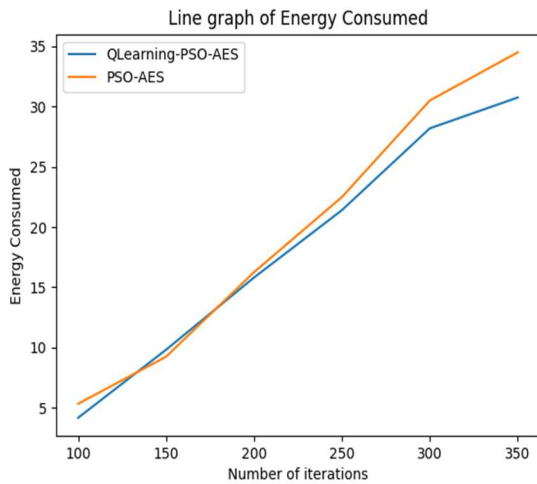Fig.9. Number of Iterations v/s Scalability

Fig.10.Number of Iterations v/s Energy consumed

Qlearning-PSO-AES algorithm enables sensor nodes to learn from their interactions with the environment and make informed decisions, leading to improved performance and convergence towards better solutions compared to hybrid PSO-AES algorithm. With increasing number of iterations efficiency increases and Convergence speed decreases because more iteration allows the algorithm to converge towards a better solution or optimize its performance. Scalability decreases and energy consumption increases due to factors such as the communication overhead, computational complexity and resource constraints.

V. CONCLUSION AND FUTURE SCOPE

The proposed hybrid Qlearning-PSO-AES key management technique for location-based security management in Wireless Sensor Networks (WSNs) leverages the strengths of Qlearning, Particle Swarm Optimization and Advanced Encryption Standard algorithm. By combining these three techniques, the Qlearning-PSO-AES algorithm addresses some limitations of existing approaches and offers several benefits. It provides a more efficient and robust optimization process, allowing WSNs to achieve better performance in terms of energy efficiency, coverage, and network lifetime. Moreover, the algorithm enhances the security of data transmission by protecting sensitive information from unauthorized access. The results demonstrated that this approach achieves better security and energy efficiency.

Trust management is an essential aspect of WSNs to ensure the reliability of data and nodes. Qlearning-PSO-AES does not explicitly address trust management, which can be crucial in WSNs to detect and mitigate malicious or compromised nodes. This work can be enhanced further by incorporating trust management mechanisms into Qlearning-PSO-AES algorithm to support trustworthiness of the system.

REFERENCES

[1] Mamoona Majid Shaista Habib 1, Abdul Rehman Javed Muhammad Rizwan Gautam Srivastava, Thippa Reddy Gadekallu and Jerry Chun-Wei Lin, "Applications of Wireless Sensor Networks and Internet of Things Frameworks in the Industry Revolution 4.0: A Systematic Literature Review", Published online 2022 Mar 8. doi: 10.3390/s22062087.

[2] Elhadi Shakshukia, Abdulrahman Abu Elkhailb, Ibrahim Nemerb, Mumin Adamb, Tarek Sheltamib, "Comparative Study on Range Free Localization Algorithms", The 10th International Conference on Ambient Systems, Networks and Technologies (ANT) April 29 - May 2, 2019.

[3] Shweta Singh, Ravi Shakya, Yaduvir Singh, "Localization Techniques in Wireless Sensor Networks", (IJCSIT) International Journal of Computer Science and Information Technologies, Vol. 6 (1), 2015, 844-850.

[4] D. Moore, J. Leonard, D. Rus, and S. Teller, "Robust distributed network localization with noisy range measurements",Proceedings of the Second ACM Conference on Embedded Networked Sensor Systems (SenSys '04), Baltimore, MD, pp. 50-61, November 2004.

[5] A. Boukerche, A. A. F. Loureiro, and A. Oliveira, "Localization systems for wireless sensornetworks", IEEE Wireless Communications", vol. 14, no. 6, pp. 6-12, 2007.

[6] Murat Dener Graduate School of Natural and Applied Sciences, Gazi University, Ankara, Turkey, "Comparison of Encryption Algorithms in Wireless Sensor Networks", ITM Web of Conferences 22, 01005(2018) https://doi.org/10.1051/itmconf/20182201005 CMES-2018.

[7] Sudhakar Avareddy and RajashreeV.Biradar, "Comparative Analysis of Localization Techniques and Security Mechanisms in WSN", IEEE International Conference on Mobile Networks and Wireless Communications (ICMNWC), 3rd - 4th Dec. 2021, at Tumkur, Karnataka, India.

[8] Vimalathithan R. and M.L.Valarmathi, "Cryptanalysis of Simplified-AES using Particle Swarm Optimisation", Government College of Technology, Coimbatore–641 013, India E-mail: athivimal@gmail.com.

[9] Nabil Ali Alrajeh, Maryam Bashir,and Bilal Shams, "Localization Techniques in Wireless Sensor Networks", international journal of distributed sensor networks vol-9,issue-6 june 2013

[10] Raghavendra V. Kulkarni, Senior Member, IEEE and Ganesh Kumar Venayagamoorthy, Senior Member IEEE, "Particle Swarm Optimization in Wireless Sensor Networks: A Brief Survey", IEEE transactions on systems,MAN,CYBERNETICS PART-C:APPLICATIONS AND REVIEWS.

[11] Ako Muhammad Abdullah, "Advanced Encryption Standard (AES) AlgorithmtoEncryptandDecryptData",https://www.researchgate.net/publication/317615794_Advanced_Encryption_Standard_AES_Algorithm_to_Encrypt_and_Decrypt_Data, Publication Date: June 16, 2017.

[12] Murat Dener. "Comparison of Encryption Algorithms in Wireless Sensor Networks", ITM Web of Conferences 22, 01005 (2018) https://doi.org/10.1051/itmconf/20182201005 CMES-2018.

[13] Beakcheol jang (member, IEEE), myeonghwi kim gaspard harerimana (member, IEEE), and jong wook kim(member, IEEE), "Q-Learning Algorithms: A Comprehensive Classification and Applications", vol 7, 2019, digital object identifier 10.1109/access 2019

[14] Fadi AlMahamid,Senior Member, IEEE, and Katarina Grolinger, Member, IEEE "Reinforcement Learning Algorithms: An Overview and Classification", Department of Electrical and Computer Engineering Western University London, Ontario, Canada arXiv:2209.14940v1 29 Sep 2022.

[15] Ms.S.Manju, Asst Professor, Dr.Ms.M.Punithavalli, "An Analysis of Q-Learning Algorithms with Strategies of Reward Function" S.Manju et al. / International Journal on Computer Science and Engineering (IJCSE). ISSN : 0975-3397 Vol. 3 No. 2 Feb 2011.

An automatic feature extraction technique from the images of granular parakeratosis disease

Original Scientific Paper

Sheetal Janthakal

Department of Computer Science and Engineering,
Ballari Institute of Technology and Management,
Ballari, Karnataka, India
Department of Computer Science and Engineering,
Rao Bahadur Y. Mahabaleswarappa Engineering College,
Ballari, Karnataka, India
sjanthakal@yahoo.co.in

Girisha Hosalli

Rao Bahadur Y. Mahabaleswarappa Engineering College,
Department of Computer Science and Engineering,
Ballari, Karnataka, India
hosalligiri@gmail.com

Abstract – *The largest and most vital part of the human body is skin and any change in the features of skin is termed as a skin lesion. The paper considers granular parakeratosis lesion that is an epidermal reaction occurring due to the disorder of keratinization, and mainly seen in intertriginous areas. The manual inspection of the lesion features is a bit cumbersome due to which an automated system is proposed in this paper. The main goal is to determine the size and depth of granular parakeratosis lesions using the proposed ensemble algorithm, partition clustering and region properties method. As a flow of the proposed model, segmentation is done using U-net with binary cross entropy, features are extracted using partition clustering and region properties method, and classification is done using SVM 10-fold model. The proposed feature extraction method estimates the depth and absolute size of K lesions in each image by predicting the absolute height and width of the lesion in terms of pixel square. After extracting the features, classification is done, thereby obtaining an accuracy of 95%, sensitivity and specificity of 100%. The proposed model provides better performance compared to state-of-the-art models. The main application of this automated system is in dermatology field where some skin lesions have same features which makes the experts to diagnose the disease incorrectly. If the proposed system is incorporated, diagnosis can be done in an effective manner considering all the relevant features.*

Keywords: *U-net with Binary Cross Entropy, Partition Clustering, Region Properties, Depth and Absolute Size, SVM 10-fold*

1. INTRODUCTION

Granular parakeratosis appears as red or brown hyperkeratotic papules or plaques in intertriginous areas. Patients of various ages have been diagnosed with the illness, and is more common in women than in men [1]. Granular parakeratosis was once assumed to be a contact dermatitis caused by hygiene products like deodorants and antiperspirants; however, cases have been documented even without the application of any personal hygiene products in the affected areas, ruling out contact dermatitis as the cause [2]. Other intertriginous and non-intertriginous body parts, such as the face, have also been reported to develop granular parakeratosis.

As described above, Granular parakeratosis is a type of skin disease. For the diagnosis of such type of diseases, most of the dermatologists rely on traditional methods. Though these methods have shown improved performance, they are still not feasible for a variety of factors such as a large number of patients, infrastructure, technical equipment, etc. Further, granular parakeratosis shares many of the characteristics of benign lesions in its early stages, making it difficult to distinguish. Experts find it difficult to detect the disease with the naked eye. Also, the diagnosis process is quite challenging as the analysis depends on the clinical expertise of the experts.

To overcome this problem, there is a requirement of an automated system that can adapt to technological advancements in the discipline of dermoscopy and assist specialists in detecting lesions accurately and giving a better path to diagnosis. Computer-aided diagnosis (CAD) systems use a variety of machine learning techniques for extracting the features from a given lesion dataset. Several texture analysis techniques like Principal Component Analysis (PCA) and Gray-Level Co-Occurrence Matrix (GLCM) have recently been presented in this arena, and their models have gained widespread acceptance for feature extraction, resulting in enhanced classification [3]. These techniques adopt dermoscopic images and are able to detect the most required features of the affected area.

"The malignant and benign lesions are classified using several feature extraction algorithms such as the ABCD rule, the seven-point checklist method, three-point checklist, and CASH algorithm. The ABCDE rule (Asymmetry, Border, Color, Diameter, Evolve), the 7-point checklist, and the Menzies technique are three clinical diagnosis methods used by dermatologists to distinguish melanoma from nevus [4]. These feature extraction techniques are dependent on lesion color, shape, geometry, texture, and structure [5]. An important screening tool for the detection of melanoma with accurate sensitivity and specificity is ABCD [6]".

Feature extraction is regarded as a necessary tool for properly analysing an image. Many authors explored a variety of features for classification as explained above; however none of them properly distinguish benign and malignant lesions. Several lesion extraction techniques have been developed in the past to aid specialists in finding the lesions automatically. However, due to variations in shapes and sizes, extracting the features from dermoscopic lesions is a hard task since it results in inaccurate extraction and increases the computational time. To tackle the aforementioned hurdles for more accurate lesion extraction, a new technique for extracting the features from lesion is created.

The novelty of the proposed work lies in feature extraction that is described as follows:

- In this paper, different digital images of parakeratosis have been analyzed.

- Initially, U-net with binary cross entropy technique is applied to segment the dataset, followed by which features (size and depth) of the segmented lesion are extracted using the region properties method, and finally classification of the lesion into starting or later stage is done using the SVM 10-fold validation model.

- Following that, a thorough discussion based on the findings is presented.

The paper comprises four sections, starting with the literature review, where a brief overview of the existing literature is presented. Next, the proposed methodol-ogy section describes the system architecture and the method implemented. The results and discussion section gives the results obtained from the experiments and discussions on them, and eventually, the final section concludes the paper.

2. LITERATURE REVIEW

Feature selection is a technique used in both machine learning and statistical pattern recognition. This is crucial in a variety of applications, including classification. Many methods for detecting melanoma have been reported in the last decade [7], [8]. Some of these attempts were to imitate dermatologists' performance by extracting and detecting most dermoscopic structures, such as pigment networks, irregular streaks, granularities, blotches, etc. Many studies utilised global approaches to classify skin lesions, whereas others employed local ones [9]. Several feature extraction techniques for various types of skin lesions investigated so far are described.

Features, which are retrieved using local, global, or local–global scenarios, play an important part in classification. For melanoma detection using dermoscopic pictures, Barata et al. [10] used a local–global technique. Local methods were employed to extract features using bag-of-words, whereas global methods were studied for skin lesions categorization in terms of higher sensitivity and specificity, with encouraging results.

The author of [11] suggested an entropy-controlled neighbourhood component analysis paradigm for most discriminant feature selection and dimensionality reduction (ECNCA). A model for lesion classification is also proposed that leverages deep feature information to build the best discriminant feature vector. The ECNCA framework improves fused characteristics by removing the duplicate and superfluous data and selecting the most important components. After the application of the proposed feature framework, the classification is done by testing on four datasets: PH2, ISIC MSK, ISIC UDA, and ISBI-2017, leading to an accuracy of 98.8%, 99.2%, 97.1%, and 95.9%, respectively. The drawback of the method is that it is applicable only to a limited dataset.

The article [12] proposed a diagnosis guided feature fusion (DGFF) that uses lesion information from the melanoma to improve skin lesion segmentation pixel-wise classification performance. It creates feature representations that distinguish between melanoma and non-melanoma lesions and also improves the network's ability to recognise various sorts of skin lesions using dermoscopic images. The extracted features are fed into the pixel-wise classification task, leading to an accuracy of 88.2%, a sensitivity of 63.3%, and a specificity of 94.2%. This method has the limitation of not considering some of the dermoscopic images that contain redness around the lesion area and black spots in an image.

The framework of [13] proposes the Self-supervised Topology Clustering Network (STCN) to segment the skin images automatically. The STCN consists of a transformation-invariant network that comprises a feature extraction function, a self-expression function, and a self-supervision deep topology clustering algorithm. The main goal is to determine the appearance characteristics and keep them consistent across multiple variations. These features will further be automatically partitioned into groups using the Deep Topology Clustering (DTC) algorithm, which will be used to construct pseudo labels for skin images. Finally, the DTC module is used as the self-supervision component to train a classification network using the estimated annotations. But the model is unable to use hand-craft features due to which the required information will be ignored.

To investigate the textural complexity of a skin lesion, a fractal-based regional texture analysis (FRTA) technique was created. FRTA separated the lesion area into smaller subregions based on textural complexity. Successful feature extraction from dermoscopic images has been achieved using a fractal-based border irregularity measurement and regional texture analysis technique. The performance of classification is increased when the Support Vector Machine (SVM) recursive feature elimination (RFE) technique is applied before each stage of the layered structured model [14], but the difficult cases present in an image cannot be classified correctly.

The labels are defined as a method of grouping items into clusters in which objects in one cluster are almost identical and objects in other clusters are significantly different. Clustering's main purpose is to extract sets of patterns, points, or objects from natural groupings [15]. Clusters of various forms and densities are determined using the MDCUT algorithm (Multi-Density ClUsTering) [16]. It is a density based clustering algorithm that can handle noisy data and discover neighbouring and imbricated clusters. The drawback is that only a few pre-processing methods are applied to the dataset.

Trabelsi et al. [17] used a variety of clustering techniques, including fuzzy c-means, modified fuzzy c-means, and K-means, to segment a skin disease with an 83% true positive rate. The clustering algorithms depend on the identification of a centroid that can generalise a cluster of data. However, the performance of these algorithms degrades with the presence of noisy data and outliers.

Table 1.: Overview of the literature

Method	Major contributions	Limitations
ECNCA	Improves fused characteristics	Works only for Small dataset
DGFF	Improves pixel-wise classification performance	Doesn't consider black spots in an image
STCN	Determines the appearance characteristics	Ignores the required information
FRTA	Improves the performance	Difficult cases are ignored

According to literature, there are various problems with successful feature extraction. The proposed integrated system plays a significant role in overcoming the obstacles of accurate disease diagnosis based on visual and simulated evaluation by measuring the effective features and diagnosing the disease with a higher degree of accuracy. The proposed method employs the conjunction of clustering and region properties methods to overcome these. The suggested approach extracts the size and depth of lesions in an image by applying several morphological functions to the given dataset.

3. PROPOSED METHODOLOGY

3.1. FEATURE EXTRACTION

"Relevant information for accomplishing the computing tasks associated with a certain application" is defined as a feature. There are two types of features: local ones and global ones [18]. In order to build a classification rule, a collection of numerical criteria that describe the object or phenomena seen (supervised or not) is described. Several feature extraction algorithms have been developed, each with their own set of principles [19]. Here, a feed-form method of partition clustering and the region properties method are proposed.

3.2 SYSTEM ARCHITECTURE

The architecture of the proposed system is shown in figure 1. To begin, 224x224 lesion images are acquired, segmentation is performed using the U-net method, followed by watershed-based separation of lesions (formation of clusters), then, extracting the features using regionprop and finally, classification is done using SVM 10-fold model.

If features extracted from the lesion are efficient, it can lead to a better classification of granular parakeratosis. Here, the parakeratosis image consists of several lesions that can be easily identified by labeling the lesions and then determine the width, height, and depth of a lesion. The detailed steps of pre-processing and feature extraction using clustering and region properties are shown in figure 2. Some transformations like thresholding and morphology are applied to the clustered lesion to extract the most descriptive set of features. Using the regionprops approach, the size and depth of the clustered lesions obtained in figure 1 are extracted.

The proposed feature extraction method, being an unsupervised one, extracts the size and depth of a lesion in the following manner:

- Morphology pre-processing techniques remove any small objects and holes in the image.
- The touching cells in an image can be effectively separated using distance transform and thresholding. Thus, leading to the separation of lesions and non-lesions, followed by which a number of clusters of lesions are created.

- Different lesions in the clusters are labeled, after which watershed filling is applied. For each label, the size and depth of the lesion is extracted using the regionprops method of skimage.

3.3 CLUSTERING

One of the most prominent approaches for skin disease segmentation and classification is the clustering algorithm. Clustering, often known as cluster analysis, is a machine learning technique for organizing unlabeled data. It is defined as "***grouping similar data points into different clusters***". Clustering is a form of unsupervised learning that works with unlabeled data. The advantage of clustering algorithms is that they are flexible, easy to implement, and can generalize features having a similar statistical variance. *Here, lesions in a group have possible similarities and have fewer or no similarities with another group.*

Partition Clustering

It's a type of clustering in which data is split into non-hierarchical groups. This strategy is also known as the centroid-based method [20]. In this type, the dataset is divided into K groups, with K denoting the number of pre-defined groups. The cluster centre is designed in such a way that the distance between one cluster data point is the smallest when compared to the cluster centroid of the other cluster.

The type of clustering used in the implementation is partitioning clustering. The patterns like size and depth of lesions are considered, and the data points having the same size and depth are formed into a cluster (group). After the application of the clustering technique, each cluster is provided with a cluster ID (or label id) and the area and depth of each cluster (lesion) are found.

Mathematical analysis involved in the partition clustering

An image can be partitioned into K clusters such that the total of Manhattan distances (L1) between locations and the cluster's centre is kept to a minimum. Then, the sum of L1 absolute errors (SAE) can be minimised by using the following equation 1.

$$SAE = \sum_{i=1}^{K} \sum_{x \in C_i} dist_{L_1}(c_i, x) \qquad (1)$$

where $dist_{L_1}$ is L_1 distance, C_i is the ith cluster, x is a point in C_i, and c_i is the ith cluster average.
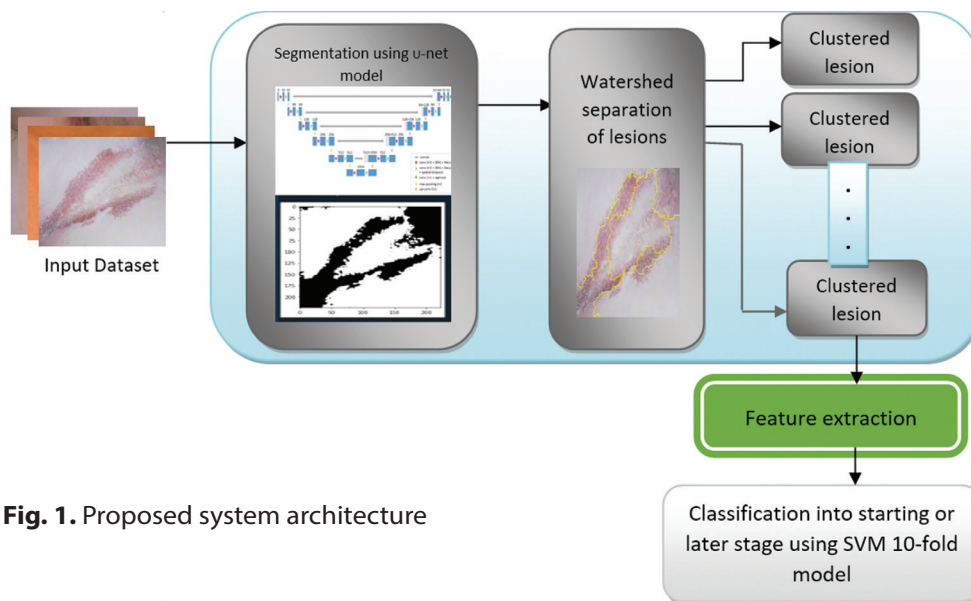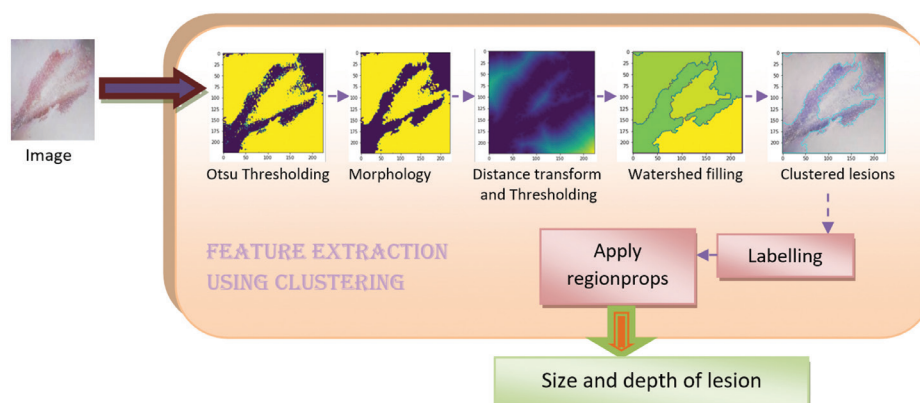

Fig. 1. Proposed system architecture

Fig. 2. Feature extraction using clustering

3.4 Dataset

To test the proposed methodology, publicly available DermnetNZ and DermIS datasets are chosen [21], [22]. These datasets consist of several RGB images of granular parakeratosis and is partitioned into two classes, starting stage and later stage wherein 79 samples are considered for each class. For the implementation of size and depth features, the OpenCV library and the python machine learning package, Scikit-learn library, are adapted. All the experiments are run on a Windows 10 system with an i5 processor. Figure 3 shows some of the sample images of granular parakeratosis.

Fig. 3. Samples of granular parakeratosis

3.5 Implementation

The given skin image undergoes several steps like normalization, clustering (form the clusters of skin lesion), extract the size and depth features, and pass them to the classification model.

In this section, the implementation of the distance transform, watershed, and clustering algorithms for extracting the features from the granular parakeratosis dataset is described. The model is trained on 79 dermoscopy images.

The below mentioned algorithm describes the generalised steps incorporated by the proposed model:

Step 1: Initially, import the libraries required for feature extraction

Step 2: Then, read an image by defining pixel size

Step 3: Perform segmentation using the U-net model. The result of the U-net model is transformed to binary image (threshold image to separate lesion boundaries) using Otsu thresholding

Step 4: Watershed based separation of lesions: Apply morphological functions to enhance the boundaries and create a mask

Step 5: Label the lesions in an image

Step 6: Extract the size and depth of each lesion using regionprops method

Step 7: Output results into a csv file

A detailed description of the flow of the implementation is as follows:

1. Initially, segmentation is done using the encoder-decoder process of the U-net model with binary cross entropy as a loss function. The main aim of choosing binary cross entropy is to minimise the loss so as to improve performance of the model. A 224x224 image is passed into the network for which 32 filters are applied. Then, it gets converted into 112x112x64, 56x56x128, 28x28x256, 14x14x512, and 7x7x1024 as it passes through different levels of the network. In the decoder path, each level concatenates with the corresponding level in the encoder path, leading to a 7x7x1024, 14x14x512, 28x28x256, 56x56x128, 112x112x64, and 224x224x32 image. To this image, the last layer with a filter of size 1x1 and a sigmoid activation function is applied, generating 224x224x1 segmented-image.

2. Otsu thresholding: It is an auto-thresholding technique that automatically calculates a threshold value for a binary image. The flags cv2.THRESH_BINARY & cv2.THRESH_OTSU are passed as parameters to the cv2.threshold() function with the threshold value set as zero. The main goal of Otsu's approach is to minimise the variance by choosing the correct value for the threshold. If it is chosen wrong, the variance of one or more classes will be significant. Thus, to get the total variance, add all the within-class and between-class variances together as shown in equation

$$\sigma_T^2 = \sigma_w^2(t) + \sigma_b^2(t) \qquad (2)$$

where $\sigma_w^2(t) = w_1(t)\sigma_1^2(t) + w_2(t)\sigma_2^2(t)$ and

$$\sigma_b^2(t) = w_1(t)w_2(t)[\mu_1(t) - \mu_2(t)]^2$$

$w_1(t)\ and\ w_2(t)$ → probabilities of the classes divided by threshold t (0-255)

μ_i → class i^{th} mean

3. Morphological transformations are straightforward operations that are usually applied to binary images. OpenCV's morphologyEx() function is as follows:

• Morphological transformations are simple procedures done on images depending on their shape to remove noise, small holes in foreground objects, and so on. Erosion, dilation, opening, and closing are some of the morphological operations. In implementation part, after otsu thresholding, opening morphology is done. To execute opening morphological procedures on a given image, the MORPH_OPEN operation in the morphologyEx() method is used.

4. To extract the exact lesion in an image, a distance transform followed by a threshold is applied [23]. The distance transform function calculates the approximate distance from every pixel in the image to the zero pixel. For zero pixels, it will be zero. Out of several distance types available, DIST_L2 is chosen which runs the linear-time algorithm. This algorithm makes use of squared Euclidean (or quadratic) distance described as follows. Let G stand for regular grid and $f{:}G \rightarrow R$ be

a grid function where R is the range of distance function d. The distance transform of f is defined by equation 3.

$$D_f(p) = \min_{q \in G}\big(d(p,q) + f(q)\big) \quad (3)$$

where $d(p, q)$ is a distance measure between p and q. A point q that is close to p and with a small f(q) is discovered for each point p.

Let $G = \{0, \ldots, n-1\}$ be a one dimensional grid, and $f : G \to R$ an arbitrary grid function. The squared Euclidean (or quadratic) distance transform of f is described by equation 4.

$$D_f(p) = \min_{q \in G}\big((p-q)^2 + f(q)\big) \quad (4)$$

5. The non-lesion area can be found by applying dilation to the result obtained in the previous step. To determine the area which is not sure of a lesion or non-lesion (also called boundaries or border of lesion, where lesion and non-lesion touch each other), watershed algorithm is applied.

6. A *watershed* is a transition defined on a grayscale image. This technique aids in the detection of touching and overlapping lesions in an image. The watershed algorithm extracts the completely lesion area and the completely non-lesion area, leading to the creation of clusters. Several clusters of lesions are identified and then markers are applied to detect the exact boundaries (labeling). These markers assign positive numbers to completely lesion and non-lesion areas and zero to the area that is not sure to be lesion or non-lesion **using cv2.connectedComponents()**. Finally, after labelling the regions, apply the watershed algorithm for filling.

7. After identifying labelled lesions in an image, the features of these lesions can be determined using the regionprops() module of the skimage library. The size and depth of lesions in an image are calculated by measuring the cluster's height and width in pixel square.

8. The features obtained are then given as an input to the SVM 10 fold cross validation model. The reason for chosing SVM is that it finds the best separator to differentiate the classes. Thus, SVM serves as a binary classifier. Here, it classifies the lesions into starting stage or later stage. In SVM 10 fold model, 224x224 images from which the features extracted using the region properties technique are input into the SVM classifier with hinge loss and linear activation function. Hinge loss is a function that is mainly used to train the SVM classifier. The linear activation function decides the output of the model and when associated with neurons, it decides whether a neuron should be activated or not depending on the input provided. The output of this SVM

classifier is then fed into the 10 fold validation model wherein the model is trained on one partition and evaluated on other nine partitions, thereby increasing an accuracy to 95%, sensitivity to 100% and specificity to 100%. The output of classification is shown in figure 4.
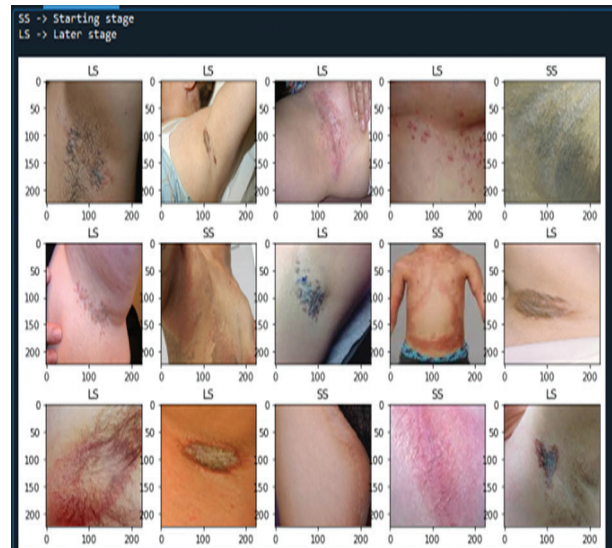

Fig. 4. Classification of granular parakeratosis into starting or later stage

4. RESULTS AND DISCUSSION

4.1 QUANTITATIVE EVALUATION

The model is evaluated quantitatively using accuracy, sensitivity, and specificity metrics. This is computed as

$$\text{Accuracy} = \frac{TP+TN}{TP+FN+TN+FP}$$
$$\text{Sensitivity} = \frac{TP}{TP+FN}$$
$$\text{Specificity} = \frac{TN}{TN+FP}$$

Abbreviations: TP - True Positive, TN - True Negative, FP - False Positive and FN - False Negative

4.2 ANALYSIS

The size and depth of the lesion (segmented object) are determined in the model. Figure 5 shows the samples of original image, an overlay on the original image, a segmented image, and the size and depth extracted from the lesions of sample images. The results obtained for other images are shown in Table 2. The table shows that for each image, different lesions are identified and labeled with a unique number. For each label, the area and depth of the lesion are found. For example, the first four rows (excluding the heading) of the table correspond to an image, images.bmp. This image consists of four lesions identified by lesion numbers 1, 2, 3, and 4 (second column). For each of these lesions, an area and depth are computed. The same thing is repeated for the other images in the dataset (from the fifth row).
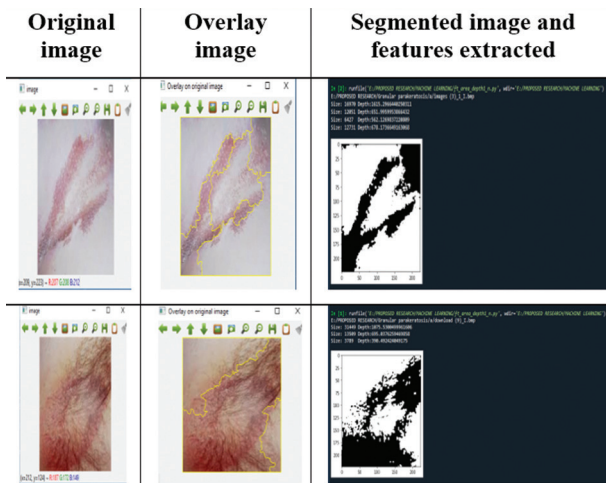
Original image	Overlay image	Segmented image and features extracted

Fig. 5. Original image, overlay image, segmented image and features extracted

Table 2. Simulation results of the model

Image Name	Lesion#	Area	Depth
images.bmp	1	4242.5	1615.297
images.bmp	2	3012.75	651.996
images.bmp	3	1606.75	562.127
images.bmp	4	3182.75	678.1737
download.bmp	1	7862.25	1075.53
download.bmp	2	3377.25	695.0376
download.bmp	3	947.25	390.4924
Axillary Granulary Parakeratosis.bmp	1	2846.5465	1207.022
Axillary Granulary Parakeratosis.bmp	2	8344	1199.578
Axillary Granulary Parakeratosis.bmp	3	934.5	313.2203
Axillary-Granular-Parakeratosis-1.bmp	1	6636.25	1308.71
Axillary-Granular-Parakeratosis-1.bmp	2	1522.75	479.2031
Axillary-Granular-Parakeratosis-1.bmp	3	1146	419.2386
Axillary-Granular-Parakeratosis-1.bmp	4	111.25	89.25483
Axillary-Granular-Parakeratosis-1.bmp	5	101.25	114.1604
Axillary-Granular-Parakeratosis-1.bmp	6	91	104.332
Axillary-Granular-Parakeratosis-1.bmp	7	140.75	119.1665
Axillary-Granular-Parakeratosis-1.bmp	8	41.25	59.35534
Axillary-Granular-Parakeratosis-1.bmp	9	280.5	171.3797
Axillary-Granular-Parakeratosis-1.bmp	10	26	47.83452
Axillary-Granular-Parakeratosis-1.bmp	11	172.25	137.3026
Axillary-Granular-Parakeratosis-1.bmp	12	136.5	121.3026
Axillary-Granular-Parakeratosis-1.bmp	13	53.75	95.01219
Axillary-Granular-Parakeratosis-1.bmp	14	67.25	73.39697
Axillary-Granular-Parakeratosis-1.bmp	15	207.25	144.6518
Axillary-Granular-Parakeratosis-1.bmp	16	16.5	33.14214
Axillary-Granular-Parakeratosis-1.bmp	17	270.5	196.5097

Experiment shows that the proposed strategy produces good results. The performance of the proposed model provides a better result compared to the state-of-art methods. After the application of the partition clustering and region properties method to the given dataset, the output is fed to SVM 10-fold model that achieved an accuracy of 95%, a sensitivity of 100% and a specificity of 100%. The performance of each fold in 10-fold model is presented in table 3.

Table 3. Fold-wise performance of 10-fold

Fold	Accuracy	Sensitiviy	Specificity
1	95	99.99	99.99
2	94.99	99.99	100
3	94.99	99.98	99.98
4	95	100	99.99
5	94.99	100	100
6	95	99.99	100
7	94.99	100	99.99
8	95	100	100
9	95	100	100
10	95	100	100
Average	94.99	99.99	99.99

Table 4 shows the performance of the existing models and compares them with the proposed model after feature extraction.

Table 4. Comparison of the proposed method to state-of-the-art techniques in terms of classification performance

Model	Feature extracted	Accuracy	Sensitivity	Specificity
Morphological geodesic active contour [24]	Color	94.59	91.72	97.99
Fuzzy clustering [25]	Area, perimeter, and centroid	97.6	96.82	96.94
Scattered Wavelet Transform[26]	Hand-crafted features	93.14	-	-
Stationary Wavelet Transform[27]	Entropy	91.5	90	93
RESNET-50 [28]	Contrast	89.8	-	-
Proposed model	**Size and depth**	**95**	**100**	**100**

The model proposed by salih et al. achieved an accuracy of 97.6 which is bit higher than the proposed model. Though this model achieved higher accuracy, it didn't work well with few of the skin lesions and couldn't achieve higher sensitivity and specificity. Thus, the proposed hybrid model can be used for parakeratosis feature extraction that not only works well with all of the training samples but also achieved better performance metrics, including accuracy, sensitivity, and specificity.

Figure 6 shows the graphical representation of the performance comparison of proposed and existing models.
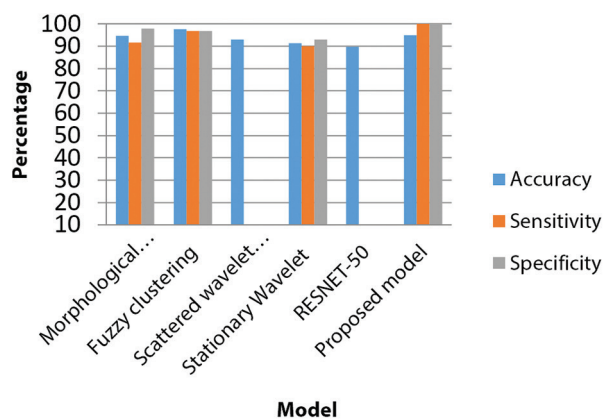
Fig. 6. Performance comparison

5. CONCLUSION

An estimation of the features of lesions in an image is an important application of medical image processing. The paper proposes an automatic method for size and depth extraction using partition clustering and the region properties method. The model performs the segmentation of the given dataset using U-net with binary cross entropy technique, extracts the features using partition clustering and region properties methods, and finally classify into starting or later using SVM cross validation model. The proposed method estimates the depth and absolute size of K lesions in each image by predicting the absolute height and width of the lesion in terms of pixel square. After extracting the size and depth, classification is performed using SVM 10-fold model. The experiment results demonstrate that the proposed model provides a better performance compared to the other models.

The model has the limitation that it works well only for the limited number of samples. As a future work, the model can be improvized in such a way that it works well even for a large dataset.

6. REFERENCES:

[1] J. Mcgrath, "Dermatology, Venereology & Leprology", Vol. 74, No. 1, 2008, pp. 53-55.

[2] P. Chirasuthat, S. Chirasuthat, P. Suchonwanit, "Follicular Granular Parakeratosis: A Case Report, Literature Review, Proposed Classification", Skin Appendage Disorder, Vol. 7, No. 2, 2021, pp. 144–148.

[3] G. Pavithra, C. Palanisamy, S. S. Rajasekar, R. S. Soundariya, "Skin Lesion Analysis - Feature Extraction Methods Using Dermoscopy Image", International Journal of Aquatic Science, Vol. 12, No. 3, 2021, pp. 1821-1829.

[4] Q. Abbas, F. Ramzan, M. U. Ghani, "Acral melanoma detection using dermoscopic images and convolutional neural networks", Visual Computing for Industry, Biomedicine, Art, 2021.

[5] S. Sengupta and N. Mittal, "Analysis of Various Techniques of Feature Extraction on Skin Lesion Images", Proceedings of the 6th International Conference on Reliability, Infocom Technologies and Optimization, Noida, India, 20-22 September 2017.

[6] S. Majumder and M. A. Ullah, "A Computational Approach to Pertinent Feature Extraction for Diagnosis of Melanoma Skin Lesion", Pattern Recognition and Image Analysis, Vol. 29, No. 3, 2019, pp. 503-514.

[7] K. Chinpong et al., "ABCD Feature Extraction for Melanoma Screening Using Image Processing: A review", The Journal of Chulabhorn Royal Academy, Vol. 5203, No. 4, 2021, pp. 230-245.

[8] L. Hoang, S. H. Lee, E. J. Lee, K. R. Kwon, "Multiclass Skin Lesion Classification Using a Novel Lightweight Deep Learning Framework for Smart Healthcare", Applied Sciences, Vol. 12, No. 5, 2022.

[9] H. A. Mahmood, "Appending Global to Local features for Skin Lesion Classification on Dermoscpic Images", Journal of Engineering Research, Vol. 10, 2022, pp. 1-19.

[10] M. Francisco, "Two Systems for the Detection of Melanomas in Dermoscopy Images using Texture and Color Features", IEEE Systems Journal, Vol. 8, No. 3, 2013, pp. 965-979.

[11] T. Akram et al. "A multilevel features selection framework for skin lesion classification", Human-centric Computing and Information Sciences, Vol. 10, No. 1, 2020.

[12] X. Wang, X. Jiang, H. Ding, Y. Zhao, J. Liu, "Knowledge-aware deep framework for collaborative skin lesion segmentation and melanoma recognition", Pattern Recognition, Vol. 120, 2021, p. 108075.

[13] D. Wang, N. Pang, Y. Wang, H. Zhao, "Biomedical Signal Processing and Control Unlabeled skin lesion classification by self-supervised topology clustering network", Biomedical Signal Processing and Control, Vol. 66, 2021, p. 102428.

[14] S. Chatterjee, D. Dey, S. Munshi, "Integration of morphological preprocessing and fractal based

feature extraction with recursive feature elimination for skin lesion types classification", Computer Methods and Programs in Biomedicine, Vol. 178, 2019, pp. 201-218.

[15] J. Oyelade, I. Isewon, O. Oladipupo, O. Emebo, Z. Omogbadegun, "Data Clustering : Algorithms and Its Applications", Proceedings of the 9th International Conference on Computational Science and Its Applications, St. Petersburg, Russia, 1-4 July 2019, pp. 71-81.

[16] S. Louhichi and B. Abdallah, "Skin Lesion Segmentation Using Multiple Density Clustering Algorithm MDCUT And Region Growing", Proceedings of the IEEE/ACIS 17th International Conference on Computer and Information Science, 6-8 June 2018, pp. 74-79.

[17] O. Trabelsi, "Skin Disease Analysis and Tracking based on Image Segmentation.", 2013 International Conference on Electrical Engineering and Software Applications, 2013.

[18] E. Salahat, M. Qasaimeh, "Recent advances in features extraction and description algorithms: A comprehensive survey", Proceedings of the IEEE International Conference on Industrial Technology, Toronto, ON, Canada, 22-25 March 2017, pp. 1059-1063.

[19] S. Benyahia et al. "Multi-Features Extraction Based on Deep Learning for Skin Lesion Classification",, Tissue and Cell, Vol. 74, 2021.

[20] S. Ayram and T. Kainen, "Introduction to partitioning-based clustering methods with a robust example", Reports of the Department of Mathematical Information Technology Series C. Software and Computational Engineering, Vol. 35, No. C, 2006.

[21] "Granular parakeratosis images | DermNet NZ." https://dermnetnz.org/topics/granular-parakeratosis-images?stage=Live (accessed: 2021).

[22] DermIS, https://www.dermis.net/dermisroot/en/32551/diagnose.htm." .

[23] P. F. Felzenszwalb, D. P. Huttenlocher, "Distance transforms of sampled functions", Techincal Report, TR20041963, Vol. 4, 2004, pp. 1-15.

[24] F. F. Ximenes Vasconcelos, A. G. Medeiros, S. A. Peixoto, P. P. Rebouças Filho, "Automatic skin lesions segmentation based on a new morphological approach via geodesic active contour", Cognitive Systems Research, Vol. 55, 2019, pp. 44-59.

[25] S. H. Salih and S. Al-Raheym, "Comparison of skin lesion image between segmentation algorithms", Journal of Theoretical and Applied Information Technology, Vol. 96, No. 18, 2018, pp. 6085-6094.

[26] S. Raja, S. Kotra, R. Babu, P. Goriparthi, V. Kotra, L. Chiau, "Journal of King Saud University - Science Dermoscopic image classification using CNN with Handcrafted features", Journal of King Saud University - Science, Vol. 33, No. 6, 2021, p. 101550.

[27] S. M. Kumar, J. R. Kumar, K. Gopalakrishnan, "Skin Cancer Diagnostic using Machine Learning Techniques - Stationary Wavelet Transform and Random Forest Classifier", International Journal of Innovative Technology and Exploring Engineering, Vol. 3075, No. 2, 2019, pp. 4705-4708.

[28] M. A. Khan, T. Saba, M. Sharif, "Multi-Model Deep Neural Network based Features Extraction and Optimal Selection Approach for Skin Lesion Classification", Proceedings of the International Conference on Computer and Information Sciences, Sakaka, Saudi Arabia, 3-4 April 2019, pp. 1-7.

(12) PATENT APPLICATION PUBLICATION

(19) INDIA

(22) Date of filing of Application :25/02/2023

(21) Application No.202341012928 A

(43) Publication Date : 17/03/2023

(54) Title of the invention : Sentiment Analysis of College Survey using AI

(51) International classification :G06F 403000, G06N 030800, G06Q 300200, G06Q 502000, G09G 032000
 	
(86) International Application No
Filing Date :PCT//
:01/01/1900
 	
(87) International Publication No: NA
 	
(61) Patent of Addition to Application Number
Filing Date :NA
:NA
 	
(62) Divisional to Application Number
Filing Date :NA
:NA
	(71)**Name of Applicant :**
	  1)**Ballari Institute of Technology and Management**
	   Address of Applicant :Ballari Institute of Technology and Management, Ballari-583104, Bellary, Karnataka, India ----------- -----------
	  2)**Dr. Abdul Lateef Haroon P S**
	  3)**Mohammed Shafiulla**
	  4)**Aswatha Narayana**
	  5)**Prithviraj Y J**
	  6)**Dr K M Sadyojatha**
	  7)**Dr R N Kulkarni**
	  8)**Sathyanarayana S**
	  9)**Sathyanarayana K B**
	Name of Applicant : NA
	Address of Applicant : NA
	(72)**Name of Inventor :**
	  1)**Ballari Institute of Technology and Management**
	Address of Applicant :Ballari Institute of Technology and Management, Ballari-583104, Bellary, Karnataka, India ----------- -----------
	  2)**Dr. Abdul Lateef Haroon P S**
	Address of Applicant :Associate Professor, Department of Electronics and Communication Engineering, Ballari Institute of Technology and Management, Ballari-583104 ----------- -----------
	  3)**Mohammed Shafiulla**
	Address of Applicant :Assistant Professor, Department of Computer Science and Engineering, Ballari Institute of Technology and Management, Ballari-583104, Ballari, Karnataka, India ----------- -----------
	  4)**Aswatha Narayana**
	Address of Applicant :Assistant Professor, Department of Electronics and Communication Engineering, Ballari Institute of Technology and Management, Ballari-583104 ----------- -----------
	  5)**Prithviraj Y J**
	Address of Applicant :Deputy Director, Ballari Institute of Technology and Management, Ballari-583104, Bellary, Karnataka, India ----------- -----------
	  6)**Dr K M Sadyojatha**
	Address of Applicant :Professor & HOD, Department of Electronics and Communication Engineering, Ballari Institute of Technology and Management, Ballari-583104 ----------- -----------
	  7)**Dr R N Kulkarni**
	Address of Applicant :Professor & HOD, Department of Computer Science and Engineering, Ballari Institute of Technology and Management, Ballari-583104 ----------- -----------
	  8)**Sathyanarayana S**
	Address of Applicant :Assistant Professor, Department of Computer Science Engineering, J N N College of Engineering, Shivamogga-577204 ----------- -----------
	  9)**Sathyanarayana K B**
	Address of Applicant :Assistant Professor, Department of Information Science Engineering, J N N College of Engineering, Shivamogga-577204 ----------- -----------

(57) Abstract :
Sentiment Analysis of College Survey using AI Abstract This system presents a combination of Machine Learning and NLP based approaches for sentiment analysis of student's feedback. The textual feedback, typically collected towards the end of a semester, provides useful insights into the overall teaching quality, and suggests valuable ways for improving teaching methodology. The system describes a sentiment analysis model trained using BERT and VADER to analyse the sentiments expressed by students in their textual feedback. A comparative analysis is also conducted between the proposed model and other methods of sentiment analysis. The experimental results suggest that the proposed model performs better than other methods.

No. of Pages : 14 No. of Claims : 7

SPRINGER LINK

Log in

≡ Menu   🔍 Search   🛒 Cart

Home > Proceedings of the 2nd International Conference on Cognitive and Intelligent Computing > Conference paper

Novel Approach to Abstract Object Features from Java Program

R. N. Kulkarni ✉ & P. Pani Rama Prasad

Conference paper | First Online: 02 October 2023

2 Accesses

Part of the Cognitive Science and Technology book series (CSAT)

Abstract

Nowadays, the software developers use unified modeling language tool (UML) to design the application software for an organization. The present UML tool available in the market supports thirteen different diagrams, which represents the static behavior and dynamic behavior of the software. In this paper, an automated tool is proposed that abstracts the object features from the Java program. To abstract these object features, initially the tool extracts all the necessary components related to the class such as class name, attributes associated with the class, methods, and visibility information like private, public, and protected. Finally, all the extracted features are stored in the form of a table called class table. Further, the information available in the class table, and input Java program is used to abstract the features of object such as object name, attributes, methods used by the object, visibility, and associations.

Keywords

UML   **Restructuring**   **Class table**   **Object table**   **Java program**

This is a preview of subscription content, access via your institution.

⌄ Chapter **EUR 29.95**	⌄ eBook **EUR 277.13**	⌄ Hardcover Book **EUR 329.99**
Price includes VAT (India)	Price includes VAT (India)	Price excludes VAT (India)
• Available as PDF • Read on any device • Instant download • Own it forever	• Available as EPUB and PDF • Read on any device • Instant download • Own it forever	• Durable hardcover edition • Dispatched in 3 to 5 business days • Free shipping worldwide - see info
Buy Chapter	Buy eBook	Buy Hardcover Book

Tax calculation will be finalised at checkout

Purchases are for personal use only

Learn about institutional subscriptions

References

1. Kulkarni R N, Pani Rama Prasad P (2021) Abstraction of UML class diagram from the input Java program. Int J Adv Netw Appl 12(04):4644–4649

2. Kulkarni R N, Patil P (2020) Abstraction of functional modules from a Legacy 'C' Program using program slicing, perspectives in communication, embedded-systems and signal-

processing 4(4):39–44

3. Mazumder SF, Latulipe C, Are variable, array and object diagrams in Java textbooks explanative? In: Proceedings of the 2020 ACM conference on innovation and technology in computer science education, 2020, pp 425–431

4. Sharaff A, Rath SK (2020) Formalization of UML class diagram using colored Petri Nets. In: IEEE 1st International conference on power, control and computing technologies (ICPC2T), Raipur, 2020, pp 256–261

5. Sabir U, Azam F et al (2019) A model driven reverse engineering framework for generating high level UML models from Java source code. IEEE Access 2019, pp 312–318

6. Kulkarni R N, Pani Rama Prasad P (2019) Restructuring of Java program to be amenable for reengineering. J Eng Sci Technol 02(06):45–51

7. Mahanto P, Barisal SK, Mohapatra DP (2019) Achieving MC/DC using UML object diagram. In: IEEE International conference on information technology (ICIT), Bhubaneswar, 2019, pp 182–189

8. Kästner A, Gogolla M, Selic B (2018) From (imperfect) object diagrams to (imperfect) class diagrams: new ideas and vision paper. In: Proceedings of the 21th ACM/IEEE international conference on model driven engineering languages and systems, 2018, pp 71–80

9. Kästner A, Gogolla M, Selic B (2018) Towards flexible object and class modeling tools: an experience report. In: MODELS'18: Proceedings of the 21th ACM/IEEE international conference on model driven engineering languages and systems, 2018, pp 13–22

10. Singh D (2018) A scrutiny study of various unified modeling language (UML) diagrams, software metrics tool and program slicing technique. J Emerg Technol Innov Res (JETIR) 5(6)

11. Singh D, Sidhu HJS (2018) A scrutiny study of various unified modeling language (uml) diagrams, software metrics tool and program slicing technique 5(6), 254–262

12. Handigund SM, Sajjanar S, Arunakumari BN (2015) Resuscitation of syllogism within unified modeling language levels through the renovation of object diagram. In: IEEE International conference on advances in computing, communications and informatics (ICACCI), pp 114–121

13. Torchiano M, Torchiano M, Ricca F, Leotta M (2017) Do UML object diagrams affect design comprehensibility? Results from a family of four controlled experiments. J Vis Lang Comput, pp 135–143

14. Duc BM (2015) Uniform object modeling methodology and reuse of real-time system using UML. In: Proceedings of the 5th ACM international conference on Embedded software, 5(2), pp 44–47

15. Zeaaraoui A, Ettifouri EH, Bouchentouf T (2015) An automated object-based approach to transforming requirements to class diagrams. In: IEEE Second world conference on complex systems (WCCS), 2(1), pp 69–75

16. Parada AG, Siegert E, de Brisolara LB (2014) Generating Java code from UML class and sequence diagrams. IEEE Explore, 33–38

Author information

Authors and Affiliations

Department of Computer Science & Engineering, Ballari Institute of Technology and Management, Ballari, India

R. N. Kulkarni & P. Pani Rama Prasad

Corresponding author

Correspondence to R. N. Kulkarni .

Editor information

Editors and Affiliations

BioAxis DNA Research Centre Private Limited, Hyderabad, Andhra Pradesh, India

Amit Kumar

Department of Computer Science, Brunel University, Uxbridge, UK

Gheorghita Ghinea

CMR College of Engineering and Technology, Hyderabad, India

Suresh Merugu

Rights and permissions

Reprints and Permissions

Copyright information

About this paper

Cite this paper

Attendance Certificate

This is to certify that **Dr. R N Kulkarni** of **Ballari Institute of Technology and Management, Ballari** has attended the one day Awareness Workshop on Outcome Based Education (OBE) and Accreditation organized by National Board of Accreditation (NBA), New Delhi in collaboration with Visvesvaraya Technological University, Belagavi at B.M.S. College of Engineering, Bengaluru on 16th January, 2023.

Dr. Shambhavi B R
Chief-Coordinator- IQAC, BMSCE

Chief Coordinator-IQAC
B.M.S. College of Engineering
Bengaluru - 560 019

2024/2/7 14:21

BRIDGE'22
REVITALIZING INDIA THROUGH NEW AGE SKILLS

Certificate of Participation

Presented To

DR. R N KULKARNI

Ballari Institute of Technology and Management
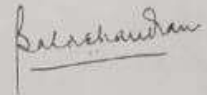
for participating in the 48th Edition of

BRIDGE 2022 - Bengaluru (A High Impact Industry-Institute Interaction Event of India),

Organized by ICT Academy held on 19 October 2022 at The Lalit Ashok, Bangalore.

C.NO: 160273

Hari Balachandran
Chief Executive Officer
ICT Academy

2024/2/7 14:21

GOVERNMENT OF INDIA

INTELLECTUAL
PROPERTY INDIA

Date/Time : 06/12/2022

CHALLAN : TR-5
DOCKET NO:118521

Agent Number:

To,
BALLARI INSTITUTE OF TECHNOLOGY & MANAGEMENT (BITM)
JNANA GANGOTRI CAMPUS, HOSPETE ROAD, NEAR ALLIPUR, BALLARI, KARNATAKA, INDIA 583104.
rnkulkarni@bitm.edu.in

Sr. No.	CBR No.	Reference Number /Application Type	Application Number	Title/Remarks	Amount Paid
1	49338	R20224044251	202241038278	---	4400
2		E-101/21213/2022-CHE	202241038278	Correspondence	0
Total :					4400

Received a sum of Rs. 4400 (Rupees Four Thousand Four Hundred only) through

Payment Mode	Bank Name	Cheque/Draft Number	Cheque/Draft Date	Amount in Rs
Draft	KARNATAKA GRAMIN BANK	747574	30/11/2022	4400

Note: This is electronically generated receipt hence no signature required.

PATENT OFFICE
INTELLECTUAL PROPERTY BUILDING
G.S.T. Road, Guindy, Chennai-600032
Tel No. (091)(044) 22502081-84 Fax No. 044 22502066
E-mail : Chennai-patent@nic.in
Web Site : www.ipindia.gov.in

GOVERNMENT OF INDIA

INTELLECTUAL
PROPERTY **INDIA**

CHALLAN : TR-5
DOCKET NO:61285

Date/Time : 06/07/2022

To,
BELLARI INSTITUTE OF TECHNOLOGY & MANAGEMENT
"JNANA GANGOTRI" CAMPUS, HOSPETE ROAD, NEAR ALLIPUR, BALLARI, KARNATAKA, INDIA-583104.
rnkulkarni@bitm.edu.in

Agent Number:

Sr. No.	CBR No.	Reference Number /Application Type	Application Number	Title/Remarks	Amount Paid
1	26805	ORDINARY APPLICATION	202241038775	BLOCK CHAIN FOR ENSURING CORRECTNESS OF DATA STORED IN UNTRUSTED CLOUD STORAGE	1750
2		E-101/11674/2022-CHE	202241038775	Correspondence	0
3		E-2/3001/2022-CHE	202241038775	Form2	0
4		E-3/20492/2022-CHE	202241038775	Form3	0
5		E-5/2594/2022-CHE	202241038775	Form5	0
6	26805	E-12/5072/2022-CHE	202241038775	Form9	2750
7		E-106/4079/2022-CHE	202241038775	Form28	0
8		E-101/11675/2022-CHE	202241038775	Others(EDUCATIONAL INSTITUTION ELIGIBILITY DOCUMENT)	0
Total :					4500

Received a sum of Rs. 4500 (Rupees Four Thousand Five Hundred only) through

Payment Mode	Bank Name	Cheque/Draft Number	Cheque/Draft Date	Amount in Rs
Draft	KARNATAKA GRAMIN BANK	747559	15/06/2022	4500

Note: This is electronically generated receipt hence no signature required.

Novel Approach to Identify and Eliminate Deadlocks in the 'C' Program

R. N. Kulkarni, Pratibha Mishra, J. Vedavyas, and Arun Biradar

Abstract The programming system of any organization comprises various types of interrelationships, like period dependency, sequence dependency, called-calling in-hierarchy dependency, and other types of application-dependent dependencies. The functionalities in the 'C' program are normally un-modular and may scatter in number of interdependent programs group. The control flow graph of the C program helps in identifying the navigational paths within the interdependent programs groups. A deadlock is a situation in which two programs, functional units, or modules that share the same resource effectively prevent each other from accessing the resource. Different techniques are available to detect potential deadlocks in the programming system. Analyzing and comprehending each potential deadlock in order to determine whether the deadlock is viable in a real-world execution requires significant programmer effort. In this paper, a novel approach is proposed to detect deadlock and also eliminate deadlock, which is designed by considering the control flow of the program. In the beginning, the control flow of the entire program is abstracted, and then the entries of each called and calling function are entered in a four-column program dependency table. After performing the entry for the entire program, scan the entire table from left to right and top to bottom. If any row in the program dependency table appears more than once, then there is a possibility of deadlock. After identifying the repeated row, find out the functions that are repeated, and then the deadlock is resolved by copying the functions in the appropriate place without modifying the functionality.

R. N. Kulkarni · P. Mishra · J. Vedavyas (✉)
Department of Computer Science and Engineering, Ballari Institute of Technology and Management, Ballari, India
e-mail: vedavyas@bitm.edu.in

R. N. Kulkarni
e-mail: rnkulkarni@bitm.edu.in

P. Mishra
e-mail: prathibhamishra@bitm.edu.in

A. Biradar
School of CSE, Reva University, Bangalore, India
e-mail: arun.biradar@reva.edu.in

Effective ANN Model based on Neuro-Evolution Mechanism for Realistic Software Estimates in the Early Phase of Software Development

Ravi Kumar B N[1]
Dept. of Computer Science and Engineering
BMS Institute of Technology and Management
Bangalore, India

Dr. Yeresime Suresh[2]
Dept. of Computer Science and Engineering
Ballari Institute of Technology and Management
Ballari, India

Abstract—There is no doubt that the software industry is one of the fastest-growing sectors on the planet today. As the cost of the entire development process continues to rise, an effective mechanism is needed to estimate the required development cost to control better the cost overrun problem and make the final software product more competitive. However, in the early stages of planning, the project managers have difficulty estimating the realistic value of the effort and cost required to execute development activities. Software evaluation prior to development can minimize risk and upsurge project success rates. Many techniques have been suggested and employed for cost estimation. However, computations based on several of these techniques show that the estimation of development effort and cost vary, which may cause problems for software industries in allocating overall resources costs. The proposed research study proposes the artificial neural network (ANN) based Neural-Evolution technique to provide more realistic software estimates in the early stages of development. The proposed model uses the advantages of the topology augmentation using an evolutionary algorithm to automate and achieve optimality in ANN construction and training. Based on the results and performance analysis, it is observed that software effort prediction using the proposed approach is more accurate and better than other existing approaches.

Keywords—Software cost estimation; COCOMO-II; neuro-evolution; artificial neural network; genetic algorithm

I. INTRODUCTION

The software industry is undoubtedly one of the greatest innovations in the modern world [1]. The software development process broadly requires various discrete actions such as understanding the client requirements, analysis, preparing the user requirement specification, technical requirement specification, software requirement specification, and hardware requirement specification in the initial stages [2]. Further actions architecture design of the software, design of the modules, coding, integration, testing, and debugging. The overall development cost estimation depends on the individual cost and efforts required for each of the actions involved in the SDP. However, estimating the cost in software development has been a challenge facing researchers and professionals in software engineering over the past few years. The purpose of cost estimation is to help with decisions made during the development of a software project. Many factors affect the

accuracy of cost estimation. If the cost is underestimated, the project may be delayed, lack implemented features, or not be completed. On the other hand, an overestimated cost can lead to higher software costs, a waste of resources, and even loss of opportunities for competing markets [3]. These factors can have negative consequences for the project, the development organization, and the customers. Thus, the quality of estimates can affect the quality of the software project.

Many software cost estimation models have been developed and improved, which can be categorized into algorithmic and non-algorithmic models [4]. In algorithmic cost model (ACM), typically a mathematical model or expressions are formulated using factors like i) source line of codes (SLOC), ii) risk calculation, and iii) skill levels obtained from the historical records; however, it fails to enumerate many vital factors including i) complexities, ii) reliability and experiences of the projects and due to this, it leads to the imprecise estimation. The constructive cost model- COCOMO is the most popular method in this category [5]. Further, it has evolved as COCOMO-II and has been widely used to design software cost predictors with various strategies considering basic cost indicators like lines of codes (LOC) and the function points [6-7]. The non-algorithmic approach is basically concerned with soft-computing approaches that overcome the limitations of the algorithmic model. The soft-computing approaches handle a better approximation of the solutions of the complex problems where many nonlinear and uncertain parameters are involved. Table I highlights the comparison of algorithmic and non-algorithmic models. Specifically, the existing approaches for the estimation, such as COCOMO and iii) function point-based model, all lack providing desirable accuracy as they ignore many of the critical drivers. So, these methods limit their applicability in the real-time scenario. In order to address these challenges, the soft-computing approaches are being extensively attracted the focus of the researchers by including approaches either individual or by hybrid techniques like- swarm optimization, fuzzy logic, genetic algorithm, machine learning, and neural network [8-10]. The advantage of the soft-computing approach is that it approximates the solutions created by the mess due to nonlinear factors that are uncertain and imprecise. In recent years, neural networks have gained prominence in software development. However, the literature presents several studies on applying neural networks and machine learning techniques

to estimate cost [11-12]. However, there is no consensus on which method best predicts software costs. The neural network architecture involves different configuration and hyperparameters such as layers, neuron nodes, transfer function, and learning parameters (weights and biases). Generally, the design of the learning model is specific to the particular data set and problem context. If the same model is introduced with a different dataset, it may not perform similarly. Therefore, the parameters mentioned above affect network performance. However, the evolution of models that produce good results in different environments is still a driving force for current research work. This paper suggests a unique approach to software development cost estimation based on Neuro-evolution. The proposed Neuro-evolution approach implements a mechanism of artificial intelligence (AI) that employs an evolutionary algorithm to generate optimal Artificial Neural Network (ANN) architecture. Further, the constructed ANN model in the proposed work is trained to adopt characteristics of software attributes using the previous dataset to produce accurate software estimates.

TABLE I.   ANALYSIS OF ALGORITHMIC AND NON-ALGORITHMIC TECHNIQUES

Techniques	Category	Advantages	Limitations
Analogy	Non-Algorithmic	Independent of new resources	Dependent on past information & huge data requirement.
Expert-based		Highly responsive and fast process	Biased outcome
Bottom-Up		Stable	Inaccurate timings & needs huge data
Top-Down		Faster & low cost	less stable outcome & decisions
COCOMO	Algorithmic	Flexible analysis, input modification, & clear outcomes	Inaccurate estimates & practically infeasible
Function Point		Tool independent	Not good enough
Neural Network	Machine learning	Precise predictive estimates	Highly dependent on the dataset and no standard rule for implementation

The ANN model constructed is a feedforward neural network utilizing backpropagation learning mechanisms. The entire configuration and learning parameter is realized with the evolutionary algorithm, particularly a genetic algorithm (GA) implemented via the Neuro-evolution concept. The proposed study aims to achieve:

- A unique ANN model with an optimal selection of its parameters, including the size of hidden layers, number of neuron units at each layer, and transfer functions, from the given interval (linear, Relu, and sigmoid).

- The stable training process of the constructed ANN model that supports large training data samples.

- Self-adjustment in the weight and biases in an optimal manner from the training samples.

- Enhanced generalization in the training phase and efficient identification of dependencies of the predicted values from the input observations.

- Higher accuracy in the prediction to achieve realistic estimates of the cost required for the software development compared to the existing techniques.

The remaining sections of this paper are organized in the following manner: Section-II presents the review of the literature in the context of software cost and effort estimations; Section III discusses the material and methodology adopted in the proposed work; Section IV presents the system design and implementation procedure adopted in the proposed system; Section V presents the outcome and discusses the performance of the proposed system concerning its scope and effectiveness compared to the existing approaches, and finally, the entire contribution of the proposed work is summarized in Section VI.

II.   RELATED WORK

Currently, the literature consists of several types of techniques and schemes for software cost estimation and prediction. This section discusses some of the recent research works carried in the context of enhancing prediction of the cost required for software development.

A. Algorithmic Approaches

The algorithmic approaches are concerned with mathematical models or expressions for cost predictions. To date, various methods have been suggested based on the algorithmic approaches. Work carried out by Kumawat, and Sharma [13] focuses on estimating the size metric for computing the cost required for the software project development (SPD). The authors have used the function point analysis (FPA) technique to compute cost estimates. The work of Khan et al. [14] suggested a cost estimation model by customizing features of the COCOMO-II that integrates additional cost drivers for computing the estimates of actual cost and effort required for SDP. Similarly, the study of Keil et al. [15] has introduced a different version of COCOMO-II to fit in the context of global software development (GSD). Two additional cost drivers are added in this version of cost drivers concerning collaboration and communication among different sites. The researchers in the above-discussed literature have tried to provide a significant contribution. All the factors are determined and devised based on the literature analysis and researchers' knowledge. However, there is a lack of empirical support, effective benchmarking, and validation of the scope of the suggested schemes. The authors in the study of Menzies et al. [16] have introduced a tool that encompasses case studies and previous experience to reduce the execution time, the effort required, and the number of defects in the project's development. Their results were obtained from small data sets, and they recommend conducting other tests where large volumes of information are handled. They do not explicitly use control indicators from other areas of knowledge, for example, to measure human and logistical resources. In the existing literature, few extensions to COCOMO were suggested, including dynamic multistage models to meet the analytical needs of prototyping SPD models. These models consider the

dynamics of varying requirements, system design, and other strategies, but all lack desirable accuracy as they ignore many critical drivers. So, these methods limit their applicability with varied IDEs models, languages, and tools.

B. Non-Algorithmic Approaches

The non-algorithmic approach generally implies the soft-computing techniques that handle ambiguity and nonlinearity in the cost estimation techniques. The previous section discusses the conventional approaches regarding software cost and effort estimation. However, software project requirements constantly change over time, which also causes the estimates of cost and effort to change. The researchers realized the need for soft computing approaches that include machine learning techniques, fuzzy logic, and various metaheuristic method. This section discusses the existing soft computing approaches for software effort and cost estimation to analyze the current research trend. Nandal and Sangwan [17] a hybrid Bat and Grautational algorithm is used to estimate the effort of software, whereas fuzzy regression models are used to overcome the problem of imprecise in the dataset for the prediction software effort (Nassif et al. [18]). All these approaches provide a good solution but at the cost of huge computational complexity. The application of evolutionary algorithms like GA is used in the study of Zaidi et al. [19] and Reena et al. [20] to optimize the coefficients of different estimation models in the presence of nonlinear data. The approach of intelligent techniques like the neural network deals with the complexities and uncertainty in the software effort estimation is presented in Venkataiah et al. [21] [22]. Few recent research studies have also focused on applying the hybrid approach in the SPD process. The joint approach of nature-inspired algorithm and ML is adopted by authors in [23-25] to compute the estimates of effort in project development. The work of Singh et al. [26] evaluated different ML techniques in the software effort estimation. The outcome reported in this study showed better performance achieved by LR in terms of error percentage analysis. A neural network approach [27-28] has also been widely accepted in software cost estimation. In the work of Choetkiertikul et al. [29], a long short-term memory (LSTM) and recurrent highway network (RHN) are employed to estimate the effort required for completing user stories or issues. Also, Bayesian Network is used to estimate the work time required in the SPD process [30].

C. Motivation of the Research

A wide range of schemes and techniques have been described in the literature for predicting SPD's costs. The recent literature has been observed more focused on applying metaheuristic techniques, neural networks, and machine learning algorithms. Building a model based on the dataset is difficult due to the complexity and nonlinearity involved in the data attributes. Also, the learning model's design is affected by a variety of factors concerned with network parameters, data modeling, and feature engineering. Apart from this, the factors that determine the connectivity among nodes are complicated to analyze before the training phase to develop an ideal network. Generally, the building and training of the learning model involves a lot of human effort and is specific to the particular context, which is a significant concern as software attributes vary over time. However, even small changes in parameters can dramatically alter the result of the trained model.

A unique model with accurate estimation is presented based on the neuro-evaluation augmenting topology to evolve with an optimized ANN architecture to address and overcome these problems. This type of approach for the cost estimation problem has not yet been applied to the software cost estimation problem. The proposed study aims to explore the effectiveness of augmenting the topology mechanism to automate the construction and training of the ANN model that generates better solutions.

III. MATERIALS AND METHODOLOGY

The material used for evaluating the proposed model is the COCOMO dataset. The methodology used for designing and developing the proposed ANN model for cost estimation is based on the Neuro-evolution AI technique, which constructs an optimal ANN model using a genetic algorithm. This section briefly highlights the dataset and methodology adopted in the proposed system.

A. Dataset

The COCOMO (Constructive Cost Model) is a widely known software estimation model introduced by Barry Boehm [31]. This model utilizes an approach of statistical correlation between software attributes and lines of the code. In other words, it basically adopts regression analysis with the responsible parameters that are representative of the estimates of the cost required in software development. In the current research work, the study uses the COCOMO NASA-2 dataset publicly accessible at the promise software engineering repository. This dataset consists of a total of 24 vital cost attributes from 93NASA projects.

B. Artificial Neural Network

In recent years, ANN has received wide attention to address complex nonlinear problems in various fields such as computer vision, image processing, natural language processing, and many more. ANN can be viewed as a function approximator that takes an input from observation state and maps to the output state (decision), such that: $f(x) \rightarrow y$. Typically, the function approximators consist of neurons, often referred to as cells or units, composed of summation and activation functions. The typical function of ANN cell is described in Fig. 1 as follows:
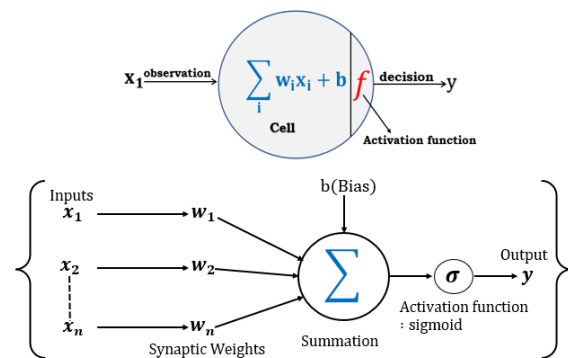

Fig. 1. Typical Function of ANN Cell.

In Fig. 1, the architecture of the basic ANN cell is described where x is the n input such that:$x \in [x_1, x_2, x_3 \cdots x_n]$, w indicates synaptic weight, such that: $w \in [w_1, w_2, w_3 \cdots w_n]$. Each weight 'w' are associated with input sample $'x'$ both together served as input to the cell function, where all x is multiplied with w and are summed with biased (b) using summation function as described as follows:

$$x \cdot w = (x_1 \times w_1) + (x_2 \times w_2) + \cdots + (x_n \times w_n) \qquad (1)$$

Equation 25 describes the dot product of vector x and vector w, and their summation is given in equation 26 as follows:

$$\sum = x \cdot w \qquad (2)$$

The weights'w_i' can be considered as a strength of the association between cells, and it also decides how much influence the given input will have on the cell's output. Another essential component of the ANN cell is the offset value added to the summation of dot product $x \cdot w$. This offset value is often called a bias that allows shifting the phenomenon of the nonlinear activation function to produce the expected result correctly to the output state. Moreover, the w and b are also often called learning parameters of the ANN model; the relationship between w and b can be numerically represented as follows:

$$(x \cdot w) + b \qquad (3)$$

Equation 3 is then passed to the nonlinear function, which is generally a sigmoid function that enables nonlinearity in the ANN cell as numerically represented as follows:

$$y = \sigma(x \cdot w) + b \qquad (4)$$

Where y denotes the output of the cell and nonlinear σ sigmoid function. Sigmoid or Logistic: takes a real-valued input and returns output in the range [0,1]. The ANN cells are arranged into several layers, typically classified as input layers, hidden layers and output layers all interconnected to each other.

Usually, the topological structure of the artificial neural network is selected based on empirical analysis, and the learning parameters are determined using the training process, which is related to the trial-and-error process. Therefore, developing an ANN model is not a big problem. However, training ANN models to accomplish certain tasks is a real challenge. In this regard, Neuro-Evolution can be an effective mechanism for determining the optimal topology of neural networks and learning parameters (weights and biases) to construct an ideal ANN model.

C. Neuro-Evolution of Augmenting Topologies

Neuro-Evolution of Augmenting Topology (NEAT) is a neuroevolutionary AI technology that deals with topology augmentation to automate the construction and training of ANN models using evolutionary algorithms (EA) [32]. The EA in NEAT is a kind of genetic algorithm (selection, crossover, and mutation), which allows the evolution of ANN units, learning parameters (weight and biases), and structure, trying to determine stability between the fitness of the obtained

solution and assortment. Fig. 2 shows a sample visualization of the topology construction of ANN using the NEAT algorithm.

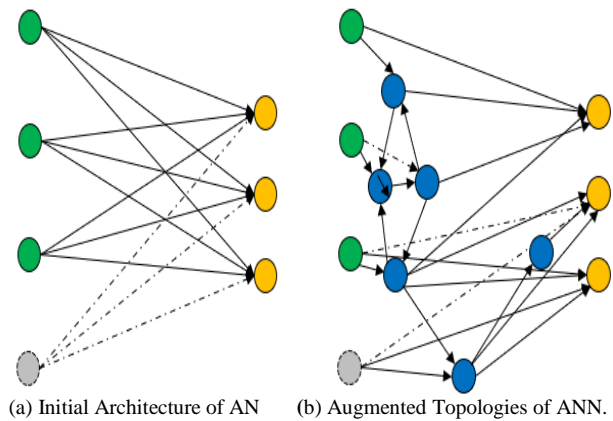(a) Initial Architecture of AN   (b) Augmented Topologies of ANN.

Fig. 2.   Topology Construction of ANN using NEAT.

In the above Fig. 2, visualization of initial topology (a) and final topology construction of ANN model (b) after several iterations is shown using NEAT. The flow process of topology augmentation in the construction and training of the ANN model is shown in Fig. 3.

The mechanism of topology augmentation for the optimal ANN model requires the initialization of variables concerning network hyperparameter and loss function. The initialization of hyperparameter variables (such as learning rate and the number of neurons) is crucial to determine the training performance of the network during the crossover and mutation process of EA. On the other hand, the loss function determines the optimality of the neuron genes (bias) and synapse genes (weight) in the learning phase. The loss function in NEAT is also regarded as a fitness function, and a set of neuron genes and synapse genes are called genomes.
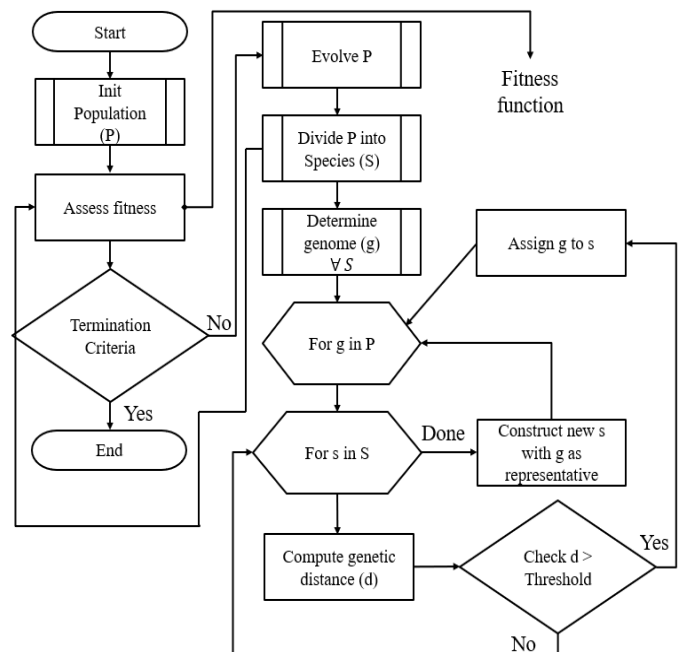

Fig. 3.   Flow Process of Topology Augmentation using NEAT.

The algorithm generates a genome considering single input and output layer during the initialization of an initial set of solution candidates (population). Therefore, in the first generation, the genomes only vary in weights and biases but not network topology. After assessing the fitness value of each genome, the algorithm stops if the termination criterion is met. Otherwise, it generates a new set of solution candidates by executing crossovers phase y between genomes and then performs mutations in the subsequent offspring. All these processes are carried out randomly, and prior to computing the fitness of neuron genes and synapse genes, i.e., optimality of weight and biases, the algorithm splits the set of solution candidates into species (a particular class with the common characteristics) based on the computation of the genetic distance between each set of neuron weight and biases. The computation of the genetic distance is carried out using the following numerical equation:

$$d = d_b + d_w \tag{5}$$

The above equation 6 represents the computation of distance (d) based on the summation of neuron (d_b i.e., bias) and synapse (d_w i.e., weight). The computation of the d_b and d_w are shown in equations 6 and 7 as follows:

$$d_b = c_n \times \frac{\Delta_b}{\max(B(g_1),B(g_2))} \tag{6}$$

$$d_w = c_s \times \frac{\Delta_w}{\max(W(g_1),W(g_2))} \tag{7}$$

Where c_n and c_s are the user-defined variables for fine-tuning the model parameters.

IV. PROPOSED COST ESTIMATION MODEL

This section discusses the proposed cost estimation implementation procedure based on the ANN model determined using the NEAT algorithm discussed in the previous section. In the proposed study, the cost estimation problem is being studied as a regression problem rather than an optimization problem to predict kilo line of code (KLOC). The proposed cost estimation model design involves three core modules; namely, i) data exploration module ii) data preprocessing, and iii) design of ANN Model.

A. Dataset Exploration

In the current study, the data is available on the NASA website. The data is downloaded by sending an HTTP GET request to the respective URLs. When the request is sent, the data can be retrieved in the form of an a.arff file. However, this is not readable readily by our system. Hence, the data is sub-set from the 'Arff file', which contains 10 parts, including {Title, Past Usage, Relevant Information, Number of instances, Number of attributes, Attribute information, Missing attributes, Class distribution, Data}. The sub-set extracts only the Data. The Data Store stores the data in the form of a simple CSV file. Each column is separated by a (delimiter), and a new line character separates each sample. Many data science platforms can read and process this format, including pandas used in the current study. The data imported into the numerical computing environment (NCE) describes 124 entries ranging from the index number 0 to 123 with 24 columns. The dataset consists of 24 variables with type numeric and two categorical

variables. The memory taken to upload the data is more than 25 KB. Table II presents a statistical description of all the 25 predictors and an output KLOC. The closer shows that the counts of all the parameters are identical to the number of samples, which indicates there are no missing values. The differential between the consecutive pair between {0, 25%}, {25%, 50%}, {50%, 75%} and {75%, 100%} sometimes are not less than standard deviation (σ) that means there is the presence of outliers in the data, as well if RMSE and MAE of the model have a difference more than mean KLOC then outliers need to be corrected. Another important observation on the dataset is that certain parameters show a specific correlation with the effort. The correlations are either negative correlation or positive correlation. In positively correlated parameters, the effort decreases with a decrease in the parameter's values, whereas, in negatively correlated parameters, the effort decreases if the parameters increase. The positively correlated parameters are the cost drivers (CD) $\in$ {acap, pcap}, and negatively correlated parameters such that CD $\in$ {rely, Cplx, data, time, stor, sced}. Further, on the analysis of co-efficient using linear regression analysis, it is found that reduced reusability (ruse) and 'site' have a higher multiplier effect on cost/effort compared to other CDs, as evident in Fig. 4. It is clear that the correlation of data points with the actual effort is highly non-uniform in nature. Therefore, a custom feature engineering process for the proposed ANN-based CEM is being carried out.

B. Preprocessing

In this section, the preprocessing operation is carried out from the perspective of the feature engineering task and the extraction of suitable input for the proposed learning model. The core module in this stage contains i) correlation analysis and ii) dataset normalization. In the correlation analysis, the relationships between various variables are analyzed using a mathematical approach that helps find correlations between various cost drivers. The formula for correlation is shown in the equation as follows:

$$r_{x,y} = \frac{\sum(x_i-x').(y_i-y')}{\sqrt{\sum(x_i-x')^2.\sum(y_i-y')^2}} \tag{8}$$

Where, x_i and y_i denotes cost drivers, x' and y' are means values of the cost drivers and $r_{x,y}$ is the correlation factor between x and y that ranges from -1 to +1. As it can be observed from the formula if $x \propto y$, which means that $x = ky$, then the following outcome is achieved when the same is substituted in equation 9.

$$r_{x,y} = \frac{\sum(x_i-x').k(x_i-x')}{\sqrt{\sum(x_i-x')^2.k^2\sum(x_i-x')^2}} \tag{9}$$

$$r_{x,y} = \frac{\sum k(x_i-x')^2}{k\sqrt{(\sum(x_i-x')^2)^2}} \tag{10}$$

$$r_{x,y} = \frac{k\sum(x_i-x')^2}{k\sum(x_i-x')^2} \tag{11}$$

$$r_{x,y} = 1 \tag{12}$$

The above equation 12 proves that when the two cost drivers are proportional, the correlation between them is one. Similarly, when one cost driver reduces and another cost driver

increases, in other words, x=k-ly, then the correlation is said to be -1 and considered as an ideal scenario when there is a perfect linear relationship between two CDs. However, a zero correlation refers to total randomness and no relation between two CDs. The correlation plot for among CDs is given in Fig. 5. It can be analyzed that there is a strong correlation between the 'prec', 'flex', 'resl' and 'team'. As it can be observed that except for exponential CDs such that {'prec', 'flex', 'resl', 'team' and 'pmat'} all other CDs have (>10%) correlation. Hence, all variable turns out to be significant while building an ANN model.

TABLE II. DESCRIPTIVE STATISTICS

| Cost Drivers	count	mean	std	min	25%	50%	75%	max
ACT_EFFORT	124.0	563.334677	1029.227941	6.00	71.50	239.500	581.750	8211.00
prec	124.0	3.110000	1.292409	0.00	2.48	2.480	4.9600	4.960000
flex	124.0	2.618952	1.041618	0.00	103	2.030	4.0500	5.070000
resl	124.0	3.688871	1.403707	0.00	2.83	2.830	5.6500	6.010000
team	124.0	1.837097	1.094185	0.00	1.10	1.100	3.2900	4.660000
pmat	124.0	5.602984	1.288265	2.84	4.68	4.680	6.2400	7.800000
relay	124.0	1.078522	0.103427	0.85	1.00	1.100	1.1000	1.740000
Cplx	124.0	1.189892	0.163256	0.87	1.17	1.170	1.2125	1.740000
Data	124.0	1.014919	0.117179	0.90	0.90	1.000	1.1400	1.280000
Ruse	124.0	0.996935	0.014605	0.95	1.00	1.000	1.0000	1.070000
Time	124.0	1.124516	0.184476	1.00	1.00	1.000	1.2900	1.630000
Stor	124.0	1.107097	0.163149	1.00	1.00	1.000	1.1700	1.460000
Pvol	124.0	0.927406	0.095456	0.87	0.87	0.870	1.0000	1.150000
Acap	124.0	0.880276	0.101079	0.71	0.85	0.850	1.0000	1.016667
Pcap	124.0	0.918817	0.085625	0.76	0.88	0.895	1.0000	1.000000
pcon	124.0	1.000544	0.035766	0.81	1.00	1.000	1.0000	1.205000
Apex	124.0	0.925712	0.083496	0.81	0.88	0.880	1.0000	1.220000
Plex	124.0	1.004590	0.080974	0.91	0.91	1.000	1.0000	1.190000
ltex	124.0	0.966781	0.089415	0.91	0.91	0.910	1.0000	1.200000
Tool	124.0	1.115847	0.078542	0.83	1.09	1.170	1.1700	1.170000
Sced	124.0	1.043065	0.063760	1.00	1.00	1.000	1.1400	1.140000
Site	124.0	0.925040	0.017623	0.86	0.93	0.930	0.9300	0.947500
docu	124.0	1.024940	0.057830	0.91	1.00	1.000	1.1100	1.230000
Physical Delivered KLOC	124.0	103.443901	141.455891	0.00	20.00	51.900	131.7500	980.000000
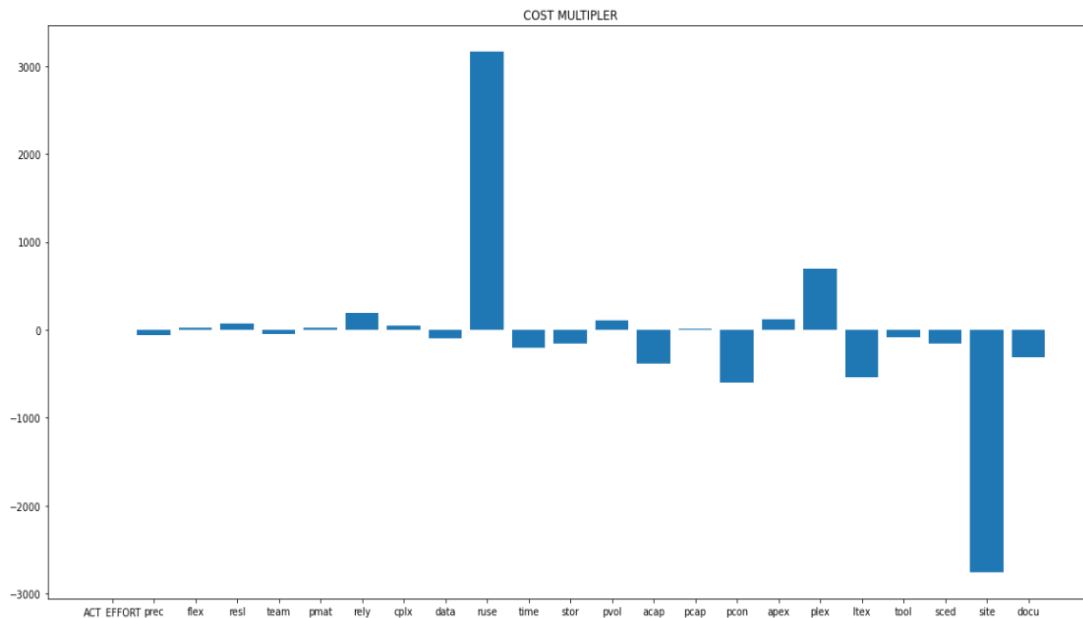
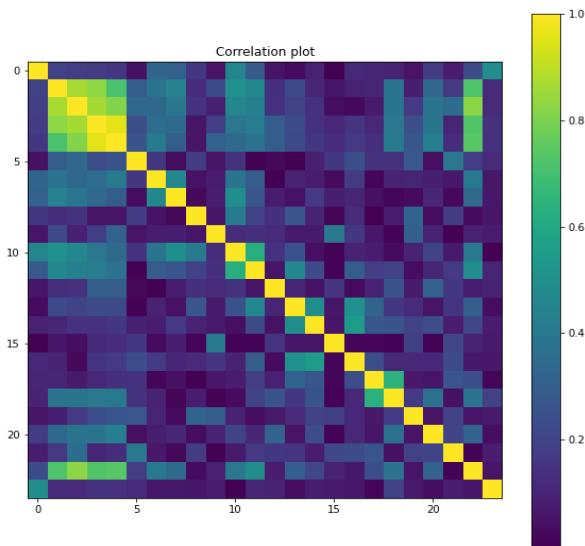Fig. 4. Representation of Cost Multiplier.

Fig. 5.   Correlation Plot among CDs and KLOC.

In order to provide an input to a learning model, the input data is required to be in a vector form. Feature vectorization refers to converting a row of values into a usable vector. In this phase of implementation, the data is normalized with the help of the Min-Max scaling method. Further, each row is transposed and fed to neural networks. The typical formula for data normalization for feature vectors is numerically expressed in equation 13.

$$x' = \frac{x - min(x)}{max(x) - min(x)} \qquad (13)$$

Where, x is the input data, i.e., original CDs feature samples, which is normalized using min and max function and

rescaled in the range of [0,1], and x' normalized CDs feature samples which are further fed to the proposed learning model.

C. Design of the Proposed ANN Model

This section discusses the ANN model design and its implementation procedure with the support of the algorithmic steps. The implementation procedure utilizes the NEAT library of python executed in the Anaconda distribution. The dataset is split into training and testing sets, where 80% of the dataset is kept for the model training, and 20% of the dataset is kept for model testing. The design configuration of the proposed ANN model is carried out using neural evolution mechanisms, where the features from the input observation are considered for determining weights and biases. In this process, the optimality of the ANN architecture is determined through topology augmentation using a genetic algorithm. The configuration parameters considered in the ANN construction consist of hidden layers, neurons unit at each hidden layer, and a set of transfer functions. The proposed study considers three transfer functions: linear, Relu, and nonlinear sigmoid. On the other hand, mean square error (MSE) is considered a fitness function. Since the proposed study has considered MSE, the fitness evaluation is carried out based the less error. Therefore, the inverse roulette selection (IRS) technique is considered for the proportionate fitness selection. The core configuration and training process of ANN construction using topology augmentation is shown in Fig. 6. The topology augmentation begins with the initialization of population (a set of candidate solutions), basically a pool of random neural networks. The process iterates several times, which is also called a generation where the algorithm chooses the optimal ANN based on the fitness value, which is then further cross overed according to the selection/decision process.
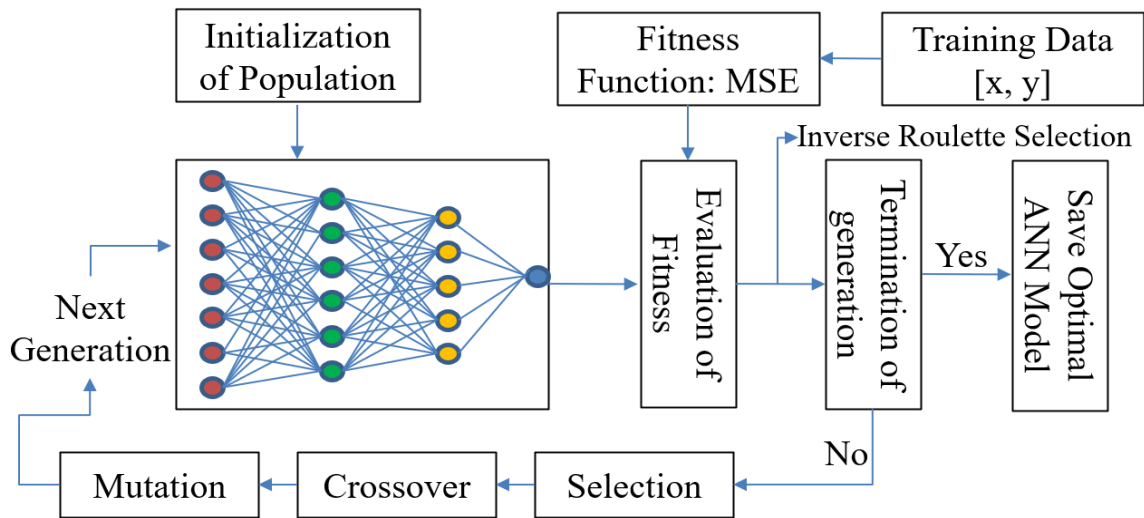

Fig. 6.   Generation of Optimal ANN Model using Neuro-evolution Technique.

Afterward, a new ANN model is generated, and after mutation, an evolved version of the ANN model is further carried out for the training process. All these processes continue until the termination criteria are met. This termination criterion is based on the specified number of generations, wherein each generation, the trained model is evaluated and selected according to the prediction performance. The implementation steps for the above-discussed procedure are mentioned as follows:

Algorithm:1 Neuro evolution training

Step 1. Create population pool

In this step, the population pool is generated, a set of random neural networks with random layers and neurons and random activation functions. Inputs to the algorithm are given in the form of a finite number of layers and neurons and, at the same time, a set of activation functions. The activation functions allowed are, Sigmoid, Linear, and relu.

Step 2. Evaluate fitness of the population

The MSE fitness function measures the fitness of the population. The MSE of the input data is considered with the output in the training set.

Step 3. Select the fittest individual to reproduce

The inverse Russian roulette process selects the individuals for the repopulation pool. The lower the fitness function value, the higher the probability of the selection. The following equation decides the probability of selection.

$$P_i = 1 - \frac{MSE_i}{\sum_{i=1}^{n} MSE_i} \qquad (14)$$

Step 4. Repopulate using copies of the fittest network

Most fit individuals among the population are selected and used for further processing. The crossover of these individuals is made here, and also mutation is applied according to the mutation probability.

Step 5. Introduce normally distributed mutations to the network weights

The neural networks are finalized in this step, and the newly formed networks are introduced to the population pool.

V. RESULT AND PERFORMANCE ANALYSIS

This section discusses the performance metrics followed by outcome analysis to justify the scope and effectiveness of the proposed system.

A. Neuro Evolution Model Parameters

The design and development of the proposed system are done using python programming language and execution on Anaconda. The parameters considered for executing proposed neuroevolutionary technique for obtaining optimal ANN model is mentioned in Table III.

The parameter namely population size is the total number of offspring (networks) present in each generation and total number of generations is number of times the fitness is measured. In 15% of the cases a new neuron is added to the network. In 10% of the cases an existing neuron is deleted from the network. Addition and deletion of neurons happen within a single generation. Either relu, sigmoid or linear

activation functions are chosen. Initial bias is assigned according to the normal distribution. Maximum value of weights and bias are set to 30 however the minimum weight is set to 0 in order avoid negative values. At the same time, minimum bias is set to -5 in order to cancel out certain values.

Mutation probability is 5%. This is necessary to display the stochastic nature of the system. After successful execution of the neuro-evolution training, the proposed algorithm returns optimal ANN model discussed in Table IV.

The architecture of the obtained ANN model is shown in Fig. 7. After evolution through several iteration, the neuro-evolution algorithm provides optimal number of layers and number of neurons unit at each layer as mentioned in Table IV.

TABLE III. NEURO-EVOLUTION HYPERPARAMETERS

Parameters	Values
Population size	200
Number of generations	100
Probability of adding a new neuron	0.15
Probability of deleting a neuron	0.1
Activation function	Sigmoid, Relu, Linear
Initial bias	according to normal distribution
Mutation probability	0.5
Minimum neuron bias	-5
Maximum neuron bias	30
Minimum weight	0
Maximum weight	30
Weight mutation probability	0.5

TABLE IV. CONFIGURATION DESCRIPTION OF OBTAINED OPTIMAL ANN MODEL

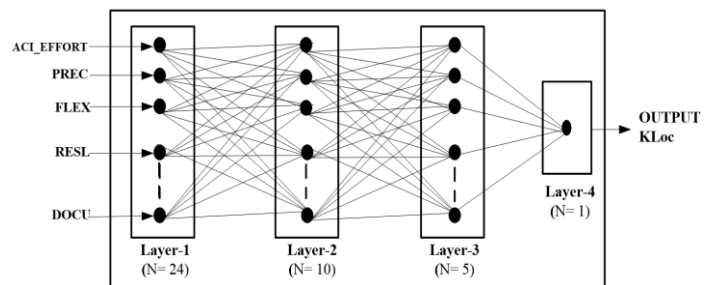| Layer	Number of neurons	Trainable parameters
Layer 1 (input)	24	N/A
Layer 2	10	(24*10) + 10 = 250
Layer 3	5	(10 * 5) + 5 = 55
Layer 4 (output)	1	(5 * 1) + 1 = 7
Loss Function (MSE)	-	-
Activation Function (Relu)	-	-
	Total neurons: 40	Total trainable parameters: 312

Fig. 7. Architecture of Optimal ANN Model.

B. Performance Metrics

1) MMRE (Mean Magnitude of Relative Error): The MMRE performance metric is the most common basis for the assessment of the effort estimation process. The matric MMRE is computed for the given dataset of software projects whose estimated efforts are compared with their actual efforts. The estimation process with minimum MMRE is considered to be the most accurate. The formula for calculating MMRE is given as Eq. 15.

$$\text{MMRE} = \frac{1}{N} \cdot \sum_{i=1}^{n} \frac{\lfloor (y-y\prime) \rfloor}{y} \tag{15}$$

Where, y is the actual effort, and $y\prime$ denotes estimated work effort for project pi, and N is the total project (PI) under consideration. Mathematically, MMRE gives an average percentage of error between y and $y\prime$.

2) MSE (Mean Squared Error): MSE is being calculated in proposed implementations to analyze the performance of proposed methods over other LR and SVR. MSE is more critical function while building better models while optimizing the learning model. The formula for calculating MSE is given as Eq. 16.

$$\text{MSE} = \frac{1}{n} \sum_{i=1}^{n} (y-y\prime)^2 \tag{16}$$

Where y is the actual effort, and $y\prime$ denotes estimated work effort for project pi, and N is the total number of the project under consideration.

3) RMSE (Root Mean Square Error): Since the unit of MSE is squared, RMSE is the square root of MSE used since the unit of MSE is Nl^2 where Nl is the number of lines of code in the project. Though MSE is significant for optimizing the model, it would make no sense to human beings. Hence, the study considers $\text{RMSE} = \sqrt{\text{MSE}}$. Since the unit of RMSE is Nl, it can be assumed that the most probable range for y can be $y = y\prime \pm \text{RMSE}$. The computation of RMSE can be numerically represented as follows in eq. 17:

$$\text{RMSE} = \sqrt{\frac{1}{n} \sum_{i=1}^{n} (y-y\prime)^2} \tag{17}$$

4) MAE (Mean Absolute Error): This is similar to MMRE, representing average absolute error instead of providing average percentage error. In MAE abs function is used to remove the error from simple error, and the average is calculated. Due to this, some of the extreme points, like outliers, will provide less significance; hence this measure is less sensitive to outliers. MAE can be numerically represented as follows in eq. 18:

$$\text{MAE} = \frac{1}{N} \cdot \sum_{i=1}^{n} \lfloor (y-y\prime) \rfloor \tag{18}$$

Since the unit of MAE and output (actual cost) is the same, MAE represents total cost overrun or underrun.

5) Pred: PRED is the de facto standard for cost model accuracy measurement. It is called the percentage of predictions falling within the K% of the actual known value. The formula for PRED calculation is shown in equation 19:

$$\text{PRED} = \frac{1}{n} \sum_{i=1}^{n} \left| \frac{\text{EstimationEffort} - \text{ActualEffort}}{\text{Actual Effort}} \right| K \% \tag{19}$$

Where k% is the percentage error between AE and EE, PRED represents the percentage of a number of projects whose cost overrun or underrun is below 25% in some researches 30%.

C. Outcome Analysis

This section discusses the outcome obtained for the proposed system based on the comparative analysis. The proposed study implements two machine learning algorithms for the comparative analysis such as Linear regression (LR) and supports vector regression (SVR). In order to compare ANN with LR and SVR, the performance metrics MSE, RMSE, and MAE are considered. To justify the scope of the proposed optimal ANN model, the study also considers performance analysis with similar existing approaches such as estimation technique based on fuzzy-genetic [33] and based Dolphin optimization technique [34], Bat optimization [34], and combined Dolphin-BAT [34], the performance metric PRED and MMRE is used. The quantitative outcome obtained for the proposed system and its comparison is shown in Table V.

As it can be observed in Table V, that LR, SVR is associated with 151% and 128% errors, respectively, which means the predicted/estimated value could be more than twice as big as the actual value; therefore, making LR and SVR unfit for real-world implementations. However, even the most basic benchmarked algorithms (GA) are giving 29.9% error which is below 30%, which is an acceptable cost overrun ratio for software projects in general. It is also far below 77%, which is the average cost overrun ratio of the NASA project from which the dataset is collected. The overall numerical outcome shows the proposed ANN's effectiveness regarding the cost overrun ratio. Performance analysis regarding MAE is shown in Table VI.

TABLE V. QUANTITATIVE OBSERVATION IN TERMS OF MMRE

Methods	Performance Metrics
LR	1.510457
SVR	1.281522
GA	0.299469
BAT	0.1698
DOLPHIN	0.1665
DOLPHIN-BAT	0.14576
ANN	0.113518

TABLE VI. QUANTITATIVE OBSERVATION IN TERMS OF MAE

Methods	Performance Metrics
LR	119.266357
SVR	81.872095
ANN	22.151230

The performance metric MAE is used to calculate the performance of proposed methods over other LR and SVR. Since the unit of MAE is in Nl, the MAE value 22.15 obtained for ANN represents a number of lines of codes in the projects that may vary by 22,151 lines in ANN. An average developer writes 250 lines of production code per week (40 hours of working per week). An extra 22151 lines represent 88 weeks of work (3520-man hours). Considering that an average developer in the USA earns approximately $34 per hour, the total cost overrun might come to $119,680. In the cases of LR and SVR, the cost overrun is quite more than ANN, which is impractical for real-time implementation? The performance of the learning models implemented in this study regarding MSE is shown in Table VII.

The metric MSE is being considered in proposed implementations to assess the performance of the proposed ANN over other LR and SVR. MSE represents the overall training of the algorithm as it is used for optimization. Even though the MSE does not directly represent the algorithm's performance, it does represent the quality and level of training given to the algorithm. Lower MSE represents higher knowledge of the algorithm. More trainable parameters can store more knowledge among them. The MSE score is higher in both LR and SVR as they contain fewer trainable parameters than ANN. The quantified outcome indicates that ANN is less associated with error compared to LR and SVR. Therefore, it can be concluded that SVR and LR are subjected issue of underfitting. The performance analysis in terms of RMSE is mentioned in Table VIII.

Similarly, the metric RMSE is considered to evaluate the training performance of the learning models. The RMSE also helps to understand the requirement re-training model by the preprocessing step. From the quantified outcome, the proposed ANN scored 39.33 % RMSE and 22.15% MAE from Table VI, i.e., a difference of 17.18 % compared to mean KLOC of all projects, i.e., 103.44. This indicates minor variation with 16%-17%, which is within the acceptable limit of 20 %. The performance analysis regarding PRED is shown in Table IX.

PRED represents the ratio of projects which has less than a threshold percentage of cost overrun. Hence, this performance measurement is more practical than the other metrics since it represents the number of projects that will fall below the acceptable cost overrun ratio. In most of the studies, the threshold is set to 30%. In this study, 25% of the threshold value is considered to perform comparative analysis. From Table IX, it can be observed that the proposed model ANN achieved a higher PRED value, i.e., 68.91, compared to other ML methods and existing approaches. Bat, Dolphin, hybrid Dolphin-Bat, and the proposed ANN are more practical to implement as they have PRED value much higher than GA. But among them, the proposed ANN method has the highest PRED value, which indicates its suitability and scope in the real-world system. The following analysis mentions the overall improvement (%) of ANN concerning MMRE in Fig. 8 and PRED in Fig. 9 over other implemented ML models and existing approaches.

TABLE VII. QUANTITATIVE OBSERVATION IN TERMS OF MSE

Methods	Performance Metrics
LR	42545.810081
SVR	29240.145478
ANN	1547.247493

TABLE VIII. QUANTITATIVE OBSERVATION IN TERMS OF RMSE

Methods	Performance Metrics
LR	206.266357
SVR	170.997501
ANN	39.335067

TABLE IX. QUANTITATIVE OBSERVATION IN TERMS OF PRED

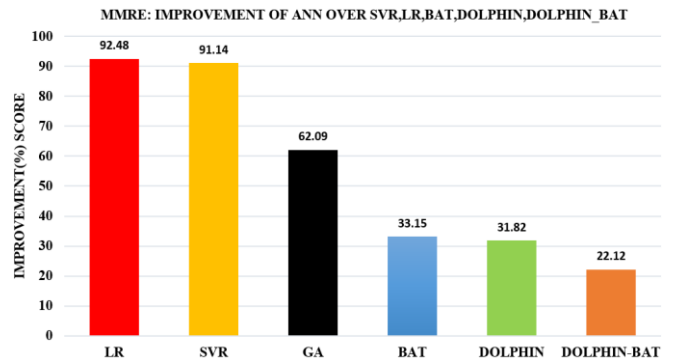| Methods	Performance Metrics
LR	2.335234
SVR	5.297425
GA	11.66
BAT	61.66
DOLPHIN	61.66
DOLPHIN-BAT	66.66
ANN	68.91522

Fig. 8. MMRE Improvement (%) of ANN over SVR, LR and existing Methods.
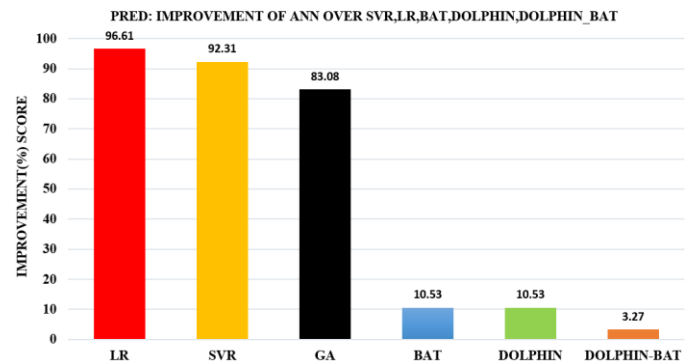

Fig. 9. PRED Improvements (%) of ANN over SVR, LR and Existing Methods.

The analysis from Fig. 8 shows ANN has achieved 92.4% improvement over LR, 91.14% improvement over SVR, and 62.09%, 33.15%, 31.82%, 22.12% over Fuzzy-GA, BAT, Dolphin, and Dolphin-Bat, respectively. The analysis from Fig. 9 shows that ANN has achieved 96.91% improvement over LR, 92.31% improvement over SVR, and 83.08%, 10.53%, 10.53%, 3.27% over Fuzzy-GA, BAT, Dolphin, and Dolphin-Bat, respectively. Hence, it can be seen that the proposed offers a good result regarding software cost estimates. The overall analysis shows effectiveness of the proposed neuro-evolution algorithm towards devising suitable learning model for achieving realistic estimates of the cost required in the initial stage of the software development process. Hence, the proposed research work suggested a technically-efficient method acquainted with recent trends and technologies to benefit real-world applications.

VI. CONCLUSION

The development of software projects involves various phases like initial planning, risk assessment, effort, and cost estimation. Among these, cost estimation is the key concern in the software industry. The conventional approaches do not provide accurate estimation due to the lack of precise system and cost drivers modeling. In this paper, the study has presented a novel and unique approach to predict realistic estimates of the cost needed to develop a software project. The proposed study applied a mechanism of neural evolution in conjunction with evolutionary technique, namely genetic algorithm top construct ANN, which predicts actual estimates of the cost required to develop a software. The application of neural evolution in ANN modeling proves its effectiveness and scope that it can compete with the existing techniques in terms of realistic estimates of the cost and effort. Once developed and trained, the proposed ANN can estimate the development costs in real-time as it computes cost estimates based on the responsible attributes required in the development of the software. The execution complexity grows linearly with the problem context and size of data samples. Based on the result analysis, it is observed that the proposed ANN is producing better results than other previously proposed algorithms and other machine learning models being implemented. The existing works adopted global optimization algorithms that require huge computing resources due to recursive operation in parallel. However, the proposed ANN model is constructed optimally using the mechanism of augmenting topology, and it better adopts generalization of the feature from the input observations, therefore, providing accurate estimates of the cost compared to the existing approaches.

REFERENCES

[1] Alt, R., Leimeister, J.M., Priemuth, T. et al. Software-Defined Business. Bus Inf Syst Eng 62, 609–621 (2020).

[2] Trendowicz, A., 2013. Software Cost Estimation, Benchmarking, and Risk Assessment: The Software Decision-Makers' Guide to Predictable Software Development. Springer Science & Business Media.

[3] Mittas, N. and Angelis, L., 2013, September. Overestimation and underestimation of software cost models: Evaluation by visualization. In 2013 39th Euromicro Conference on Software Engineering and Advanced Applications (pp. 317-324). IEEE.

[4] Khan, B., Khan, W., Arshad, M. and Jan, N., 2020. Software Cost Estimation: Algorithmic and Non-Algorithmic Approaches. International Journal of Data Science and Advanced Analytics (ISSN 2563-4429), 2(2), pp.1-5.

[5] Kaushik, A., Chauhan, A., Mittal, D. and Gupta, S., 2012. COCOMO estimates using neural networks. International Journal of Intelligent Systems and Applications, 4(9), pp.22-28.

[6] Singh, B.K., Tiwari, S., Mishra, K.K. and Punhani, A., 2021. Extended COCOMO: robust and interpretable neuro-fuzzy modelling. International Journal of Computational Vision and Robotics, 11(1), pp.41-65.

[7] Coelho, E. and Basu, A., 2012. Effort estimation in agile software development using story points. International Journal of Applied Information Systems (IJAIS), 3(7).

[8] Bedi, R.P.S. and Singh, A., 2017. Software Cost Estimation using Fuzzy Logic. Indian Journal of Science and Technology, 10, p.3.

[9] Singh, B.K. and Misra, A.K., 2012. Software effort estimation by genetic algorithm tuned parameters of modified constructive cost model for nasa software projects. International Journal of Computer Applications, 59(9).

[10] Nassif, A.B., Azzeh, M., Capretz, L.F. and Ho, D., 2016. Neural network models for software development effort estimation: a comparative study. Neural Computing and Applications, 27(8), pp.2369-2381.

[11] Tayyab M.R., Usman M., Ahmad W. (2018) A Machine Learning Based Model for Software Cost Estimation. In: Bi Y., Kapoor S., Bhatia R. (eds) Proceedings of SAI Intelligent Systems Conference (IntelliSys) 2016. IntelliSys 2016. Lecture Notes in Networks and Systems, vol 16. Springer, Cham.

[12] Sakhrawi, Z., Sellami, A. & Bouassida, N. Software enhancement effort estimation using correlation-based feature selection and stacking ensemble method.

[13] Kumawat P., Sharma N. (2019) Design and Development of Cost Measurement Mechanism for Re-Engineering Project Using Function Point Analysis. In: Kamal R., Henshaw M., Nair P. (eds) International Conference on Advanced Computing Networking and Informatics. Advances in Intelligent Systems and Computing, vol 870. Springer, Singapore.

[14] J. A. Khan, S. U. R. Khan, T. A. Khan and I. U. R. Khan, "An Amplified COCOMO-II Based Cost Estimation Model in Global Software Development Context," in IEEE Access, vol. 9, pp. 88602-88620, 2021.

[15] P. Keil, D. J. Paulish, and R. S. Sangwan, "Cost estimation for global software development," in Proc. Int. Workshop Econ. Driven Softw. Eng. Res. (EDSER), 2006, pp. 7–10.

[16] Menzies T, Brady A, Keung J, Hihn J, Williams S, El-Rawas O, Green P, Boehm B. Learning project management decisions: a case study with case-based reasoning versus data farming. IEEE Transactions on Software Engineering. 2013 Sep 16;39(12):1698-713.

[17] D. Nandal and O. P. Sangwan, "Software cost estimation by optimizing COCOMO model using hybrid BATGSA algorithm," Int. J. Intell. Eng. Syst., vol. 11, no. 4, pp. 250–263, 2018.

[18] A. B. Nassif, M. Azzeh, A. Idri, and A. Abran, "Software development effort estimation using regression fuzzy models," Comput. Intell. Neurosci., vol. 2019, pp. 1–17, Feb. 2019.

[19] Zaidi SA, Katiyar V, Abbas SQ (2017) Development of a framework for software cost estimation: design phase. Int J Tech Res Appl 5(2):68–72.

[20] Reena, Bhatia PK (2017) Application of genetic algorithm in software engineering: a review. Int Refereed J Eng Sci 6(2):63–69.

[21] V. Venkataiah, R. Mohanty, M. Nagaratna, Prediction of software cost estimation using spiking neural networks, in: Smart Intell. Comput. Appl. Smart Innov. Syst. Technol., Springer, Singapore, 2019, pp. 101–112, http: //dx.doi.org/10.1007/978-981-13-1927-3_11.

[22] V. Venkataiah, R. Mohanty, M. Nagaratna, Prediction of software cost estimation using spiking neural networks, Smart Innov. Syst. Technol. 105 (2019) 101–112, http://dx.doi.org/10.1007/978-981-13-1927-3_11.

[23] S. Kumari, S. Pushkar, Cuckoo search based hybrid models for improving the accuracy of software effort estimation, Microsyst. Technol. 24 (2018) 4767–4774, http://dx.doi.org/10.1007/s00542-018-3871-9.

[24] M. Pandey, R. Litoriya, P. Pandey, Validation of existing software effort estimation techniques in context with mobile software applications, Wirel. Pers. Commun. 110 (2020) 1659–1677, http://dx.doi.org/10.1007/s11277-019-06805-0.

[25] S. Goyal, P.K. Bhatia, Feature selection technique for effective software effort estimation using multi-layer perceptrons, Lect. Notes Electr. Eng. 605 (2020) 183–194, http://dx.doi.org/10.1007/978-3-030-30577-2_15.

[26] A.J. Singh, M. Kumar, Comparative analysis on prediction of software effort estimation using machine learning techniques, SSRN Electron. J. (2020) 1–6, http://dx.doi.org/10.2139/ssrn.3565822.

[27] M. Qin, L. Shen, D. Zhang, L. Zhao, Deep learning model for function point based software cost estimation -an industry case study, in: Proc. - 2019 Int. Conf. Intell. Comput. Autom. Syst. ICICAS 2019, 2019, pp. 768–772, http://dx.doi.org/10.1109/ICICAS48597.2019.00165.

[28] V. Resmi, S. Vijayalakshmi, Kernel fuzzy clustering with output layer self-connection recurrent neural networks for software cost estimation, J. Circuits, Syst. Comput. 29 (2019) 1–17, http://dx.doi.org/10.1142/S0218126620500917.

[29] M. Choetkiertikul, H.K. Dam, T. Tran, T. Pham, A. Ghose, T. Menzies, A deep learning model for estimating story points, IEEE Transactions on Software Engineering, 45 (2019), 637–656, http://dx.doi.org/10.1109/TSE.2018.2792473.

[30] Dragicevic, S., Celar, S., & Turic, M. (2017). Bayesian network model for task effort estimation in agile software development. Journal of Systems and Software, 127, 109- 119. DOI: 10.1016/j.jss.2017.01.027.

[31] http://promise.site.uottawa.ca/SERepository/datasets/cocomonasa_v1.arff

[32] Stanley, K.O., Miikkulainen, R., 2002a. Evolving neural networks through augmenting topologies. Evolutionary Computation 10 (2), 99–127.

[33] X Chhabra, S., Singh, H. Optimizing design parameters of fuzzy model based COCOMO using genetic algorithms. Int. j. inf. tecnol. 12, 1259–1269 (2020). https://doi.org/10.1007/s41870-019-00325-7.

[34] A. A. Fadhil, R. G. H. Alsarraj and A. M. Altaie, "Software Cost Estimation Based on Dolphin Algorithm," in IEEE Access, vol. 8, pp. 75279-75287, 2020, doi: 10.1109/ACCESS.2020.2988867.

A Recommendation-Based Contextual Model for Talent Acquisition

[1]Channabasamma A. and [2]Yeresime Suresh

[1]*Department of Computer Science and Engineering, Gokaraju Rangaraju Institute of Engineering and Technology Hyderabad, India*
[2]*Department of Computer Science and Engineering, Ballari Institute of Technology and Management, "Jnana Gangotri" Campus, Ballari, India*

Corresponding Author:
Channabasamma A.
Department of Computer
Science and Engineering,
Gokaraju Rangaraju Institute of
Engineering and Technology
Hyderabad, India
Email: channu.ar@gmail.com

Abstract: It is important to assist the job seekers in selecting the perfect jobs, which suit candidates' current skills and career objectives. Given the job description and resumes in the unstructured form, choosing the best job manually is a tedious task, so there is a need for an automated system to deal with raw data. The extraction of structured information from applicant resumes is needed not only to support the automatic screening of candidates but also to efficiently route candidates to the corresponding occupational categories based on their respective skills. The primary objective of this article is to process and extract relevant information from the unstructured data, like resumes in the form of .pdf, .doc, etc., using natural language processing. This study also proposes machine learning algorithms that exploit user context information to shortlist for the desired job role and also recommends alternative jobs to the candidates. Based on existing skills, new opportunities and possibilities will be introduced, which the candidate wouldn't have explored before. In addition, it also focuses on formalizing the problem of identifying the additional skills, taking into account the employee's existing skills. To exhibit the effectiveness of the proposed algorithms, various resumes have been passed and tried for different formats. The results obtained by the proposed method excel the traditional methods mathematically and practically.

Keywords: Talent Acquisition, Recommender System, Natural Language Processing, Eligible Candidates, Potential Candidates and Latent Candidates

Introduction

People can find jobs online using many websites such as Monster and Indeed.com. These web platforms have been providing services for more than a decade; helping job seekers and organizations by saving a lot of money and time. To automate the workflow, the candidate has to enter long forms about different entities though most of the information is already present in the candidate's resume. Long forms demotivate users and may introduce delay and also there is a tendency of skipping non-mandatory fields even though the information is available.

Traditional approaches to information retrieval may not be appropriate for users. The reason being a greater number of results returned to a job seeker requires a lot of time to analyze options. Usually, many potential resumes may be excluded from the search results or may not be examined due to the complexity of the database and

stringent timelines. However, most people don't identify what is needed until it is shown. People may love a product, a movie, job opening- but may not be known that exists. Further, automatic parsing of resume documents is very challenging as resumes may contain partial sentences or full; may differ in the type of information, and order; conversion from different formats like.pdf, .doc, and .docx to text yields unexpected formats of information (Aluvalu and Jabbar, 2018; Deepa and Rajeswara, 2020).

To automate the recruitment process, the system should be independent of the order and type of information in the documents to parse effectively and efficiently. Taking into account the above-mentioned challenges, the primary objective of this article is to process and extract relevant information from the unstructured data, like resumes in the form of .pdf, .doc, etc., using natural language processing and shortlisting for the desired job role. This study also recommends

alternative jobs to the candidates based on the skills to introduce new opportunities and possibilities, which the candidate wouldn't have explored before. Recommender systems are broadly recognized in several fields to suggest services, products, and information to latent customers (Faqihi *et al.,* 2020; Le *et al.,* 2022; Boorugu and Ramesh, 2020; Ramesh and Madhavi, 2019). A recommendation is an important aspect of an organization's workforce for creating and maintaining the right skilled profiles. Proposed job recommendation is primarily aimed at supporting the discovery of jobs that may interest the user as it automatically returns suitable and prospective jobs.

Literature Survey

The recommendation system is an eminent research area, which includes a lot of applications in the field of e-banking, e-health, and e-commerce (Aggarwal, 2016; Bobadilla *et al.,* 2013; Xavier Amatriain *et al.,* 2011; Shahab, 2019). Especially, in the field of e-recruiting, the role of a recommendation system is imperative (Kantipudi *et al.,* 2021). This section outlines the contributions of various researchers towards matching candidates with respective jobs.

Srivastava *et al*. (2018) focused on algorithms to provide training recommendations in an industrial setup. By keeping a record of the employee's training details and work experience, the authors formalized the problem of the next training recommendation. Past training data has been mined using several unsupervised algorithms to generate the next training recommendations. Though these algorithms beat several recommendation algorithms and also sequence mining algorithms, still there is a scope to enhance these algorithms to predict a sequence of training required for an employee's long-term career (Srivastava *et al.,* 2018).

Kumar *et al*. (2017) designed a method to explore the hiring pattern and intelligence behind it. To accommodate the known intelligence, machine learning methods are applied. This method offered a ranking system based on hiring patterns. Highly trained models were used to predict the ranking and sorting of resumes (Kumar *et al.,* 2017).

Belsare and Deshmukh (2018) presented the employment recommendation system, which uses various recommendation methods. Which are simple matching, collaborative and content-based filtering Belsare and Deshmukh (2018). Personalized recommendations can be generated using both content-based recommendation and collaborative filtering, hence these are more suitable for the job aspirants; however, collaborative filtering suffers from a cold start problem whereas with content-based recommendation too precise results might be created.

The main bottleneck in generating information retrieval systems is to stabilize the available expertise of the text analysis methods and the capability to evaluate the model for quick interpretation. Prokhorov and Safronov (2019) provided an outline of natural language processing and machine learning approaches, which are very much essential to modern information systems to search and filter text documents (Prokhorov and Safronov, 2019; Deepa and Rajeswara, 2017).

Rodriguez and Chavez (2019) identified the required key attributes of profile in the process of job matching. This study implemented a prominent feature selection approach that extracts the most cogent attributes required for job matching.

Conventional recommender systems focused on either finding the best match between a candidate's preferences and the job description(content-based) or finding candidates with the same desires (collaborative filtering) (Ricci *et al.,* 2015; Jalili *et al.,* 2018). However, information regarding the user environment (contextual knowledge) can be used to amend the candidate's initial desires (Adomavicius and Tuzhilin, 2011; Lappas, 2020; Raj *et al.,* 2022). Several candidates prefer jobs closer to their skills, but some candidates seek jobs far beyond their skills. The recommendations for improving their lacking skills will help them in achieving their dream job.

Materials and Methods

This article proposes two algorithms viz, JOB_DJ and JOB_Alternate for shortlisting a resume for the desired job role and alternate job recommendations respectively. It also identifies additional skills required by other candidates; keeping it as side information, the designed method not only improves the procedure of resume shortlisting but also can perform recommendations for new experts or skills.

The Basic Idea

Generally, it can be observed that most of the skills are commonly present in every resume. An individual resume may include special distinct skills which differentiate it from other resumes in the set. The basic idea here is that identification of special skills from each resume will reduce the time required to select an appropriate resume when compared to the time required to look for complete information.

Skill-Based Talent Acquisition

Talent acquisition is an approach to finding specialists for a position that requires a very specific skillset. This article explores the skill section of the candidate's resume and develops a strategy to identify potential resumes with special skills. This approach uses a blend of Natural Language Processing (NLP) and other sub-recommendations to suggest jobs to candidates. In our previous work, using an advanced library of NLP, Spa Cy,

an attempt has been made to capture candidates' special skills required for data scientist job selection (Suresh and Manusha Reddy, 2021). In this article, the work is extended to focus on shortlisting candidates for any desired jobs and generating alternative job recommendations that the candidate is most likely to select or interact with. The dataset includes seven resumes, which are in different formats and layouts.

Organization of Special Skills Knowledge

The main bottleneck is to measure the quality of content in the resume's skills section. This study extends the concept of special skills to develop a technique for selecting appropriate resumes. Each part of the skill information can be organized into "skill_type" and their corresponding "skill_values". For example, 'programming-languages' is a skill_type, and 'Java, Python' is skill_values. From the resume's skills information, two types of skillsets can be extracted using NLP. The first is the Skill-type-Desired Jobst (SDJ) and the second is Skill-type-Alternate Jobs (SAJb).

Approach to Build SDJ and SAJb

The approach to building data frame SDJ includes several steps: First, Information from the documents can be extracted using one of the Python libraries, PyPDF2, it includes extracting the text information, cleaning it, and then exporting it easily readable text files. Next, to program the model to process and analyze such a huge amount of data, NLP is used. The NLP's Spa Cy library has the Matcher tool, which can be used to specify custom rules for phrase matching. The process of the matcher tool involves: First, defining the required patterns, it involves creating a dictionary-1 with the set of skill types required for the desired job role. Next, these patterns are added to the Matcher tool and finally, the Matcher tool parses the resume documents to extract the skill values for the skill types mentioned in the dictionary-1. Once the phrases are found, the count of the respective skill type in the data frame is updated. It is important to assist the job seekers in selecting other alternative jobs, which suit with his/her current skills and career desires. Dictionary-2, skill types required for other alternative jobs are constructed. Considering the dictionary-2, SAJb is constructed; the approach of constructing SAJb is exactly similar to the SDJ.

Organization of Candidates Based on Skills

After extracting the count of skill values to all skill types in the data-sets, the next part of the process is to well organize the candidates' resumes. Based on the count of the skill values, candidates can be categorized into one of the three categories: Eligible candidates, who have perfect skills required for the desired job role. Potential candidates, who have near potential skills. Latent candidates, other candidates who are not skilled enough and may require additional skills.

Setting Skills Threshold Value

The count of skill values of SDJ is compared against the threshold, T_{SDJ} in function JOB_DJ. It helps to cluster the candidates into eligible candidates, potential candidates, and latent candidates. The objective of clustering the candidates is to improve the efficiency of HR analytics in meeting the need for talent acquisition. T_{SDJ} could be chosen effectively by considering the number of skills to eliminate candidates with common skills. The value of the threshold can be increased gradually to analyze the total number of eligible candidates' resumes. If the number of eligible candidates is shown to be decreased, the threshold value can be reduced and monitored. From the experiments, it is noticed that by decreasing the threshold value, the number of candidates with common skills would increase. Another Threshold, T_{SAJb}, is used much similar to T_{SDJ}, to recommend alternative jobs in function JOB_Alternate.

Operation of the JOB_DJ and JOB_Alternate

This article proposes an algorithm JOB_DJ to better serve the latent candidates who miss an opportunity due to the lack of a few required skills. The major goals of the algorithm are: First shortlisting the candidates for the Desired job role. Second, based on existing (near potential) skills, candidates will be recommended for alternative job positions. Third, identifying and providing recommendations to improve their lacking skills to apply for the desired job role.

It takes SDJ as input, the count of each skill type in the SDJ constitutes a major part; which is compared against the threshold, T_{SDJ}. Due to a lack of few 'near potential skills', the candidates shouldn't lose opportunities. With this objective, the JOB_DJ incorporates another function JOB_Alternate. It attempts to identify the skills that potential candidates possess and maps with the skills required for alternative job roles. This function takes SAJb as input. The values of this data frame are compared against another threshold, T_{SAJb} to recommend alternate jobs based on existing skills. Furthermore, the approach is also extended to identify the additional skills required by latent candidates. Thereby recommendations can be generated on these skills to improve profiles. Let *Ci* be an individual candidate and Si be an individual skill type in SDJ/SAJb. The detailed steps involved are shown in JOB_DJ and JOB_Alternate:

```
Sub program function of JOB_Alternate {
for each Cᵢ in SAJb
        Lᵢ = []
        for each Si in SAJb
                count2←SAJb[Cᵢ , Sᵢ ]
                if (count2>T_SAJb)
                        Lᵢ←append si if
```

```
        if (len (L_i>0))
                AltJb←append L_i return
                AltJb /* Holds the list of alternative
                jobs to be recommended for potential
                candidates. */
        else

                Write (No alt job)
Return
}
```

Sub program function of JOB_DJ   {
for each C_i in SDJ
L_i= []   //holds the list of skill types
        for each S_i in SDJ count←
        SDJ [C_i, S_i] if(count<T_{SDJ})
                        L_i←append S_i // identifying
                        lacking skills
        if (len(L_i)==0)
                Write (Shortlisted: Yes) else
                    Write (Shortlisted: No)
                    Write (Feedback: There is a scope to
        improvement in L_i)
                    AltL_i←append C_i /*
                    Holds list of candidates not shortlisted
        for desired job role. Which can be further
        considered for recommending alternate jobs. */
if (ci = = AltL_i) // Not shortlisted and looking for
alternative job positions
        AltJb =JOB_Alternate()
        Write (Recommended for Alternative jobs,
        Altjb)
else
        Write (Not applicable because you are
shortlisted for desired job role: Congratulations)
}

Case Study

To gather insights from industry experts on IT demand, a survey has been made. Survey questionaries include Q1. As per your knowledge, what is the most required factor to be considered for an IT job? Q2. Do you feel the data scientist job is the highest-paid job in the IT industry? Q3. Can you please list out a few other highest-paying jobs? Q4. To what extent do you feel the following skills (Table 1) are most required for the data scientist role, please rate the following: (1: Low, 10: High). As per the survey responses it has been observed that special skills are the most contributing factors to IT jobs and the highest paid job is the data scientist.

A data scientist is a proficient person, who knows how to discover meaningful information from raw data. To become a data scientist, one should possess the right set of skills related to various underlying fields of statistics and computer science. However, the list of skills mentioned in the Table 1 got the highest score from survey responses. Henceforth, to validate the proposed algorithms, this article

focused on extracting the special skills required for the data scientist role (Desired job role) as a case study.

As per industry experts' opinions, besides the data scientist role, many other alternative jobs are also in demand nowadays. So, it is important to assist the job seekers in selecting the perfect jobs, which suit with his/her current skills and career desires. Focusing on a few, for example, software developers, web developers, system engineers, quality assurance engineers, power programmers, etc., dictionary-2 (Table 2) is constructed. It includes a set of skill types required for other alternative jobs (respective skills required for these alternative jobs also gathered from industry experts).

Required sample patterns for data scientist job roles are defined in dictionary-1 and patterns for other alternative jobs are defined in dictionary 2 (Table 1 and 2 respectively). Results of a count of each skill type for the data scientist role are plotted using Matplotlib as shown in Fig. 1. The graph has been plotted by considering the count of skill values against X- the axis and candidates against the Y-axis.

The detailed roadmap of how JOB_DJ and JOB_Alternate are applied to the data scientist job role and other alternative job roles is shown in Fig. 2. It includes several steps, the steps followed are:

1. The knowledge base, Dictionary-1 is created, which includes the special skill set required for the data scientist role (Table 1)
2. Another knowledge base, Dictionary-2 is created, which includes the other alternative job roles and respective skill types required. It can be considered for generating alternative job recommendations (Table 2)
3. Resumes are parsed by Spa Cy, an advanced library of NLP
4. The NLP Spa Cy library has the Matcher tool, which parses the whole resume to match the respective phrases in the Dictionary-1
5. For each of the phrases found in the data frame, the count of the respective skill type in the SDJ will be updated
6. Once the SDJ is built, JOB_DJ is used to match candidates' skills with skill types of data scientist job role by comparing with the threshold, TSDJ
7. If the candidate's skill values meet the threshold value, TSDJ, the candidate is assumed to be eligible and gets shortlisted for the data scientist role. Else it identifies the lacking skills and will be recommended to the candidate so that the candidate can improve
8. Step 3 will be repeated to look for the phrases in the dictionary-2
9. For each of the phrases found, the count of the respective skill type in the SAJb will be updated
10. Once the SAJb is built, JOB_Alternate is used to match candidates' skills with skill types of alternate jobs specified in the dictionary-2

11. If the candidate's skill values meet the threshold value, TSAjb, the candidate is assumed to be potential and alternative jobs will be recommended

12. Else, in addition to this, the model also identifies the other candidates who don't possess the required skills; recommendations can be generated to improve on these skills

Table 1: Dictionary-1: Skill set for SDJ (Data scientist)

Statistics	Machine learning	Deep learning	R language	Python language	NLP	Data engineering
Statistics statistical	Linear regression	Neural network	R	PYTHON	Nlp	Aws
Models	Logistic regression	Keras theano	Ggplot	Flask django	Topic	ec2
Statistical	K means random	Face detection	Shiny	Pandas	Modeling	Amazon
Modeling	Forest	Neural network	Cran dplyr	Numpy	Lda named	Redshift s3
Probability normal	XGBOOST Svm	Convolutional	Tidyr	Scikitlearn	Entity	Docker
Distribution	Naive bayes Pca	Neural network	Lubridate	Sklearn	Recognition	Kubernetes
Poisson	Decision trees	(cnn)	Knitr	Matplotlib	Pos tagging	Scala
Distribution	SVD ensemble	Recurrent		Scipy bokeh	Word2vec	Teradata
Survival models	Models boltzman	Neural		Statsmodel	Word	Google big
Hypothesis testing	Machine	Network (RNN)			Embedding	Query aws
Bayesian inference		Object			Spacy	Lambda aws
Factor analysis		Detextion yolo			Gensim nltk	Emr hive
Forecasting		Gpu cuda			Doc2vec	Hadoop
Markov chain		Tensorflow			Applications	Sql
		ISTM gan			Cbow bag od	
		Opencv			Words skip	
					Gram bert	
					Chat bot	

Table 2: Dictionary-2: Skill set for SDJ (Data scientist)

Software developer	System engineer	Power programmer	Quality assurance engineer	Android developer	Web developer
Machine learning	Assembly language	Scala	IOT	Java	HTML
and artificial	Programming	Akka	Block chain	Android SDk	CSS
Intelligence	Microsoft office	Play	RFID	Android	Analytical
Cloud computing	Oracle	Java/JEE	Artificial	Studio	Skills
Software testing	Java	Spring boot	Intelligence	XML	Back end
Docker and	SQL	Cloud foundry	Ranorex	Kotlin	basics
kubernete	Statistical methods	Docker	Test Plant eggplant	Object-oriented	Javascript
DevOps	GAMP	ReactJS	Robot Framework	oriented	Search
Python	Cisco networking	Angular JS	Watir	fundamentals	Engine
java	C++	Express JS	Unified Functional	SQL	Optimization
C	Algebra	Node.js	Testing (UFT)	Material	Jquery
C++	Computer networks	Mongo DB	Katalon Studio	Design	Graphic
PHP	GxP	Cassandra	Selenium	language	Design
C#	Linux	Hadoop HDFS		Python	Applications
				Node.js	
				.Net	
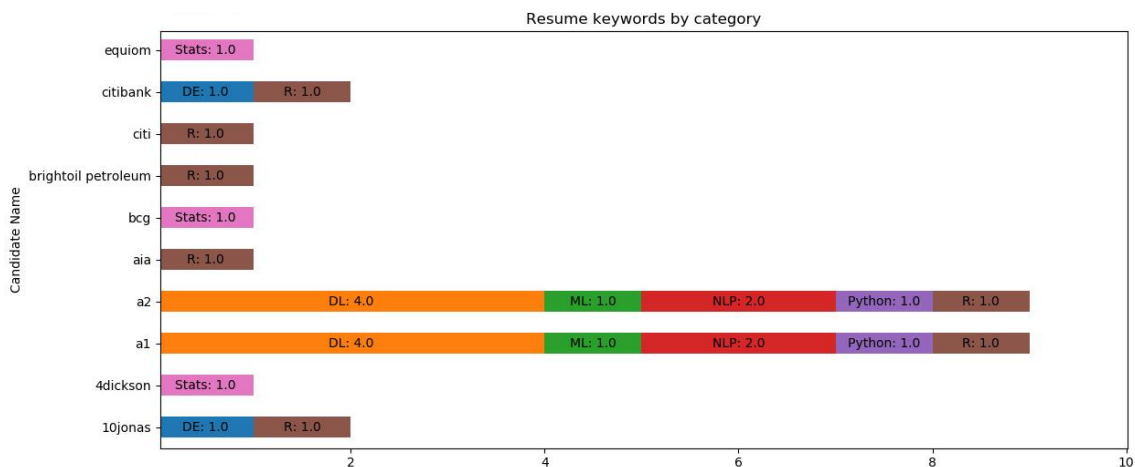
Fig. 1: SDJ (data scientist): The count of skill values for each skill type
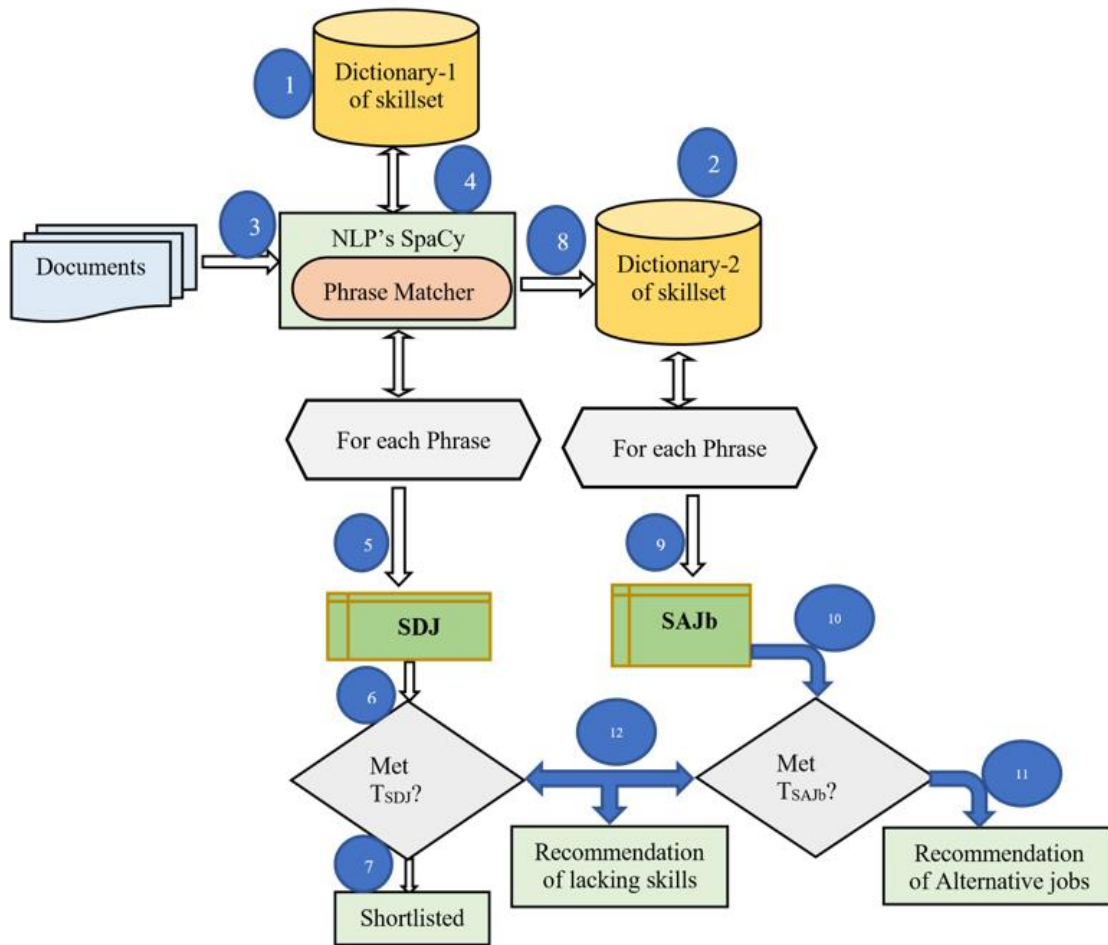
Fig. 2: High-level view of skill selection for resume shortlisting

Results and Discussion

On inputting SDJ and SAJb to JOB_DJ and JOB_Alternate respectively, another data frame (CSV) is obtained; which meets the objectives mentioned in the above algorithms. For effective visualization, Tableau is used by considering this CSV file as input. Tableau is one of the data-visualization tools, used to show the objectives of this study in an effective manner. The respective candidate's status can be viewed in Fig. 3.

In addition to shortlisting the candidates, the model also focuses on:

1. Based on the candidate's existing skills, alternative jobs can be recommended so that the potential candidate shouldn't lose an opportunity (Fig. 4)
2. Another main contribution of this article is to identify and recommend additional skills required by other latent candidates who are not skilled

enough (Fig. 5). This helps candidates in improving their profile to meet career goals

A tree map chart has been used to describe all the candidates' details like their status, feedback, and alternative jobs (Fig. 6) Treemapping is a data visualization technique under Tableau that is used to display hierarchical data.

The primary objective of this article is to shortlist the candidates for the data scientist role. In this article, an objective is to eliminate candidates with common skills, therefore, the Threshold (TSDJ) value is set to two. Among seven input candidate resumes, it can be observed that only one candidate is known to be eligible and shortlisted for the data scientist role; one candidate is known to be potential, alternate jobs can be recommended; and for the other five latent candidates, feedback can be generated to improve upon the skills which candidate doesn't possess. The value of the threshold can be increased gradually to analyze the total number of eligible candidates' resumes.

Table 3: The performance of JOB_DJ and JOB_Alternate

Input TSDJ and TSAJB		Algorithm	TP	FP	TN	FN	Accuracy
7	2	JOB_DJ	2	1	2	2	0.57
	2	JOB_Alternate					
30	2	JOB_DJ	8	7	6	9	0.46
	1	JOB_Alternate					
1096	1	JOB_DJ					
	1	JOB_Alternate	279	153	446	218	0.66

Table 4: The performance of different resume recommendation systems

System #	# Shortlisted resumes	Accuracy
System-1	51	51/67 = 0.761
System-2	53	53/67 = 0.791
System-3	48	48/67 = 0.716
Proposed system (Using JOB_DJ)	56	56/67 = 0.835

Table 5: Comparison of JOB_DJ with traditional systems

Criteria	JOB_DJ	Traditional systems
Unstructured data (.pdf, .jpeg, .doc etc.)	Yes	No
Utilization of existing skills	Yes	Partially
Feedback to improve lacking skills	Yes	No
Alternate job Recommendations	Yes	Yes

Fig. 3: Candidates' status

If the number of eligible candidates is shown to be decreased, the threshold value can be reduced and monitored. It can be noticed that by decreasing the value To exhibit the effectiveness of the proposed algorithms, various numbers of resumes have been passed and tried for a different levels of thresholds. The performance of both JOB_DJ and JOB_Alternate algorithms has been shown in Table 3. The performance of the model is evaluated by comparing the results obtained by JOB_DJ with the results of manual inspection. With the manual verification, it is confirmed that out of 100 candidates, only 67 candidates are having the minimum required skills to be shortlisted. To predict the accuracy, the same set of resumes was given as input to different resume recommendation systems (System-1, System-2, and System-3), and the prediction is recorded in Table 2. Figure 7 shows the graphical representation.

of the threshold, the candidates with common skills would increase. The value of the threshold can be gradually changed as per the requirement of Human Resources.

The performance of the proposed system using JOB_DJ is compared with the results of the most preferable recommender systems in the literature survey. The results obtained by the proposed method excel the traditional methods mathematically and practically (Table 3 to 5).

The article proposes algorithms that can be applied to any of the job roles given the dictionary of skillset for the respective jobs; taking one as the desired one and the other as alternative job roles. It focuses mainly on the extraction of information from resumes. The proposed system parses resumes effectively and efficiently as the system is independent of the order and format of the documents; thereby reducing the burden of entering long forms by the candidate.

Candidate Name	Alternative Job Recommendation
arunkumar	Sorry we didnot find any alternative jobs
elonmusk	Sorry we didnot find any alternative jobs
ganesh	Sorry we didnot find any alternative jobs
jaggu	Sorry we didnot find any alternative jobs
rajesh	['AndDev', 'PP', 'QA', 'SD', 'WebDev']
ramu	Sorry we didnot find any alternative jobs
shiva	Not applicable because your resume is shortlised for Data Science Role

Fig. 4: Recommendations for alternative jobs

Candidate Name	feedback
arunkumar	('There is scope of improvement in', ['DE', 'DL', 'ML', 'NLP', 'Python', 'R', 'Stats'])
elonmusk	('There is scope of improvement in', ['DE', 'DL', 'ML', 'NLP', 'Python', 'R', 'Stats'])
ganesh	('There is scope of improvement in', ['DE', 'DL', 'ML', 'NLP', 'Python', 'R', 'Stats'])
jaggu	('There is scope of improvement in', ['DE', 'DL', 'ML', 'NLP', 'Python', 'R', 'Stats'])
rajesh	('There is scope of improvement in', ['DL', 'ML', 'NLP', 'Python', 'R', 'Stats'])
ramu	('There is scope of improvement in', ['DE', 'DL', 'ML', 'NLP', 'Python', 'R', 'Stats'])
shiva	Your techinical skills are good . Wait for the further updates about interview

Fig. 5: Identifying and recommending required skills

Fig. 6: Visualizing the individual candidate's summary
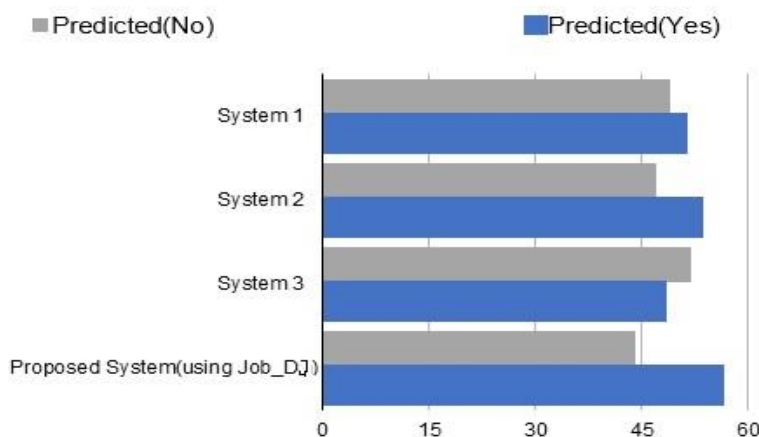
Fig. 7: Performance of different resume recommendation systems

Conclusion

In this study, two algorithms have been proposed with the objective of skill matching with the desired job role and alternate job recommendations by incorporating raw data (.pdf, .doc). Further, it incorporates the feedback to improve the algorithm performance along with identifying the lacking skills as side information. It has been proved that adding user contextual information in the JOB_Alternate algorithm (such as the skills that an employee currently possesses, to recommend alternative jobs) generally improves the prediction accuracy for talent acquisition. The proposed system parses resumes effectively and efficiently as the system is independent of the order and format of the documents; thereby reducing the burden of entering long forms by a candidate. To enhance the accuracy of the system's recommendation results, the shortlisting process can be further enhanced to drill down from the data scientist role to include sub-roles in the future. Further, it focuses on a two-way recommendation system. In this study, an approach was developed by exploring only the skill section to identify potential resumes. Future work can be extended to explore more contextual information about the employee in other sections of the resume.

Acknowledgment

We are thankful to the people who gave us a comments on the work, to the people who participated in data collection and questionnaire distribution.

Author's Contributions

Channabasamma A: Contributed in drafting the article and contributed to conception and design, or acquisition of data, and analysis and interpretation of data.

Yeresime Suresh: Contributed in reviewing it critically for significant intellectual content and gave final approval of the version to be submitted.

Ethics

This article is an original research work. The corresponding author confirms that all of the other authors have read and approved the manuscript and no ethical issues involved.

References

Adomavicius, G., & Tuzhilin, A. (2011). Context-aware recommender systems. In recommender systems handbook (pp. 217-253). Springer, Boston, MA. https://link.springer.com/chapter/10.1007/978-0-387-85820-3_7

Aggarwal, C. C. (2016). "An introduction to recommender systems" in recommender systems, springer Cham Heidelberg New York Dordrecht London. pp, 1-28.

Aluvalu, R., & Jabbar, M. A. (2018). Handling data analytics on unstructured data using MongoDB. doi.org/10.1049/cp.2018.1409

Amatriain, X., Jaimes, A., Oliver, N., & Pujol J. M. (2011). "Data mining methods for recommender systems" in recommender systems handbook, Springer New York Dordrecht Heidelberg London, pp. 39-67.

Belsare, R. G., & Deshmukh, D. V. (2018). Employment recommendation system using matching, Collaborative filtering and content-based recommendation. International Journal Computer Applied Technology Res, 7(6), 215-220.

Bobadilla, J., Ortega, F., Hernando, A., & Gutiérrez, A. (2013). Recommender systems survey. Knowledge-Based Systems, 46, 109-132. doi.org/10.1016/j.knosys.2013.03.012

Boorugu, R., & Ramesh, G. (2020, July). A survey on NLP-based text summarization for summarizing product reviews. In 2020 2nd International Conference on Inventive Research in Computing Applications (ICIRCA) (pp. 352-356). IEEE. doi.org/10.1109/ICIRCA48905.2020.9183355

Deepa, A., & Rajeswara, R. R. (2017). An Eigen character Technique for Offline-Tamil Handwritten Character Recognition. In Proceedings of the First International Conference on Intelligent Computing and Communication (pp. 495-505). Springer, Singapore.

Deepa, A., & Rajeswara, R. R. (2020). A novel nearest interest point classifier for offline Tamil handwritten character recognition. Pattern Analysis and Applications, 23(1), pp, 199-212.

Faqihi, B., Daoudi, N., Hilal, I., & Ajhoun, R. (2020). Pedagogical resources indexation based on ontology in an intelligent recommendation system for content production in a d-learning environment. Journal of Computer Science, 16(7), 936-949. doi.org/10.3844/jcssp.2020.936.949

Jalili, M., Ahmadian, S., Izadi, M., Moradi, P., & Salehi, M. (2018). Evaluating collaborative filtering recommender algorithms: A survey. IEEE Access, 6, 74003-74024. doi.org/10.1109/ACCESS.2018.2883742

Kantipudi, M. V. V., Moses, C. J., Aluvalu, R., & Goud, G. T. (2021). Impact of COVID-19 on Indian Higher Education. Library Philosophy and Practice, 4992, 1-11.

Kumar, A., Pandey, A., & Kaushik, S. (2017, January). Machine learning methods for solving complex ranking and sorting issues in human resourcing. In 2017 IEEE 7th International Advance Computing Conference (IACC) (pp. 43-47). IEEE. doi.org10.1109/IACC.2017.0024.

Lappas, T. (2020). Mining career paths from large resume databases: Evidence from IT professionals. ACM Transactions on Knowledge Discovery from Data (TKDD), 14(3), 1-38. doi.org/10.1145/3379984

Le, Q., Vu, S. & Le, A. (2022). A comparative analysis of various approaches for incorporating contextual information into recommender systems. Journal of Computer Science, 18(3),187-203. doi.org/10.3844/jcssp.2022.187.203

Prokhorov, S., & Safronov, V. (2019, September). Ai for ai: What NLP techniques help researchers find the right articles on NLP. In 2019 International Conference on Artificial Intelligence: Applications and Innovations (IC-AIAI) (pp. 76-765). IEEE. doi.org/10.1109/ICAIAI48757.2019.00023.

Raj, H., Harsh, K., Khattri, P. & Haider, T. U. (2022). "Knowledge-based System of Indian Culture using Ontology with Customized Named Entity Recognition", Journal of Computer Science, 18(3), 172-186. doi.org/10.3844/jcssp.2022.172.186

Ramesh, G., & Madhavi, K. (2019). summarizing product reviews using nlp-based text summarization. International Journal of Scientific and Technology Research.

Ricci, F., Rokach, L., & Shapira, B. (2015). Recommender systems: Introduction and challenges. In recommender systems handbook (pp. 1-34). Springer, Boston, MA. doi.org/10.1007/978-1-4899-7637-6_1

Rodriguez, L. G., & Chavez, E. P. (2019, February). Feature selection for job matching application using profile matching model. In 2019 IEEE 4th International Conference on Computer and Communication Systems (ICCCS) (pp. 263-266). IEEE., doi.org/10.1109/CCOMS.2019.8821682

Shahab, S. (2019). Next Level: A course recommender system based on career interests. https://scholarworks.sjsu.edu/etd_projects/684/

Srivastava, R., Palshikar, G. K., Chaurasia, S., & Dixit, A. (2018). What's next? a recommendation system for industrial training. Data science and engineering, 3(3), 232-247. doi.org/10.1007/s41019-018-0076-2.

Suresh, Y., & Manusha Reddy, A. (2021). A contextual model for information extraction in resume analytics using NLP's spacy. In Inventive Computation and Information Technologies (pp. 395-404). Springer, Singapore. doi.org/10.1007/978-981-33-4305-4_30.

Confirmation For "IMPACT OF DIGITAL SKILLING ON GETTING INDUSTRY-READY" | August 24, 2022

DATAQUEST <chanda@c2cm.com>
Mon 22-Aug-22 9:19 PM

To: Dr. R N Kulkarni <rnkulkarni@bitm.edu.in>

Dear Dr. Kulkarni,

Greetings from Dataquest!

Thank you for registering for the Dataquest x IBM event on **"IMPACT OF DIGITAL SKILLING ON GETTING INDUSTRY-READY" on August 24, 2022.**

It gives us immense pleasure to Confirm your participation for the physical conference on **Wednesday, 24 August 2022** at **Hyatt Hotel Hilton, Bangalore Embassy Golf links, Bangalore**

The details for the itinerary are given below for your reference.

Date: Wednesday, 24 August 2022
Time: 9:30 AM – 3:00 PM
Theme: Impact of Digital Skilling on Getting Industry-Ready
Venue: Hotel Hilton, Bangalore Embassy Golf links
Location: https://bit.ly/3BBoitH

Please Join us for at 10.00 AM for morning tea with snacks.

In case of any queries, you can reach out RSPV: Chanda | email id- chanda@c2cm.com | Mobile No: 97172.11060.

Looking forward to your presence to grace the conference.

Regards
Team Dataquest

Department of Mechanical Engineering
The National Institute of Engineering
(An Autonomous Institute under VTU, Belagavi)
Mysuru-570008

CERTIFICATE

Sponsored by
Ministry of MSME,
Government of India

In association with
Visweswarnya Technological
University, Belagavi

This is to certify that

Mr. Shivaramakrishna A.

Ballari Institute of Technology
& Management

Participated in

Five Days Workshop On

RECENT TRENDS IN AUTOMATION
TECHNOLOGIES FOR MSME DEVELOPMENT

Organized by the Department of Mechanical Engineering

From 30th January to 03rd February 2023
at The National Institute of Engineering, Mysuru

INDUSTRY PARTNERS

HYDAC JANATICS VIDYUT AUTOMATION rexroth A Bosch Company AUTOMATION STUDIO

X:NG

Shri Akadas G
Director, MSME- DFO, Bengaluru

Dr. Shivakumar H R
Regional Director, VTU - RO, Mysuru

Dr. Rohini Nagapadma
Principal, NIE

Department of Mechanical Engineering
The National Institute of Engineering

(An Autonomous Institute under VTU, Belagavi)
Mysuru-570008

CERTIFICATE

This is to certify that

Mr. **Pavankumar B. K.**

Ballari Institute of Technology & Management

Participated in

Five Days Workshop On

RECENT TRENDS IN AUTOMATION TECHNOLOGIES FOR MSME DEVELOPMENT

Organized by the Department of Mechanical Engineering

From 30th January to 03rd February 2023
at The National Institute of Engineering, Mysuru

INDUSTRY PARTNERS

HYDAC   JANATICS Pneumatic   VIDYUT AUTOMATION   rexroth A Bosch Company   AUTOMATION STUDIO

XNG   FLUIDTECHNIK SOLUTIONS
Fluid Power Piping Services & Training

Shri Akadas G
Director, MSME- DFO, Bengaluru

Dr. Shivakumar H R
Regional Director, VTU - RO, Mysuru

Dr. Rohini Nagapadma
Principal, NIE

Department of Mechanical Engineering
The National Institute of Engineering

(An Autonomous Institute under VTU, Belagavi)
Mysuru-570008

Sponsored by
Ministry of MSME,
Government of India

CERTIFICATE

In association with
Visweswaraya Technological
University, Belagavi

This is to certify that

Akkasali Taranath

Ballari Institute of Technology
& Management

Participated in

Five Days Workshop On

RECENT TRENDS IN AUTOMATION TECHNOLOGIES FOR MSME DEVELOPMENT

Organized by the Department of Mechanical Engineering

From 30th January to 03rd February 2023
at The National Institute of Engineering, Mysuru

INDUSTRY PARTNERS

HYDAC   Pneumatic   rexroth
A Bosch Company   AUTOMATION STUDIO

XNG

Shri Akadas G
Director, MSME- DFO, Bengaluru

Dr. Shivakumar H R
Regional Director, VTU - RO, Mysuru

Dr. Rohini Nagapadma
Principal, NIE

Technical Note

Mechanical behavior and fractography analysis of Zn-Sn alloy matrix composites reinforced with nano B₄C particles

Santosh V Janamatti[1,a], Veerabhadrappa Algur[2,b], Madeva Nagaral[3,c], V Auradi[4,d]

[1]Department of Mechanical Engineering, Ballari Institute of Technolog and Management, Ballari, Karnataka, India
[2]Department of Mechanical Engineering, Rao Bahadur Y Mahabaleswarappa Engineering College, Ballari, Karnataka, India
[3]Aircraft Research and Design Centre, HAL, Bengaluru, Karnataka, India
[4]Department of Mechanical Engineering, Siddaganga Institute of Technology, Tumakuru, Karnataka, India

Article Info	Abstract
	The effect of nano-sized B₄C particulates on the Zn85-Sn15 alloy has been investigated. Composites reinforced with B₄C of (0%, 2%, 4% and 6%, by weight) are manufactured by two step stir casting. Microstructural studies carried out by SEM, EDS, and XRD and mechanical testing like tensile, hardness, and impact were performed on cast samples. The criteria for determining strength and fractography are met. EDS analysis confirms the homogeneous distribution of B₄C particles in the Zn-Sn matrix seen in SEM micrographs. XRD examination revealed the B₄C phases in the Zn-Sn alloy matrix as well. When B₄C reinforcement is added to the basic matrix alloy, it improves its hardness and tensile strength with slight decrease in the ductility and impact strength. Further, tensile and impact fractured surfaces were studied to know the different fracture mechanisms.

1. Introduction

Materials are the starting point for determining human age and the ability to meet daily demands. For a long time, people have had access to and used materials. We can understand that human advancements are about human usage and utilization of materials for social beneficial capacities, research, and innovation if we focus on the historical environmental variables of human growth [1].

As a novel material system, metal matrix composites (MMCs) have staked a claim in a wide variety of engineering fields. Domain-specific applications for these materials can be found in a variety of fields, such as transportation, aerospace, and medicine. Increased strength, increased stiffness, resistance to corrosion and wear, superior damping characteristics, a low coefficient of thermal expansion, etc. are just some of the properties that can be combined in metal matrix composites.

It exemplifies humanity's ability to comprehend and alter nature. When a new process for creating material is developed, the benefit will also increase dramatically, and human culture will advance [2, 3]. As a result, materials have evolved into a picture of human progress and have progressed toward being achievements for separating periods of human history. B₄C nanoparticles were supported to Zinc-compound composite using a

liquid metallurgical course, in which the blending strategy was accomplished while pouring the particles to avoid agglomeration of particulates and to achieve a normal homogeneous dispersion of nano particulates in the molten [4, 5].

Copper, zinc, and aluminium alloys are some of the most frequently used materials for bearing applications. These days, copper-zinc alloys and copper-tin alloys are used in a wide variety of commercial industries in place of pure copper. A lot rides on the properties constituents for MMCs to be successfully produced, used, and have their desired properties. Much of the fundamental research in MMCs has focused on the structure and behavior of the interface region. Researchers have created composites of Al, Cu, Zn, and Mg by incorporating SiC, Al_2O_3, B_4C, and graphite particles into the alloys in liquid, semisolid, and powder metallurgical forms (PM).

There are benefits to using a stir casting method, but it is still difficult to create high-quality particulate reinforced MMCs. The true challenges lie in achieving a strong bond between the Cu matrix combination and the reinforcement, limiting or avoiding the interfacial response between the framework compound and the fortification, and increasing the wettability of the fortification in the lattice material. It is common practice to add trace amounts of reactive metals like magnesium, titanium, and the like to copper melt in order to increase its wettability. In addition, wettability can be improved by employing metallic covered fortifications such as graphite, TiO_2, Al_2O_3, and SiC.

In addition, studies using B_4C as reinforcement to synthesize zinc-tin alloy with B_4C composites by liquid melt technique are extremely limited. The microstructure and mechanical properties of the prepared composites of Zn-Sn alloy with boron carbide are then analyzed.

By adding particles in preheated cast iron die by two step method. Prepared samples are machined according to ASTM principles to complete essential tests such as tensile, hardness, wear, and microstructure tests [6]. Because of its remarkable hardness, outstanding strength, high wear and impact strength, B_4C is a more prominent support material [7, 8]. The aim of this work is focusing on a wide scope of utilizations in airplane, vehicle, auto and other designing applications further writing survey uncovers that many works have been done on the utilization of micro-particles as reinforcement to blend copper-micro composites by liquid metallurgy procedure [9, 10]. The expected micro-particles molecule has thickness viable with that of aluminum and copper for all intents and purposes high hardness. Upgraded two phase mix stir cast successions is created for the composite. Delivered Zn-15Sn alloy with 500 nano size B_4C reinforcement composites are then suspended to different analyses to concentrate on mechanical and wear conduct [11, 12].

2. Experimental Details

Composites using a two-stage melt stir strategy with Zinc 85 percent-Tin15 percent wt. (Fig. 1a) were synthesized. Boron carbide particles with 2, 4 and 6 wt. % were used as the reinforcement in the Zn-Sn matrix alloy. For casting, an electric furnace with a power rating of 60 kW and a maximum temperature of 800℃ is used (Fig. 2a). A graphite crucible with the required weight percent of Zn-Sn composite network material in billet shapes was placed inside the heater and kept at a temperature of roughly 450°C. At this temperature, the entire Zn-Sn compound melted, allowing the base combination to dissolve and works out the needed wt. % of B_4C powder [13, 14].

The nano B_4C composites with Zn-Sn alloy matrix with 2% B_4C are made using a liquid metallurgy method and a stir technique. Metal ingots of a specific amount of Zn-Sn alloy are loaded into an electric furnace and heated until they melt. As, zinc-tin alloys melt at

around 419°C, but here, the molten metal has already been superheated to 450°C. Melting and superheating temperatures are recorded using thermocouples calibrated for the appropriate temperature range. Crucibles are filled with solid hexachloroethane (C_2Cl_6) for about three minutes to degas the superheated molten metal. Zirconium ceramic is applied to a steel rotor mounted on a shaft stirrer to agitate the liquid metal. By rotating the stirrer at a speed of about 300 rpm, the molten metal is agitated to the point where a vortex is created. The stirrer is immersed in the molten metal, taking up about 60% of the depth in the crucible. In addition to stirring the molten metal, a small amount of nano B_4C particulates, equal to about 2% by weight of charged zinc-tin alloy, must be heated to about 300°C in a separate heater before being slowly poured into the molten metal vortex. Wetability between the Zn-Sn alloy matrix and the B_4C reinforcement particulates is brought to a point where interfacial shear strength can be established by continuing to stir the mixture for an extended period of time. The nano composites with a Zn-Sn and 2 wt.% B_4C composition are made by pouring a molten metal mixture containing a Zn-Sn alloy matrix and B_4C composites into cast iron moulds of 125 mm length and 15 mm diameter dimensions. Further, Zn-Sn alloy with 4 and 6 wt. % of nano B_4C reinforced composites were synthesized by similar process. Figure 2 (a-b) are showing the stir cast set up and die used to prepare composites.

(a)

(b)

Fig. 1 (a) Zn-Sn matrix (b) Nano B_4C particles

(a)

(b)

Fig. 2 (a) Stir cast set up (b) Cast iron die

3

For the purpose of determining whether or not reinforcing particles are distributed uniformly throughout the Zn-Sn alloy, the cast specimen is then subjected to a scanning electron microscopy (SEM) (TESCAN VEGA 3 LMU, Czech Republic) microstructural investigation. Both Zn-Sn alloy and Zn-Sn reinforced composites containing 2 to 6, wt.% of B_4C are imaged microscopically. The microstructure sample is 15mm in diameter and 5mm in height.

The specimen is machined in accordance with ASTM standard E10 [15] for hardness testing. A Brinell hardness tester (Krystal Industries, Ichalkaranji) is used to get an idea of the material's tensile strength, or how tough it is. The surface of the polished specimen is flawless. The depression is made using a ball indenter with a 5 mm diameter and 250 kg of pressure. Three indentations are made into the surface of the specimen and the results are recorded and counted.

The specimens are machined in accordance with ASTM standard E8 to investigate the tensile behavior of Zn-Sn alloy and Zn-Sn alloy with various percentages of B_4C composites. Testing tensile strength, studying the behavior of ZN-Sn alloy reinforced composites under unidirectional tension, and evaluating the uniform distribution effect are all possible with the help of a computer-measured tensile machine by Instron. This specimen measures 104 mm in total length, 45 mm in gauge length, and 9 mm in gauge diameter. This tensile test is useful for assessing the mechanical properties of composites and as cast alloys. The schematic diagram of tensile test specimen is shown in Fig. 3.
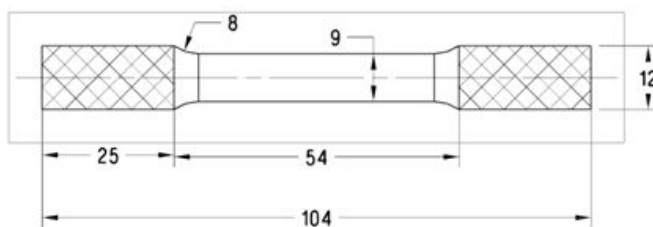
Fig. 3 Schematic diagram of tensile test specimen

Impact test is conducted by using Charpy impact testing machine. The specimen used for the impact test is shown in the Fig. 4. The test is conducted on the Zn-Sn alloy and Zn-Sn alloy with 2, 4 and 6 wt. % of nano B_4C reinforced composites as per ASTM E23 standard.
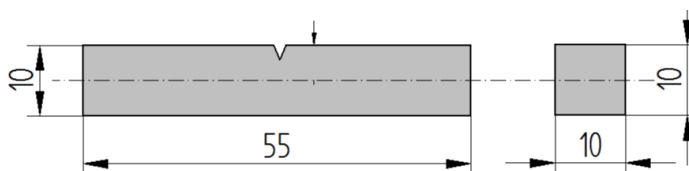
Fig. 4 Schematic diagram of impact test specimen

3. Results and Discussion

3.1. Microstructural Analysis

The microstructure of synthesized composites using as-cast Zn-Sn matrix alloy (Fig.5a), Zn-Sn-2 wt. percent B4C (Fig.5b), Zn-Sn alloy with 4 wt. percent B4C (Fig.5c), and Zn-Sn alloy with 6 wt. percent B4C composites are characterized using SEM (Fig. 5d).
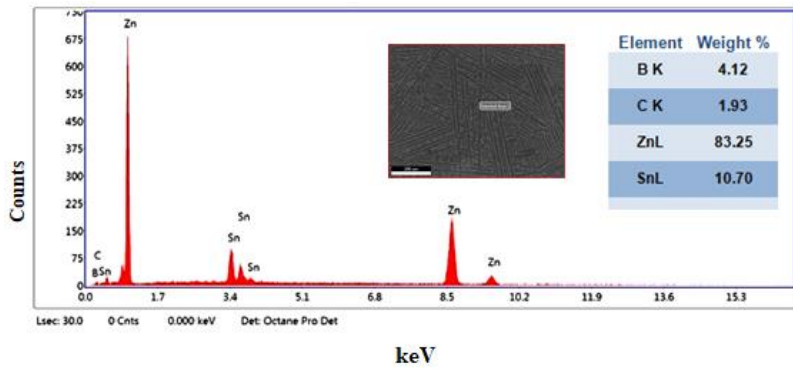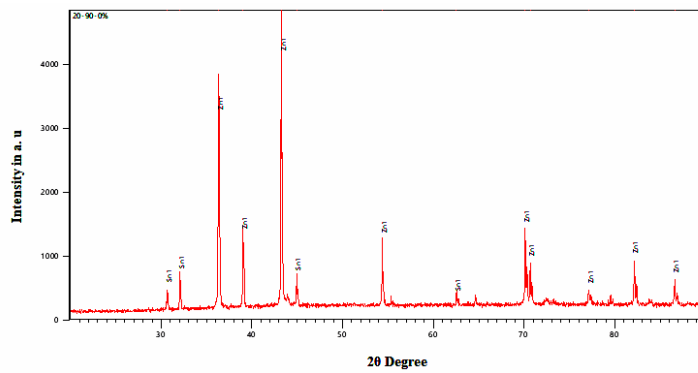
(a)

(b)

(c)

(d)
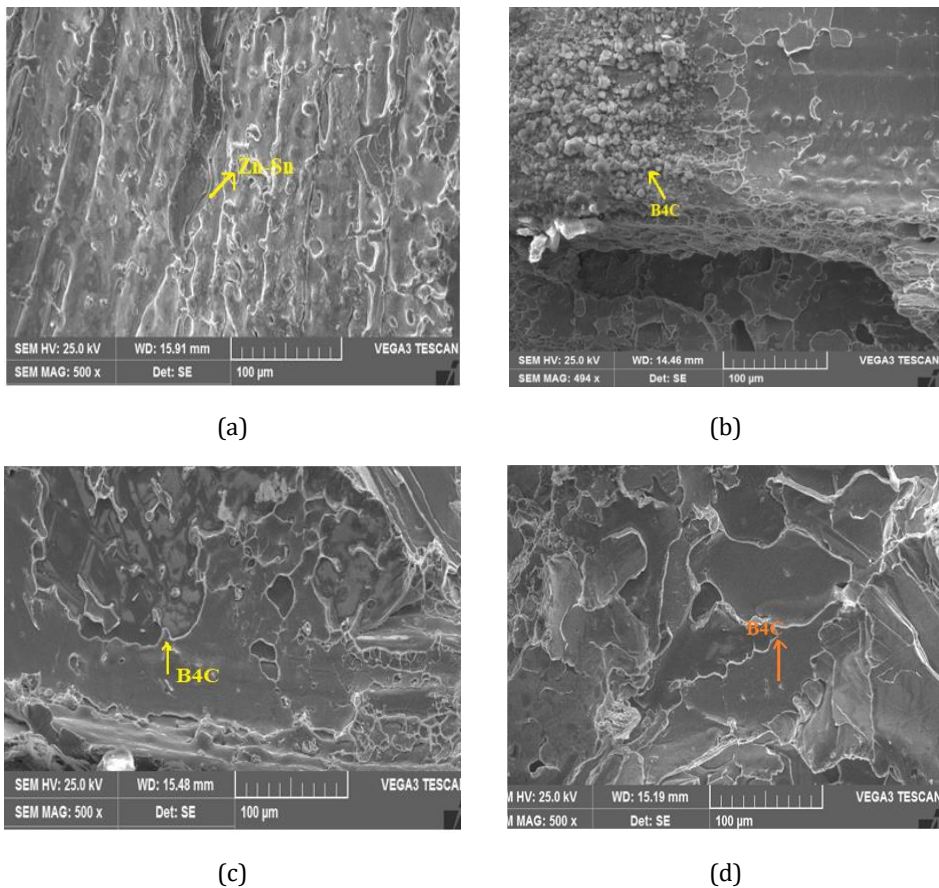
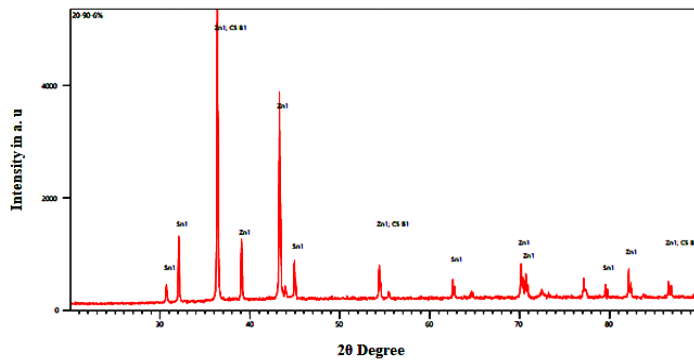Fig. 5 SEM micrographs of (a) as-cast Zn-Sn matrix (b) Zn-Sn alloy matrix with 2 wt.% of B_4C (c) Zn-Sn alloy matrix with 4 wt. % of B_4C (d) Zn-Sn alloy matrix with 6 wt. % of B_4C composites

Fig. 5 (b-d) demonstrates the appropriation of B_4C support particulates in various wt. % of B4C, and it can be seen that the particles were dissolved finely and uniformly with no formation clustering. Furthermore, due to its sophisticated two-stage support blending method, the predicted metal grid composites show remarkably low isolation [16].

Fig. 6(a) represents the EDS of the Zn-Sn matrix whereas Fig. (b-d) can demonstrate the presence of boron particles in the Zn-Sn compound lattice. By displaying B and C materials in EDS testing, this diagram further revealed that boron and carbide components may be found in the Zn –Sn alloy matrix.

Fig. 7 shows an XRD examination of Zn-Sn alloy and Zn-Sn alloy with 6 wt. % B_4C particles (Fig. 7b). XRD investigation confirms the presence of the Sn stage over the Zn network and boron carbide stage in the Zn- Sn matrix.
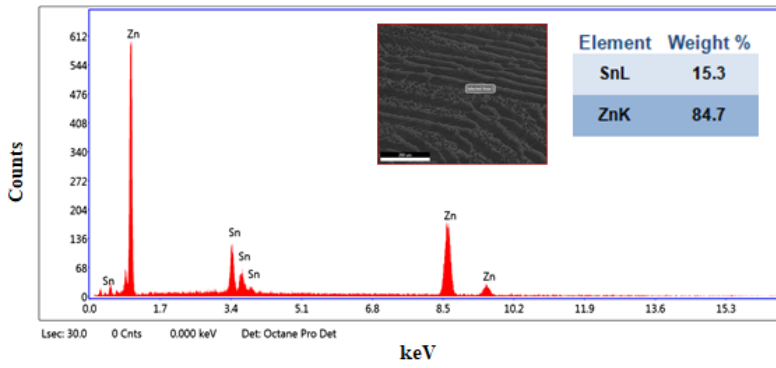
(a)
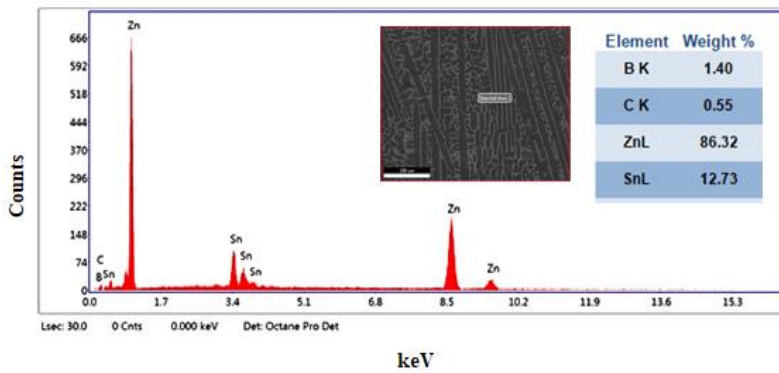
(b)
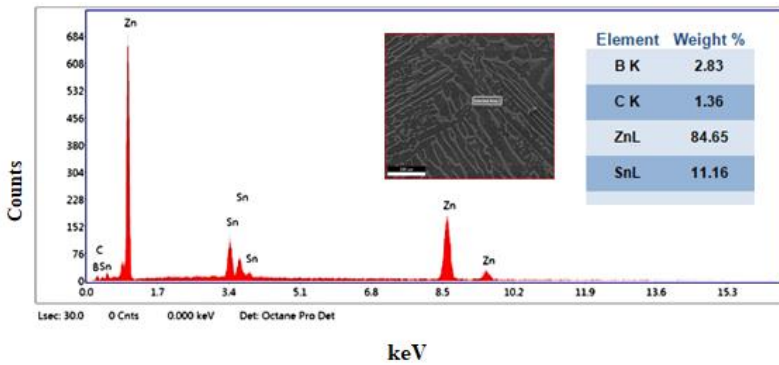
(c)

(d)

Fig. 6 EDS spectrums of (a) as-cast Zn-Sn matrix (b) Zn-Sn alloy matrix with 2 wt.% of B$_4$C (c) Zn-Sn alloy matrix with 4 wt. % of B$_4$C (d) Zn-Sn alloy matrix with 6 wt. % of B$_4$C composites

(a)

(b)

Fig. 7 XRD patterns of (a) as-cast Zn-Sn matrix (b) Zn-Sn alloy matrix with 6 wt. % of B$_4$C composites

3.2. Hardness Measurements

Hardness benefits from a combination of Zn-2, and 6wt. % in the current research. Brinell hardness analyzer has found percent B_4C composites. Fig. 8 shows the hardness of Zn-2, 4& 6, wt% of B_4C composite is higher than Zn basis matrix in terms of percentage [17]. With increasing of B_4C particles, a significant increase in the composite matrix hardness can be detected. The presence of B_4C particles in the framework Zn alloy is the main reason for this. The hardness of the composite material is improved whenever firm reinforcement is consolidated into a delicate base alloy. As can be seen in Figure.8, the Brinell hardness increases as the B_4C particles are increased. The tougher particles are responsible for the increase in hardness [18].

Table 1. Hardness of Zn-Sn alloy and its nano B_4C composites with standard deviation

Material Composition	Hardness (BHN)
Zn-Sn Alloy	82.03 ± 1.50
Zn-Sn – 2 wt. % B_4C	88.53 ± 1.43
Zn-Sn – 4 wt. % B_4C	100.20 ± 1.15
Zn-Sn – 6 wt. % B_4C	115.02 ± 1.16

± - SD (Standard Deviation)
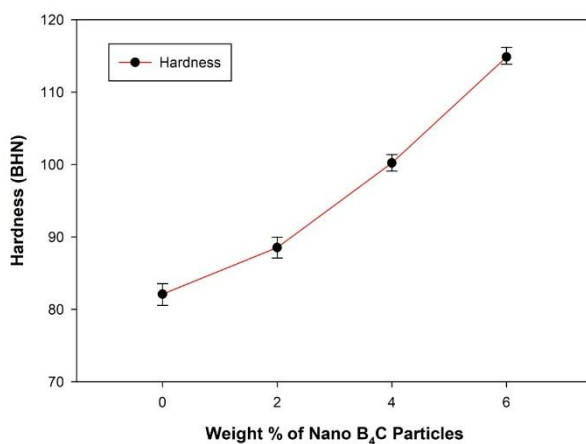
Fig. 8 Hardness of Zn-Sn alloy and its nano B_4C composites

3.3. Tensile Properties

Fig.9 shows the ultimate strength (UTS) and yield strength (YS) for Zn alloy, and 2, 4 and 6 wt. percent B_4C composites. The proximity of hard B_4C particles is credited with the improvement in ultimate and yield strength.

Ultimate and yield strength of as-cast Zn alloy with 2, 4 & 6 wt. % B_4C reinforcement, as illustrated in the Fig. 9. Boron carbide particles enhanced the yield Strength of the base matrix. Zn-Sn combination. In a fine Zn composite base network, ceramic particles are uniformly combined [19]. Many ceramics, such as boron ceramics, will resist external weight in contrast to delicate materials, and as a result, they will not twist plastically successfully, increasing their yield resistance rate.

The tensile properties of these materials might be affected by the consistency of the particle dispersion. It has been demonstrated that these are currently quite homogeneous, so it is anticipated that they will not significantly affect the trends of the

current work. Clusters can cause localized damage that compromises a material's strength and ductility. In this sense, such aggregations may be viewed as pre-loading danger zones. It is important to note that clustering is often more prevalent in composites reinforced with small particulates, despite the fact that these composites appear to have greater strength and ductility than materials containing coarse particles. Any areas of clustering must be kept to a minimum if top performance is desired, and this is especially true for nanoparticle-reinforced composites.

Table 2. Tensile properties of Zn-Sn alloy and its B_4C composites with standard deviation

Material Composition	Ultimate Tensile Strength (MPa)	Yield Strength (MPa)
Zn-Sn Alloy	315.15 ± 1.54	248.37 ± 1.21
Zn-Sn – 2 wt. % B_4C	330.32 ± 1.12	266.86 ± 1.33
Zn-Sn – 4 wt. % B_4C	357.44 ± 1.39	295.09 ± 0.97
Zn-Sn – 6 wt. % B_4C	394.46 ± 0.56	326.03 ± 0.94

± - SD (Standard Deviation)
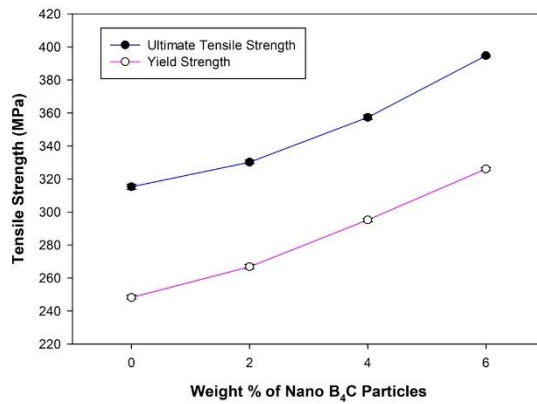
Fig. 9 Ultimate and yield strength of Zn-Sn alloy and its nano B_4C composites
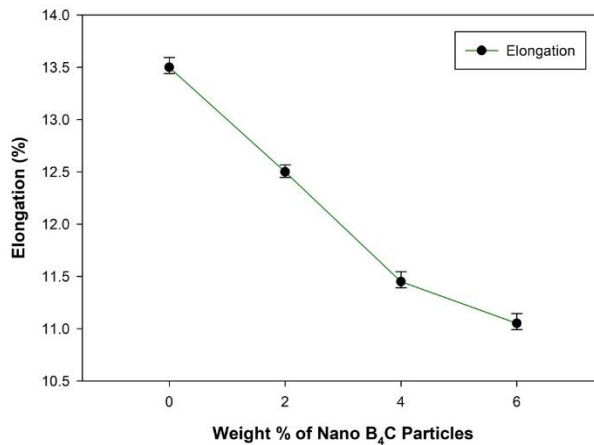
Fig. 10 Elongation of Zn-Sn alloy and its nano B_4C composites

Elongation of as-cast Zn composite with 2, 4 6 wt. % of B$_4$C reinforcement is shown Fig. 10. It was shown that as boron carbide particles increased in base matrix the % of elongation is reduced, as shown in Figure.11. Harder particles are consistently integrated into the Zn-Sn base alloy [20]. Due to two step stir action hard boron carbide particles are distributing uniformly throughout the base solution, hence substitution solid solution was achieved. As results, boron is influencing on delicate base alloy, then base alloy successfully opposes plastically, increasing yield strength rate and diminishes the machinability and % of elongation.

Fig. 11 (a-d) are representing stress-strain graphs of as cast Zn-Sn alloy, Zn-Sn alloy with 2, 4 and 6 wt. % of nano B$_4$C reinforced composites. Boron carbide reinforced Zn-Sn alloy composites exhibited superior load carrying capacity as compared to the as cast Zn-Sn alloy. The ultimate tensile stress of as cast Zn-Sn alloy is 311115 MPa, as weight percentage of B$_4$C particles content increased in the Zn-Sn alloy, the tensile strength incraesed. Zn-Sn alloy with 2, 4 and 6 weight % of boron carbide reinforced composites exhibits 330.32 MPa, 357.44 MPa and 394.46 MPa respectively with reduced strain. The increase in load carrying capacity with addition of B$_4$C is mainly due to the load bearing capacity of hard carbide particles during tensile laoding onditions.
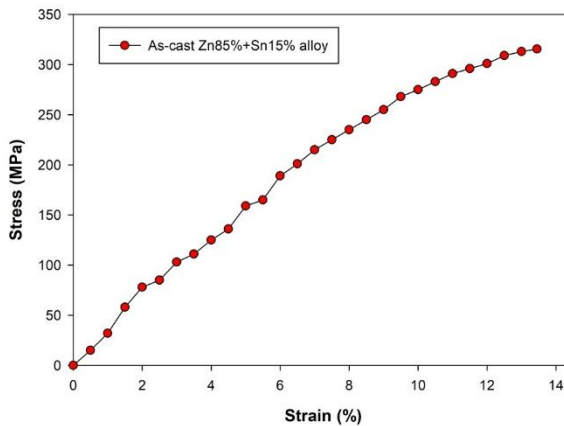
(a)
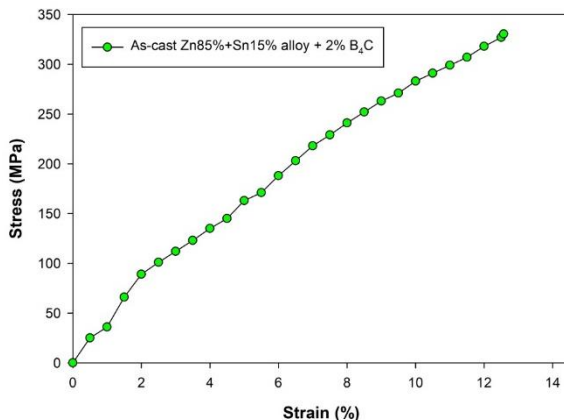
(b)
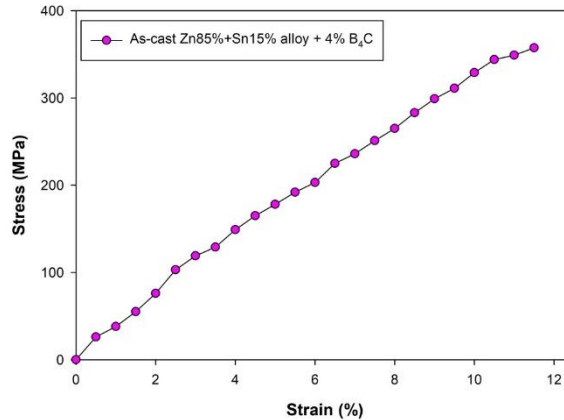
(c)
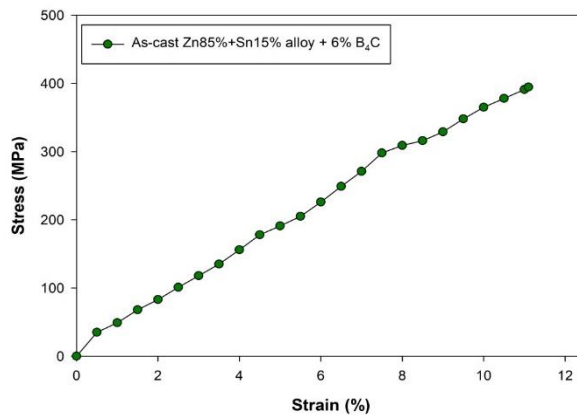
(d)

Fig. 11 Stress-strain graphs of (a) as-cast Zn-Sn matrix (b) Zn-Sn alloy matrix with 2 wt.% of B_4C (c) Zn-Sn alloy matrix with 4 wt. % of B_4C (d) Zn-Sn alloy matrix with 6 wt. % of B_4C composites

3.4. Tensile Fractography

Fig. 12 shows the tensile fractured surfaces of as-cast Zn alloy and Zn-Sn alloy with 6 wt. percent of B4C composites (a-b). The goal of the tensile fracture surfaces research is to see how boron carbide particles alter Zn alloy fracture behavior [21]. The particles were equally distributed throughout the matrix alloy in the current investigation, boosting microhardness, ultimate, and yield strength while lowering ductility. Interfaced cohesion between the Zn –Sn alloy matrix and B4C particles, reinforcement fracture, and matrix failure are all causes of failure in particle-reinforced metal composites [22].

The as-cast Zn alloy's tensile cracked surface in Fig. 12 (a) shows larger and more uniform dimples, indicating malleable fracture. On the cracked surfaces of Zn alloy reinforced with 6 wt .% of B_4C particles (Fig.12b), the size dimples are less than on the as-cast Zn matrix. On the fracture surfaces of composites, electron microscopy revealed particle decohesion with the matrix and reinforcement [23]. The particle fracture is less

11

ductile in the majority of cases, and the surface is smooth and crisp, showing that the particle is broken rather than decreased, implying that high interface strength dominates these composites.
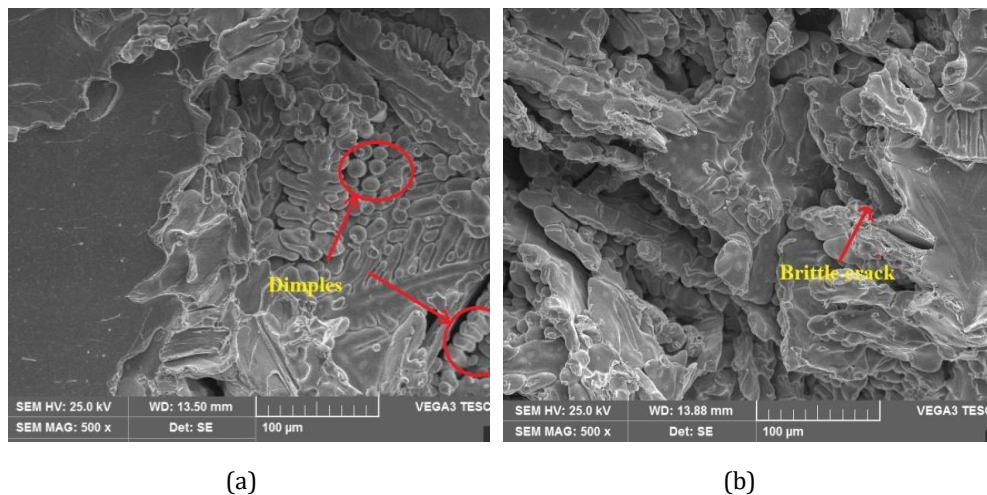

(a)   (b)
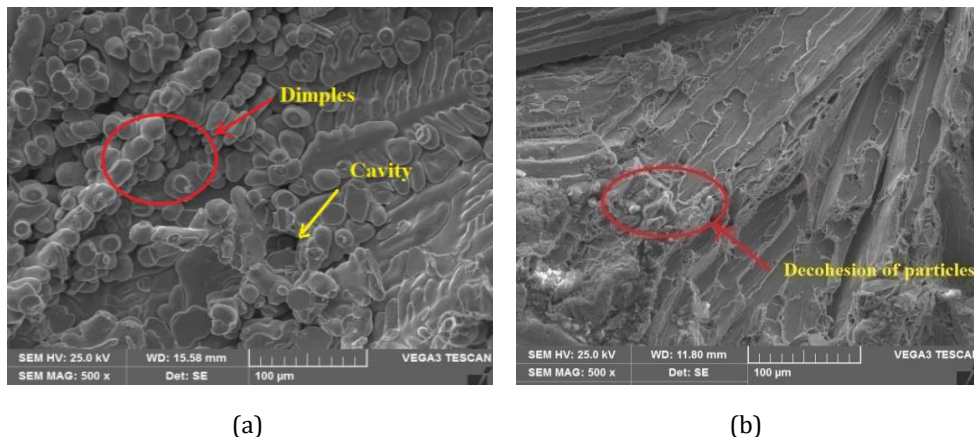
Fig. 12 Tensile fractured surfaces SEM images of (a) as-cast Zn-Sn matrix (b) Zn-Sn alloy matrix with 6 wt. % of B_4C composites

3.5. Impact Strength and Fractography

The impact strength of Zn alloy reinforced metal composites containing 2 to 6 wt.% B_4C particles is shown in Fig 13. The impact strength of Zn alloy as-cast is 3.5 J, but the impact strength of Zn-Sn alloy with 2, 4 and 6 wt.% of B_4C composites are 3.0, 2.49 and 2.0 J respectively with the addition of ceramic particles. Because of the hard particle and matrix contact, composites absorb less energy than as-cast Zn matrix. The creation of a hard interface between the matrix and reinforcement is influenced by load transfer, which is critical for improving composite brittleness [24].
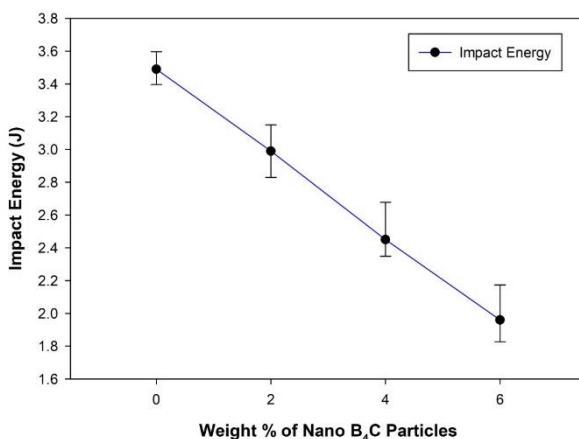
Fig. 13 Impact strength of Zn-Sn alloy and its nano B_4C composites

Impact cracked surfaces of as-cast Zn alloy, Zn-2 wt. per cent, and Zn-6 wt. percent, SEM micrographs Figure 10 depicts B_4C reinforced composites. The Zn-Sn alloy matrix has larger dimples with voids, as shown in Fig. 14 (a), while the matrix alloy tends to have smaller dimples and voids after introducing B_4C particles, as shown in Fig. 14 (b). The

soft matrix was turned into a brittle substance by the inclusion of ceramic particles. The impact strength of the newly developed composites is reduced due to strong interfacial bonding between the Zn matrix and B_4C- particles. The impact strength of the newly generated composites is lowered due to strong interfacial bonding between the Zn matrix and B_4C- particles. Brittle materials absorb fewer loads than soft or ductile materials; however, the impact strength of the newly developed composites is reduced. The fracture surfaces of particles reinforced composites containing 2 and 6 weight per cent particles indicate a sharp brittle fracture mode [25].

(a)   (b)

Fig. 14 Impact fractured surfaces SEM images of (a) as-cast Zn-Sn matrix (b) Zn-Sn alloy matrix with 6 wt. % of B_4C composites

4. Conclusions

A stir casting process was used to make Zn-Sn alloy with 2, 4 and 6 wt. % of B_4C composites. The prepared composites were studied for microstructural characterization by using SEM, EDS and XRD. Scanning electron micrographs were shown the dispersion of boron carbide particles in the Zn-Sn alloy matrix. Further, boron carbide particles in the Zn-Sn alloy matrix were confirmed by the EDS spectrums containing the Boron and Carbon elements, XRD patterns recognized by the Zn, Sn and B_4C phases in the prepared matrix. With the incorporation of nano sized boron carbide particles various mechanical properties like, hardness, ultimate and yield strengths were improved. The percentage improvement in the hardness of Zn-Sn alloy with 6 wt. % of boron carbide particles is 40%. As weight percentage of boron carbide particles were increased to 2 to 6 wt. % in the Zn-Sn alloy, ultimate and yield strengths were improved. Ultimate tensile strength of as-cast Zn-Sn alloy was 315.15 MPa, with 6 wt. % of nano boron carbide particles it was found 394.46 MPa. Addition of hard ceramic particles decreased ductility of Zn-Sn alloy, the lowest ductility was observed in the case of Zn-Sn alloy with 6 wt. % of B_4C particles. Stress-strain patterns of Zn-Sn alloy with boron carbide particles reinforced composites exhibited superior load carrying capacity as compared to the as-cast Zn-Sn alloy. Tensile fractured surfaces of as-cast Zn-Sn alloy indicated the ductile mode of fracture, whereas composites shown brittle fracture. Hard particles addition affected on the impact energy of Zn-Sn alloy, impact strength of Zn-Sn alloy decreased as weight percentage of boron carbide particles increased from 2 to 6 weight percentage in the Zn-Sn alloy. Further, different fracture mechanisms were observed in the case of as-cast Zn-Sn alloy and its

boron carbide reinforced composites. Hence, these Zn-Sn alloys with nano born carbide particles composites can be used for future load bearing applications.

References

[1] Nagesh SN, Siddaraju C, Prakash SV, Ramesh MR. Characterization of brake pads by variation in composition of friction materials. Procedia Materials Science, 2014; 5: 295-302. https://doi.org/10.1016/j.mspro.2014.07.270

[2] Manjunatha SS, Manjaiah M, Basavarajappa S. Analysis of factors influencing dry sliding wear behaviour of laser remelted plasma sprayed mo coating using response surface methodology. Achieves of Metallurgy and Materials, 2018; 63 (1): 217-225. https://doi.org/10.1080/17515831.2017.1407473

[3] Dineshkumar S, Sriram S, Surendran R, Dhinakaran V. Experimental investigation of tensile properties of Ti-6Al-4V alloy at elevated temperature. International Journal of Recent Technology and Engineering, 2019; 8(1):103-107.

[4] Prasad GP, Chittappa HC, Nagaral M, Auradi V. Influence of B4C reinforcement particles with varying sizes on the tensile failure and fractography of LM29 alloy composites. Journal of Failure Analysis and Prevention, 2020; 20(6): 2078-2088. https://doi.org/10.1007/s11668-020-01021-6

[5] Ali Z, Muthuraman V, Rathnakumar P, Gurusamy P, Nagaral M. Studies on mechanical properties of 3 wt.% of 40 and 90 μm size B4C particulates reinforced A356 alloy composites. Materials Today: Proceedings, 2022; 52: 494-499. https://doi.org/10.1016/j.matpr.2021.09.260

[6] Anne G, M. Ramesh MR, Shivananda Nayaka, Arya SB, Sahu S. Microstructure evolution and mechanical and corrosion behavior of accumulative roll bonded Mg-2%Zn/Al-7075 multilayered composite. Journal of Materials Engineering and Performance, 2017;26 (4):1726-1734. https://doi.org/10.1007/s11665-017-2576-z

[7] Kumar HSV, Kempaiah UN, Nagaral M. Impact, tensile and fatigue failure analysis of boron carbide particles reinforced Al-Mg-Si (Al6061) alloy composites. Journal of Failure Analysis and Prevention, 2021; 21: 2177-2189. https://doi.org/10.1007/s11668-021-01265-w

[8] Pathalinga PG, Chittappa HC, Nagaral M, Auradi V. Effect of the reinforcement particle size on the compressive strength and impact toughness of LM29 alloy B4C composites. Structural Integrity and Life, 2019;5 (7):231-236.

[9] Nagaral M, Auradi V, Kori SA, Vijaykumar H. Investigations on mechanical and wear behavior of nano Al2O3 particulates reinforced AA7475 alloy composites. Journal of Mechanical Engineering and Sciences, 2019; 13(1):4623-4635. https://doi.org/10.15282/jmes.13.1.2019.19.0389

[10] Harti J, Prasad TB, Nagaral M, Rao KN. Hardness and tensile behavior of Al2219-TiC metal matrix composites. Journal of Mechanical Engineering and Automation, 2016; 6(5A): 8-12.

[11] Ali Z, Muthuraman V, Rathnakumar P, Gurusamy P, Nagaral M. Investigation on the tribological properties of copper alloy reinforced with Gr/ZrO2 particulates by stir casting route. Materials Today: Proceedings, 2020; 33: 3449-3453. https://doi.org/10.1016/j.matpr.2020.05.351

[12] Balaraj V, Nagaraj K, Nagaral M, Auradi V. Microstructural evolution and mechanical characterization of micro Al2O3 particles reinforced Al6061 alloy metal composites. Materials Today: Proceedings, 2021; 47: 5959-5965. https://doi.org/10.1016/j.matpr.2021.04.500

[13] Krishna Prasad S, Samuel Dayanand, Rajesh , Madeva Nagaral, Auradi V, Rabin Selvaraj. Preparation and Mechanical Characterization of TiC Particles Reinforced Al7075 Alloy Composites, Advances in Materials Science and Engineering, 2022,

Article ID 7105189, https://doi.org/10.1155/2022/7105189. https://doi.org/10.1155/2022/7105189

[14] Nagaral M, Auradi V, Kori SA, Reddappa HN, Jayachandran, Shivaprasad V. Studies on 3 and 9 wt. % of B4C particulates reinforced Al7025 alloy composites. In AIP Conference Proceedings, 2017; 1859, 1: 020019. https://doi.org/10.1063/1.4990172

[15] Nagaral M, Deshapande RG, Auradi V, Satish BP, Samuel D, Anilkumar MR. Mechanical and wear characterization of ceramic boron carbide-reinforced Al2024 alloy metal composites. Journal of Bio-and Tribo-Corrosion, 2021; 7(1):1-12. https://doi.org/10.1007/s40735-020-00454-8

[16] Nagara M, Auradi V, Bharath V. Mechanical characterization and fractography of 100 micron sized silicon carbide particles reinforced Al6061 alloy composites. Metallurgical and Materials Engineering, 2022; 28 (1): 17-32. https://doi.org/10.30544/639

[17] Fazil N, Venkataramana V, Nagaral M, Auradi V. Synthesis and mechanical characterization of micro B4C particulates reinforced AA2124 alloy composites. International Journal of Engineering and Technology UAE, 2018; 7 (2.23): 225-229. https://doi.org/10.14419/ijet.v7i2.23.11954

[18] Marco Z, Carlos ES, Alicia EA. Investigation on Al2O3 reinforced zinc aluminium matrix composites. Procedia Materials Science, 2015;8:424-433. https://doi.org/10.1016/j.mspro.2015.04.093

[19] Jeng J, Xu J, Hua W, Xia L, Deng X, Wang S, Tao P, Ma X, Yao J, Jiang C, Lin L. Wear Performance of the lead free tin bronze matrix composite reinforced by short carbon fibers. Applied Surface Science, 2009;255:6647-6651. https://doi.org/10.1016/j.apsusc.2009.02.063

[20] Ferguson JB, Schultz BF, Rohatgi PK. Zinc alloy ZA-8 shape memory alloy self healing metal matrix composite. Materials Science and Engineering A, 2015;620(3):85-88. https://doi.org/10.1016/j.msea.2014.10.002

[21] Halil BK, Hasan U, Ahmet CT, Okan D, Ahmet A. Influence of sea water on mechanical properties of SiO2-epoxy polymer nanocomposites. Research on Engineering Structures and Materials, 2019;5(2):147-154.

[22] Ahmet CT, Halil BK, Hasan U, Okan D, Ahmet A. Evaluation of low-velocity impact behavior of epoxy nanocomposite laminates modified with SiO2 nanoparticles at cryogenic temperatures. Research on Engineering Structures and Materials, 2019;5(2):115-125.

[23] Mei Z, Zhu YH, Lee WB, Yue TM, Pang GKH. Microstructure investigation of a SiC whisker reinforced eutectoid zinc alloy matrix composite. Composite Part A: Applied Science and Manufacturing, 2006;37(9):1345-1350. https://doi.org/10.1016/j.compositesa.2005.08.011

[24] Wenlong Z, Xiang M, Dongyan D. Aging behavior and tensile response of a SiCw reinforced eutectoid zinc-aluminium-copper alloy matrix composite. Journal of Alloys and Compounds, 2017;727:375-381. https://doi.org/10.1016/j.jallcom.2017.08.130

[25] Uppada RK, Putti SR, Mallarapu GK. Mechanical behavior of fly ash-SiC particles reinforced Al-Zn alloy based metal matrix composites fabricated by stir casting method. Journal of Materials Research and Technology, 2019;8(1):737-744. https://doi.org/10.1016/j.jmrt.2018.06.003

ALL INDIA COUNCIL FOR TECHNICAL EDUCATION

Nelson Mandela Marg, Vasant Kunj, New Delhi – 110 070

AICTE Training and Learning (ATAL) Academy

Certificate

This is certified that **V. Venkata Ramana**, **Professor** of **Ballari Institute of Technology and Management** participated & completed successfully AICTE Training And Learning (ATAL) Academy **Blended/Hybrid** FDP on "**Leadership Excellence**" from **2023-01-02-2023-01-07** to **2023-01-16-2023-01-20** at **DEENBANDHU CHHOTU RAM UNIVERSITY OF SCI AND TECH**.

Advisor-I, ATAL Academy
Mamta Rani Agarwal

Coordinator

ALL INDIA COUNCIL FOR TECHNICAL EDUCATION

Nelson Mandela Marg, Vasant Kunj, New Delhi – 110 070

AICTE Training and Learning (ATAL) Academy

Certificate

This is certified that **Raghavendra Joshi**, **Professor** of **BITM Ballari** participated & completed successfully AICTE Training And Learning (ATAL) Academy **Blended/Hybrid** FDP on "**Leadership Excellence**" from **2023-01-02-2023-01-07** to **2023-01-16-2023-01-20** at **DEENBANDHU CHHOTU RAM UNIVERSITY OF SCI AND TECH** .

Advisor-I, ATAL Academy
Mamta Rani Agarwal

Coordinator

K.L.E. Society's

K.L.E. INSTITUTE OF TECHNOLOGY

(Affiliated to VTU, Belagavi, Approved by AICTE, New Delhi and ISO 21001: 2018 Certified Institute)

(All UG Programmes NBA Accredidated)

Gokul, Hubballi-27

Organized by

Department of Mechanical Engineering

In Association with

School of Mechanical Engineering, KLE Technological University, Hubballi-580031.
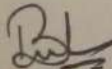
Certificate of Participation
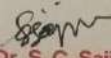
This is to certify that

Mr. RAGHAVENDRA . KARNOOL
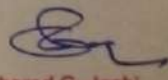
has Attended One Week Faculty Development Programme on

INDUSTRIAL ENTERPRISE APPLICATION MANAGEMENT (PLM & ERP)

held from 21st to 25th November 2022 at KLE Institute of Technology Hubballi.

Dr. Basukumar H. K.	Vinayak N. Kulkarni	Dr. S. C. Sajjan	Dr. Manu T. M.	Dr. Sharad G. Joshi
FDP Co-ordinator	FDP Co-ordinator	Professor, HoD Mech Engg.	Dean (Academic)	Principal

ICFAI

ಕರ್ನಾಟಕ ರಾಜ್ಯ ಮಹಾವಿದ್ಯಾಲಯ ಶಿಕ್ಷಕ ಸಂಘ (ರಿ.)

KARNATAKA RAJYA MAHAVIDYALAYA SHIKSHAK SANGH (R)

A Nationalistic Teachers' Movement...

and

Karnataka Rajya Tantrika Mahavidyalaya Shikshak Sangh

Affiliated to

Akhil Bhartiya Rashtriya Shaikshik Mahasangh, New Delhi

In Collaboration with

Bengaluru City University, Bengaluru

Bengaluru North University, Bengaluru

Organizes

Two Days National Seminar on

BHARAT @75
Unnat Shikshan
Unnat Bharat

CERTIFICATE

This is to Certify that

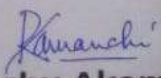Shri / Smt. / Dr. / Prof. ___RAGHAVENDRA KARNOOL___ has

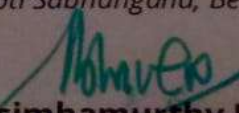participated / presented a article titled _____

_____ in

Two Days National Seminar on

BHARAT 75 Unnat Shikshan Unnat Bharat

held on 7ᵗʰ and 8ᵗʰ September, 2022 @ Jnana Jyoti Sabhangana, Bengaluru (Central College Campus)

Dr. Raghu Akamanchi	Prof. Narasimhamurthy N.	Dr. Sangappa S. B.
President KRMSS	Dean, Faculty of Arts, BCU	Director (Adm & PR), K. S. G. I.
	Seminar Convenor	Seminar Convenor

ಕರ್ನಾಟಕ ರಾಜ್ಯ ಮಹಾವಿದ್ಯಾಲಯ ಶಿಕ್ಷಕ ಸಂಘ (ರಿ.)

KARNATAKA RAJYA MAHAVIDYALAYA SHIKSHAK SANGH (R)

A Nationalistic Teachers' Movement...

and

Karnataka Rajya Tantrika Mahavidyalaya Shikshak Sangh

Affiliated to

Akhil Bhartiya Rashtriya Shaikshik Mahasangh, New Delhi

In Collaboration with

Bengaluru City University, Bengaluru

Bengaluru North University, Bengaluru

Organizes

Two Days National Seminar on

BHARAT @75
Unnat Shikshan
Unnat Bharat

CERTIFICATE

This is to Certify that

Shri / Smt. / Dr. / Prof. ___KALYAN BABU. S.T___ has

participated / presented a article titled _____

_____ in

Two Days National Seminar on

BHARAT @75 Unnat Shikshan Unnat Bharat

held on 7th and 8th September, 2022 @ Jnana Jyoti Sabhangana, Bengaluru (Central College Campus)

Dr. Raghu Akamanchi
President KRMSS

Prof. Narasimhamurthy N.
Dean, Faculty of Arts, BCU
Seminar Convenor

Dr. Sangappa S. B.
Director (Adm & PR), K. S. G. I,
Seminar Convenor

ScienceDirect

Materials Today: Proceedings

Vibrational behaviour and mechanical properties of hybrid polymer matrix composites reinforced with natural fibres: A review

Mayur D. Pawar ✉ , Raghavendra Joshi ✉

Show more ⌄

⟨ Share   " Cite

Abstract

Recent developments in technologies have amplified the practice of non-renewable resources namely natural fibres through manufacture. Composite reinforced with natural fibres toughens in a more symbolic way and extensively related in polymer composite materials. Further, the plant fibres are used widely in polymer composites is due to its little cost and noteworthy properties. The composite reinforced with natural fibres makes lighter compared to synthetic fibres. This yielded the substantial requirement for natural fibre composites in industrialized sector for a secure atmosphere. The proper deployment of composite structures is a critical issue and particularly the vibration is the key factor in the assessment of structural properties. The review focuses on hybrid polymer composite reinforced with various kinds of natural fibres and their associated mechanical properties. Also, it outlines the applications pertaining to vibrational behaviour characteristics.

Introduction

Composites are made from two or more constituent materials by retaining their individual properties. It is a single component at macroscopic level. The beginning of composites was boosted based on requirement to encapsulate different material properties as a single unit. They are widely used in light weight constructions and widely preferred over metals due to high strength to weight ratio. A Composite structure named Sandwich panels called as face sheets comprising of two thin outer laminates are used in the study. Face sheets with a thick light weight core sandwiched in between them. It provided a good compressive and tensile strength, while the core was observed with good shear strength. Sandwich panels can be made a good vibration damper by inserting a visco-elastic core between the face sheets [1].

One of the basic challenges is a vibrational control in structures for design engineers. However, most of the vibration dampers do not have sufficient strength. This can be overcome by incorporating high strength and good damping characteristics of sandwich plates. The good design concepts for sandwich panel are very important in order to have high stiffness, low weight and good damping characteristics. However, the optimization of sandwich panels is not simple as it contains many design variables, objectives and constraints to be satisfied for best suitable panel (K Senthil Kumar et al., 2013). Much research has been carried out on sandwich panels, however the limited study on the same using hybrid polymer cores. Cashew nut shell liquid, a by-product from Cashew nut tree has been used in most of the applications ranging from automotive brake linings to fabrics [2].

Natural fibres such as animal, mineral and plant fibres depends on their source. The majority natural form and common natural fibres are plant fibres. These are labeled into bast fibres, leaf fibres, /seed fibres and grass/reed fibres. Jute, hemp, flax, kenaf and ramie are common types of bast fibres. Some of the leaf fibres are Sisal, pineapple, abaca, and banana fibres. Further, the fruit/seed fibres include coir, kapok, coconut and cotton. Also bamboo, switch grass and Miscanthus are the examples of Grass/reed fibres. These fibres are far and wide used in the fortification of polymer composites. The three main ingredients such as hemicelluloses, cellulose, and lignin are present in numerous water-soluble amalgams except cotton, lignin, cellulose, waxes, hemicelluloses are few other plant fibres. The natural fibres reinforced with composites used by researchers can be referred in Fig. 1.

Section snippets

Sources and properties of natural fibres

Researchers carried out work on composites reinforced with various natural fibres based on application. Also, they were carried out different techniques like characterization after the sample preparation, evaluation of physical, mechanical and other relevant properties to suit the targeted application. Many authors and

researchers found the main use of natural fibers from the polymer composites under the application of reinforcement by the addition of jute and kenaf fibers that takes place for…

Natural fibre reinforcement for composite materials- methods

Natural fibre reinforced polymer composite materials have been noticed exceptional research in almost all engineering appliances due to advantageous possessions such as little compactness, lightweight and biodegradable material in past few decades. H. S. Basavrajet al. [6] discussed the vibrational behaviour by adding sandwich laminate to jute fibre reinforced matrix (CNSL-GP resin) that reflected in damping factors and frequencies using optimum approach. It has been observed that the potential …

Conclusions

An extensive review was done to understand the earlier work carried out by researchers in the area of polymer matrix composites. The features of the composites reinforced with natural fibres could prompt to replace other existing composites in commercial applications as they exhibits low density compared to synthetic glass fibres. The different natural fibres used for the production of polymer matrix composites have been reviewed. The fabrication techniques and testing done with various…

Declaration of Competing Interest

The authors declare that they have no known competing financial interests or personal relationships that could have appeared to influence the work reported in this paper.…

Special issue articles   Recommended articles

References (22)

P.C. Jena
Mater. Today Proc. (2018)

M. Rajesh *et al.*
Procedia Eng. (2016)

K. Senthil Kumar *et al.*
Mater. Des. (2014)

A. Bhattacharjee *et al.*
Compos. Struct. (2020)

P. Vignesh *et al.*
Mater. Today Proc. (2018)

S. Vigneshwaran
J. Clean. Prod. (2020)

K. Ramesh Babu *et al.*
Mater. Today Proc. (2020)

M.C. Seghini
Int. J. Fatigue (2020)

M. Balachandar *et al.*
Mater. Today Proc. (2019)

G. Navaneethakrishnan
Mater. Today Proc. (2020)

⌄ View more references

Cited by (3)

Combining the pineapple leaf fibre (PALF) and industrial ramie fibre to the epoxy matrix for high-strength light weight medium-density fibreboards ↗
2023, Biomass Conversion and Biorefinery

Hybrid polymer matrix development using cashew nut shell liquid as an additive into epoxy resin ↗

2023, Journal of the Chinese Institute of Engineers, Transactions of the Chinese Institute of Engineers,Series A

Physical, Mechanical and Perforation Resistance of Natural-Synthetic Fiber Interply Laminate Hybrid Composites ↗

2022, Polymers

View full text

ELSEVIER

RELX™

Taylor & Francis
Taylor & Francis Group

RESEARCH ARTICLE

Check for updates

Synthesis of Fe_3O_4–aluminium matrix composites: mechanical and corrosion characteristics

Shivaramakrishna A[a], Yadavalli Basavaraj[a] and Raghavendra Subramanya [b]

[a]Department of Mechanical Engineering, Ballari Institute of Technology and Management, Ballari, India; [b]Department of Mechanical Engineering, Sai Vidya Institute of Technology, Bangalore, India

ABSTRACT

The aim of this study is to investigate at the mechanical characteristics of Fe_3O_4 particle reinforced with 7075 aluminium alloy composite. The composites of different weight percentage 2%, 4%, 6%, and 8% of Fe_3O_4 reinforcement were prepared using stir casting technique. Prepared composite samples were examined for mechanical properties like tensile percentage elongation and hardness test along with scanning electron microscopy. Additionally, corrosion was also conducted on the prepared samples. The results of mechanical properties reveal that improvement in hardness and tensile strength and corrosion resistance values with different weight percentage combinations. When compared to the original Al7075 alloy, the Ultimate Tensile Strength is highest at a value of 64.563% for 8% Fe_3O_4 reinforcement, and variation in Ultimate Tensile Strength is highest at a value of 21.865% for an increase in reinforcement percentage from 4% to 6% weight, according to the experimental studies. .

1. Introduction

There is now a lot of interest in particle-reinforced metal-matrix composites, particularly those based on existing aluminium alloys. This is due to the fact that the addition of ceramic particles to aluminium alloys can increase mechanical and tribological characteristics [1]. Current technology advancement in aerospace, automotive, marine, construction and ease industries has made the demand for materials having high strength-to-weight ratio, good corrosion resistance and good thermal conductivity to be on the increase [2]. In the literature [3,4] studies reveal that the increase in reinforcement particles in matrix-metal results in the increase of mechanical properties like hardness, tensile strength, impact strength, etc. Al-Fe alloys are attractive for applications at temperatures beyond those normally associated with conventional Al alloys because of the stability of Fe in Al. In addition, alloying Al with Fe increases its high-temperature strength due to the dispersion of second-phase particles [5]. Compared to solid-phase processing, the liquid-phase processing methods are attractive as they are economical and also capable to produce large structural components with complex geometry. However, a major challenge in the liquid-phase processing is to achieve uniform distribution of reinforcement and to obtain strong interfacial bonding between the reinforcement and the matrix [6]. The development of $Al_{13}Fe_4$ composite provides higher hardness and

improved tensile strength with much loss of ductility as compared to base alloy. Both composite and base alloy exhibit ductile mode of facture [7].

Due to its low cost and greater free energy thermite reaction with aluminium, magnetite (Fe_3O_4) is also good filler. This reaction can increase the wettability of magnetite and aluminium matrix while also providing more energy for the operation. It is also a highly regarded filler material due to its outstanding magnetic characteristics.

Additionally, corrosion behaviour is an important factor to consider when using composites as structural materials. Reinforcing particles may interact with the matrix chemically, mechanically, or electrochemically, speeding up corrosion.

Furthermore, galvanic interactions between the matrix and reinforcement might accelerate corrosion. Several corrosion experiments of Al matrix composites were carried out in order to determine their corrosion susceptibility in NaCl. Different research studies have revealed that increasing the SiC volume and optimising the quantity of SiC improved the AMC's corrosion resistance [8–10].

The presence of reinforcements sometimes restricts the continuity of the aluminium alloy and the surface oxide coating primarily to the formation of galvanic couples at the boundary/interface between the aluminium substrate and the reinforcing material precipitates. This increases the number of potential places for electrochemical process [11].

CONTACT Raghavendra Subramanya ✉ rvs.sdly@gmail.com 🏛 Department of Mechanical Engineering, Sai Vidya Institute of Technology, Bangalore, Karnataka, India

Taylor & Francis
Taylor & Francis Group

Check for updates

Tensile hardness and wear properties of iron oxide (Fe$_3$O$_4$) reinforced aluminium 7075 metal matrix composites

Shivaramakrishna a[a], Raghavendra Subramanya [b] and Yadavalli Basavaraj[a]

[a]Department of Mechanical Engineering, Ballari Institute of Technology and Management, Ballari, India; [b]Department of Mechanical Engineering, Sai Vidya Institute of Technology, Bangalore, India

ABSTRACT

The Al-7075 aluminium alloy has been proposed for widespread use in automotive applications. This material has been researched in composite structures with various reinforcements in order to improve its usage. In this study, Fe$_3$O$_4$ (magnetite) is reinforced in an Al-7075 matrix to create a metal matrix composite by a stir casting process. Aside from the Neat Matrix samples, five samples were produced by adding Fe$_3$O$_4$ to Al 7075 matrix in various weight proportions such as 2, 4, 6, 8, and 10. The mechanical properties of the fabricated composite specimens were determined by different tests, including hardness, tensile, compression, and wear strength. The results were compared to a standard matrix alloy. In addition, SEM with EDAX studies was performed to examine the dispersion of the reinforced particles in the chosen matrix alloy. The homogeneous distribution of Fe$_3$O$_4$ particles in composites was observed to be intragranular in origin. Furthermore, Fe$_3$O$_4$ particles were found to be well attached to the matrix alloy, with a clean interface. The composite's hardness and tensile strength along with wear resistance were also found to increase as the Fe$_3$O$_4$ concentration increased.

1. Introduction

Aluminium is very attractive due to its low density, high thermal conductivity, and environmental resistance; however, it has a high thermal expansion coefficient and low mechanical strength.

Al-7075 has quite a broad range of uses, therefore it requires further reinforcing. The aluminium alloy is utilised as a matrix material and is reinforced with single and multiple reinforcement particles such as SiC, Al$_2$O$_3$, Gr, TiO$_2$, B$_4$C, fly ash, and other materials to create composites with better strength than the basic alloy material.

The potential of MMCs to significantly alter characteristics (thermal expansion, density), mechanical properties (tensile and compressive behaviour), tribological properties, and other qualities by changing constituent or filler material phase has recently attracted researchers' attention [1].

Contents lists available at ScienceDirect

Materials Today: Proceedings
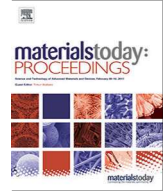
Investigation on mechanical properties of Al7075 based MMC reinforced with Fe_3O_4

Kurubara Raghavendra [a], A. Shivaramakrishna [b], Yadavalli Basavaraj [c], MJ. Sandeep [d], BK. Pavan Kumar [b]

[a] Ballari Institute of Technology and Management, Allipura, Ballari 583104, India
[b] Ballari Institute of Technology and Management, Allipura, Ballari 583104, India
[c] Principal, Ballari Institute of Technology and Management, Allipura, Ballari 583104, India
[d] Dayananda Sagar University, Kudlugate, Bengaluru 560078, India

ARTICLE INFO

ABSTRACT

This work primarily focuses on Metal Matrix Composites due to their immense usage in the engineering industry. Metal Matrix Composites (MMCs) hold considerably improved mechanical properties with huge sort of applications from automotive to aerospace. In this investigation, aluminum (Al7075) as matrix and 3%, 6%, and 9% weight proportions of iron oxide (Fe_3O_4) as reinforced Metal Matrix Composite are prepared by the help of the stir-casting method. The stir casting process is adopted due to its rewards like easy manufacturing, low manufacturing cost, and uniform distribution of reinforced particles. The reinforcing particle Fe_3O_4 takes part in a significant function in the engineering material properties. The investigation reveal enhance in mechanical properties like Tensile, Compression and Hardness Strengths. When juxtapose with primordial Al7075 alloy, the tensile strength is recorded highest as 362 MPa and Yield strength as 262 MPa for 9% wt. reinforced Fe_3O_4. Also, micro structural studies (SEM & EDS) were done on the newly fabricated Al7075-Fe_3O_4 Metal Matrix Composite which conveys uniform distribution of Fe_3O_4 reinforced particle.

Copyright © 2022 Elsevier Ltd. All rights reserved.
Selection and peer-review under responsibility of the scientific committee of 2022 International Conference on Recent Advances in Engineering Materials.

1. Introduction

Al7075 is a precipitation hardened alloy, with specific strength and specific stiffness, good fracture toughness and corrosion resistance, and excellent molding performance, belonging to super-high strength deformation Al alloy [1–4]. It is one of the crucial structural materials in aerospace and automotive industry, whose properties are unnatural by metal compound particles, solid solution particles, gain structure and dislocation [5–6]. Compared to Solid processing technique, the liquid processing technique are attractive as they are more economical and can produce complex geometrical components. Though, a major challenge in the liquid technique is to attain even distribution of reinforcement and to gain tough interfacial bonding between the reinforcement and the matrix [7]. The improvement of $Al_{13}Fe_4$ Metal Matrix composite enhances elevated hardness and tensile strength with loss of ductility as compared to the base alloy and shows ductile mode of facture [8].

Limited work has been reported in studying the Mechanical characterization of Fe_3O_4 reinforced with Al7075 matrix composite. For the present experimental study, the proposed Metal Matrix Composite is fabricated by stir casting method in an electric melting furnace.

The aim of the proposed work is to fabricated an Al7075 Metal Matrix Composite reinforced with Fe_3O_4 (weight proportions) in order to determine the optimized weight quantity of Fe_3O_4. The composite's Tensile, compression, Hardness strengths and micro structural characteristic were tabulated and shown.

2. Materials and methods

The Al7075 alloy used as a base-metal in the study for the fabrication of composite that has been reinforced with a different weight proportions of Fe_3O_4 (3%,6% and 9% wt).

The chemical composition of aluminum is shown in Table1. Fe_3O_4 300Mesh particle sizes were chosen.

The Stir casting method was employed to fabricate the Aluminum metal matrix composite. Fig. 1 shows the casting setup and the stirrer fixed to variable speed motor[8]. Fig. 2 illustrates the fabrication process flowchart.

A Neural Network Model based Approach for Critical Rotating Machine using MATLAB

Pavan Kumar B K[1], Dr.Yadavalli Basavaraj[2]

[1]Asst.prof, [2]Principal, Mechanical Department, Ballari Institute of Technology and Management, Ballari, Karnataka, India

Abstract: Rotating machines are commonly employed in a wide range of industrial applications. To minimise failures, boost dependability, and reduce maintenance costs, condition-based maintenance must be implemented for spinning machinery. It is very critical to identify the fault and predict the life of any machines. Henceforth, present study is focused on reliability of machines using neural network by the aid of statistical tool named MATLAB which ensures the proper validation which has 99% accuracy for the obtained data.

1. Introduction

In the modern era, industries have well equipped facilities to maintain the machines in stable condition. Machines operating at higher speeds starts to fail, if it's not maintained regularly that in turn affects the health of machines leading to major disaster in industries. Henceforth it is necessary to suggest the optimum solution by framework predictive maintenance approach to enhance the life of rotating machines (1). Nowadays industrial maintenance is focused only on alarm indications and expertise reviews. The hazards of motor rotating at higher rpm leads to failure of machines if properly not maintained regularly also leading to major economic losses (2).

2. Problem Identification

In a steel manufacturing industry, products of various cross sections are to be produced. One of the issues with fault classification is the high dimensionality of rotating equipment. Many factors, including as load, saturation, unexpected operating conditions, electrical noise, and temperature, may all impact the fault identification process. So, its much essential for maintaining the accuracy level for validation using the statistical tool.

3. Standard measurements for Critical Rotating Machine

The predictive maintenance or condition monitoring is among the planning maintenance part of other maintenances such as a preventive and production maintenances and it involves the trending and analysis of the machinery performance parameters to detect and identify developing problems before a catastrophic failure can occur. The motor drive end of the machine was found to be in critical condition which are above 7.1mm/s at 60Hz and 1550rpm and to be followed according to vibration severity chart. The vibration program for maintenance of rotating machines is based on factors like plant survey, machine condition, measurement points and instrumentation selections, time period, tolerance etc.,

Figure 1: ISO 10816-3 Industrial machines with nominal power and speeds between 120 r/min and 15000 r/min

The ISO 10816-3 Vibration Severity Chart as shown in above figure.1 is divided into three zones, the zone A (green) for vibration values from new machines, zone B (yellow) for machines without restriction and zone C (red)for machines in which the damage could occur any time.

Table 1: Motor Drive End representing Frequency and speed versus different Velocities such as V-H(Horizontal), V-V(vertical), V-A(Axial)

MOTOR – DRIVE END (DE)					
SL NO	Frequency		Velocity		
	X in Hz	RPM	V-H	V-V	V-A
1	20	1450	0.02	0.01	0.01
2	40	1500	0.02	0.01	0.02
3	60	1550	7.91	8.15	7.78
4	80	1600	0.06	0.05	0.03
5	100	1650	0.35	0.16	0.19
6	120	1700	0.01	0.03	0.03
7	140	1750	0.01	0.04	0.05
8	160	1800	0.02	0.05	0.03
9	180	1850	0.01	0.09	0.04
10	200	1900	0.01	0.04	0.02
11	220	1950	0.02	0.01	0.02
12	240	2000	0.01	0.01	0.01
13	260	2050	0.01	0.01	0.01
14	280	2100	0.02	0.01	0.04
15	300	2150	0.02	0.02	0.04
16	320	2200	0.01	0.01	0.03
17	340	2250	0.01	0.01	0.08
18	360	2300	0.02	0.01	0.01
19	380	2350	0.01	0.01	0.01
20	400	2400	0.01	0.01	0.01

4. Results and discussions

An Artificial Neural Network (ANN) is a data processing model inspired by how the human brain analyses data. There is a wealth of material outlining the fundamental architecture and parallels to organic neurons. The material here is restricted to a general overview of the various components involved in the ANN implementation. The network design or topology, which includes the number of nodes in hidden layers, network connections, initial weight assignments, and activation functions, is particularly crucial in ANN performance and largely relies on the situation at hand.
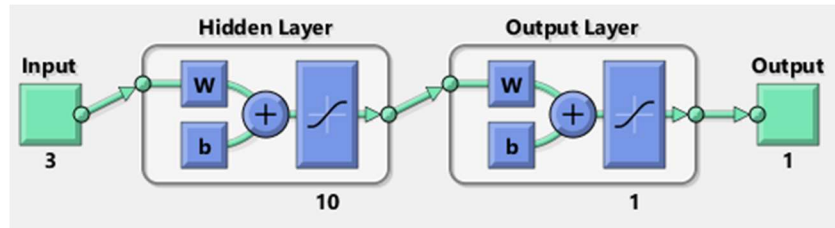

Figure 2: Neural network topology having 3 inputs and 1 output

Figure 2 shows the neural network for the motor drive end having three input and 10 hidden layers and one output wa established. Purelin and transig functions are used for further obtaining of results as a transfer functions.
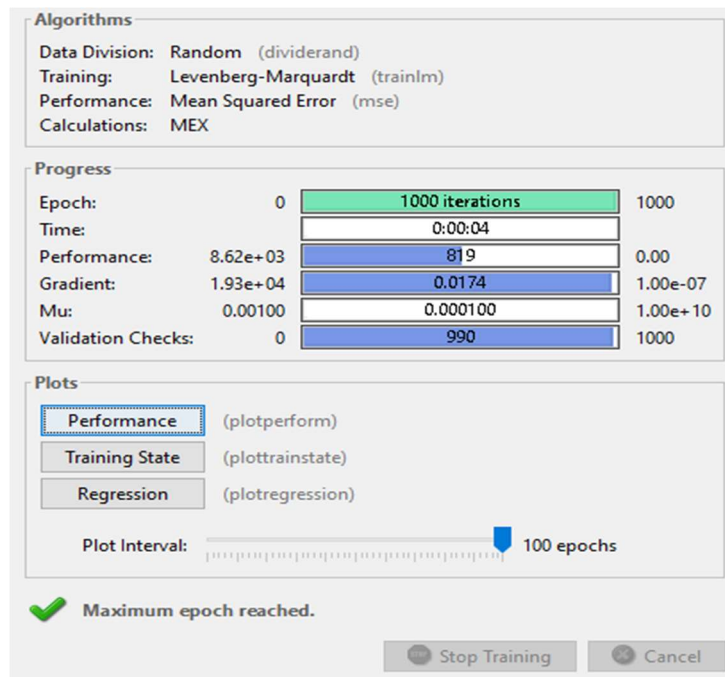

Figure 3: Algorithm and Regression window showing 1000 iterations of Epoch

The Figure 3 shows the possible regression results established upon changing the values. The epoch of 1000 iterations was trained in the network having the performance value of 8.62e+03 and gradient is 1.93e+04 with the maximum epoch readings. The values are consistent as per the literature survey examined. Hence this type of approach can be adopted for failure estimation of machines.
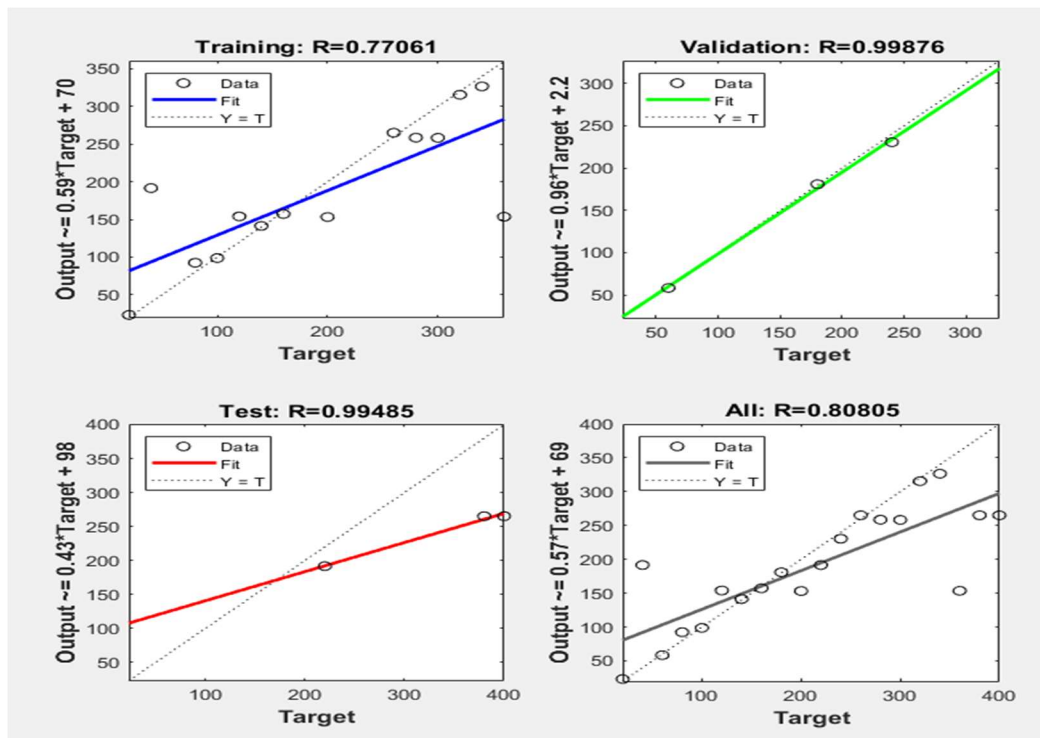
Figure 4: Regression validation output

Figure 4 shows the validation of the results using Levenberg algorithm for obtaining regression values which has higher accuracy rate of 99%.

5. Conclusion

In this study, a generic methodology for detecting machinery faults using a pattern regression technique is proposed. This entails gathering data, extracting features, reducing high-dimensional data, and classifying it using MPL and closest neighbour. Although we utilized bearing fault diagnostics as illustrative examples, the suggested technique may be used to different applications by simply altering the sensory signal properties. The approaches described are appropriate for rotating equipment defect identification and diagnosis and found to be 99% accuracy when validated using neural network. Finally, maintenance strategy is implemented such that, it will be performed prior to the scheduled date.

6. References

1. Pratesh Jayaswal, S.N. Verma, A.K. Wadhwani, "Application of ANN, Fuzzy Logic and Wavelet Transform in machine fault diagnosis using vibration signal analysis", Journal of Quality in Maintenance Engineering, Emerald Group Publishing Limited, ISSN:1355-2511, Vol. 16 No. 2, 2010.

2. J. P. Patel, S. H. Upadhyay, "Comparison between Artificial Neural Network and Support Vector Method for a Fault Diagnostics in Rolling Element Bearings", 12th International Conference on Vibration Problems, ICOVP 2015, Science Direct, Procedia Engineering 144, (2016), pages 390 – 397.

3. Md. Mamunur Rashid, Muhammad Amar, Iqbal Gondal, Joarder Kamruzzaman, "A data mining approach for machine fault diagnosis based on associated frequency patterns", Springer Science+Business Media New York, Monash University, Clayton, VIC 3800, Australia 2016, pages: 638–651.

4. Yuri Merizalde, Luis Hernandez Callejo, Oscar Duque Perez, "Diagnosis of wind turbine faults using generator current signature analysis: A review", Journal of Quality in Maintenance Engineering, Emerald Publishing Limited, Vol.26, No.3, 2020, ISSN: 1355-2511, pages. 431-458.

5. K. Droder, W. Hoffmeistera, M. Luiga, T. Tounsi, " Real-Time Monitoring of High-Speed Spindle Operations using Infrared Data Transmission", International Conference on Performance Cutting, Germany, 2014, 488 – 493

6. N. Jamaludin, R H Bannister., "Condition Monitoring Of Slow-speed Rolling Element Bearings Using Stress Waves", Journal of Engineering, Vol 215, No. 4, pp 245 – 271,2013

7.Akitoshi , Takashi, Hiroshi, "Application of Condition Monitoring System for Wind Turbines", New Energy Engineering Department Industrial Machinery Division, TECHNICAL REVIEW No.80, 2012.

8.A.A. Mohamed, R. Neilson, P. Mac Connell, "Monitoring of Fatigue Crack Stages in a High Carbon Steel Rotating Shaft Using Vibration", University of Aberdeen, UK, Procedia Engineering 10 (2012) 130–135.

9.Changxiao, Chen Yao, Hailiang, Huagang," Reliability Analysis of Aircraft Condition Monitoring Network Using an Enhanced BDD Algorithm", School of Electronics and Information Engineering, Beihang University, Beijing,2012, china, 925-930.

10.S.Sheng, "Wind Turbine Gearbox Condition Monitoring – Vibration Analysis", Applied Systems Health Management Conference,Virginia, 2011.

Vibration analysis of Frequency domain data using MATLAB asset for application of Rotating Part Machines in Industry

Pavan Kumar B K[a], Dr.Yadavalli Basavaraj[b]

[a] Assistant Professor, Ballari Institute of Technology & Management, Ballari, Karnataka, India

[b] Principal, Ballari Institute of Technology & Management, Ballari, Karnataka, India

Corresponding author: Pavan Kumar B K

Abstract: Increasing the number of Condition-Based Profitability and safety are given emphasis in monitoring activity. Maintenance is the prevention of anticipated problems by monitoring the machine in time for it to run, which involves process control, keeping the machine operating, logistics, and improvement. This paper focuses on a unique feature of predictive maintenance utilising the MATLAB tool's State space model and accuracy is more than 85%. The frequency data is primarily collected from rotating machines using vibrometers, and the obtained spectrums are analysed using MATLAB for validation, which clearly defines the severity level of vibration in a component and to estimate the life of the machine by creating a state space model and analysing it using asset tool.

Keywords: Maintenance, MATLAB, Frequency domain data, condition monitoring.

1. Introduction

Vibration analysis is an extensively measured parameter in many business programs. Vibration response measurements give valuable information on common issues. Both the analytical form and the window are included in the frequency domain data. However, frequency domain data have been used in a variety of applications, including nonlinear regression and compression. The signal is decomposed into time and frequency phrases of a wavelet, known as the mum wavelet, using frequency domain data. Frequency domain data are a powerful statistical tool that may be applied to a wide range of applications, including signal processing, data compression, and business management of gear-wheels.

2. Investigation on Critical machine and Data acquisition

The accelerometer is placed on motor non driving end to collect data using vibrometer. These measurements were done under full load conditions, and amplitude values in the axial and vertical directions were found to be dominant. Later, this gathered data is fed into a computer utilising Omnitrend software, where information is transmitted and useful in understanding the prior data also by trends, which helps in diagnosing the problem by verifying whether the readings are within allowed limits or not. The nature of the problem in

equipment is detected by its distinct vibration characteristics. By studying the vibration amplitude pattern, a localised problem may be identified without affecting the other bearings in the equipment.

Table 1: Specifications of Mill Fan motor

| Type of Equipment	Rotor Fan details
Location	Non-Drive End
Pressure	780 MM WC
Impeller diameter	2750MM
Motor	Type 3-Phase Induction Motor
Rating	590Kw
Operating Voltage	7KV
Full Load Current	71 Amp
Motor Speed	990 RPM

The reason of failure was determined by thoroughly inspecting the sources of bearing problems such as misalignment, mechanical looseness, and so on, and removing them one by one, which causes bearing failure. The details of Mill fan motor are shown in below Table 1 and identified as high vibration response.

Table 2: Data acquisition for Motor Non-drive end

MOTOR – NON-DRIVE END (NDE)				
SL NO	Frequency	Velocity		
	X in Hz	V-H	V-V	V-A
1	20	0.01	0.04	0.01
2	40	0.01	0.05	0.05
3	60	0.07	0.12	0.21
4	80	0.04	0.08	0.33
5	100	0.31	0.35	0.31
6	120	0.01	0.1	0.1
7	140	0.01	0.05	0.05
8	160	0.01	0.03	0.08
9	180	0.01	0.08	0.05
10	200	0.01	0.01	0.06
11	220	0.01	0.01	0.02
12	240	0.01	0.01	0.01
13	260	0.01	0.02	0.03

14	280	0.01	0.01	0.02
15	300	0.02	0.03	0.01
16	320	0.01	0.05	0.05
17	340	0.01	0.02	0.02
18	360	0.01	0.01	0.07
19	380	0.02	0.01	0.05
20	400	0.01	0.01	0.03

The data measurements are collected from a variety of sources and analysed to identify equipment failure trends and determine what maintenance is required. Data capture, data manipulation, status detection, health evaluation, and prognosis assessment are all activities carried out during this stage and represented in below Table 2.
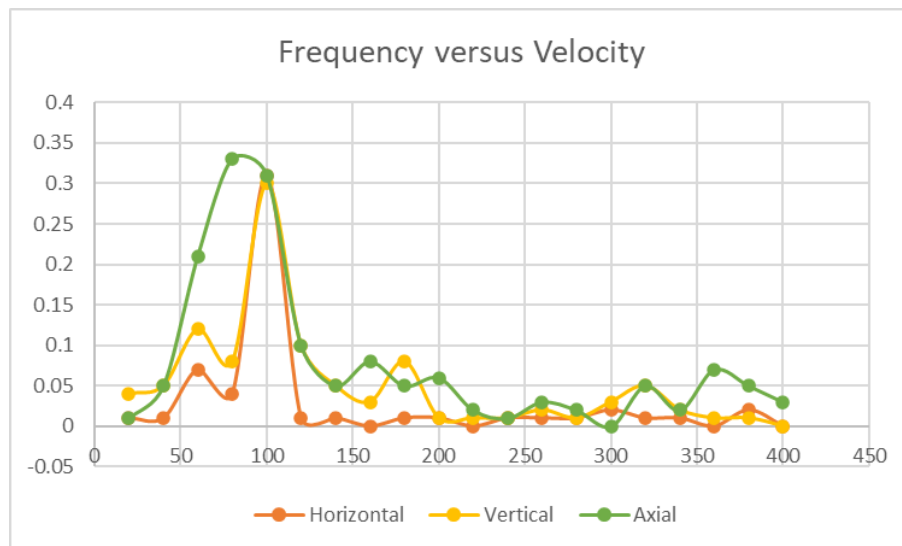
Graph 1 : Graph shows frequency versus velocity with triaxial directions

As per the above data collected with triaxial directions for different frequency, graph is drawn to show the highest peak in order to find the fault in machine. The common type of fault detection is generally categorised into two types namely data driven and model-based approaches.

3. Neural network

A Neural Network (NN) is a data processing model inspired by how the human brain analyses data. There is a wealth of material outlining the fundamental architecture and parallels to organic neurons. The material here is restricted to a general overview of the various components involved in the NN implementation. The network design or topology,

which includes the number of nodes in hidden layers, network connections, initial weight assignments, and activation functions, is particularly crucial in NN performance and largely relies on the situation at hand. Figure 1 depicts a basic NN and its elements having 3 inputs and 1 output with 10 hidden layers.
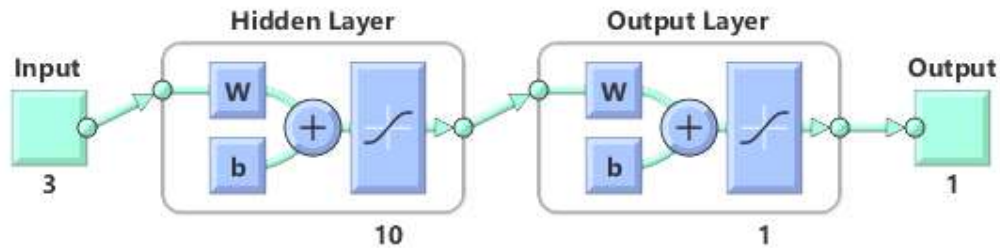

Figure 1: Neural Network flow diagram

An artificial neural network models biological synapses and neurons and can be used to make predictions for complex data sets. Neural networks and their associated algorithms are among the most interesting of all machine-learning techniques.
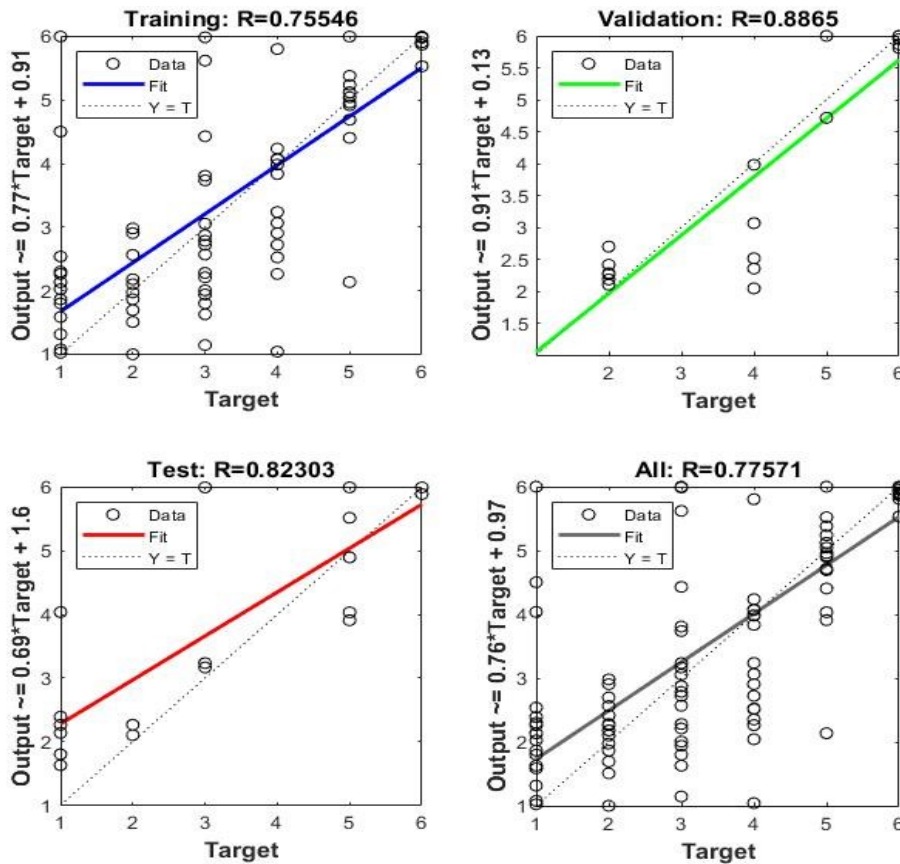

Figure 2: Regression results shown for training and test data

In this paper, explain the feed-forward mechanism, which is the most fundamental aspect of neural networks and it is much essential to show the best validation performed at certain epoch number having validation value is 88% which is greater than 85% obtained from training and test data.

4. Validation

Validation of the developed regression based simultaneous bearing fault diagnosis and severity identification methods on a bearing test rig with vibration signals utilizing seeded fault tests.
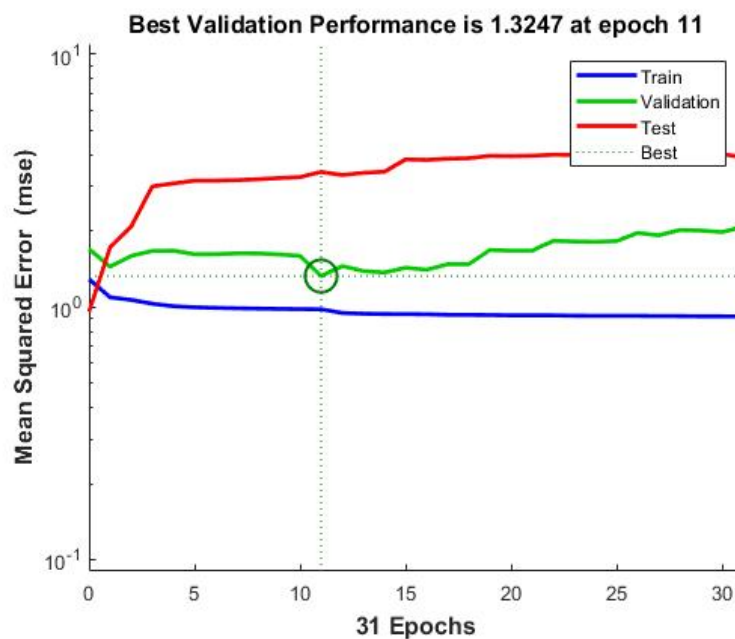

Figure 3: Performance validation results having MSE and epochs

The Figure 3 validates the best performance validated is 1.3247 at the epoch 11. The accuracy of the diagnostic outperforms the previously published values. This study concentrated on imbalance and misalignment since these two flaws are the most typical errors that may be detected in bearing difficulties. Both the unbalance and misalignment rigs have 150000 data points in their data.
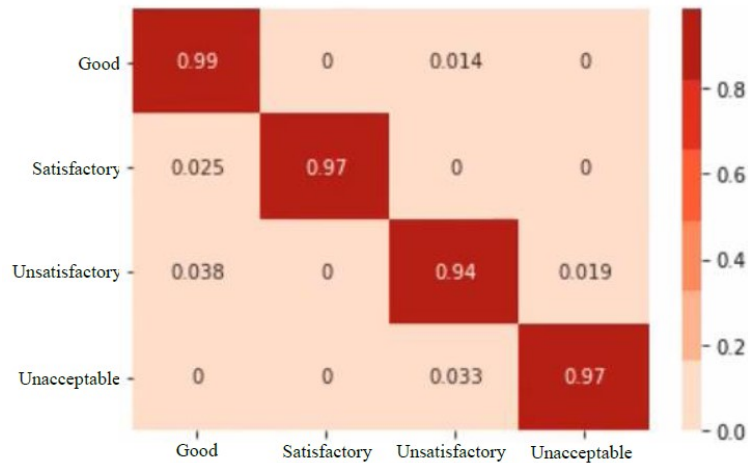
Figure 4: Forest Qualifier matrix

The above figure 4 matrix shows the best breakdown error in predictions for an unseen data. Each value of the row is standardised by listing different colours with different values. We can easily identify the diagonal values with those of the positions which exactly shows the best performance in the matrix. Image classification can be finished with the least error rate.

5. CONCLUSION

A generic methodology for detecting machinery faults using a pattern recognition technique is proposed. This entails gathering data, extracting features, reducing high-dimensional data, and classifying it using MPL and closest neighbour. Although we utilized bearing fault diagnostics as illustrative examples, the suggested technique may be used to different applications by simply altering the sensory signal properties. This paper concludes towards validation from regression and forest qualifier matrix having more than 85% from literature survey using MATLAB tool for diverging fault detection and prognosis in vibration size techniques for machine factors.

5. REFERENCES

[1] Mazzoleni, Y. Maccarana, F. Previdi. "A comparison of data-driven fault detection methods with application to aerospace electro- mechanical actuators", IFAC-Papers, 2017.

[2] Van Tung, Tran, and Bo-Suk Yang. Machine fault diagnosis and prognosis: The state-of-the-art International Journal of Fluid Machinery and Systems 2.1 (2009): 61-71.

[3] Rezaei, Aida. Fault Detection and Diagnosis on the rolling element bearing. Masters Abstracts International. Vol. 46. No. 03. 2007.

[4] Lu, Bin, and Santosh Sharma. A literature review of IGBT fault diagnostic and protection methods for power inverters. Industry Applications Society, 2008.IEEE.

[5] Attoui, I., B. Oudjani, W. Richi, K. Chettah, N. Fergani, And N. Boutasseta. Fault Diagnosis Of Rotating Machinery Based On Vibration Signal Analysis. In 3rd International conference on advances in mechanical engineering. 2017.

[6] Duan, Zhihe, et al. Development and trend of condition monitoring and fault diagnosis of multi-sensors information fusion for rolling bearings: a review. The International Journal of Advanced Manufacturing Technology 96.1-4 (2018): 803-819.

[7] Mellit, Adel, Giuseppe Marco Tina, and Soteris A. Kalogirou. Fault detection and diagnosis methods for photovoltaic systems using neural network: A review. Renewable and Sustainable Energy Reviews 91 (2018): 1-17.

[8] Katipamula, Srinivas, and Michael R. Brambley. Methods for fault detection, diagnostics, and prognostics for building systems—a review, part I. Hvac&R Research 11.1 (2005): 3-25.

[9] Cerrada, Mariela, et al. A review on data-driven fault severity assessment in rolling bearings. Mechanical Systems and Signal Processing 99 (2018): 169-196.

[10] Janssens, Olivier, et al. Convolutional neural network-based fault detection for rotating machinery. Journal of Sound and Vibration 377 (2016): 331-345.

[11] Li, Fanbiao, et al. Fault detection filtering for nonhomogeneous Markovian jump systems via a fuzzy approach. IEEE Transactions on Fuzzy Systems 26.1 (2018): 131-141.

[12] Li, Linlin, et al. Diagnostic Observer Design for T–S Fuzzy Systems: Application to Real-Time-Weighted Fault-Detection Approach."IEEE Transactions on Fuzzy Systems 26.2 (2018): 805-816.

[13] Aherwar, A. 2012, "An investigation on gearbox fault detection using vibration analysis techniques: A review", Australian Journal of Mechanical Engineering, Vol. 10, No. 2, pp. 169-184.

[14] Berge, S. P., Lund, B. F., & Ugarelli, R. (2014) Condition Monitoring for Early Failure Detection. Frognerparken Pumping Station as Case Study. Procedia, 70, 162–171.

[15] Y H Kim, A C C Tan & V Kosse (2008) Condition monitoring of low speed bearings - A review, Australian Journal of Mechanical Engineering, 6:1, 61-68.

Original Article

Vibration Analysis of Frequency Domain Data using MATLAB for Application of Rotating Part Machines in Industry

B. K. Pavan Kumar[1], Yadavalli Basavaraj[2]

[1,2]*Mechanical, Ballari Institute of Technology and Management, Karnataka, India*

Abstract - Increasing the number of Condition-Based Profitability and safety are given emphasis in monitoring activity. Maintenance is the prevention of anticipated problems by monitoring the machine in time for it to run, which involves process control, keeping the machine operating, logistics, and improvement. This paper focuses on a unique feature of predictive maintenance utilizing the MATLAB tool's State space model, and accuracy is more than 85%. The frequency data is primarily collected from rotating machines using vibrometers, and the obtained spectrums are analyzed using MATLAB for validation, which clearly defines the severity level of vibration in a component and estimates the machine's life by creating a state space model and analyzing it using the asset tool.

Keywords - Maintenance, MATLAB, Frequency domain data, Condition monitoring, Vibration analysis.

1. Introduction
Vibration analysis is an extensively measured parameter in many business programs. Vibration response measurements give valuable information on common issues. The frequency domain data includes both the analytical form and the window. However, frequency domain data have been used in a variety of applications, including nonlinear regression and compression.

The signal is decomposed into time and frequency phrases of a wavelet, known as the mum wavelet, using frequency domain data. Frequency domain data are a powerful statistical tool that may be applied to a wide range of applications, including signal processing, data compression, and business management of gear wheels.

2. Literature Survey
Mazzoleni et al. [1], experimental data are collected for the cylindrical bearing NJ305, and four conditions are considered: inner race defect, outer race defect, roller defect, and healthy bearing. Kurtosis, crest factor, energy, skewness, and other characteristics are calculated for all 900 signals in the database. ANN is trained and tested first for condition auto-identification, and then various classifiers are analysed here to determine the best method. The Support Vector Machine technique as a classifier was found to be the most efficient, with nearly 86% efficiency.

Attoui et al. [5] this paper centres around fostering a convolutional brain organization to gain includes straightforwardly from the first vibration signals and afterwards analyze deficiencies. The viability of the proposed technique is approved through PHM gearbox challenge information and a planetary gearbox test rig which was contrasted with the other three conventional strategies; the outcomes show that the one-layered convolution brain organization (1-DCNN) model has higher exactness for fixed-shaft gearbox and planetary gearbox issue determination than that of the customary indicative ones.

Katipula et al. [8], By comparing the proposed method to previous works, two main contributions are concluded: first, the proposed method directly uses raw vibration signals to carry out fault diagnosis in an end-to-end way, greatly reducing the reliance on human expertise and manual intervention; second, the appropriate network architecture of the MLCNN model is designed to realise compound fault diagnosis of the gearbox effectively and efficiently. Finally, two case studies are used to validate the presented method. The results show that it is more accurate than other existing methods in the literature. Furthermore, its stability performance is quite good.

Li et al. [12], In this research, domain adaptation is employed to facilitate the effective implementations of intelligent fault detection. Specifically, we suggested a framework based on a multilayer multiple kernel form of Maximum Mean Discrepancy. In order to provide consistent findings and enhance accuracy, the kernel approach is developed to replace the high dimensional map of Maximum

Mean Discrepancy. As a result, characteristics from various domains are near one another in the Hilbert Space. Furthermore, two separate domains' characteristics contribute to domain adaptation in each feature layer. Two bearing datasets are utilised to evaluate the suggested method's effectiveness. The experimental findings suggest that the proposed technique can overcome the limits of existing methods and attain conditioned performance.

Pankaj et al. [19], The following methods for CBM fault prognostics are examined in this study: logical data analysis, artificial neural networks, and proportional hazard models. A technique for applying and comparing these models is created, which comprises data pre-processing, model construction, and model output analysis. The outcomes are evaluated using three metrics: error, half-life error, and cost score. According to the findings of this investigation, the LAD and feed-forward ANN models outperform the PHM model. The feedback ANN, on the other hand, performs poorly, with substantially larger variation than the other three approaches' predictions. The purpose of this research is to give suggestions on when and where to employ these three prognostic models based on these findings.

3. Critical Machine Identification

The accelerometer is placed on the motor's non-driving end to collect data using a vibrometer. These measurements were done under full load conditions, and amplitude values in the axial and vertical directions were found to be dominant.

Later, this gathered data is fed into a computer utilising Omnitrend software, where information is transmitted and useful in understanding the prior data and trends, which helps diagnose the problem by verifying whether the readings are within allowed limits. The nature of the problem in equipment is detected by its distinct vibration characteristics.

By studying the vibration amplitude pattern, a localised problem may be identified without affecting the other bearings in the equipment. The details of the Mill fan motor are shown below in Table 1 and identified as high vibration response.

**Table 1. Specifications of Mill Fan motor**

Type of Equipment	Rotor Fan details
Location	Non-Drive End
Pressure	780 MM WC
Impeller diameter	2750MM
Motor	Type 3-Phase
Rating	590Kw
Operating Voltage	7KV
Full Load Current	71 Amp
Motor Speed	990 RPM

Table 2. Data acquisition for Motor Non-drive end

	Motor – Non-Drive End (NDE)			
	Frequency	Velocity		
SL NO	X in Hz	V-H	V-V	V-A
1	20	0.01	0.04	0.01
2	40	0.01	0.05	0.05
3	60	0.07	0.12	0.21
4	80	0.04	0.08	0.33
5	100	0.31	0.35	0.31
6	120	0.01	0.1	0.1
7	140	0.01	0.05	0.05
8	160	0.01	0.03	0.08
9	180	0.01	0.08	0.05
10	200	0.01	0.01	0.06
11	220	0.01	0.01	0.02
12	240	0.01	0.01	0.01
13	260	0.01	0.02	0.03
14	280	0.01	0.01	0.02
15	300	0.02	0.03	0.01
16	320	0.01	0.05	0.05
17	340	0.01	0.02	0.02
18	360	0.01	0.01	0.07
19	380	0.02	0.01	0.05
20	400	0.01	0.01	0.03

The data measurements are collected from a variety of sources and analysed to identify equipment failure trends and determine what maintenance is required. Data capture, data manipulation, status detection, health evaluation, and prognosis assessment are all carried out during this stage and are represented in Table 2.

As per the above data collected with triaxial directions for different frequencies, a graph is drawn to show the highest peak to find the fault in the machine. The common type of fault detection is generally categorised into two types: data-driven and model-based approaches.
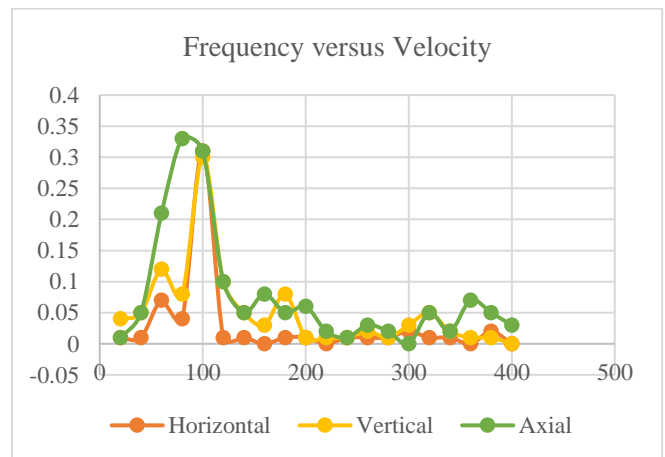
Graph 1. The graph shows frequency versus velocity with triaxial directions
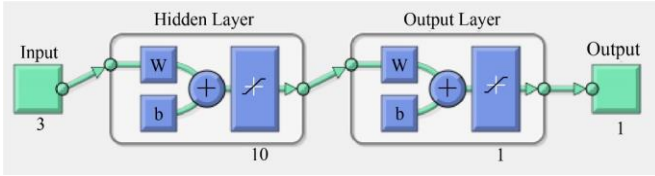
Fig. 1 Neural Network flow diagram

The reason for failure was determined by thoroughly inspecting the sources of bearing problems, such as misalignment, mechanical looseness, and so on, and removing them one by one, which causes bearing failure

4. Neural network

A Neural Network (NN) is a data processing model inspired by how the human brain analyses data. A wealth of material outlines the fundamental architecture and parallels to organic neurons. The material here is restricted to a general overview of the various components involved in the NN implementation. The network design or topology, which includes the number of nodes in hidden layers, network connections, initial weight assignments, and activation functions, is particularly crucial in NN performance and largely relies on the situation at hand. Figure 1 depicts a basic NN and its elements having 3 inputs and 1 output with 10 hidden layers.

An artificial neural network models biological synapses and neurons and can be used to make predictions for complex data sets. Neural networks and their associated algorithms are among the most interesting of all machine-learning techniques.

This paper explains the feed-forward mechanism, which is the most fundamental aspect of neural networks. It is essential to show that the best validation performed at a certain epoch number with a validation value of 88%, which is greater than 85% obtained from training and test data.
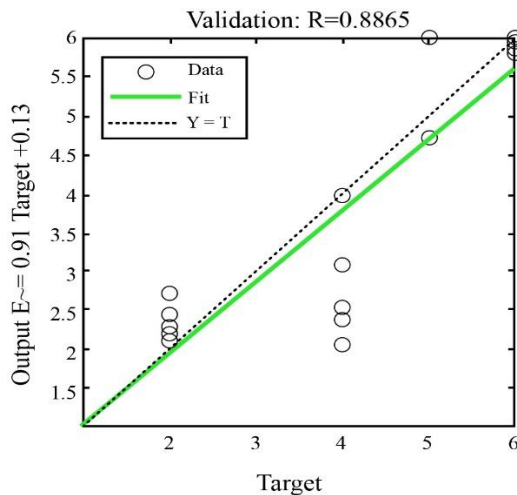

Fig. 2 Validation results showing R-value

5. Validation

Validate the developed regression-based simultaneous bearing fault diagnosis and severity identification methods on a bearing test rig with vibration signals utilizing seeded fault tests.
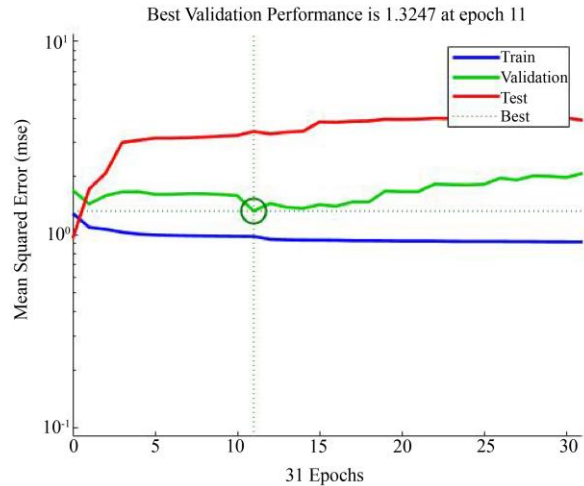

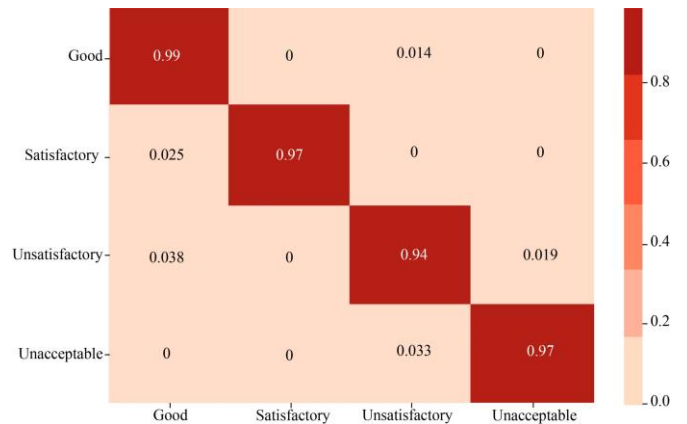**Fig. 3 Performance validation results having MSE and epochs**

Fig. 4 Forest Qualifier matrix

Figure 3 validates that the best performance validated is 1.3247 at epoch 11. The accuracy of the diagnostic outperforms the previously published values. This study concentrated on imbalance and misalignment since these two flaws are the most typical errors that may be detected in bearing difficulties. Both the unbalance and misalignment rigs have 150000 data points in their data.

The above figure 4 matrix shows the best breakdown error in predictions for unseen data. Each value of the row is standardised by listing different colours with different values. We can easily identify the diagonal values with those of the positions showing the best performance in the matrix. Image classification can be finished with the least error rate.

6. Conclusion

A generic methodology for detecting machinery faults using a pattern recognition technique is proposed. It entails

gathering data, extracting features, reducing high-dimensional data, and classifying it using MPL and closest neighbor. Although we utilized bearing fault diagnostics as illustrative examples, the suggested technique may be used in different applications by simply altering the sensory signal properties.

This paper concludes towards validation from regression and forest qualifier matrix having more than 85% from literature survey using MATLAB tool for diverging fault detection and prognosis in vibration size techniques for machine factors.

References

[1] Mazzoleni, Y. Maccarana, and F. Previdi, "A Comparison of Data-Driven Fault Detection Methods with Application to Aerospace Electro-Mechanical Actuators," *IFAC-Papers*, vol. 50, no. 1, pp. 12797-12802, 2017.

[2] Van Tung, Tran, and Bo-Suk Yang, "Machine Fault Diagnosis and Prognosis: the State-of-the-Art," *International Journal of Fluid Machinery and Systems*, vol. 2, no. 1, pp. 61-71, 2009. *Crossref*, https://doi.org/10.5293/IJFMS.2009.2.1.061

[3] Aida Rezaei, "Fault Detection and Diagnosis on the Rolling Element Bearing," *Masters Abstracts International*, vol. 46, no. 03, 2007.

[4] Bin Lu, and Santosh Sharma, "A Literature Review of IGBT Fault Diagnostic and Protection Methods for Power Inverters," *2008 IEEE Industry Applications Society Annual Meeting,* pp. 1-8, 2008. *Crossref*, https://doi.org/10.1109/08IAS.2008.349

[5] Attoui, I et al., "Fault Diagnosis of Rotating Machinery Based on Vibration Signal Analysis," *In 3rd International Conference on Advances in Mechanical Engineering*, 2017.

[6] Zhihe Duan et al., "Development and Trend of Condition Monitoring and Fault Diagnosis of Multi-Sensors Information Fusion for Rolling Bearings: A Review," *The International Journal of Advanced Manufacturing Technology*, vol. 96, no.1-4, pp. 803-819, 2018.

[7] Mellit, Adel, Giuseppe Marco Tina, and Soteris A. Kalogirou, "Fault Detection and Diagnosis Methods for Photovoltaic Systems Using Neural Network: A Review," *Renewable and Sustainable Energy Reviews*, vol. 91, pp. 1-17, 2018. *Crossref*, https://doi.org/10.1016/j.rser.2018.03.062

[8] Srinivas Katipamula, and Michael R. Brambley, "Methods for Fault Detection, Diagnostics, and Prognostics for Building Systems-A Review, Part I," *Hvac&R Research*, vol. 11, no. 1, pp. 3-25, 2005.

[9] Mariela Cerrada et al., "A Review on Data-Driven Fault Severity Assessment in Rolling Bearings," *Mechanical Systems and Signal Processing*, vol. 99, pp. 169-196, 2018. *Crossref*, https://doi.org/10.1016/j.ymssp.2017.06.012

[10] Olivier Janssens et al., "Convolutional Neural Network-Based Fault Detection for Rotating Machinery," *Journal of Sound and Vibration*, vol. 377, pp. 331-345, 2016. *Crossref*, https://doi.org/10.1016/j.jsv.2016.05.027

[11] S.P. Pirogov et al., "Simulation of Forced Oscillations of Pressure Monitoring Devices," *International Journal of Engineering Trends and Technology*, vol. 70, no. 3, pp. 37-47, 2022. *Crossref*, https://doi.org/10.14445/22315381/IJETT-V70I2P205

[12] Linlin Li et al., "Diagnostic Observer Design for T–S Fuzzy Systems: Application to Real-Time-Weighted Fault-Detection Approach," *IEEE Transactions on Fuzzy Systems*, vol. 26, no. 2, pp. 805-816, 2018.

[13] A Aherwar, "An Investigation on Gearbox Fault Detection Using Vibration Analysis Techniques: A Review," *Australian Journal of Mechanical Engineering*, vol. 10, no. 2, pp. 169-184, 2011. *Crossref*, https://doi.org/10.7158/M11-830.2012.10.2

[14] S.P. Berge, B.F. Lund, and R. Ugarelli, "Condition Monitoring for Early Failure Detection. Frognerparken Pumping Station as Case Study," *Procedia Engineering*, vol. 70, pp. 162–171, 2014. *Crossref*, https://doi.org/10.1016/j.proeng.2014.02.019

[15] Y H Kim, A C C Tan, and V Kosse, "Condition Monitoring of Low Speed Bearings - A Review," *Australian Journal of Mechanical Engineering*, vol. 6, no. 1, pp. 61-68, 2015. *Crossref*, https://doi.org/10.1080/14484846.2008.11464558

[16] I. M. Jamadar et al., "Model-Based Condition Monitoring for the Detection of Failure of a Ball Bearing in a Centrifugal Pump," *Journal of Failure Analysis and Prevention*, vol. 19, pp. 1556-68, 2019. *Crossref*, https://doi.org/10.1007/s11668-019-00792-x

[17] M. Lokesha et al., "Fault Detection and Diagnosis Ingears Using Wavelet Enveloped Power Spectrum and ANN," *International Journal of Research In Engineering and Technology*, vol. 2, no. 9, pp. 146-158, 2013. *Crossref*, http://dx.doi.org/10.15623/ijret.2013.0209023

[18] Chunzhi Wu et al., "Intelligent Fault Diagnosis of Rotating Machinery Based on One-Dimensional Convolutional Neural Network," *Computers in Industry*, vol. 108, pp. 53-61, 2019. *Crossref*, https://doi.org/10.1016/j.compind.2018.12.001

[19] Pankaj Gupta, and M. K Pradhan, "Fault Detection Analysis In Rolling Element Bearing: A Review," *Materials Today: Proceedings*, vol. 4, no. 2, pp. 2085–2094, 2017. *Crossref*, https://doi.org/10.1016/j.matpr.2017.02.054

[20] V. Devaraj, and M. Kumaresan, "An Elite LOA-TFWO Approach for Load-Frequency Control of Islanded Micro-Grids Incorporating Renewable Sources," *International Journal of Engineering Trends and Technology*, vol. 70, no. 10, pp. 166-187, 2022. *Crossref*, https://doi.org/10.14445/22315381/IJETT-V70I10P217

[21] James Wakiru et al., "A Data Mining Approach for Lubricant-Based Fault Diagnosis," *Journal of Quality in Maintenance Engineering*, vol. 27, no. 2, pp. 1355-1365, 2020. *Crossref*, https://doi.org/10.1108/JQME-03-2018-0027

[22] Pengfei Liang et al., "Compound Fault Diagnosis of Gearboxes via Multi-Label Convolutional Neural Network and Wavelet Transform," *Computers In Industry*, vol. 113, no. c, 2019. *Crossref*, https://doi.org/10.1016/j.compind.2019.103132

[23] Soumava Boral, Sanjay Kumar Chaturvedi, and V.N.A. Naikan, "A Case Based Reasoning System for Fault Detection and Isolation, A Case Study on Complex Gearboxes," *Journal of Quality In Maintenance Engineering*, vol. 25, no. 2, pp. 213-235, 2019. *Crossref*, https://doi.org/10.1108/JQME-05-2018-0039

[24] Weiwei Qian et al., "A Novel Transfer Learning Method for Robust Fault Diagnosis of Rotating Machines Under Variable Working Conditions," *Journal of Measurement*, vol. 138, pp. 514-525, 2019. *Crossref*, https://doi.org/10.1016/j.measurement.2019.02.073

[25] Fafa Chen et al., "Performance Degradation Prediction of Mechanical Equipment Based on Optimized Multi-Kernel Relevant Vector Machine and Fuzzy Information Granulation," *Measurement,* vol. 151, 2020. *Crossref*, https://doi.org/10.1016/j.measurement.2019.107116

[26] Ana Gonzalez Muniz, Ignacio Diaz, and Abel Cuadrado, "DCNN for Condition Monitoring and Fault Detection in Rotating Machines and Its Contribution to the Understanding of Machine Nature," *Heliyon Journal*, vol. 6, no. 2, pp. 3395-3405, 2020. *Crossref*, https://doi.org/10.1016/j.heliyon.2020.e03395

[27] Fanbiao Li et al., "Fault Detection Filtering for Nonhomogeneous Markovian Jump Systems via a Fuzzy Approach," *IEEE Transactions on Fuzzy Systems*, vol. 26, no. 1, pp. 131-141, 2018. *Crossref*, https://doi.org/10.1109/TFUZZ.2016.2641022

RAMAIAH
Institute of Technology

CELEBRATING 60 Years
DIAMOND JUBILEE

DR. M.S. RAMAIAH CENTENARY YEAR CELEBRATIONS

ICARES-2022

CERTIFICATE

This is to certify that

Dr. SUNILKUMAR A

BALLARI INSTITUTE OF TECHNOLOGY AND MANAGEMENT, BALLARI

has presented a paper/poster titled **"AC Conductivity and Dielectric behavior of Polypyrrole – Holmium oxide Composites."** at the *International Conference on Applied Research in Engineering Sciences -(ICARES-2022)* held on 24th & 25th November 2022. The conference is jointly organized by the Department of Physics, Chemistry, Mathematics & Humanities at Ramaiah Institute of Technology, Bengaluru-560054.

Dr. N. L. Ramesh
Professor & Head
Dept. of Mathematics & Humanities

Dr. A. Jagannatha Reddy
Professor & Head
Dept. of Physics

Dr. B. M. Nagabhushana
Professor & Head
Dept. of Chemistry

Dr. N. V. R. Naidu
Principal
Ramaiah Institute of Technology

INTERNATIONAL CONFERENCE OF

INTERNATIONAL ACADEMY OF PHYSICAL SCIENCES (CONIAPS XXVIII)

On

INNOVATIONS IN COMPUTATIONAL AND PHYSICAL SCIENCES FOR SUSTAINABLE DEVELOPMENT (ICPSSD-2022)

Organized by

VIJAYANAGARA SRI KRISHNADEVARAYA UNIVERSITY, BALLARI

21-23, December 2022

Certificate of Participation

This is to certify that ....Dr. Sunilkumar A...

of ......BITM Ballari.. has participated in

the International Conference as **Invited Speaker/Delegate/Participant** held at VSK

University, Ballari, Karnataka and delivered the presentation on ..Highly effective Nitrogen

dioxide Sensor Based on Polyaniline/Vanadium Pentoxide /Lead Tetroxide Ternary

composite.

Prof K.V. Prasad
Conference Convenor, VSK University

Prof S.N. Shukla
Secretary, IAPS

Prof S.C. Patil
Registrar, VSK University

Date: 19.01.2023

To,

The deputy director,
Ballari institute of technology & management,
Ballari – 583 104.

Sir,

Sub: Reimbursement for the publication of the paper in **Scopus** – reg

Ref: https://doi.org/10.1016/j.matpr.2021.08.079

I, Dr. Machappa. T, Professor and Head of the department, department of physics, has published the original research paper title "Conducting polyaniline doped with zinc tungstate matrix film as gas sensing composite" in **Scopus** indexed research journal with citation: Materials Today: Proceedings 49 (2022) 1899–1904, and ISSN: ~~1899~~ ~~1904~~ as corresponding author with E-mail address: machappa@bitm.edu.in.

Thanking you sir

Yours sincerely

[signature] 19/1/23

Dr. Machappa T.
Head of The Department,
Dept. of Physics,
Ballari Institute of Technology & Management.
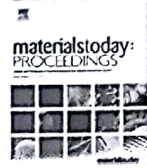BELLARY

Authentication from dean R & D:

[handwritten notes: Indexed in Scopus, citation scm 2-3, since 2004 :this in scopus, (25,000)]

[signatures and dates: 28/1/2023, 31/1/23]

[handwritten: PAY Rs 5000/-]

Conducting polyaniline doped with zinc tungstate matrix film as gas sensing composite

T. Machappa [a,*], S. Badrunnisa [b], M.V.N. Ambika Prasad [c]

[a] Department of Physics, Ballari Institute of Technology & Management, Bellari 583 104, Karnataka, India
[b] Krupanidhi Degree College, Bengaluru 560 035, Karnataka, India
[c] Department of Physics, Gulbarga University, Gulbarga 585 106, Karnataka, India

ARTICLE INFO

ABSTRACT

Conducting polyaniline (PANI) is doped with a bi-metal oxide, Zinc tungstate ($ZnWO_4$) in the chemical polymerization method, and the composite matrix is sintered on the substrate to form a film. The characterization of composite by FTIR spectrum to confirm the formation of emeraldine salt phase of PANI from monomer aniline. X-RD spectra and SEM images to confirm the presence of crystalline $ZnWO_4$ in PANI matrix. The difference in conductivity versus temperature shows exponentially thermal activated behavior, in which conductivity increases with temperature due to the curling effect of polymer composite. When exposed to liquid petroleum gas (LPG), due to depletion in the number of conduction electrons at the surface and grain boundaries, there is a barrier formation at the interface of sensing films of PANI/$ZnWO_4$ composite, via Fermi energy exchange control mechanism, thereby composite film increases its resistance with LPG concentration.

1. Introduction

The gas sensor is always operated in a gas environment known as a chemical sensor. These chemical sensor converts change in chemical information into an electrical signal, based on the chemical change and concentrations of the different gaseous species under different conditions. The sensor response (sensitivity) is defined as the ratio between the steady response of the chemical sensor when exposed to the sample gas environment to the sensor response when exposed to the reference atmosphere without sample gas. When a chemical sensor is exposed to sample gas, then sensor materials interact with the sample gas, this kind of interaction may lead to oxidation increases the resistance/reduction decreases the resistance, these chemical reactions is on the surface of the film or bulk material. Some of the physical properties will be changed in sensing material due to the interaction of sample gas, such as conductivity. The changes in resistance/conductivity will be measured by a voltage drop across the resistor connected in ser-

ies with the sensor [1]. Fig. 1 shows the solid-gas sensor working principle. The physical properties of different materials have been modified when interacted with a chemical gas environment, materials such as metals, metal oxides (ionic compounds) supermolecular structures, and polymers. Sensing material properties along with characteristics is governed by the type of interaction, material properties like polarizability, affinity, molecular size, and structural changes. There are two types of interaction between the sensing materials and the existence of gas.

The first type of interaction is "Lock and key" interaction, this happens usually in a sensing material that consists of organic materials. In this interaction, there is an arrangement of a monolayer of the identified molecule or specifically identified sites in a polymer matrix. [2]. The second one is the chemical sensing within inorganic materials. Reactions between the molecules present at the surface of sensing material and/or chemisorptions in the sensing material and/or catalytic reactions between gas and sensing material. Thus, there is a change in carrier density and mobility dues to the change in charge distribution at the surface while interacting with gas [3]. Household LPG (liquefied petroleum gas) and CO (carbon monoxide gas) are flammable gases. These gases are

From,
Dr. Sunilkumar A
Department of physics
BITM, Ballari

TO,
The Deputy Director,
BITM, Ballari

Respected Sir,

subject: Requesting for incentive for publication

With reference to above cited subject, I hereby inform you that one of my paper has published in Science Citation index expanded journal in Jan 2023 (online). please consider my request and do the needful

thanking you.

your's faithfully
tW.A

Date: 25/1/2023
place: Ballari

PA-/R 15,000/-
81/1/23

Wos indexed
Expanded.
published
25 JAN 2023
(15,000)
30/01/2023

Humidity sensing performance of the magnesium oxide nanoparticles

S. S. Shanawad[1], B. Chethan[2,*] , V. Prasad[2], A. Sunilkumar[3], and V. S. Veena[4]

[1] Department of Physics, JSS Banashankari Arts Commers and SK Gubbi Science College, Dharawad 580004, Karnataka, India
[2] Department of Physics, Indian Institute of Science, Bengaluru 560012, Karnataka, India
[3] Department of Physics, Ballari Institute of Technology and Management, Ballari 583104, Karnataka, India
[4] Department of Physics, Government First Grade College, Madhugiri 572132, Karnataka, India

ABSTRACT

In this present scenario, the humidity sensing response of the green synthesized Magnesium oxide Nanoparticles (MgO NPs) had been viewed. Here the MgO NPs synthesized by green synthesis method with green tea extract as fuel. The structural, functional and morphological characterizations like XRD (x-Ray diffraction), FTIR (Fourier transform infrared spectroscopy), SEM (scanning electron microscope), EDS (Energy dispersive X-ray spectroscopy), TEM (transmission electron microscopy), SEAD (Selected area electron diffraction) were performed for the sample. The important observation in the morphological studies is that: The MgO NPs shows the irregular clusters of particles which can be clearly distinguished has been confirmed from TEM images. The rise in the surface area and porosity confirmed from SEM studies. For the humidity sensing measurements, the sensing film of the MgO NPs prepared by groomed the sample on the glass plate using spin coating unit. The MgO NPs has shown an epitome sensitivity of 99.84% at room temperature with a rapid response time and recovery time of 14 and 26 s, respectively. The MgO NPs has gained a least real sensitivity with less LOD (Limit of detection). Also, the sample has recorded a trifling hysteresis, good linearity and shown an exact stability. The physical parameters for MgO NPs also calculated to determine the potentiality as a perfect sensor. The sensing mechanism also hashed out on the basis of the establishment of chemisorption and physisorption layers.

Address correspondence to E-mail: chethanbchetu@gmail.com; chethanb@iisc.ac.in

 Springer

,om,

Dr. Sunilkumar A
Department of physics
BITM, Ballari

TO,
The Deputy Director.
BITM, Ballari

Respected Sir,

PAY ₹,5000/-

Physics R& D,

31/1/23

Subject: Requesting for incentive for publication.

With reference to the above cited subject,
I hereby inform you that one of my paper
has published in Science Direct journal in December
2022. please consider my request and do the
needful

Thanking you.

your's faithfully
W. A

Date: 29/12/2022
place; Ballari

Scopus Indexed
Since 2020 - 9501
ISSN: 2666 - 9501
Citation Score 05
(5000)
02/01/2023. -

A study on the effect of reaction temperature on the synthesis of magnesium hydroxide nanoparticles: Comparative evaluation of microstructure parameters and optical properties

M.G. Kotresh [a,*], M.K. Patil [b], A. Sunilkumar [c], A. Sushilabai [d], S.R. Inamdar [b]

[a] Department of Studies in Physics, Vijayanagara Sri Krishnadevaraya University, Ballari 583105, India
[b] Laser Spectroscopy Programme, Department of Physics, Karnatak University, Dharwad 580003, India
[c] Department of Physics, Ballari Institute of Technology and Management, Ballari 583 104, India
[d] Department of Mathematics, Ballari Institute of Technology and Management, Ballari 583 104, India

ARTICLE INFO

ABSTRACT

In the present work, magnesium hydroxide nanoparticles were synthesized using the coprecipitation method with the variation of the reaction temperature. The effects of variation of the reaction temperature on the morphological and optical properties were discussed in this paper. The synthesized NPs were characterized using X-ray diffraction, Scanning electron microscope with energy dispersive X-ray spectroscopy, Fourier transform infrared spectrometer, UV–visible absorption, and fluorescence techniques. The crystallite size of the NPs was estimated using various theoretical methods such as Debye-Scherrer (DS), Williamson-Hall (WH), size-strain plot (SSP), and Halder-Wagner (HW) methods and noticed that all the methods have yielded nearly same crystallite size, which ranges between 10 -12 nm for MH A and 7–8 nm for MH B NPs, respectively. The synthesized NPs have shown the shape of flakes and agglomerated particle distribution. These NPs have also shown broad absorption and narrower emission band in the visible region, which suggests that these have potential applications in the field of biological markers, sensors and light-harvesting devices.

1. Introduction

Lately, magnesium hydroxide $[Mg(OH)_2]$ nanoparticles (NPs) have paid attention due to their elite properties, namely excellent fire retardant quality, great thermal stability, nontoxic, and low cost (Wu et al., 2020; Henrist et al., 2003). These NPs were already extensively utilized in flame inhibitors, therapeutic products, chemosensors, biosensors, and as the major starting material to process magnesium oxide (MgO) from magnesium chloride $(MgCl_2)$ which is present in ocean water or brackish water (Liang, 2017; Li et al., 2016; Ganguly et al., 2011). There are various methods are available to produce magnesium hydroxide (MH) NPs namely hydrothermal (Ding et al., 2001), ultrasonic-assisted (Song et al., 2010), microwave-assisted (Beall et al., 2013), co-precipitation (Calderón et al., 2020), and sol–gel methods (Minami et al., 2012). Out of all these techniques, co-precipitation emerged to be economically proficient and easy, which enables tuning crystallite size, structure, and surface modifications as a function of reaction condi-

tions such as pH, reaction temperature, and concentration of precursors used (Kotresh et al., 2021).

There are few previous reports that are available on the successful synthesis, and potential utilization of MH NPs in biomedical and industrial applications. Ding et al. have successfully produced rod, tube, needle, or lamella-structured MH NPs by employing the hydrothermal method using various magnesium precursors and reducing agents (Ding et al., 2001). Zhao et al. have shown the production of MH nanoplatelets by simple blending and casting processes and these NPs have shown excellent antibacterial and flame retardant activity (Zhao et al., 2014). Vatsha et al. synthesized MH NPs functionalized with organic fluorophores, which enables NPs to be traced during an in-vivo experiment (Calderón et al., 2020). Most of the researchers use various markers and organic fluorophores linked to the synthesized NPs to assess in vivo interaction with biomolecules due to their weak fluorescent characteristics. Hence, it is very important to synthesize good fluorescent NPs to get good signal strength during the in-vivo interaction and which is the recent highest priority of the research community for vari-

· Corresponding author at: Assistant professor, Department of Studies in Physics, Vijayanagara Sri Krishnadevaraya University, Jnana Sagara Campus, Cantonment, Ballari 583 105, India.
E-mail address: kotreshm20@gmail.com (M.G. Kotresh).

To,

The deputy director,

Ballari institute of technology & management,

Ballari – 583 104.

Sir,

      Sub: Reimbursement for the publication of the paper in **Scopus** – reg.

      Ref: https://doi.org/10.1557/s43579-023-00336-3
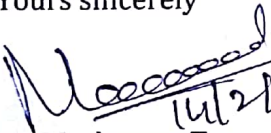
      I, Dr. Machappa. T, Professor and Head of the department, department of physics, has published along with co-research group the original research paper title "Humidity sensing performance of polyaniline-Neodymium oxide composites" in **Scopus** indexed research journal with citation: MRS communications (Springer), Volume 20, Issue 20 (2023) 01–108, and ISSN: 2159-6867 as co-author.

Thanking you sir

Yours sincerely

Dr. Machappa. T.
Head of The Department,
Dept. of Physics,
Ballari Institute of Technology & Management
BELLARY
Authentication from dean R & D:

MRS **Communications**

Research Letter

Check for updates

Humidity sensing performance of polyaniline-neodymium oxide composites

L. B. Gunjal, Department of Physics, VTU-RC, RYM Engineering College, Ballari 583104, India
S. Manjunatha, Department of Physics, V.V. Sangha's Independent PU College, Ballari 583104, India
B. Chethan, Department of Physics, Indian Institute of Science, Bengaluru, Bengaluru 560012, India
N. M. Nagabhushana, Department of Physics, VTU-RC, RYM Engineering College, Ballari 583104, India
Y. T. Ravikiran, Department of PG Studies & Research in Physics, Government Science College, Chitradurga 577501, India
T. Machappa, Department of Physics, VTU-RC, Ballari Institute of Technology & Management, Ballari 583104, India
S. Thomas, School of Energy Materials, Mahatma Gandhi University, Kottayam, Kerala, India 686560

Address all correspondence to N. M. Nagabhushana at **nagabhushananm@gmail.com** and Y. T. Ravikiran at **ytrcta@gmail.com**

Abstract

Humidity sensing response of conducting polymer composite such as Polyaniline-Neodymium Oxide (PNO) composite with varying wt% of Nd_2O_3 in PANI [PANI-Nd_2O_3-10% (PNO-1), PANI-Nd_2O_3-30% (PNO-2) and PANI-Nd_2O_3-50% (PNO-3)] was studied. These samples were prepared by in situ chemical polymerization and were structurally and morphologically characterized by various analytical techniques. Humidity sensing performance of the PNO composites was evaluated in the range of 11–97% RH. Composite PNO-3 showed the highest sensing response of 99% with a response and recovery times of 28 and 29 s, respectively. Other sensing parameters like hysteresis, limit of detection, and sensing stability were also determined for the composites.

Introduction

Humidity sensors have gained vital significance in the food production, food storage, medical field, agriculture, museums, libraries, electronic industry and nuclear power plants due to the increase in demand for their use in monitoring the controlled environments.[1] Recently, humidity sensors fabricated from materials such as metal oxides, ceramics, thin layers of aluminium oxide films have attracted considerable attention in the field of sensor research.[2] But most of these sensors have encountered many limitations, such as complex device fabrication, high operating temperature, high-power consumption, and high cost.[3] To overcome these disadvantages, conducting polymer-based humidity sensors have emerged as a competitive class of alternating material with a number of advantages, such as ease of fabrication, hygroscopicity and ambient temperature operability.[4] In addition, the sensing dependent electrical and related mechanical properties of the conducting polymers can be tuned in various ways; including doping, production of blends and composites, and use of various preparation procedures.[5]

Among all the conducting polymers, polyaniline (PANI) has emerged as an excellent polymer due to its chemical expediency and ease of synthesis along with the wide range of attractive applications in sensors, EMI shielding, corrosion protection, supercapacitors, etc.[6] PANI alone has exhibited very less sensitivity to humidity due to its less hygroscopicity. To fabricate efficient humidity sensors, PANI has been composited with diverse materials like metals, semiconductors, non-metals, metal oxides, and carbon materials such as fullerene, carbon nanotubes, graphene, graphene oxide.[7] To further enhance the scope of PANI based composites, in terms of water adsorption capacity, improved sensitivity, response, and recovery times, limit of detection and linearity, in the present work we have chosen PANI and composited with neodymium oxide (Nd_2O_3). Since it is a rare earth oxide with a hexagonal crystal system, which has a high dielectric constant and insolubility in water and favorable band offset with semiconductors, it finds applications in many microelectronic devices such as sensors.[8]
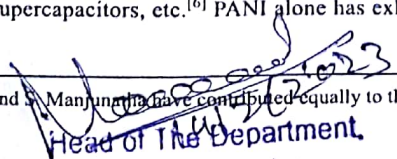
In this perspective, PNO composites with different wt% of Nd_2O_3 in polyaniline were synthesized by employing the in situ chemical polymerization, and then morphologically and structurally characterized by FESEM, TEM, XRD, FTIR and Raman studies before humidity sensing studies.

Experimental

Materials

Aniline ($C_6H_5NH_2$), Hydrochloric acid (HCl), Ammonium persulphate [$(NH_4)_2S_2O_8$], Neodymium oxide (Nd_2O_3) and de-ionized water all these analytical reagents (AR) grade chemicals were procured from SD fine chemicals, Mumbai, India.

L. B. Gunjal and S. Manjunatha have contributed equally to this work.

Head of The Department,
Dept. of Physics,
Ballari Institute of Technology & Management
BELLARY

Scanned by CamScanner

From,
Dr. Sunilkumar A
Department of physics
BITM, Ballari

To,
The Deputy Director,
BITM, Ballari

Respected sir,

Sub: Requesting incentive for publication.

With reference to above cited subject, I hereby inform you that one of my paper has published in Science citation index expanded journal in Feb-2023. please consider my request subject and do the needful.

thanking you

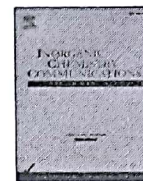your's faithfully

~W. A

Date: 25|2|2023

place: Ballari

Pay Rs, 15,000/-

17|2|23

WOS Expanded (SCIE)

ISSP 1388-7003.

Sweek 1958.

(Rs 15,000/-)

13/02/2023

Short communication

Ultrahigh sensitive and selective room temperature operable poisonous carbon monoxide gas sensor based on polyaniline ternary composite

A. Sunilkumar[a], B.S. Khened[b], B. Chethan[c,*], V. Prasad[c], M.G. Kotresh[d], T.M. Sharanakumar[e], V.S. Veena[f]

[a] Department of Physics, Ballari Institute of Technology and Management, Ballari 583104, Karnataka, India
[b] Department of Electrical and Electronics Engineering, Ballari Institute of Technology and Management, Ballari 583104, Karnataka, India
[c] Department of Physics, Indian Institute of Science, Bengaluru 560012, Karnataka, India
[d] Department of Studies in Physics, Vijayanagara Sri Krishnadevaraya University, 583104 Karnataka, India
[e] Department of Chemistry, Ballari Institute of Technology and Management, 583104 Karnataka, India
[f] Department of Physics, Government First Grade College, Madhugiri 572132, Karnataka, India

ABSTRACT

In this research paper, the influence of vanadium pentoxide (V_2O_5) and lead tetroxide (Pb_3O_4) on poisonous carbon monoxide (CO) gas sensing performance of polyaniline (PANI) at ambient temperature was deliberately discussed. Through in-situ polymerization method, the PANI/ V_2O_5 + Pb_3O_4 (PVL) ternary composites was prepared by taking vanadium pentoxide and lead tetroxide in proportionate order of 10, 20, 30, 40 and 50 wt% with polyaniline. The synthesized composites were characterized and confirmed by using XRD, FTIR, SEM, HRTEM and TGA studies. To support the CO sensing, the DC conductive studies are carried out at the temperature range 20 to 200 ^{0}C. The PVL-3 (PANI/ V_2O_5 + Pb_3O_4 – 30 %) ternary composite has shown an increased conductivity compare to pristine PANI and other ternary composites. Using, DC conductivity graphs the activation energy was determined. For the CO gas sensing studies, the film of all the composites was prepared using spin coating unit. Among PANI and all the ternary composites, PVL-3 ternary composite has shown a good variation in resistance. This composite has shown a better sensitivity of 82 % at 25,000 PPMv level. Along with this the ternary composite has depicted an appreciable response time of 34 s a recovery time of 37 s. The sensing stability of the composite also tested for 60 days. The detailed CO sensing mechanism was discussed thoroughly.

1. Introduction

In these centuries, modernization and industrialization is the prime cause to lead the sophisticated life for mankind. While enhancing the comfortable life to humans, more undeniable problems hinder the ecosystem and public health. The increase in the quantity of the non-bio degradable constituents, toxic gases, heavy metals, e-waste brings the non-curable threats to the living beings. The detection and decomposition of these wastes gained researchers attention. In this modern world increased concentration of the toxic gases namely; ammonia, nitrogen dioxide, carbon monoxide (CO) and sulfur dioxide bring serious diseases. Among the toxic gases, CO is the most dangerous pollutant which dangerous for both flora and fauna. CO is colorless, odorless, tasteless gas which has formed due to the incomplete combustion of the organic materials [1]. The perilous effects like decrease the oxygen caring efficiency in blood, irritation on skin, dizziness, hallucination, loss of locomotory and respiratory problems are caused due to increase in the CO concentration. So, CO detection and monitoring sensors are very essential and effective for today.

The conducting polymers plays a vital role in most of the research fields [2]. The research in conducting polymer science has become inter disciplinary subject, as it consolidates in physics, chemistry, biology, environmental science and engineering field. As a consequence of the diverse applications of conducting polymers it has become major endowment in every aspect of society. Among the conducting polymers polyaniline (PANI), polypyrrole and polyacetylene are more advantageous, because they are associated with π-bonds and σ-bonds [3]. In the group of conducting polymers polyaniline has captured more attention due to its chemical feasibility, cost effectiveness and eas-y synthesis [4–8]. In recent years, polymer-based composites have sought greater

---

* Corresponding author.
  E-mail address: chethanbchetu@gmail.com (B. Chethan).

From,
Dr. Sunilkumar A
Department of physics
BITM, Ballari

To,
The Deputy Director,
BITM, Ballari

Respected sir,

Sub:- Requesting incentive for publication

With reference to above cited subject, I hereby inform you that one of my paper has published in Science citation index expanded journal in Feb-2023, please consider my request ~~subject~~ and do the needful.

thanking you

yours faithfully

W.A

Date: 15/2/2023
place: Ballari

PAY Rs 15,000

WoS citation
Since 1990. ISSN 0157-4522
WoS - expanded C 167/000

17/2/23

15/02/2023

Polyaniline/vanadium pentoxide/lead tetroxide ternary composite for LPG sensing

S. S. Shanawad[1], A. Sunilkumar[2], B. S. Khened[3], B. Chethan[4],* , V. Prasad[4], M. G. Kotresh[5], T. M. Sharanakumar[6], and V. S. Veena[7]

[1] Department of Physics, JSS Banashankari Arts Commers and SK Gubbi Science College, Dharawad, Karnataka 580004, India
[2] Department of Physics, Ballari Institute of Technology and Management, Ballari, Karnataka 583104, India
[3] Department of Electrical and Electronics Engineering, Ballari Institute of Technology and Management, Ballari, Karnataka 583104, India
[4] Department of Physics, Indian Institute of Science, Bengaluru, Karnataka 560012, India
[5] Department of Studies in Physics, Vijayanagara Sri Krishnadevaraya University, Ballari, Karnataka 583104, India
[6] Department of Chemistry, Ballari Institute of Technology and Management, Ballari, Karnataka 583104, India
[7] Department of Physics, Government First Grade College, Madhugiri, Karnataka 572132, India

ABSTRACT

In the present work, Gas sensing performance of the amalgamated vanadium pentoxide (V_2O_5) and lead tetroxide (Pb_3O_4) in proportionate order with 10, 20, 30, 40, and 50 wt% in polyaniline (PANI) ternary composites has been studied. For the study, the samples are synthesized by in situ polymerization technique. The synthesized composites were characterized and confirmed using Fourier transform infrared spectroscopy (FTIR), X-ray diffraction (XRD), and scanning electron microscope (SEM) studies. Supporting to gas sensing, AC conductive studies are carried out at room temperature in the frequency ranging from 50 to 1 MHz. The PV3 ternary composite (PANI/ V_2O_5 + Pb_3O_4—30%) has depicted an enhanced conductivity compared to pristine PANI and other ternary composites. The complex plane impedance plots depict good agreement with the conductivity studies. The liquified petroleum gas (LPG) sensing studies are carried out at ambient temperature (29 °C) and at relative humidity of 45%. For the study, the film of all the samples is made using spin coating unit. Among PANI and all the ternary composites, PV3 ternary composite has shown a good variation in resistance. This composite has shown a better sensitivity of 97.05% at 25,000 PPMv level. Along with this, the PV3 ternary composite has depicted an appreciable response time of 29.15 s and a recovery time of 35.26 s. The sensing stability of the composite was also tested for 60 days. The detailed LPG sensing mechanism was discussed deliberately.

S. S. Shanawad and A. Sunilkumar have contributed equally to this work.

Address correspondence to E-mail: chethanbchetu@gmail.com; chethanb@iisc.ac.in

To,
Deputy Director,
BITM, Ballari

Date
13|3|23

From,
Dr. Sunil Kumar A
Associate professor
BITM, Ballari

Sub: Regarding incentive for publication.

Respected sir,

With reference to above cited subject I have published a paper in Science Citation index (Scopus) journal. please consider and grant one incentive for publication.

thanking you

ISSN: 0097-6156

Since 1916.

Scopus indexed - book chapter.

₹ 3,000

13/03/2023

yours faithfully

th. A
Dr. Sunilkumar A

PAY R 3000/-

17/3/23

ACS Publications
Most Trusted. Most Cited. Most Read.

Q ≡

RETURN TO BOOK

< PREV   **CHAPTER**   NEXT >

ACS SYMPOSIUM SERIES eBooks

Trends in Development of Nanomaterial-Based Sensing Devices

B. Chethan*, V. Prasad, A. Sunilkumar, V. S. Veena, and S. Thomas

Read Online

PDF (4 MB)

SUBJECTS: 3D printing, Electrodes, ˅

Abstract

Department of Mechanical Engineering
The National Institute of Engineering

(An Autonomous Institute under VTU, Belagavi)
Mysuru-570008

CERTIFICATE

NIE
ESTD 1946

MED

Sponsored by
Ministry of MSME,
Government of India

In association with
Visweswaraya Technological
University, Belagavi

This is to certify that

Dr. Raghavendra P

Ballari Institute of Technology & Management

Participated in

Five Days Workshop On

RECENT TRENDS IN AUTOMATION
TECHNOLOGIES FOR MSME DEVELOPMENT

Organized by the Department of Mechanical Engineering

From 30th January to 03rd February 2023
at The National Institute of Engineering, Mysuru

INDUSTRY PARTNERS

HYDAC   JANATICS Pneumatic   VIDYUT AUTOMATION   rexroth A Bosch Company   AUTOMATION STUDIO

XNG   FLUIDTECHNIK SOLUTIONS
Fluid Power Piping, Services & Training

Shri Akadas G
Director, MSME- DFO, Bengaluru

Dr. Shivakumar H R
Regional Director, VTU - RO, Mysuru

Dr. Rohini Nagapadma
Principal, NIE

An Analysis of the Performance of a Grid-Connected Hybrid Power Generation System Combining Wind and SOFCs, with an Ultracapacitor Storage Unit

Dr. Santhosha Kumar A
Department of Electrical and Electronics,
Central University of Karnataka,
Gulbarga, India
0000-0002-3336-6215

Ramakrishna S S Nuvvula
Department of Electrical and Electronics,Engineering
GMR Institute of Technology
Rajam, India
nramkrishna231@gmail.com

Hasan Koten
Mechanical Engineering
Istanbul Medeniyet University
Istanbul, Turkiye
0000-0002-1907-9420

Raghavendra P
Department of Electrical and Electronics,Engineering
Ballari Institute of Technology and Management,
Ballari, India
0000-0002-3874-7033

Polamarasetty P Kumar
Department of Electrical and Electronics,Engineering
GMR Institute of Technology
Rajam, India
praveenindia.p@gmail.com

Abstract - **This paper explores the usage of hybrid power generation system based on a Solid Oxide Fuel Cell (SOFC), Wind, and an Ultra-Capacitor (UC) in a grid-connected scheme. The UC acts as an energy storage system to compensate for the slow dynamic response of the SOFC. This combination of components effectively maintains a stable output of power from the Wind system. Control systems are implemented to manage the power converters associated with the energy system to meet the expected demand. The SOFC needs to increase its power in the face of changes in the inverter power or a decrease in Wind power, and in both cases, the UC supplies energy until the SOFC reaches the desired power output level. Recharging of the UC is done using Wind power. The hybrid system is capable of providing constant power irrespective of fluctuations in wind speed. Results obtained from simulations are presented to demonstrate the performance of the hybrid system with respect to the changing wind speed and load.**

Keywords—component, formatting, style, styling, insert (key words)

I. INTRODUCTION

The demand for electrical power is increasing rapidly while meeting the increasing demand at the same pace is difficult due to economical, environmental and time constraints associated with building new power plant. The strive for clean power generation has became a priority for energy sector due to increased awareness regarding environmental issues on using fossil fuels. Clean energy generation and reducing the demand-generation gap can be achieved using small scale generation placed near the load centre. The power generation in range of few kilowatts to a megawatts are termed as distributed generation (DG) [1]. The distributed generators are placed near load centre and have advantages like utilization of local resources, reduction of stress on distribution system, voltage support. However the DG can affect the system adversely if proper care is not taken in sizing and placement [1]. The distributed generation based on renewable resources uses naturally available resources to produce electricity such as PV (photo voltaic), wind, tidal, geothermal. The fuel cell and micro-turbine are the DG's gaining importance nowadays due to high efficiency and combined heat and power applications.

Among the renewable based distributed power generation the PV and wind has gained more importance and has well established technology. The wind system is one of the old technology utilizing wind power to generate electrical power. The wind based power generation has disadvantage as the output is fluctuating as wind speed varies widely, seasonally and timely [2]. However the load requirement is constant hence wind systems are associated with energy storage systems. The batteries are commonly used as storage system with wind system to store the energy when the wind power is available and release it as per load requirement. The system output is limited by wind power availability, battery capacity and it's state of charge. The batteries are high energy density devices and suitable for constant output requirements. However as wind varies widely the battery also undergoes uneven charging and discharging cycle which affects the life of battery [3]. In order to support the battery life the UC are used [4]. The ultra- capacitor is a high power density device, able to deliver the burst of power instantly and can undergo high number charging/discharging cycles. The better way to tackle the issue with wind system is to combining different resources to supply constant power. The combining different resources leads to hybrid generation system.

AI-based technologies are gaining prominence as a means

Research Article

Voltage Profile Analysis in Smart Grids Using Online Estimation Algorithm

P. Raghavendra [iD],[1] **Ramakrishna S. S. Nuvvula** [iD],[2] **Polamarasetty P. Kumar,**[2] **Dattatraya N. Gaonkar** [iD],[3] **A. Sathoshakumar** [iD],[4] **and Baseem Khan** [iD][5]

[1]*Department of Electrical and Electronics, Ballari Institute of Technology and Management, Ballari, India*
[2]*Department of Electrical and Electronics, GMR Institute of Technology, Rajam, Andhra Pradesh 532127, India*
[3]*Department of Electrical and Electronics, National Institute of Technology Karnataka, Surathkal, India*
[4]*Department of Electrical and Electronics, Central University of Karnataka, Gulbarga, India*
[5]*Department of Electrical and Computer Engineering, Hawassa University, Hawassa, Ethiopia*

Correspondence should be addressed to Ramakrishna S. S. Nuvvula; nramkrishna231@gmail.com and
Baseem Khan; baseem.khan04@ieee.org

Voltage rise is the main obstacle to prevent the increase of distributed generators (DGs) in low-voltage (LV) distribution grids. In order to maintain the power quality and voltage levels within the tolerance limit, new measurement techniques and intelligent devices along with digital communications should be used for better utilization of the distribution grid. This paper presents a real-time sensor-based online voltage profile estimation technique and coordinated Volt/VAR control in smart grids with distributed generator interconnection. An algorithm is developed for voltage profile estimation using real-time sensor remote terminal unit (RTU) which takes into account topological characteristics, such as radial structure and high R/X ratio, of the smart distribution grid with DG systems. A coordinated operation of multiple generators with on-load tap changing (OLTC) transformer for Volt/VAR control in smart grids has been presented. Direct voltage sensitivity analysis is used to select a single DG system for reactive power support in multi-DG environment. The on-load tap changing transformer is employed for voltage regulation when generators' reactive power contributions are not enough to regulate the voltages. Simulation results show that the reported method is capable of maintaining voltage levels within the tolerance limit by coordinated operation of DG systems and on-load tap changing transformer.

1. Introduction

Proliferation of distributed generation is expected to change the operation and control of existing power grids. Interconnection of distributed generators at low voltage levels improves network reliability, power quality, and efficiency and reduces overall power loss. In order to achieve these benefits with large penetration of DG source in existing utility networks, several technical problems are to be faced such as voltage regulation, islanding of DG, degradation of system reliability, power quality problems, and protection and stability of the network [1, 2]. Voltage rise problem is the main obstacle for the growth of distributed generators in low-voltage distribution grids [3]. This is very important as traditional distribution networks are designed to maintain customer voltage constant within the tolerance limit. Therefore, new measurement techniques and intelligent devices along with digital communications should be employed in low-voltage distribution grids in order to maintain the power quality and voltage levels within the tolerance limit. Emerging smart grid technologies will address the enormous challenges to be faced by the integration of high levels of DG sources into future distribution grids. A key feature of a smart grid system is the use of

Elite

NPTEL Online Certification
(Funded by the MoE, Govt. of India)

This certificate is awarded to

MALLULA VIJAYA KRISHNA

for successfully completing the course

Electric Vehicles - Part 1

with a consolidated score of **86** %

Online Assignments	21.67/25	Proctored Exam	64.28/75

Total number of candidates certified in this course: **1010**

Prof. Devendra Jalihal
Chairperson,
Centre for Outreach and Digital Education, IITM

Jan-Feb 2023
(4 week course)

Prof. Andrew Thangaraj
NPTEL, Coordinator
IIT Madras

Indian Institute of Technology Madras

FREE ONLINE EDUCATION
swayam

EDUXLABS
edu's Xpert (Esoir Solution)

MECHANICA 2022
IIT-MADRAS

CERTIFICATE OF COMPLETION

THIS IS PRESENTED TO

Shridhar S M

has successfully completed

3-Days Live Online workshop on

Basics of Electric Vehicles and its Design Process

From 27th Oct - 29th Oct 2022

Organized by: EduxLabs (Esoir Business Solution LLP)

in Association with Mechanica IIT Madras

AJAY SINGH SITOLE
Secretary
MEA, IIT-MadrAs

Issued on:
30th Oct 2022

MD.NAFISH
Eduxlabs Director
(Esoir Business Solution)

GSSS | GEETHA SHISHU SHIKSHANA SANGHA®

INSTITUTE OF ENGINEERING AND TECHNOLOGY FOR WOMEN

(Affiliated to VTU, Belagavi, Approved by AICTE, New Delhi & Govt. of Karnataka)

K R S ROAD | METAGALLI | MYSURU - 570016 | KARNATAKA | INDIA

NBA NATIONAL BOARD OF ACCREDITATION — Accredited Branches: ECE, CSE, ISE Validity : 01.07.2017 - 30.06.2023 & EEE Branch up to 30.06.2024

Accredited with Grade 'A' NAAC

QS I·GAUGE INDIAN COLLEGE RATING SILVER

ATAL RANKING OF INSTITUTIONS ON INNOVATION ACHIEVEMENTS Recognised Band EXCELLENT Colleges / Institutes (Private / Self Financed) Technical

IEEE BANGALORE SECTION

IEEE MYSORE SUBSECTION

IEEE PES Power & Energy Society® BANGALORE CHAPTER
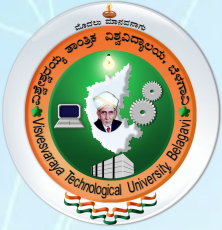
Participation Certificate

This is to certify that

SHRIDHAR S M , Assistant Professor

Ballari Institute of Technology and Management

has actively participated in the workshop on *"Recent Developments in Smart Grid and Applications"* in association with VTU, Belagavi and IEEE PES Chapter, from **05th- 07th September 2022,** Organized by Department of Electrical and Electronics Engineering, GSSSIETW, Mysuru.

HOD-EEE
Dr. G Sreeramulu Mahesh

Principal
Dr. Shivakumar M

Technical Co-Sponsor

IEEE BANGALORE SECTION

2nd IEEE International Conference on
Distributed Computing and Electrical Circuits and Electronics
ICDCECE-2023

Organized by
Ballari Institute of Technology and Management, Ballari

CERTIFICATE OF APPRECIATION

Sharana Reddy

For the paper titled...... Transient Analysis of Motor Terminal Voltage, Common Mode Voltage and Bearing Voltage in 2-level and Multilevel PWM Inve ....

presented by.............**Sharana Reddy**..........................which has been selected as the Best Paper amongst presented papers in the 2nd IEEE International Conference on Distributed Computing and Electrical Circuits and Electronics (ICDCECE-2023), organized by the Ballari Institute of Technology and Management, Ballari, India in association with IEEE Bangalore Section and IEEE Information Society on 29th-30th April, 2023.

Dr. Abdul Lateef Haroon P S
Publication Chair
ICDCECE-23

Dr. Yadavalli Basavaraj
Principal
BITM

Mr. Prithviraj Y J
Trustee/Dy. Director
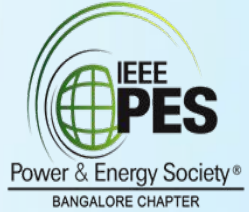BITM

GSSS | GEETHA SHISHU SHIKSHANA SANGHA®

INSTITUTE OF ENGINEERING AND TECHNOLOGY FOR WOMEN

(Affiliated to VTU, Belagavi, Approved by AICTE, New Delhi & Govt. of Karnataka)

K R S ROAD | METAGALLI | MYSURU - 570016 | KARNATAKA | INDIA

NBA NATIONAL BOARD OF ACCREDITATION — Accredited Branches: ECE, CSE, ISE
Validity : 01.07.2017 - 30.06.2023 & EEE Branch up to 30.06.2024

Accredited with Grade 'A' NAAC

QS I-GAUGE INDIAN COLLEGE RATING SILVER

ATAL RANKING OF INSTITUTIONS ON INNOVATION ACHIEVEMENTS
Recognised
Band EXCELLENT
Colleges / Institutes (Private / Self Financed) Technical

IEEE BANGALORE SECTION

IEEE MYSORE SUBSECTION

IEEE PES Power & Energy Society®
BANGALORE CHAPTER
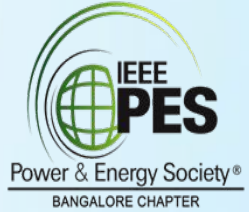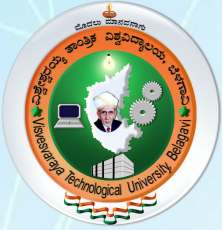
Participation Certificate

This is to certify that

Dr Sharana Reddy , Professor

Ballari Institute of Technology and Management

has actively participated in the workshop on *"Recent Developments in Smart Grid and Applications"* in association with VTU, Belagavi and IEEE PES Chapter, from **05ᵗʰ- 07ᵗʰ September 2022,** Organized by Department of Electrical and Electronics Engineering, GSSSIETW, Mysuru.

HOD-EEE
Dr. G Sreeramulu Mahesh

Principal
Dr. Shivakumar M

Elite

NPTEL Online Certification

(Funded by the MoE, Govt. of India)

This certificate is awarded to

SANTHOSHA B M

for successfully completing the course

Electric Vehicles - Part 1

with a consolidated score of **84** %

Online Assignments	22.5/25	Proctored Exam	61.22/75

Total number of candidates certified in this course: **1010**

Devendra Jalihal

Prof. Devendra Jalihal
Chairperson,
Centre for Outreach and Digital Education, IITM

Jan-Feb 2023

(4 week course)

Prof. Andrew Thangaraj
NPTEL, Coordinator
IIT Madras

Indian Institute of Technology Madras

FREE ONLINE EDUCATION
swayam
शिक्षित भारत, उन्नत भारत

Roll No: NPTEL23EE01S44440128

To validate the certificate

No. of credits recommended: 1 or 2

International conference on

Indian Knowledge Systems

Issues, Strategies and a Way Forward

16th -18th March 2023
Yuvapatha
31st Cross, 11th Main Rd, 4th Block,
Jayanagar, Bengaluru

CHANAKYA UNIVERSITY

THE ART OF LIVING

Certificate of participation

This is to certify that

Prof/Dr/Sri/Smt...... Y KAMAL KISHORE

ASSISTANT PROFESSOR, BITM, BALLARI

has participated as

Chairperson/Discussant/Rapporteur/Delegate

at the International conference on

Indian Knowledge Systems: Issues, Strategies and A way forward

at Bengaluru from 16th – 18th March 2023

Prof H S Ashok
Dean-Research (I/C), Chanakya University

Prof Ganti Suryanarayana Murthy
Director, IKS-GOI

Prof Shrinivasa Varakhedi
Vice chancellor, Central Sanskrit University

RJC

NOVEL SYNTHESIS, CHARACTERIZATION AND ANTIMICROBIAL ACTIVITY OF N-(5BROMO-2-(5-PHENYL-1,3,4-OXADIAZOL-2-YL)NAPHTHA[2,1-B]FURAN-1-YL)ACETAMIDE AND N-(5-NITRO-2-(5-PHENYL-1,3,4-OXADIAZOL-2-YL)NAPHTHA[2,1-BFURAN-1-YL]ACETAMIDE AND THEIR DERIVATIVES

K. M. Nagarsha[1], T. M. Sharanakumar[2], D. Ramesh[3], N. Y. Praveen Kumar[4], M. N. Kumarswamy[3], D. R. Ramesh[5] and K. P. Latha[1,✉]

[1]Department of Chemistry, Sahyadri Science College, Kuvempu University, Shivamogga-577202, Karnataka, India

[2]Department of Chemistry, Ballari Institute of Technology and Management, Ballari-583104, Karnataka, India

[3]Department of Chemistry, Sir M V Government Science College, Bhadravathi-577303, Shivamogga, Karnataka, India

[4]Department of Chemistry, Vijayanagara Srikrishnadevaraya University, Ballari-583103, Karnataka, India

[5]Department of Chemistry, Government First Grade College, Shikaripura-577427, Shivamogga, Karnataka, India

[✉]Corresponding Author: latha119@gmail.com

ABSTRACT

The novel derivatives of naphtho-furan such N-(5bromo-2-(5-phenyl-1,3,4-oxadiazol-2-yl)naphtha[2,1-b]furan-1-yl)acetamide (8), N-(5-bromo-2-(hydrazinecarbonyl)naphtha[2,1-b]furan-1-yl]acetamide (7), ethyl-1-acetamido-5-bromonaphtho[2,1-b]furan-2-carboxylate (6), N-(5-nitro-2-(5-phenyl-1,3,4-oxadiazol-2-yl)naphtha[2,1-bfuran-1-yl]acetamide (5), N-(2-(hydrazinecarbonyl)-5-nitronaphtho[2,1-b]furan-1-yl)acetamide (4), ethyl-1-acetamido-5-nitrpnaphtho[2,1-b]furan-2-carboxylate (3), are prepared by ethyl-1-acetamidonaphtho[2,1-b]furan-2-carboxyate and ethyl 1-aminonaphtho[2,1-b]furan-2-carboxylate. All newly synthesized compounds were confirmed by Mass, NMR, and FTIR spectroscopic techniques. Those compounds were used for antimicrobial activity it exhibits good antibacterial and anti-functional activity.

Keywords: Naphthofuran, Furan, Antibacterial Activity, Antimicrobial Activity, Oxidiazoles.

RASAYAN J. Chem., Vol. 16, No.1, 2023

INTRODUCTION

The Survey of the literature revealed that the attraction the researchers in the field of heterocyclic chemistry[1] is high, a wide range of heterocyclic molecules that have the greatest deal with their biological activeness and also they make good development of novel compounds with their unique properties. The new synthesis of a variety of heterocyclic moieties has to pay high attention to organic chemists over many years mainly due to their importance in pharmacological activity.[2] The existence of nitrogen and oxygen in a heterocyclic ring system has attracted the organic researcher because of their multiple effects on biological activities[3] and pharmacological activities.[4] Oxidiazoles[5] are important five-membered heterocyclic compounds having nitrogen and oxygen as hetero atom. Oxadiazoles have shown a key role in the evolution of principles in heterocyclic chemistry and also are considered advantageous in the medicinal field. Oxadiazole forms four possible isomers. Now a day's most researchers are more attracted to the 1,3,4-oxadiazole[6] isomer due to its high potential biological activeness.[7] The synthesis of series 1,3,4-oxadiazole molecule with 2,5-disubstituted[8] is known substantial pharmaceutical importance.[9]

International Conference

CERTIFICATE

This is to certify that....SHARAN....KUMAR....T.M.....

....BALLARY....INSTITUTE....OF....TECHNOLOGY & MANAGEMENT has participated as
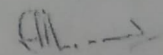
~~Chair person~~ / ~~Resource person~~ / ~~Oral Presenter~~ / Poster Presenter / ~~Delegate~~ in the International

Conference on "Recent Advancements in Chemistry" held on 23rd November 2022, organised by the

Department of Chemistry, Field Marshal K.M. Cariappa College, Madikeri.

. Poster presentation - Third place

Dr. Manjunatha J. G.
Convener

Dr. C Jagath Thimmaiah
Principal

From,

Dr. Sharanakumar T M
Asst Prof
Dept of Chemistry
BITM, Ballari

To,

The Director/Deputy Director
BITM, Ballari

Through HOD & Dean R&D

Respected Sir,

Subject:- Requesting for Incentive for publication regarding.

With reference to the above subject, I hereby inform you that our one of the paper title Determination of OAP by Novel Co(II) phthelocyanine with Appliance of composite MW CNTs was published in the Electrocatalysis Science Direct Journal. So please I request you to Sanction incentive for the above publication at the earliest..

28/12/22

PAY R 15,000/-
chem - R&D

Thanking you

your's faithfully

(Dr. Sharanakumar T M)

Forwarded to
Dean (R&D) & Deputy Director

28.12.22   23/12/2022

pos indexed.
forwarded verition.
R (15,000)   28/12/2022

Date:-
place:- Ballari

Determination of o-Aminophenol by Novel Co(II) Phthalocyanine with Appliance of Composite MWCNTs

T. M. Sharanakumar[1,2] · Mounesh[1] · N Y Praveen Kumar[1] · KR Venugopala Reddy[1] · A. Sunilkumar[3]

Abstract

A novel peripherally tetra naphthol substituted Co(II) phthalocyanine (NCoPc) was synthesized by the reaction of naphthol linked phthalonitrile, and cobalt chloride, in the presence of catalytic amount of DMF, DBU, and K_2CO_3. The NCoPc and its composite with MWCNTs were characterized by FTIR, NMR, UV–Vis, XRD, TGA, and mass spectroscopic techniques. The NCoPc and NCoPc-MWCNTs-coated glassy carbon electrodes (GCEs) were used to electrochemically detect and quantify ortho amino phenol (oAP) oAP in aqueous solutions. Cyclic voltammetric data established a linear response between the oAP oxidation current (ipa) and its molar concentration (10–190 μM). The limit of detection (LoD) of the two modified electrodes was comparable (1.5 μM and 25 nM, respectively). The NCoPc and NCoPc-MWCNTs-GCEs (in the concentration range of 10–160 μM) were both low and comparable. The LoD values for oAP at the NCoPc-GCE and NCoPc-MWCNTs by DPV were 1.2 μM and 42 nM and CA were 10 nM and 6.5 nM, respectively. They are exhibited good electrocatalytic activity towards the oxidation of oAP, and this was aided by the improved conductivity of the composite modifiers.

Keywords Naphthol · Co(II) phthalocyanine · Ortho-aminophenol · Electrocatalytic activity · Sensors

Introduction

Researchers of new materials for electrochemical sensing are playing more attention towards electrode modification via electrochemical-polymerization [1]. These modified electrodes have found applications in electrocatalysis [2], biosensors [3], electrochromic devices [4], chemically modified electrodes [5], and corrosion protector [6].

The MPc and their derivatives are soluble in most common organic solvents; they exhibit good electrochemical and photovoltaic activities [7, 8]. Due to their high chemical and physical stability, the MPc compounds show excellent optical properties like nonlinear optical devices [9], medicinal and therapeutic agents [10], photodynamic therapy [11], semiconductors [12], catalysts [13], gas sensors, and dye industry. Jilani et al. have previously reported detection of oAP by a sorbaamide substituted electrode modified with a Co(II) phthalocyanine complex [1]. The Co(II) and Cu(II) phthalocyanine-modified electrodes have been used to detect the various environmental pollutants such as 2-amino-4-chlorophenol, p-aminophenol, o-aminophenol, and p-nitrophenol [14].

o-aminophenol is considered hazardous chemical which exceedingly affects the mankind. The high concentration phenol compound affects the nervous system, liver, kidney, and blood of human and animals [15]. Phenolic compounds are added as minor components of electrolytic strip tin coating, resin manufacturing, pesticide productions, pharmaceuticals, textile, paint, wood products, oil refining, plastics, explosives, ceramics, paper [16–18], hair-dyeing agents [19], antipyretic drugs [20], photographic developers [21], the reduction of o-aminophenol to ladder polymer [22], and dyes and pesticides [16].

We have prepared naphthol substituted Co(II) phthalocyanine (NCoPc) complex and its composite with MWCNTs, and these materials were used to prepare GCE-modified electrodes for oAP detection. The electrochemical oxidation of oAP at the electrodes exhibits excellent responses marked

✉ KR Venugopala Reddy
   venurashmi30@gmail.com

1   Department of Studies and Research in Chemistry, Vijayanagara Sri Krishnadevaraya University, Bellary 583105, Karnataka, India

2   Department of Chemistry, Ballari Institute of Technology and Management, Bellary 583104, Karnataka, India

3   Department of Physics, Ballari Institute of Technology and Management, Bellary 583104, Karnataka, India

Springer

From,
Mr. Sharanakumar T M
Asst prof
Dept. of chemistry
BITM, Ballari

To,
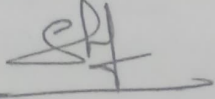The Director/ Deputy Director,
BITM, Ballari

Through HOD, Dean research & Development

Respected Sir,
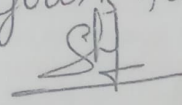
Subject:- Requesting for incentive for publication regarding.

With reference to the above subject, I am herewith submitting details of publication in scopus indexed journal.

Face page of the publication along with their Scopus details have been enclosed. I request you to Sanction incentive for the above publication at your earliest

Thanking you

yours faithfully

(Sharanakumar TM)

Date:- 14/11/22

Place :- Ballari

chemistry R & D

Pay R. 5000/-
14/11/22

warded to
ean (R&D)
Deputy Director
m, Ballary
14.11.22

In Scopus up to Present
Since 2008
Citation Score 2.0
SJR
14/11/2022

Journal details
Rasayan Journal of chemistry
Scopus indexed with Impact factor 1.45
ISSN NO:- 0974-1496

SYNTHESIS, CHARACTERIZATION, AND ANTIBACTERIAL ACTIVITIES OF NAPHTHO[2,1-b]FURAN DERIVATIVES

K. M. Nagarsha[1], T. M. Sharanakumar[2], D. Ramesh[3], M. N. Kumarswamy[3], and K. P. Latha[1,✉]

[1]Department of Chemistry, Sahyadri Science College, Kuvempu University, Shivamogga-577202, Karnataka, India

[2]Department of Chemistry, Ballari Institute of Technology and Management, Jnana Gangotri Campus, Bellary-583104, Karnataka, India

[3]Department of Chemistry, Sir M V Government Science College, Bhadravathi-577303, Shivamogga, Karnataka, India

✉Corresponding Author: latha119@gmail.com

ABSTRACT

The naphthofuran and its derivatives are important biological compounds so we have focused on the synthesis of naphthofuran derivatives. The synthesized compounds of ethyl 1-(acetylamino)-5-nitronaphtho[2,1-b]furan-2-carboxylate (3), and N-[2-((2Z)-2-benzylidenehydrazinyl)carbonyl]-5-nitronaphtho[2,1-b]furan-2-derivatives 5 (a-d) and 1-acetamido-5-nitro-N-(5-oxo-2-phenylthiazolidin-3-yl)naphtha[2,1-b]furan-2-carboxamide compounds of four derivatives 6 (a-d). The prepared compounds were confirmed by FTIR NMR, and mass methods. The prepared naphthofuran derivatives used for the antibacterial activity versus both Gram(+ve) and Gram(-ve) bacteria show excellent results. Therefore the synthesized compounds are used for further antibacterial studies in the medical field.

Keywords: Naphthofuran, Antibacterial, Heterocyclic, Biological Activity, Naphthol.

RASAYAN J. Chem., Vol. 15, No.4, 2022

INTRODUCTION

In medicinal chemist , nitrogen, oxygen, and sulfur-containing heterocycles are important f compounds. The naphthofuran is an organic derivative formed from the naphthalene ring into a heterocyclic furan ring.[1] Naphthofuran molecule has good structural moieties so it is used in important natural biological products and shows good biological and pharmacological activities.[2-4] Therefore, an attempt has been made to synthesize various novel N-substituted naphthofuran carboxamides carrying naphthofuryl rings and to study their antibacterial activities. So that we selected the naphtho[2,1-b]furan derivatives are chosen in the research work. Many synthetic compoundwith furan ring skeleton correlateed with novel biological activities like antibacterial, antifungal[5-7] antitumor[8,9], antiviral[10], anti-trypanosomal, cytotoxicity[11], and anthelmintic.[12]Thiazole is yet another major class of five-membered heterocyclic ring systems. Various naphtho [2,1- b]furan derivatives are fused with thiazole moiety and have been prepared and studied for many biological and pharmacological activities such as antibacterial, antifungal, diuretic, anthelmintic antimicrobial, analgesic, and anti-inflammatory.[13]
In this present work in order to study the various antibacterial activities we have described the synthesis of new naphthofuran derivatives of compound (3), and compound (4) used for the synthesis of N-(2-{[(2Z)-2-benzylidenehydrazinyl]carbonyl}-5-nitronaphtho[2,1-b]furan-1-yl)acetamide compounds of four derivatives 5 (a-d) and 1-acetamido-5-nitro-N-(5-oxo-2-phenylthiazolidin-3-yl)naphtha[2,1-b]furan-2-carboxamide compounds of four derivatives 6 (a-d). The prepared compounds were confirmed by NMR, FTIR, and mass, methods. The prepared naphthofuran derivatives were used for the antibacterial activity versus both Gram(+ve) and Gram(-ve) bacteria shows excellent results.

Journal Voucher

Dated : 10-Nov-22

No. :

Particulars		Amount
Travelling Expenses (Chemistry Dept.)	Dr	4,160.00
To Mrs. Vindhya R. - Chemistry Dept		4,160.00

On Account of :
TA & DA expenditure for trip to Bengaluru to attend FDP @ BMSIT-Bengaluru

₹ 4,160.00   ₹ 4,160.00

Authorised Signatory

3. Accounts department is required to disperse the above expenditure to the members accordingly

by Department of Chemistry at BI

Bengaluru – 560 064, from 31.10.2022 to 05.11.2022.

Coneveners

HoD, Chemistry

FINDING SOFTWARE FLAWS WITH DEEP NEURAL NETWORKS: A COMPARISON AND OPTIMIZATION

Gayatri Bajantri

Department of Computer Science & Engineering, BLDEA's V. P. Dr. P. G. Halakatti College of Engineering & Technology, Vijayapur-586103, Karnataka, INDIA
cse.gayatri@bldeacet.ac.in

Dr. Noorullah Shariff

Department of Artificial Intelligent and Machine Learning, Ballari Institute of Technology and Management, Ballari-583104, Karnataka, INDIA
cnshariff1@gmail.com

Abstract— The present detection performance has to be substantially enhanced because of the numerous flaws in complex software. Several methods of finding security flaws in code have been presented. There is a family of methods that use DL its means Deep Learning techniques that show promise. This study is an attempt to use Code BERT, a deep contextualised model, as an embedding solution to make it easier to find security flaws in C open-source projects. Code BERT's use for code analysis unearths previously unseen patterns in software, which may improve the efficiency of subsequent processes like software vulnerability identification. Based on BERT's design, Code BERT offers a bidirectional stacked encoder of transformers to make it easier to study security flaws in code via long-range dependency analysis. Furthermore, transformer's multihead attention method allows for several essential variables of a data flow to be concentrated on, which is vital for evaluating and tracking potentially sensitive data faults, and ultimately results in optimum detection performance. Word2Vec, Glove, and Fast Text are four mainstream-embedding approaches that are compared to one another in order to determine the efficacy of the proposed Code BERT-based embedding solution for creating software code embeddings. The experimental findings demonstrate that when it comes to downstream vulnerability detection tasks, Code BERT-based embedding works better than other embedding methods. In order to further improve efficiency, we recommended include synthetic vulnerable functions and performing fine tuning using both real-world and synthetic data to aid the model in learning susceptible code patterns in C. While doing so, we investigated which settings would best fit Code BERT. Evaluation results reveal that the updated model outperforms various state-of-the-art identification techniques on our dataset.
Keywords—BERT, Vulnerability, Embedding

I. INTRODUCTION

The vulnerability of software has been a major problem in cybersecurity research [1-3]. These security flaws pose a risk to the internet and computer systems of businesses and governments.

MANIPAL INSTITUTE OF TECHNOLOGY

MANIPAL

(A constituent unit of MAHE, Manipal)

Department of
Instrumentation and Control Engineering

CERTIFICATE OF PARTICIPATION

This is to certify that

Ms Syeda Badrunnisa Begum
Ballari Institute of Technology and Management

has Participated the DST-SERB and ISSE Manipal Chapter sponsored three-day workshop on

"Machine Learning Concepts for Modeling and Control of Nonlinear Systems"

organized by Department of Instrumentation and Control Engineering,

Manipal Institute of Technology, Manipal, between June 27-29, 2022.

Dr. Thirunavukkarasu Indiran
Convenor

Dr. Shreesha. C
HOD-ICE

Dr. (CDR). Anil Rana
Director-MIT

Basavarajeswari Group of Institutions

BITM
ESTD - 1997

ಬಳ್ಳಾರಿ ವಾಲೆಟಾಜೇಶ್ವರಿ ಆಫ್ ಟೆಕ್ನಾಲಜಿ & ಮ್ಯಾನೇಜ್‌ಮೆಂಟ್, ಬಳ್ಳಾರಿ
BALLARI INSTITUTE OF TECHNOLOGY & MANAGEMENT, Ballari
AUTONOMOUS INSTITUTE UNDER VTU, BELAGAVI
(Recognized by Govt. of Karnataka, Approved by AICTE, New Delhi)

Certificate

This is to certify that _____ **C.T.M. PRAVEEN KUMAR** _____ of CSE/AIML Department has participated in a **5-Day** Faculty Development Program on *"Industrial Advancement in Artificial Intelligence & Machine Learning"*, Organized by Department of CSE & Department of AIML, in association with Institution's Innovation Council, BITM, Ballari from 22-09-2022 to 26-09-2022.

Dr. B. M. Vidyavathi
HOD, AIML

Dr. R. N. Kulkarni
HOD, CSE

Dr. Y. Basavaraj
Principal

Mr. Y. J. Prithviraj Bhupal
Deputy Director

INSTITUTION'S INNOVATION COUNCIL

NATIONAL BOARD OF ACCREDITATION — NBA

NAAC ACCREDITED WITH A+ GRADE

Article

Gaussian Mutation–Spider Monkey Optimization (GM-SMO) Model for Remote Sensing Scene Classification

Abdul Lateef Haroon Phulara Shaik [1], Monica Komala Manoharan [2], Alok Kumar Pani [3], Raji Reddy Avala [4] and Chien-Ming Chen [5,*]

[1] Department of Electronics and Communication Engineering, Ballari Institute of Technology and Management, Ballari 583104, India
[2] School of Computer Science and Engineering, Vellore Institute of Technology, Chennai 600127, India
[3] Department of Computer Science and Engineering, CHRIST (Deemed to be University), Bangalore 560029, India
[4] Department of Mechanical Engineering, CMR Technical Campus, Hyderabad 501401, India
[5] College of Computer Science and Engineering, Shandong University of Science and Technology, Qingdao 266590, China
[*] Correspondence: chienmingchen@sdust.edu.cn

Abstract: Scene classification aims to classify various objects and land use classes such as farms, highways, rivers, and airplanes in the remote sensing images. In recent times, the Convolutional Neural Network (CNN) based models have been widely applied in scene classification, due to their efficiency in feature representation. The CNN based models have the limitation of overfitting problems, due to the generation of more features in the convolutional layer and imbalanced data problems. This study proposed Gaussian Mutation–Spider Monkey Optimization (GM-SMO) model for feature selection to solve overfitting and imbalanced data problems in scene classification. The Gaussian mutation changes the position of the solution after exploration to increase the exploitation in feature selection. The GM-SMO model maintains better tradeoff between exploration and exploitation to select relevant features for superior classification. The GM-SMO model selects unique features to overcome overfitting and imbalanced data problems. In this manuscript, the Generative Adversarial Network (GAN) is used for generating the augmented images, and the AlexNet and Visual Geometry Group (VGG) 19 models are applied to extract the features from the augmented images. Then, the GM-SMO model selects unique features, which are given to the Long Short-Term Memory (LSTM) network for classification. In the resulting phase, the GM-SMO model achieves 99.46% of accuracy, where the existing transformer-CNN has achieved only 98.76% on the UCM dataset.

Keywords: AlexNet; Gaussian Mutation–Spider Monkey Optimization; generative adversarial network; scene classification; VGG19

1. Introduction

Remote sensing images have a higher resolution from the advancement of imaging technology. Remote sensing images are used in many fields such as environmental monitoring, land use classification, change detection, image retrieval, and object detection. The remote sensing image scene classification task aims to classify the scene into remote sensing images based on semantic information, which is highly useful in practical applications [1]. Remote sensing image scene classification attracts many researchers due to its wide applications. Deep learning performs well for remote sensing scene classification for each category that has a sufficient number of labeled images [2]. Scene classification provides the accurate classification of satellite images and this is an essential problem in remote sensing images for a correct category such as farm, highway, river, and airplane for unlabeled images that are applied to interpretation tasks such as land resource management, residential planning, and environmental monitoring. Remote sensing scene classification has higher

image resolution than natural images, different target orientations, dense distribution, and small target objects [3]. Remote sensing scene classification is considered an assigned task for the specific semantic label of the remote sensing scene. This is used in a wide range of practical applications such as land use classification, natural disaster detection, environment prospecting, and urban planning [4,5].

In deep learning technology, Convolutional Neural Network (CNN) models provide efficient classification performance in various fields [6–13]. Common techniques of low-level feature extraction or hand-crafted features are structure, texture, spectrum, and color or combination of features to distinguish remote sensing images. Most representative feature descriptors such as SIFT, texture features, and color histograms are among the hand-crafted features. The low-level feature extraction performs better in remote sensing images for spatial arrangements and uniform structures that has limited performance in remote sensing images of semantic information [14,15]. Deep learning technique automatically extracts global features or high-level features for better learning of the input images. Recently, deep CNN methods have become the state-of-art model for remote sensing classification, yet they still have some limitations [16]. The existing CNN models have limitations of imbalanced data problem, overfitting and lower efficiency in classify similar images [17,18]. The contribution and objectives of this study are discussed in this research:

- Proposed GM-SMO to select the unique features from the extracted features that reduce the overfitting and imbalanced data problem. The GM-SMO model change the position of solution after exploration to increases the exploitation.
- Implemented GAN model is for augmentation of minority class and reduce the imbalanced data problem. The GAN model helps to distinguish the features for the objects and selects the unique features.
- The AlexNet and VGG19 models are used to extract high-level deep features from the input images. The deep features provide detailed information about the images that helps to achieve better classification. Further, the GM-SMO model balances exploration and exploitation ability of the model to further improve classification performance.

This paper is organized as follows: a literature survey of scene classification is given in Section 2 and the explanation of the GM-SMO model is given in Section 3. The simulation result is given in Section 4 and the result is given in Section 5. The conclusion is given in Section 6.

2. Literature Survey

The scene classification technique is helpful for many practical applications such as land utilization and planning. CNN-based models were widely applied for scene classification techniques and show considerable performance. Some of the recent CNN models in scene classification were surveyed in this section.

Xu et al. [19] applied a graph convolutional network using a deep feature aggregation technique named DFAGCN for scene classification. The pre-trained CNN model is applied for extracting multi-layer features and a graph CNN model was applied to effectively reveal convolutional feature maps. A weighted concatenation technique was applied to introduce three weighting coefficients to integrate multiple features. The graph CNN model has lower efficiency due to overfitting and imbalanced data problems. Bazi et al. [20] applied a vision transformer for scene classification in remote sensing and this is considered a state-of-art model in NLP as in the standard CNN model. Multi-head attention technique was applied as the main building block to extract information. Images in the patches were divided and flattening-embedding was used to keep the information. The first token sequence was applied to a softmax classification and several data augmentation technique was applied to generate more data for training. The overfitting problem occurs due to the generation of more features in a convolutional layer.

Alhichri et al. [21] applied a deep CNN model for remote sensing scene classification. CNN model learns feature maps from larger regions of scene and feature map was computed in attention technique as a weighted average of feature maps. The EfficientNet-

B3-Attn-2 was pre-trained CNN enhanced with attention technique. The weights are measured in the network using a dedicated branch. This model requires a greater number of images for training and has an overfitting problem. Ma et al. [22] applied a multi-objective model for scene classification named as SceneNet. Hierarchical optimization technique was applied to implement a more flexible search and coding process in remote sensing scene classification. Multi-objective optimization technique was applied to balance the performance error and computational complexity based on the Pareto solution set. The optimization technique has the limitation of local optima trap and overfitting in classification.

Zheng et al. [23] addresses the dilemma and applies multiple small-scale datasets for model generalization learning for efficient scene classification. A Multi-Task Learning Network (MTLN) was applied for training a network and handling heterogeneous data. The MTLN model considers each small dataset as an individual task and complementary information was used to improve generalization. The MTLN model has an imbalanced data problem and lower efficiency in handling the feature selection. Xu et al. [24] applied a Global Local Dual Branch Structure (GLDBS) using image discriminative features for various levels of fusion that was applied to improve performance on scene classification. CNNs model generate energy map to transform binary image to obtain a connected region. A dual branch network was constructed for CNN based models and the model was optimized using joint loss. The GLDBS model has lower efficiency in learn discriminative features and misclassification is occurring in more similar categories.

Tang et al. [25] applied an attention consistent network (ACNet) using Siamese network for remote sensing scene classification. The ACNet dual branch structure retrieves spatial rotation from image pairs of the input data and this helps to fully explore global features. The attention technique was introduced to mine the feature information from input images. The spatial rotation and similarities influences are considered in an attention model to unify the salient features. Bi et al. [26] applied Local Semantic Enhanced ConvNet (LSE-Net) for remote sensing scene classification. The LSE-Net model consists of discriminative representation and a convolutional feature extractor. A multi-scale convolution operator was combined with convolution features of multi-scale and multi-level for feature representation. The ACNet and LSE-Net models has an overfitting problem due to the generation of more features in the convolutional layer.

Cheng et al. [27] applied Inter Calibration (IC) and Self Calibration (SC) named as Siamese-Prototype Network (SPNet) for remote sensing scene classification. The support labels were used for supervised information to provide relevant features for classification. The three losses were used to optimize the model; one loss was used to learn feature representation, and thus provide an accurate prediction. The model has lower efficiency due to the overfitting problem and imbalanced data problem. Shamsolmoali et al. [28] applied a rotation equivalent feature pyramid network named REFIPN for remote sensing scene classification. The single shot detector was applied in the pyramid module for feature extraction and an optimization technique was applied to generate regions of interest. The model has lower efficiency due to overfitting and imbalanced data problem in classification.

Li et al. [29] applied Multi-Attention Gated Recurrent Network (MA-GRN) for remote sensing scene classification. Network multiple stages use features of local texture features and deep layers' global features. Spatial sequences were used for features and applied to GRU to capture long range dependency. The MA-GRN model has lower efficiency in classifying small objects and on imbalanced datasets. Zhang et al. [30] applied a combination of transformers and the CNN model for remote sensing scene classification. The self-attention was applied in ResNet model based on the Multi-Head Self-Attention model using spatial revolutions of 3×3 in bottleneck. The transformers are encoded to improve the feature representation based on attention. The transformer and CNN model have overfitting problems due to the generation of more features in the convolutional layer. In order to address the aforementioned concerns, a new model is proposed in this manuscript for effective remote sensing scene classification.

3. Proposed Method

The GAN model is applied to three datasets such as UCM, AID, and NWPU45 to augment images in minority classes. The AlexNet and VGG19 models were applied to extract the features from input images. The GM-SMO model is applied to extracted features to select relevant features for classification. The overview of GM-SMO model in scene classification is shown in Figure 1.
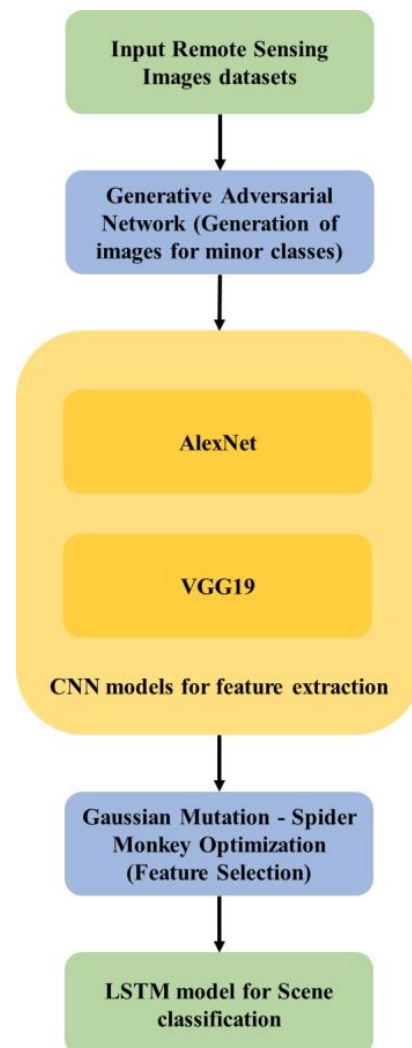
Figure 1. GM-SMO feature selection and CNN based feature extraction model for remote sensing scene classification.

3.1. Dataset Description

The proposed model's performance is analyzed on three benchmark datasets such as UCM, AID, and NWPU45. The AID includes 10,000 images with pixel size of 600×600 and 0.5 to 8 m resolution, and it includes 30 classes. Correspondingly, the UCM dataset contains 2100 images with pixel size of 256×256 and resolution of 0.30 m, and it includes 21 classes. Additionally, the NWPU45 dataset comprises 31,500 images with pixel size of 256×256 and resolution of 0.2–30 m. The NWPU45 dataset covers more than 100 nations' geo-locations and has 45 classes. The sample images of UCM, AID, and NWPU45 are represented in Figures 2–4.

Figure 2. Sample images of UCM dataset.
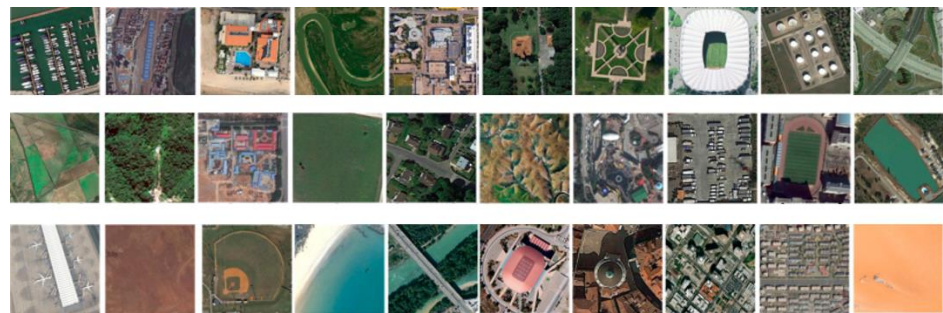
Figure 3. Sample images of AID dataset.
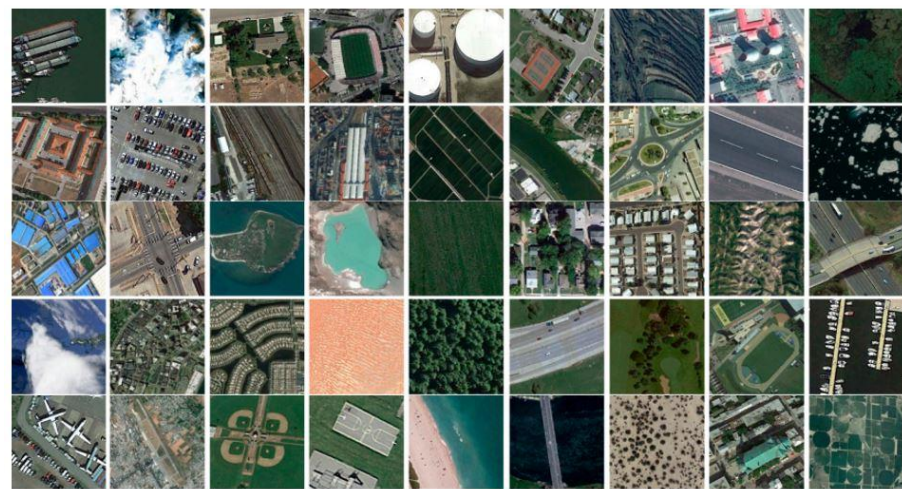
Figure 4. Sample images of NWPU45 dataset.

3.2. Generative Adversarial Network (GAN)

A generative model-specific framework is GANs. The generative model learns data distribution p_{data} from samples set x^1, ..., x^m (images) to generate new images based on learned data distribution. GANs model and its variants are used for generating labeled images: one part of the model involves learning the objects in the images based on class, separately, and the other involves class related to labeled classes.

The first variant of GAN is Deep Convolutional GAN (DCGAN). Radford et al. [31] proposed the architecture for both G and D networks of deep CNNs. This provides architectural steps for stable training of GAN and modification of Goodfellow et al. [32] original GAN, which is the basics for recent GAN research. Two neural networks are present in a model that is used to train simultaneously. The discriminator is the first network and this is denoted as D. The discriminator's role is to discriminate between samples real and fake. A sample x is imputed and output $D(x)$ is the probability of real

samples. Generator G is second network and samples are generated in the generator and D is real samples with high probability. The input samples $z^1, \ldots, z^m$ provide G from simple distribution p_z, usually a uniform distribution and the image space of distribution p_g maps $G(z)$. The objective of the model is to G achieve $p_g = p_{data}$, as in Equation (1).

$$\underset{G \quad D}{minmax} \mathbb{E}_{x \sim p_{data}} \log D(x) + \mathbb{E}_{z \sim p_z}[\log(1 - D(G(z)))] \tag{1}$$

The $D(x)$ is maximized to train the discriminator for images in the discriminator with $x \sim p_{data}$ and the model uses $x \nsim p_{data}$ for images to minimize $D(x)$. The $G(z)$ generates images in the generator to adjust D during training such that $D(G(z)) \sim p_{data}$. The generator is trained to increase $D(G(z))$, or equivalently reduce $1 - D(G(z))$. The generator increases its ability to generate more realistic images during training and the discriminator increases its ability to differentiate the real from generated images.

Generator Architecture: The generator network considers a vector of 100 random numbers from uniform distribution as input and output are provided as objects in remote sensing images in the size of $64 \times 64 \times 1$. The network architecture consists of a fully connected layer reshaped to a size of $4 \times 4 \times 1024$ and an up-sample of four fractionally strided convolutions in kernel size of 5×5 in the sample image. A deconvolution or fractionally-strided convolution is interpreted as pixels' expansion by applying zeros in between them. A larger output image was generated by convolution of the expanded image. Each network layer is applied with batch-normalization excluding the output layer. In the GAN learning process, the entire mini-batch was stabilized using normalizing responses to have unit variance and zero mean and the generator was prevented from collapsing all samples. ReLU activation function was applied in all layers and the output layer was applied with tanh activation function.

Discriminator Architecture: A typical CNN architecture has a discriminator network that considers input images in the size of $64 \times 64 \times 1$ and output is one decision (real or fake). The kernel size is set as 5×5 in four convolution layers of the network and a fully connected layer. Each convolution layer is applied with strided convolutions instead of pooling layers to reduce spatial dimensionality. Each layer of the network is applied with batch-normalization excluding input and output layers. Leaky ReLU activation functions $f(x) = \max(x, leak \times x)$ are applied in layers except for the output layer and sigmoid function with likelihood probability $(0, 1)$ image score in the output layer. The Generative Adversarial Network's [33] architecture is shown in Figure 5.
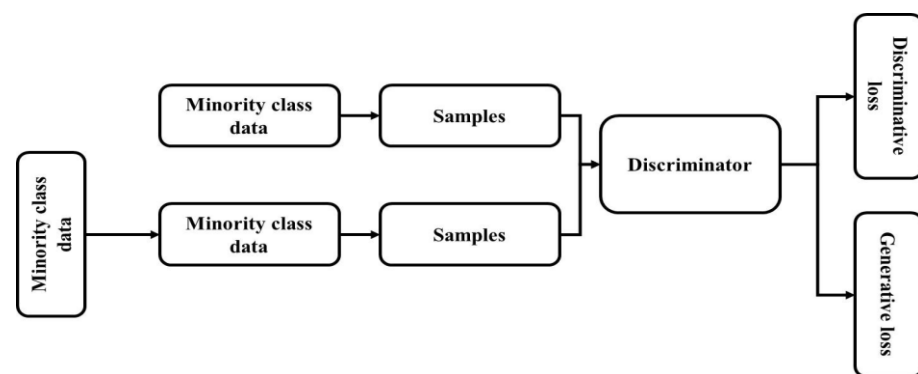
Figure 5. Generative Adversarial Network for generation of images in minority classes.

3.3. CNN-Based Feature Extraction

Convolution is a linear operation for feature extraction based on kernel, which is a small array of numbers. Kernel is applied on input for an array of numbers called a tensor [34,35].

A typical down-sampling operation is performed using a pooling layer to reduce feature maps of in-plane dimensionality. This introduces a translation invariance to small distortions and shifts, and decreases learnable parameters.

Pooling layer or final convolution of feature maps outputs are usually flattened, i.e., converted into a 1D array of numbers and connected to one or more fully connected layers, known as dense layers, so that every input is connected to a learnable weight of every output. The CNN architecture for feature extraction is shown in Figure 6.
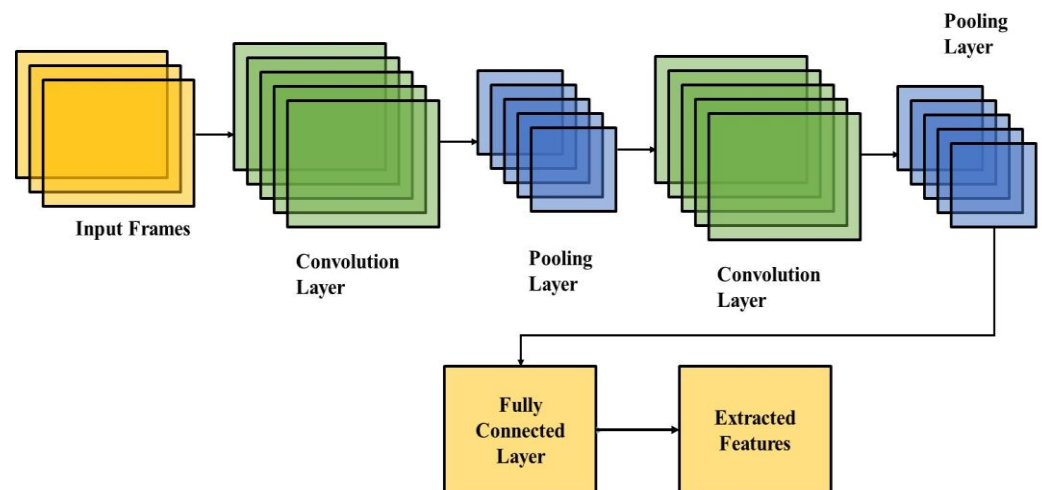
Figure 6. Convolutional Neural Network architecture for feature extraction process.

3.3.1. AlexNet

Various types of research [36,37] show AlexNet's successful performance in classification and more significant performance in image processing than previous models. The researchers in deep learning show much interest in AlexNet due to its efficiency.

AlexNet model is applied with activation function and activation function provides neural networks' non-linearity. Traditional activation functions are arctan function, tanh function, logistic function, etc. These functions generally cause gradient vanishing problems and a small range of 0 is applied with a larger gradient value. Rectified Linear Unit (ReLU) activation function is applied to overcome this problem. Equation (2) provides the ReLU model.

$$\text{ReLU}(x) = \max(x, 0) \tag{2}$$

The ReLU gradient provides 1 output if the input is not less than 0. This shows that ReLU function provides higher convergence than tanh unit in deep networks. More acceleration is gained during the training process.

The dropout layer is applied in a fully connected layer to solve the overfitting problem. The dropout layer trains only a part of the neurons and skips the remaining neurons to avoid overfitting. For instance, if dropout is set as 0.1, then 10% of the neurons are skipped in training for every iteration. Generalization is improved by dropout to minimize neurons' joint adaptation and cooperation between neurons. Dropout is applied on several sub-layers of the network. The same loss function is shared in each single sub-network and causes overfit to a certain extent. Sub-networks' entire network output is provided and dropout improves the robustness of the model.

Convolution and pooling layers automatically perform feature extraction and reduction in the model. Convolutional layers are applied for images to increase the performance. Considering image M in (m, n), size and convolution are given in Equation (3).

$$C(m, n) = (M \times w)(m, n) = \sum_{k} \sum_{l} M(m - k, n - l) w(k, l) \tag{3}$$

where kernel w size is (k, l), convolution provides a model solution to learn features of image and parameter sharing reduce complexity. Neighbouring pixel groups are applied in feature maps of pooling layer to reduce features and representation is provided by some values. The feature map size is 4×4, and every 2×2 block has max value to generate max pooling and reduce for feature dimension.

Cross change normalization improves generalization. The same position of several adjacent maps sum is provided by cross channel normalization in neurons. Normalized feature maps are applied to next layers.

Fully connected layers perform classification and neurons are connected to adjacent neurons in next layer. These layers use softmax activation function for the classification.

Softmax output is present in the range of (0, 1) to activate neurons. Overlapping pooling is performed and various input images from datasets are used for AlexNet training. The AlexNet architecture for feature extraction is shown in Figure 7.
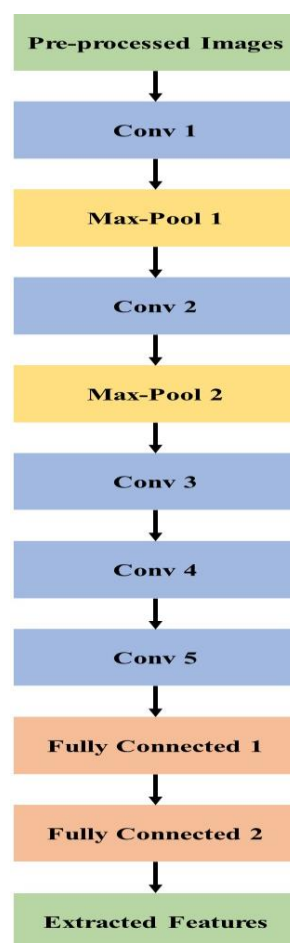
Figure 7. AlexNet model for feature extraction scene classification.

3.3.2. VGG 19

Oxford Robotics Institute developed a type of CNN model, which is named as Visual Geometry Group Network (VGG) [38,39]. VGGNet provides good performance in data cluster of ImageNet data. Five building blocks are present in VGG19. Two convolutional layers and one pooling layer are present in first and second building blocks, followed by four convolutional layers and one pooling layer which are present in the third and fourth blocks. Four convolutional layers are present in the final block and small filters 3×3 are used. The VGG19 architecture in feature extraction is shown in Figure 8.
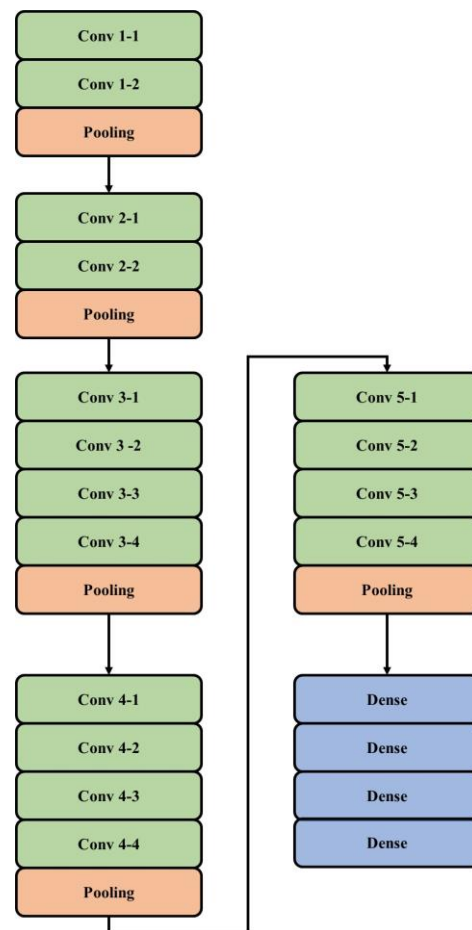
Figure 8. VGG19 architecture for feature extraction on scene classification.

3.4. Spider Monkey Optimization

The SMO technique is a metaheuristic technique based on the social behavior of the spider monkey, adopting fusion and fission swarm intelligence for foraging [40–43]. Spider monkeys are in groups of 40 to 50 members. Food searching tasks in a territory are divided by a leader. Generally, spider monkeys live with 40 to 50 members of a swarm and a leader decides to partition food searching tasks in a territory. A female lead is selected as a global leader in the swarm and, in case of food insufficiency, this creates mutable smaller groups. The group size is based on food availability of specific territory. The spider monkey's size is directly proportional to available food. The SMO based method of swarm intelligence (SI) satisfies the necessary conditions:

Labor division: smaller groups are created to divide foraging work for spider monkeys.
Self-organization: Food availability requirement is selected using group size.
An intelligent decision is carried out by intelligent foraging behavior.
Food search is initiated using swarm.
Food source individuals are measured using computing distance.
The food group members of individual's distance alter the locations for the consideration.
Food source individual distance is calculated.

SMO method uses train and error for six phases of collaborative iterative process: global leader decision phase, learning phase, global leader, global leader phase, local leader decision phase, local leader learning phase, and local leader phase. The SMO method work flow is represented in Figure 9.
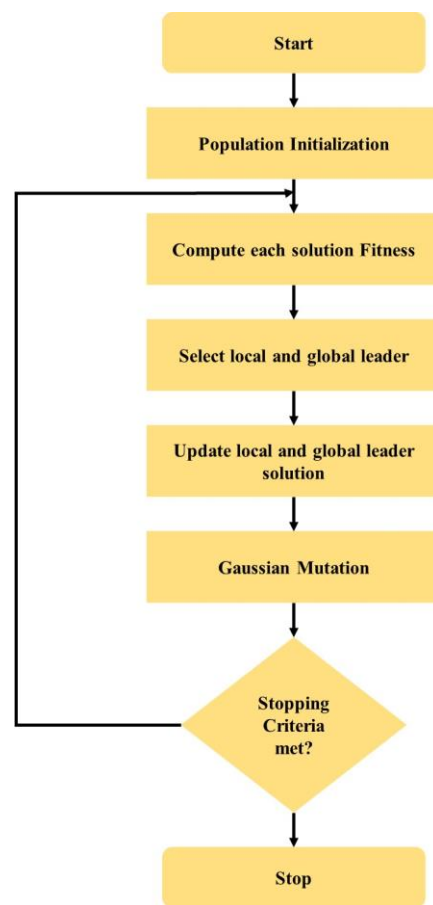
Figure 9. Gaussian Mutation–Spider Monkey Optimization for feature selection on scene classification.

The SMO method step-by-step process is given below.

3.4.1. Initializing

SMO method distributes population P of spider monkeys SM_p (where pth monkey of the population is denoted as SM_p, and $p = 1, 2\dots P$). Monkeys are M-dimensional vectors, where total number of variables is denoted as M. One possible solution of each SM_p is provided. SMO initializes each SM_p using Equation (4).

$$SM_{pq} = SM_{minq} + UR(0,1) \times \left(SM_{maxq} - SM_{minq}\right) \tag{4}$$

where
SM_{pq} is pth SM of qth dimension.
SM_p lower and upper bounds are SM_{minq} and SM_{maxq} in the qth direction for random number of UR (0, 1), uniform distribution is in range of [0, 1].

3.4.2. Local Leader Phase (LLP)

The current location is changed by SM using local group members and local leader past occurrences. The new location is updated for SM location if fitness value of new location is higher than previous location. The location update of pth SM of lth local group is provided in Equation (5):

$$SMnew_{pq} = SM_{pq} + UR(0,1) \times \left(LL_{lq} - SM_{pq}\right) + UR(-1,1) \times \left(SM_{rq} - SM_{pq}\right) \tag{5}$$

where
The lth local group leader location of qth dimension is denoted as LL_{lq}.

The *l*th local group of *l*th *SM* is randomly selected for *q*th dimension and is denoted as SM_{rq}, such that r, p.

3.4.3. Global Leader Phase (GLP)

After LLP, GLP is started to update the location. Experiences of local group members and global leader are used to update *SM* location. The location update is provided in Equation (6):

$$SMnew_{pq} = SM_{pq} + UR(0,1) \times \left(GL_{lq} - SM_{pq}\right) + UR(-1,1) \times \left(SM_{rq} - SM_{pq}\right) \quad (6)$$

where *q*th dimension of global leader location is denoted as GL_{lq} and an arbitrarily selected index is $q = 1, 2, 3, \dots M$.

The *SM* fitness calculates probability prb_p in this phase. The location of SM_p based on probability value, is updated and better location candidate has access to a number of possibilities to improve convergence. The probability calculation is given in Equation (7).

$$prb_p = \frac{fn_p}{\sum_{p=1}^{N} fn_p} \quad (7)$$

where *p*th SM fitness value is denoted as fn_p. The new location fitness of *SM*'s is calculated and compared with the previous location. The best fitness value of the location is considered.

3.4.4. Global Leader Learning (GLL) Phase

The global leader location update is performed using a greedy selection technique. The SM location updated is based on the global leader location for best fitness in the population. The global leader is applied with the optimum location. An increment of 1 is added to Global Limit Count if updates are encountered.

3.4.5. Local Leader Learning (LLL) Phase

The local group is applied using the greedy selection method to update the location of the local leader. The SM location is updated with local leader location for best fitness in a specific local group. The local leader is assigned to the optimum location. The increment of 1 is added to the Local Limit Count if no updates are encountered.

3.4.6. Local Leader Decision (LLD) Phase

Local group candidates modify the location randomly as per step 1 when a local leader does not update its location or uses the past information from local and global leaders based on *pr* using Equation (8).

$$SMnew_{pq} = SM_{pq} + UR(0,1) \times \left(GL_{lq} - SM_{pq}\right) + UR(0,1) \times \left(SM_{rq} - LL_{pq}\right) \quad (8)$$

3.4.7. Global Leader Decision (GLD) Phase

The population splits into small-size groups as per the global leader's decision if the location is not updated for a global leader up to the Global Leader Limit. The splitting process occurs for a maximum number of groups (MG) is received. A local leader is selected at each iteration for the newly shaped group. Allowed groups are created at the maximum number and the global leader does not update its position until the allowed limit of pre-fixed, then global leader aims to merge entire groups into a single group.

The SMO processing controls parameters are as follows:

Perturbation rate (pr)
Max number of groups (MG)
GlobalLeaderLimit
Value of LocalLeaderLimit

3.4.8. Gaussian Mutation

The SMO method is trapped in a local optimum in complex problems of the iterative optimization process. During iteration, the algorithm solution value remains unchanged. To increase the algorithm probability and algorithm shortcoming, this technique jumps out of the position of local optimal and adds random perturbation and Gaussian mutation and continues to process the algorithm. The Gaussian mutation formula is shown in Equation (9).

$$x^{i,iter+1} = \begin{cases} x^{i,iter} + rand & if \ r \geq 0.2 \\ x^{i,iter} \times Gaussian(\mu, \sigma) & otherwise \end{cases} \tag{9}$$

where random perturbation or Gaussian mutation selection probability is r_j and *rand* was a random number in the range of [0, 1]. The distribution of Gaussian variation is given in Equation (10).

$$Gaussian(\mu, \sigma) = \left(\frac{1}{\sqrt{2\pi\sigma}} \right) \exp \left(-\frac{(x-\mu)^2}{2\sigma^2} \right) \tag{10}$$

where the variance is denoted as σ^2 and the mean value is denoted as μ.

3.5. LSTM Model

The LSTM model is introduced by Hochreiter and Schmidhuber [44] as an evolution of the RNN model. This model overcomes the limitation of RNN using additional interactions per module. LSTMs are a type of RNN that learn long-term dependencies and remember information for a long time as a default. A chain structure of the LSTM model is given in research [45]. A different structure is present in the repeating module. Four interaction layers with unique communication method is applied instead of standard RNN or a single neural network. The LSTM structure is shown in Figure 10.
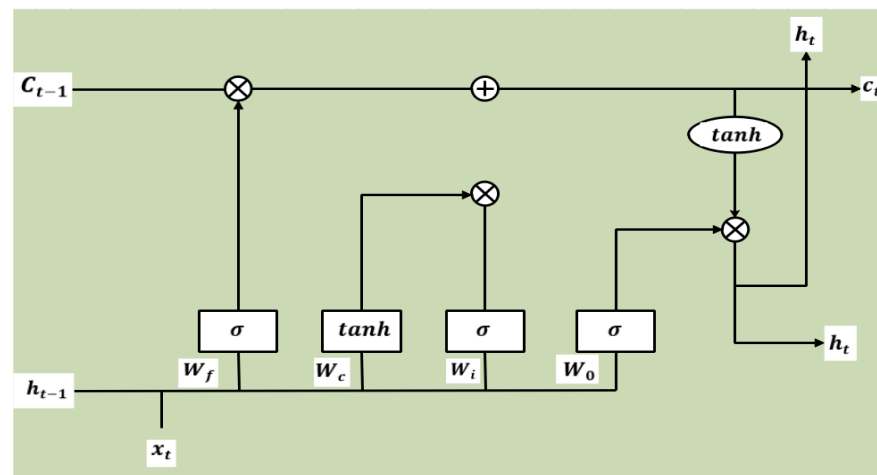
Figure 10. LSTM unit for remote sensing scene classification.

A typical LSTM network consists of cells and memory blocks. The next cell is transferred into two states: a hidden state and a cell state. The main chain of data flow is the cell state that allows data to flow essentially unchained. Some linear transformation is carried out and sigmoid is used to remove or add data in the layer. A gate is similar to a series of matrix operations or a layer that has various individual weights. LSTMs are developed to reduce long-term dependency using memorizing process to control gates [46].

4. Experimental Setup

The implementation details of datasets, parameter settings, and system requirements are discussed in this section.

Datasets: The UCM [47] dataset has 100 images per class, 21 classes, 2100 total images, 0.3 m spatial resolution, and 256×256 image size. The AID [48] dataset has 200–400 images per class, 30 classes, 10,000 total images, 0.5–0.8 m spatial resolution, and 600×600 image size. The NWPU45 [49] dataset has 700 images per class, 40 classes, 31,500 total images, 0.2–0.3 m spatial resolution, and 256×256 image size. As seen in the AID, the number of images varied per class, where this imbalanced data problem is effectively addressed by the GM-SMO model.

Parameter settings: In AlexNet and VGG19 model, the learning rate is set as 0.01, the dropout rate is set as 0.1, and the Adam optimizer is used. In LSTM network, the loss function is categorical cross entropy loss function and optimizer is Adam. In GM-SMO, the population size is set as 50, and number of iterations is set as 50. The 5-fold cross validation is applied to test the performance of the model.

System Requirement: Intel i9 processor, RAM is 128 GB, Graphics card is 22 GB, and OS is Windows 10-64 bit. MATLAB 2022a was used to evaluate the performance of the GM-SMO technique.

5. Results

The GM-SMO model is applied to scene classification to improve the efficiency of the model. The GM-SMO model is tested on three datasets and accuracy is shown for 10 epochs. The GM-SMO model is tested and compared with deep learning techniques and feature selection techniques on scene classification. The GM-SMO model is also compared with existing methods in scene classification for three datasets. The Grey Wolf Optimization (GWO), Firefly (FF), and Particle Swarm Optimization (PSO) were compared with the GM-SMO technique on scene classification.

The GM-SMO method accuracy for various numbers of epochs for three datasets is shown in Figure 11. This shows that the GM-SMO method increases the accuracy up to 8 epochs and accuracy decreases after 8 epochs. The reason for the decrease in accuracy after 8 epochs is the overfitting problem. The generation of more features in the convolutional layer and repeated learning of the features creates an overfitting problem. The Gaussian mutation in the SMO method helps to learn unique features for classification and increases the exploitation. The Gaussian mutation technique helps to reduce the overfitting problem and increases the performance of classification.
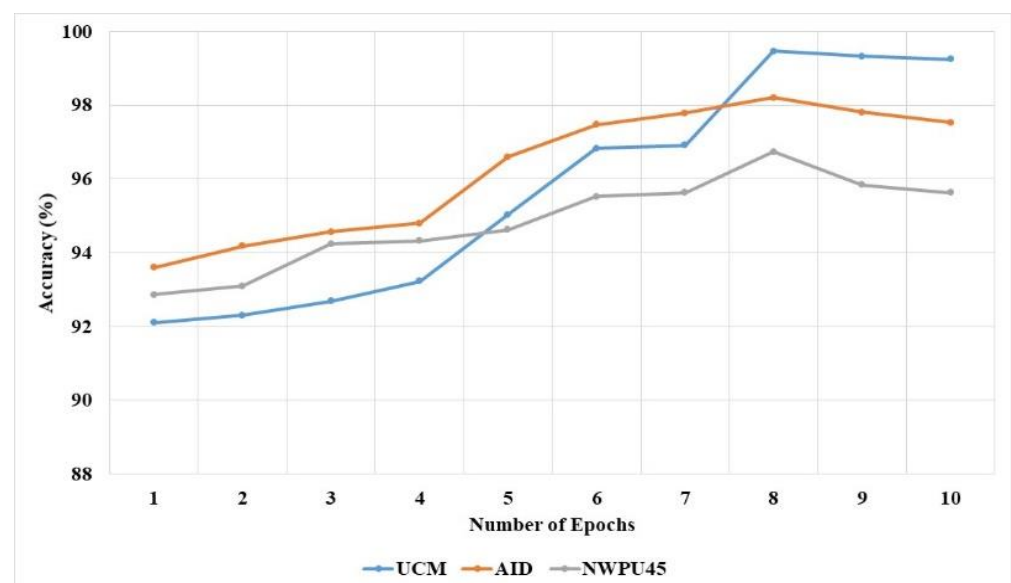
Figure 11. GM-SMO method accuracy vs. number of epochs in scene classification.

The GM-SMO method is measured with accuracy and sensitivity for three datasets and compared with deep learning techniques, as shown in Table 1 and Figure 12. The GM-SMO

model uses the AlexNet-VGG19 model for feature extraction from given images. The GM-SMO method performs feature selection with better exploitation that helps to reduce the overfitting problem in scene classification. The existing deep learning models such as GoogleNet, ResNet, Artificial Neural Network (ANN), and Recurrent Neural Network (RNN) have overfitting problems and provide lower efficiency. The existing method generates more features in the convolutional layer and lacks feature selection techniques for classification. The GM-SMO with LSTM has obtained higher performance than the existing techniques in scene classification. The GM-SMO with LSTM has 99.46% accuracy and 99.41% sensitivity, which are better than the other models. The local understanding of the images is good enough in the GM-SMO with LSTM model; therefore, it obtains better classification results compared to other classification models. In addition, the Z-test's *p*-value of individual classifiers is mentioned in Table 1.

Table 1. Deep learning techniques' performance in scene classification on three datasets.

Methods	Accuracy (%)	Sensitivity (%)	*p*-Value
GoogleNet	92.44	90.28	<0.10
ResNet	92.67	90.9	<0.10
ANN	92.67	93.89	<0.05
RNN	94.04	94.68	<0.05
LSTM with GM-SMO	99.46	99.41	<0.01
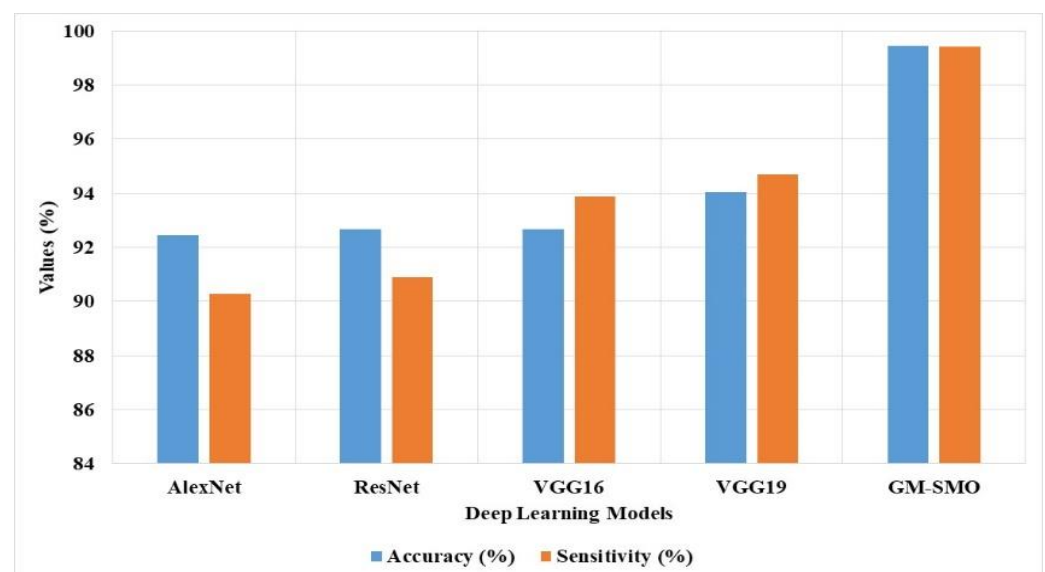
Figure 12. GM-SMO method's accuracy and sensitivity compared with deep learning in three datasets.

The GM-SMO method performance is compared with existing feature selection techniques, as shown in Table 2 and Figure 13. The existing feature selection techniques such as GWO, FF, and PSO have a limitation of local optima trap due to lower exploitation. The Gaussian mutation is applied in the SMO technique to increase the exploitation and overcome the overfitting problem. The Gaussian mutation changes the solutions related to the best solution that increases the exploitation in feature selection. The GM-SMO model selects unique features for scene classification that help to increase the sensitivity of the model. The GM-SMO model has 99.46% accuracy and 99.41% sensitivity, which are better compared to the existing optimizers.

Table 2. Feature selection techniques' comparison in scene classification on three datasets.

Methods	Accuracy (%)	Sensitivity (%)
PSO	91.23	90
FF	93.14	90.94
GWO	94.28	91.18
SMO	94.6	91.6
GM-SMO	99.46	99.41
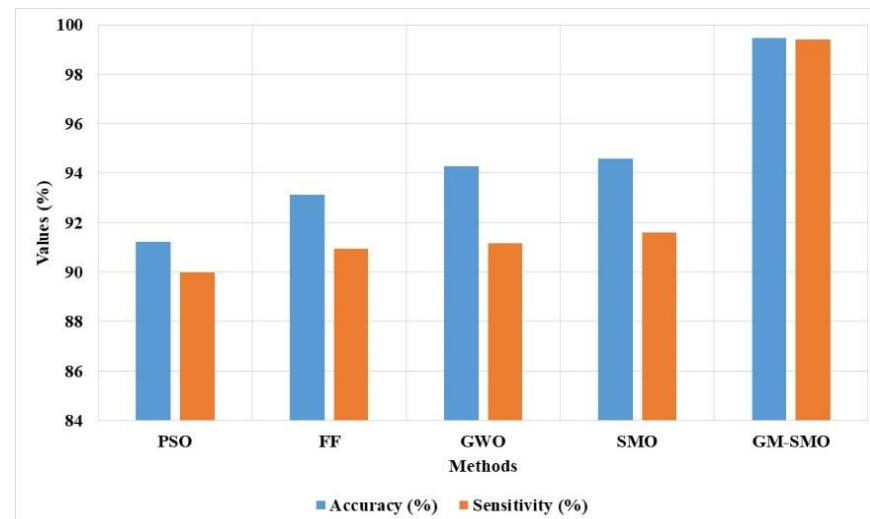
Figure 13. GM-SMO method accuracy and sensitivity compared with existing feature selection techniques.

The imbalanced data problem decreases the performance of scene classification in existing techniques. A common technique applied for imbalanced data problems is augmentation to generate similar images. Table 3 and Figure 14 show the GAN augmentation performance with standard augmentation. Although images generated by augmentation are highly similar, it is difficult to learn unique features, overfitting, and misclassification among similar categories. GAN based augmentation is applied in this study to generate similar images in minority classes and unique feature learning. The GAN based optimization technique has higher efficiency in three datasets than augmentation and SMOTE techniques. The GAM GM-SMO method has 99.46% accuracy and 99.41% sensitivity, and augmentation model has 99.24% accuracy and 98.31% sensitivity in UCM dataset.

Table 3. Sampling techniques for scene classification.

Datasets	Methods	Accuracy (%)	Sensitivity (%)
	SMOTE	97.35	96.53
UCM	Augmentation	99.24	98.31
	GAN	99.46	99.41
	SMOTE	94.2	95.14
AID	Augmentation	95.34	95.67
	GAN	98.2	98.31
	SMOTE	92.1	92.3
NWPU45	Augmentation	93.46	93.16
	GAN	96.73	96.6
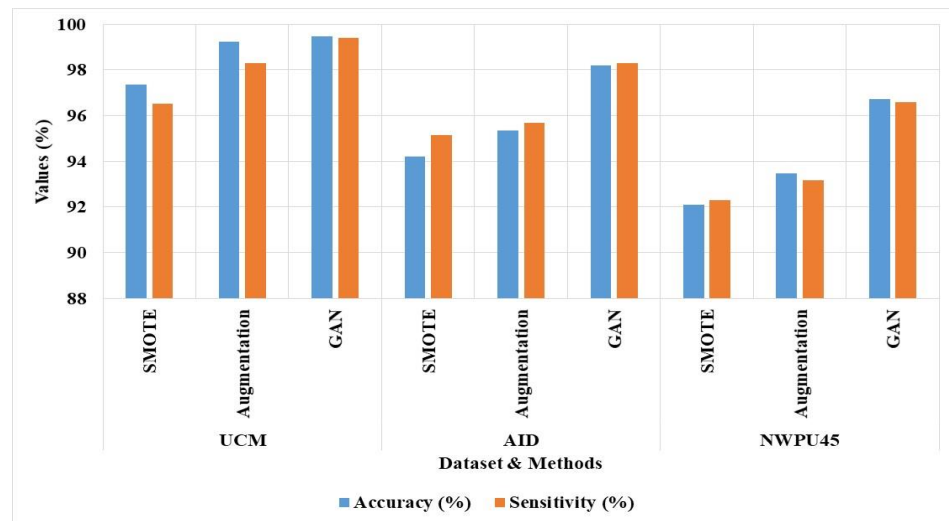
Figure 14. GM-SMO performance in the sampling process.

By inspecting Table 4, the proposed GM-SMO with LSTM classifier obtained higher classification results compared to other classifiers: GoogleNet, ResNet, ANN, and RNN, with limited computational time. As specified in Table 4, the GM-SMO with LSTM classifier consumed 12, 23, and 34 s per image of computation time on the UCM, AID, and NWPU45 datasets. Sample classification output image is depicted in Figure 15.

Table 4. Results of the GM-SMO with LSTM classifier in terms of means of computational time.

Classifiers	Computational Time (s)		
	UCM	AID	NWPU45
GoogleNet	25	41.09	50.36
ResNet	32	38.50	48
ANN	19.43	36.20	45.38
RNN	15.12	35	44
LSTM with GM-SMO	12	23	34
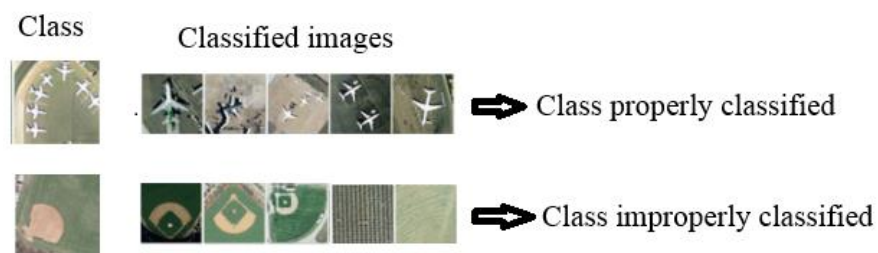
Figure 15. Sample classification output image.

Comparative Analysis

The GM-SMO model is compared with existing techniques in scene classification on three datasets such as UCM, AID, and NWPU45, and the comparative results are mentioned in Tables 5–7. The GM-SMO method is compared with existing techniques on the UCM dataset, as shown in Table 5. The existing CNN model has limitations of imbalanced data problem and overfitting problem in the scene classification. The GM-SMO model applies the GAN model to augment the minority classes and increase their performance. The Gaussian mutation changes the solution after exploration to increase the exploitation of the model. The GM-SMO method selects the unique features to overcome the overfitting and

imbalanced data problem. The GM-SMO model has achieved 99.46% accuracy, which is better compared to other methods on the UCM dataset.

Table 5. GM-SMO is compared with existing methods on the UCM dataset.

Methods	Accuracy (%)
DFAGCN [19]	98.48
vision transformer [20]	97.90
EfficientNet-B3-Attn-2 [21]	97.90
SceneNet [22]	99.10
MTLN [23]	97.66
LSE-Net [26]	98.53
MA-GRN [29]	99.29
transformers—CNN [30]	98.76
GM-SMO	99.46 ± 0.0238

Table 6. GM-SMO method comparison with existing methods on AID dataset.

Methods	Accuracy (%)
DFAGCN [19]	94.88
vision transformer [20]	94.27
EfficientNet-B3-Attn-2 [21]	96.56
SceneNet [22]	89.58
MTLN [23]	92.54
GLDBS [24]	97.01
ACNet [25]	95.38
LSE-Net [26]	94.41
MA-GRN [29]	96.19
transformers—CNN [30]	95.54
GM-SMO	98.20 ± 0.2590

Table 7. GM-SMO method comparison with existing methods on NWPU45 dataset.

Methods	Accuracy (%)
DFAGCN [19]	89.29
vision transformer [20]	93.05
SceneNet [22]	95.21
MTLN [23]	89.71
GLDBS [24]	94.46
ACNet [25]	92.42
LSE-Net [26]	93.34
SPNet [27]	83.94
MA-GRN [29]	95.32
transformers—CNN [30]	93.06
GM-SMO	96.73 ± 0.0432

The GM-SMO model is compared with existing techniques in scene classification on the AID dataset, as shown in Table 6. The GM-SMO model selects unique features for the classification to solve the overfitting problem and imbalanced data problem. The GM-SMO model changes the solution of the SMO technique to increase the exploitation of the model. The GM-SMO model has achieved 98.20% accuracy, which is superior compared to other models on the AID dataset.

The GM-SMO method is compared with existing scene classification techniques on NWPU45 dataset, as shown in Table 7. The existing CNN based models have a limitation of imbalanced data problem and overfitting problem in scene classification. The GM-SMO model changes the solution of SMO technique after exploration to increase the exploitation. The GM-SMO model maintains the tradeoff between exploration and exploitation to find

the relevant features for classification. The GM-SMO model selects unique features to overcome the overfitting and imbalanced data problem. The GM-SMO model has 96.73% accuracy, which is better compared to transformers—CNN [30], MA-GRN [29], and other comparative models.

6. Conclusions

Scene classification helps to classify the object or land use such as a farm, airplane, or stadium from remote sensing images. The existing CNN based models have limitations of overfitting problems, imbalanced data problems, and misclassification of similar categories. This research proposes a GM-SMO technique for the feature selection process to improve the classification performance of scene classification. The GM-SMO model selects unique features to overcome the imbalanced data problem and overfitting problem. The GAN model is applied for the augmentation of images and to reduce imbalanced data problems. The AlexNet and VGG19 models are applied to extract the features from remote sensing images. The GM-SMO model has 98.20% accuracy, LSE-Net has 94.41% accuracy, and MTLN has 92.54% accuracy on the AID dataset. The future work of this research involves applying the proposed model to the real time datasets to further validate the efficiency of the model. However, the proposed model is computationally complex, which can be addressed in future work by implementing an unsupervised deep learning model.

Author Contributions: The paper investigation, resources, data curation, writing—original draft preparation, writing—review and editing, and visualization were conducted by A.L.H.P.S. and M.K.M. The paper conceptualization and software were conducted by R.R.A. and A.K.P. The validation, formal analysis, methodology, supervision, project administration, and funding acquisition of the version to be published were conducted by C.-M.C. All authors have read and agreed to the published version of the manuscript.

Data Availability Statement: 1. The datasets generated during and/or analyzed during the current study are available in the (UC Merced 15 datasets) repository, http://weegee.vision.ucmerced. edu/datasets/landuse.html (accessed on 14 July 2022). 2. The datasets generated during and/or analyzed during the current study are available in the (AID datasets) repository, https://captain-whu.github.io/AID/ (accessed on 14 July 2022). 3. The datasets generated during and/or analyzed during the current study are available in the (NWPU45 datasets) repository, https://1drv.ms/u/s! AmgKYzARBl5-ca3HNaHIlzp_IXjs (accessed on 14 July 2022).

Conflicts of Interest: The authors declare no conflict of interest.

References

1. Xie, H.; Chen, Y.; Ghamisi, P. Remote sensing image scene classification via label augmentation and intra-class constraint. *Remote Sens.* **2021**, *13*, 2566. [CrossRef]
2. Li, Y.; Zhu, Z.; Yu, J.G.; Zhang, Y. Learning deep cross-modal embedding networks for zero-shot remote sensing image scene classification. *IEEE Trans. Geosci. Remote Sens.* **2021**, *59*, 10590–10603. [CrossRef]
3. Li, M.; Lin, L.; Tang, Y.; Sun, Y.; Kuang. G. An attention-guided multilayer feature aggregation network for remote sensing image scene classification. *Remote Sens.* **2021**, *13*, 3113. [CrossRef]
4. Wang, X.; Wang, S.; Ning, C.; Zhou, H. Enhanced feature pyramid network with deep semantic embedding for remote sensing scene classification. *IEEE Trans. Geosci. Remote Sens.* **2021**, *59*, 7918–7932. [CrossRef]
5. Cheng, G.; Sun, X.; Li, K.; Guo, L.; Han, J. Perturbation-seeking generative adversarial networks: A defense framework for remote sensing image scene classification. *IEEE Trans. Geosci. Remote Sens.* **2021**, *60*, 5605111. [CrossRef]
6. Srinivas, M.; Roy, D.; Mohan, C.K. Discriminative feature extraction from X-ray images using deep convolutional neural networks. In Proceedings of the 2016 IEEE International Conference on Acoustics, Speech and Signal Processing (ICASSP), Shanghai, China, 20–25 March 2016; pp. 917–921.
7. Ijjina, E.P.; Mohan, C.K. Human action recognition based on recognition of linear patterns in action bank features using convolutional neural networks. In Proceedings of the 2014 13th International Conference on Machine Learning and Applications, Detroit, MI, USA, 3–6 December 2014; pp. 178–182.

8.   Saini, R.; Jha, N.K.; Das, B.; Mittal, S.; Mohan, C.K. Ulsam: Ultra-lightweight subspace attention module for compact convolutional neural networks. In Proceedings of the IEEE/CVF Winter Conference on Applications of Computer Vision, Snowmass, CO, USA, 1–5 March 2020; pp. 1627–1636.

9.   Deepak, K.; Chandrakala, S.; Mohan, C.K. Residual spatiotemporal autoencoder for unsupervised video anomaly detection. *Signal Image Video Process* **2021**, *15*, 215–222. [CrossRef]

10.   Roy, D.; Murty, K.S.R.; Mohan, C.K. Unsupervised universal attribute modeling for action recognition. *IEEE Trans. Multimed.* **2018**, *21*, 1672–1680. [CrossRef]

11.   Perveen, N.; Roy, D.; Mohan, C.K. Spontaneous expression recognition using universal attribute model. *IEEE Trans. Image Process* **2018**, *27*, 5575–5584. [CrossRef]

12.   Roy, D.; Ishizaka, T.; Mohan, C.K.; Fukuda, A. Vehicle trajectory prediction at intersections using interaction based generative adversarial networks. In Proceedings of the 2019 IEEE Intelligent Transportation Systems Conference (ITSC), Auckland, New Zealand, 27–30 October 2019; pp. 2318–2323.

13.   Roy, D. Snatch theft detection in unconstrained surveillance videos using action attribute modelling. *Pattern Recognit. Lett.* **2018**, *108*, 56–61. [CrossRef]

14.   Zhang, P.; Bai, Y.; Wang, D.; Bai, B.; Li, Y. Few-shot classification of aerial scene images via meta-learning. *Remote Sens.* **2021**, *13*, 108. [CrossRef]

15.   Kim, J.; Chi, M. SAFFNet: Self-attention-based feature fusion network for remote sensing few-shot scene classification. *Remote Sens.* **2021**, *13*, 2532. [CrossRef]

16.   Zhang, Z.; Liu, S.; Zhang, Y.; Chen, W. RS-DARTS: A convolutional neural architecture search for remote sensing image scene classification. *Remote Sens.* **2021**, *14*, 141. [CrossRef]

17.   Wu, X.; Zhang, Z.; Zhang, W.; Yi, Y.; Zhang, C.; Xu, Q. A convolutional neural network based on grouping structure for scene classification. *Remote Sens.* **2021**, *13*, 2457. [CrossRef]

18.   Lasloum, T.; Alhichri, H.; Bazi, Y.; Alajlan, N. SSDAN: Multi-source semi-supervised domain adaptation network for remote sensing scene classification. *Remote Sens.* **2021**, *13*, 3861. [CrossRef]

19.   Xu, K.; Huang, H.; Deng, P.; Li, Y. Deep feature aggregation framework driven by graph convolutional network for scene classification in remote sensing. *IEEE Trans. Neural Netw. Learn. Syst.* **2021**, *33*, 5751–5765. [CrossRef]

20.   Bazi, Y.; Bashmal, L.; Rahhal, M.M.A.; Dayil, R.A.; Ajlan, N.A. Vision transformers for remote sensing image classification. *Remote Sens.* **2021**, *13*, 516. [CrossRef]

21.   Alhichri, H.; Alswayed, A.S.; Bazi, Y.; Ammour, N.; Alajlan, N.A. Classification of remote sensing images using EfficientNet-B3 CNN model with attention. *IEEE Access* **2021**, *9*, 14078–14094. [CrossRef]

22.   Ma, A.; Wan, Y.; Zhong, Y.; Wang, J.; Zhang, L. SceneNet: Remote sensing scene classification deep learning network using multi-objective neural evolution architecture search. *ISPRS J. Photogramm. Remote Sens.* **2021**, *172*, 171–188. [CrossRef]

23.   Zheng, X.; Gong, T.; Li, X.; Lu, X. Generalized scene classification from small-scale datasets with multitask learning. *IEEE Trans. Geosci. Remote Sens.* **2021**, *60*, 5609311. [CrossRef]

24.   Xu, K.; Huang, H.; Deng, P. Remote sensing image scene classification based on global–local dual-branch structure model. *IEEE Geosci. Remote Sens. Lett.* **2021**, *19*, 8011605. [CrossRef]

25.   Tang, X.; Ma, Q.; Zhang, X.; Liu, F.; Ma, J.; Jiao, L. Attention consistent network for remote sensing scene classification. *IEEE J. Sel. Top. Appl. Earth Obs. Remote Sens.* **2021**, *14*, 2030–2045. [CrossRef]

26.   Bi, Q.; Qin, K.; Zhang, H.; Xia, G.S. Local semantic enhanced convnet for aerial scene recognition. *IEEE Trans. Image Process* **2021**, *30*, 6498–6511. [CrossRef] [PubMed]

27.   Cheng, G.; Cai, L.; Lang, C.; Yao, X.; Chen, J.; Guo, L.; Han, J. SPNet: Siamese-prototype network for few-shot remote sensing image scene classification. *IEEE Trans. Geosci. Remote Sens.* **2021**, *60*, 5608011. [CrossRef]

28.   Zareapoor, M.; Chanussot, J.; Zhou, H.; Yang, J. Rotation Equivariant Feature Image Pyramid Network for Object Detection in Optical Remote Sensing Imagery. *IEEE Trans. Geosci. Remote Sens.* **2021**, *60*, 5608614.

29.   Li, B.; Guo, Y.; Yang, J.; Wang, L.; Wang, Y.; An, W. Gated recurrent multiattention network for VHR remote sensing image classification. *IEEE Trans. Geosci. Remote Sens.* **2021**, *60*, 5606113. [CrossRef]

30.   Zhang, J.; Zhao, H.; Li, J. TRS: Transformers for remote sensing scene classification. *Remote Sens.* **2021**, *13*, 4143. [CrossRef]

31.   Radford, A.; Metz, L.; Chintala, S. Unsupervised representation learning with deep convolutional generative adversarial networks. *arXiv* **2015**, arXiv:1511.06434.

32.   Goodfellow, I.; Pouget-Abadie, J.; Mirza, M.; Xu, B.; Warde-Farley, D.; Ozair, S.; Courville, A.; Bengio, Y. Generative adversarial nets. In Proceedings of the 28th Annual Conference on Neural Information Processing Systems 2014 (NIPS), Montreal, QC, Canada, 8–13 December 2014; p. 27.

33.   Yi, X.; Walia, E.; Babyn, P. Generative adversarial network in medical imaging: A review. *Med. Image Anal.* **2019**, *58*, 101552. [CrossRef]

34.   Niu, M.; Lin, Y.; Zou, Q. sgRNACNN: Identifying sgRNA on-target activity in four crops using ensembles of convolutional neural networks. *Plant Mol. Biol.* **2021**, *105*, 483–495. [CrossRef]

35.   Zhang, Z.; Tian, J.; Huang, W.; Yin, L.; Zheng, W.; Liu, S. A haze prediction method based on one-dimensional convolutional neural network. *Atmosphere* **2021**, *12*, 1327. [CrossRef]

36. Chen, J.; Wan, Z.; Zhang, J.; Li, W.; Chen, Y.; Li, Y.; Duan, Y. Medical image segmentation and reconstruction of prostate tumor based on 3D AlexNet. *Comput. Methods Programs Biomed.* **2021**, *200*, 105878. [CrossRef] [PubMed]
37. Zhu, Y.; Li, G.; Wang, R.; Tang, S.; Su, H.; Cao, K. Intelligent fault diagnosis of hydraulic piston pump based on wavelet analysis and improved alexnet. *Sensors* **2021**, *21*, 549. [CrossRef] [PubMed]
38. Karacı, A. VGGCOV19-NET: Automatic detection of COVID-19 cases from X-ray images using modified VGG19 CNN architecture and YOLO algorithm. *Neural Comput. Appl.* **2022**, *34*, 8253–8274. [CrossRef] [PubMed]
39. Awan, M.J.; Masood, O.A.; Mohammed, M.A.; Yasin, A.; Zain, A.M.; Damaševičius, R.; Abdulkareem, K.H. Image-Based Malware Classification Using VGG19 Network and Spatial Convolutional Attention. *Electronics* **2021**, *10*, 2444. [CrossRef]
40. Kumar, S.; Sharma, B.; Sharma, V.K.; Sharma, H.; Bansal, J.C. Plant leaf disease identification using exponential spider monkey optimization. *Sustain. Comput. Inform. Syst.* **2020**, *28*, 100283. [CrossRef]
41. Kumar, S.; Sharma, B.; Sharma, V.K.; Poonia, R.C. Automated soil prediction using bag-of-features and chaotic spider monkey optimization algorithm. *Evol. Intell.* **2021**, *14*, 293–304. [CrossRef]
42. Lee, J.G.; Chim, S.; Park, H.H. Energy-efficient cluster-head selection for wireless sensor networks using sampling-based spider monkey optimization. *Sensors* **2019**, *19*, 5281. [CrossRef]
43. Xia, X.; Liao, W.; Zhang, Y.; Peng, X. A discrete spider monkey optimization for the vehicle routing problem with stochastic demands. *Appl. Soft Comput.* **2021**, *111*, 107676. [CrossRef]
44. Jalayer, M.; Orsenigo, C.; Vercellis, C. Fault detection and diagnosis for rotating machinery: A model based on convolutional LSTM, Fast Fourier and continuous wavelet transforms. *Comput. Ind.* **2021**, *125*, 103378. [CrossRef]
45. Yang, Y.; Xiong, Q.; Wu, C.; Zou, Q.; Yu, Y.; Yi, H.; Gao, M. A study on water quality prediction by a hybrid CNN-LSTM model with attention mechanism. *Environ. Sci. Pollut. Res.* **2021**, *28*, 55129–55139. [CrossRef]
46. Kumar, S.; Damaraju, A.; Kumar, A.; Kumari, S.; Chen, C.-M. LSTM network for transportation mode detection. *J. Internet Technol.* **2021**, *22*, 891–902. [CrossRef]
47. Yang, Y.; Newsam, S. Bag-of-visual-words and spatial extensions for land-use classification. In Proceedings of the 18th SIGSPA-TIAL International Conference on Advances in Geographic Information Systems, San Jose, CA, USA, 2–5 November 2010; pp. 270–279.
48. Xia, G.S.; Hu, J.; Hu, F.; Shi, B.; Bai, X.; Zhong, Y.; Zhang, L.; Lu, X. AID: A benchmark data set for performance evaluation of aerial scene classification. *IEEE Trans. Geosci. Remote Sens.* **2017**, *55*, 3965–3981. [CrossRef]
49. Li, B.; Su, W.; Wu, H.; Li, R.; Zhang, W.; Qin, W.; Zhang, S. Aggregated deep fisher feature for VHR remote sensing scene classification. *IEEE J. Sel. Top. Appl. Earth Obs. Remote Sens.* **2019**, *12*, 3508–3523. [CrossRef]

Human Activity Recognition Using Significant Skeletal Joints

Abdul Lateef Haroon P. S., Rashmi P., Supriya M. C.

Abstract

The growing development in the sensory implementation has facilitated that the human activity can be used either as a tool for remote control of the device or as a tool for sophisticated human behaviour analysis. The prime contribution of the proposed system is to harness the potential of learning approach in order to carry out computational efficiency towards activity recognition process. A template for an activity recognition system is also provided in which the reliability of the process of recognition and system quality is preserved with a good balance. The research presents a condensed method of extraction of features from spatial and temporal features of event feeds that are further subject to the mechanism of machine learning to enhance the recognition accuracy. The importance of proposed study is reflected in the results, which, when trained using KNN, show higher accuracy performance. The proposed system demonstrated 10-15% of memory usage over 532 MB of digitized real-time event information with 0.5341 seconds of processing time consumption.

Article Preview

Top

Review Of Literature

The existing approaches based on conventional Local Spatio-Temporal (LST) are suffered from various challenges like dynamic background and illumination. To enhance this problem, the work of Zhang and Parker (2016), provides a multi-dimensional colour-depth LST feature-based feature detector technique to represent various features such as shape, pose variation, texture with local maxima as a region of interest. The authors have also used a support vector machine (SVM) with feature representation to build an effective action detection system. The study uses different standard datasets to demonstrate the effectiveness of the presented technique.

Complete Article List

Search this Journal: *Full text search term(s)*

Reset

Learn More
About IGI Global (/about/) | Partnerships (/about/partnerships/) | COPE Membership (/about/memberships/cope/) | Contact Us (/contact/) | Job Opportunities (/about/staff/job-opportunities/) | FAQ (/faq/) | Management Team (/about/staff/)

Resources For
Librarians (/librarians/) | Authors/Editors (/publish/) | Distributors (/distributors/) | Instructors (/course-adoption/) | Translators (/about/rights-permissions/translation-rights/)

Media Center
Webinars (/symposium/) | Blogs (/newsroom/) | Catalogs (/catalogs/) | Newsletters (/newsletters/)

Policies
Privacy Policy (/about/rights-permissions/privacy-policy/) | Cookie & Tracking Notice (/cookies-agreement/) | Fair Use Policy (/about/rights-permissions/content-reuse/) | Accessibility (/accessibility/) | Ethics and Malpractice (/about/rights-permissions/ethics-malpractice/) | Rights & Permissions (/about/rights-permissions/)

(http://www.facebook.com/pages/IGI-Global/138206739534176?ref=sgm)　　(http://twitter.com/igiglobal)
(https://www.linkedin.com/company/igi-global)(http://worldd-forgotten-children.org)

(https://publicationethics.org/category/publisher/igi-global)

(12) PATENT APPLICATION PUBLICATION

(21) Application No.202341012928 A

(19) INDIA

(22) Date of filing of Application :25/02/2023

(43) Publication Date : 17/03/2023

(54) Title of the invention : Sentiment Analysis of College Survey using AI

(51) International classification :G06F 403000, G06N 030800, G06Q 300200, G06Q 502000, G09G 032000	(71)**Name of Applicant :**
	  1)**Ballari Institute of Technology and Management**
	   Address of Applicant :Ballari Institute of Technology and Management, Ballari-583104, Bellary, Karnataka, India ----------- -----------
	  2)**Dr. Abdul Lateef Haroon P S**
	  3)**Mohammed Shafiulla**
	  4)**Aswatha Narayana**
	  5)**Prithviraj Y J**
	  6)**Dr K M Sadyojatha**
	  7)**Dr R N Kulkarni**
	  8)**Sathyanarayana S**
	  9)**Sathyanarayana K B**
	Name of Applicant : NA
	Address of Applicant : NA
	(72)**Name of Inventor :**
	  1)**Ballari Institute of Technology and Management**
	Address of Applicant :Ballari Institute of Technology and Management, Ballari-583104, Bellary, Karnataka, India ----------- -----------
	  2)**Dr. Abdul Lateef Haroon P S**
	Address of Applicant :Associate Professor, Department of Electronics and Communication Engineering, Ballari Institute of Technology and Management, Ballari-583104 ----------- -----------
	  3)**Mohammed Shafiulla**
	Address of Applicant :Assistant Professor, Department of Computer Science and Engineering, Ballari Institute of Technology and Management, Ballari-583104, Ballari, Karnataka, India ----------- -----------
	  4)**Aswatha Narayana**
	Address of Applicant :Assistant Professor, Department of Electronics and Communication Engineering, Ballari Institute of Technology and Management, Ballari-583104 ----------- -----------
	  5)**Prithviraj Y J**
	Address of Applicant :Deputy Director, Ballari Institute of Technology and Management, Ballari-583104, Bellary, Karnataka, India ----------- -----------
	  6)**Dr K M Sadyojatha**
	Address of Applicant :Professor & HOD, Department of Electronics and Communication Engineering, Ballari Institute of Technology and Management, Ballari-583104 ----------- -----------
	  7)**Dr R N Kulkarni**
	Address of Applicant :Professor & HOD, Department of Computer Science and Engineering, Ballari Institute of Technology and Management, Ballari-583104 ----------- ------ -----------
	  8)**Sathyanarayana S**
	Address of Applicant :Assistant Professor, Department of Computer Science Engineering, J N N College of Engineering, Shivamogga-577204 ----------- ----------
	  9)**Sathyanarayana K B**
	Address of Applicant :Assistant Professor, Department of Information Science Engineering, J N N College of Engineering, Shivamogga-577204 ----------- ----------

(86) International Application No :PCT// Filing Date :01/01/1900	
(87) International Publication No: NA	
(61) Patent of Addition to Application Number :NA Filing Date :NA	
(62) Divisional to Application Number :NA Filing Date :NA	

(57) Abstract :
Sentiment Analysis of College Survey using AI Abstract This system presents a combination of Machine Learning and NLP based approaches for sentiment analysis of student's feedback. The textual feedback, typically collected towards the end of a semester, provides useful insights into the overall teaching quality, and suggests valuable ways for improving teaching methodology. The system describes a sentiment analysis model trained using BERT and VADER to analyse the sentiments expressed by students in their textual feedback. A comparative analysis is also conducted between the proposed model and other methods of sentiment analysis. The experimental results suggest that the proposed model performs better than other methods.

No. of Pages : 14 No. of Claims : 7

पेटेंट कार्यालय, भारत सरकार | The Patent Office, Government Of India

डिजाइन के पंजीकरण का प्रमाण पत्र | Certificate of Registration of Design

डिजाइन सं. / Design No.	:	382363-001	
तारीख / Date	:	27/03/2023	
पारस्परिकता तारीख / Reciprocity Date*	:		
देश / Country	:		

प्रमाणित किया जाता है कि संलग्न प्रति में वर्णित डिजाइन जो *MACHINE LEARNING-BASED HUMANOID DEVICE FOR OBJECT IDENTIFICATION* से संबंधित है, का पंजीकरण, श्रेणी 10-05 में 1.Dr. Abdul Lateef Haroon P S 2. Mr. Premachand D R 3.Ballari Institute Of Technology And Management 4.Dr K M Sadyojatha 5.Prithviraj Y J 6.Mr. Srikantha K M के नाम में उपर्युक्त संख्या और तारीख में कर लिया गया है।

Certified that the design of which a copy is annexed hereto has been registered as of the number and date given above in class 10-05 in respect of the application of such design to *MACHINE LEARNING-BASED HUMANOID DEVICE FOR OBJECT IDENTIFICATION* in the name of 1.Dr. Abdul Lateef Haroon P S 2. Mr. Premachand D R 3.Ballari Institute Of Technology And Management 4.Dr K M Sadyojatha 5.Prithviraj Y J 6.Mr. Srikantha K M.

डिजाइन अधिनियम, 2000 तथा डिजाइन नियम, 2001 के अध्यधीन प्रावधानों के अनुसरण में।

In pursuance of and subject to the provisions of the Designs Act, 2000 and the Designs Rules, 2001.

जारी करने की तिथि : 04/01/2024
Date of Issue :

महानियंत्रक पेटेंट, डिजाइन और व्यापार चिह्न
Controller General of Patents, Designs and Trade Marks

AGRICULTURAL RESEARCH COMMUNICATION CENTRE

Reference ID. ARCC/A-6061

Date : 08-02-2023

Hemanthakumar R. Kappali,

Department of Electronics and Communication Engineering,

Ballari Institute of Technology and Management,

Ballari-583 104, Karnataka, India.

Acceptance of manuscript

Dear Dr. R.,

We are pleased to inform you that your manuscript has been accepted for publication in **Indian Journal of Agricultural Research**. Your submission is a well-thought out piece of writing and follows many of journal guidelines. The editors agreed that your submission showed great writing skills.

Manuscript Title : Computer Vision and Machine Learning in Paddy Diseases Identification and Classification: A Review

Author(s): Hemanthakumar R. Kappali, K.M. Sadyojatha, S.K. Prashanthi

Congratulations to you once again on your article acceptance in ARCC Journals, and we look forward to receiving more of your good submissions.

With Best Wishes and Seasonal Greetings,

Gaurav Gupta
Managing Editor

Participants Perspectives on P2BL Mini-Symposium

Deepak Waikar <deepak.waikar@iucee.org>

Sat 12/3/2022 7:53 PM

To:Deepak Waikar <deepak.waikar@iucee.org>

We highly appreciate your participation and we hope that you may have found the IUCEE-Vishwaniketan Mini-Symposium on Problem and Project-Based Learning (P2BL) very useful to you. Please provide your views about the Mini-Symposium on P2BL held on 2 and 3 December 2022.

Please complete the survey at the earliest.

https://forms.gle/Cfj7Zj3nDBAeGRoX6

Please note that your personal information will be kept confidential. Your responses will, only, be used for analysis and research.

Thank you,
with best wishes,
Prof. Krishna Vedula,
Prof. Sandeep Inamdar
Dr. Deepak Waikar
Dr. Vikas Shinde
For the IUCEE-Vishwaniketan Mini-Sympo on P2BL

CESS

Centre for Educational and Social Studies

Prajnanam, 6/6, 10th Block, Nagarbhavi, 2nd Stage
Bengaluru - 560072

ATTENDANCE CERTIFICATE

This is to certify that Nilam Chheda, Asst professor from BALLARI INSTITUTE OF
TECHNOLOGY AND MANAGEMENT, BALLARI has attended the Two-Day National
Conference on *"NEP Readiness: Scope and Challenges for Transforming Higher
Education"* held during *September 29-30, 2022* organized by Centre for Educational and
Social Studies at Ramaiah Institute of Management, Bengaluru.

[Seal: CENTRE FOR EDUCATIONAL AND SOCIAL STUDIES ★ BANGALORE]

Director
CESS, Bengaluru

सत्यमेव जयते
भारत सरकार
Government of India
वाणिज्य एवं उद्योग मंत्रालय
Ministry of Commerce and Industry
उद्योग संवर्धन और आंतरिक व्यापार विभाग
Department for Promotion of Industry and Internal Trade
महानियंत्रक एकस्व, अभिकल्प एवं व्यापार चिह्न का कार्यालय
Office of the Controller General of Patents, Designs & Trademarks

Rajiv Gandhi National Institute of Intellectual Property Management, Civil Lines, Nagpur. 440 001 (INDIA)

CERTIFICATE

This is to certify that,

DR. NASEERUDDIN

has successfully completed One week Public Training Program on

"Patent filing requirement in India, Patentability, Forms, fees, Examination of Patent application, Exercise on important forms filling / Patent Specification, Case study / Patent Search, IPC, how to search, Hands-on Exercise on prior art search / Hands-on Exercise of Patent Specification / Claims writing / Patent commercialization, IP Policy etc. / Copyright filing requirement in India, Design filing requirement in India, Other proceedings of Patents like Term, renewal, working of patent, opposition etc."

During 21st to 25th November 2022

Conducted by

Rajiv Gandhi National Institute of Intellectual Property Management (RGNIIPM), Nagpur

Pankaj Borkar
Deputy Controller of P & D
Team Leader - Training, RGNIIPM

25th November 2022
RGNIIPM/Trg./2022-23/A-1102

Nirmalya Sinha
Joint Controller of P & D
Head, RGNIIPM

Attendance Certificate

This is to certify that **Dr.Naseeruddin** of **Ballari Institute of Technology and Management, Ballari** has attended the one day Awareness Workshop on Outcome Based Education (OBE) and Accreditation organized by National Board of Accreditation (NBA), New Delhi in collaboration with Visvesvaraya Technological University, Belagavi at B.M.S. College of Engineering, Bengaluru on 16th January, 2023.

Dr Shambhavi B. R.
Chief Coordinator IQAC, BMSCE

Chief Coordinator IQAC
B.M.S. College of Engineering
Bengaluru - 560 019

Department of Mechanical Engineering
The National Institute of Engineering

(An Autonomous Institute under VTU, Belagavi)
Mysuru-570008

.CERTIFICATE.

This is to certify that

Mr. Ambrayya

Ballari Institute of Technology
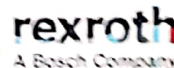& Management

Participated in

Five Days Workshop On

RECENT TRENDS IN AUTOMATION
TECHNOLOGIES FOR MSME DEVELOPMENT

Organized by the Department of Mechanical Engineering

From 30th January to 03rd February 2023
at The National Institute of Engineering, Mysuru

INDUSTRY PARTNERS

HYDAC   JANATICS   VIDYUT AUTOMATION   rexroth A Bosch Company   AUTOMATION STUDIO

XNG   FLUIDTECHNIK SOLUTIONS

Shri Akadas G
Director, MSME- DFO, Bengaluru

Dr. Shivakumar H R
Regional Director, VTU - RO, Mysuru

Dr. Rohini Nagapadma
Principal, NIE

NIE
ESTD : 1946

MED

Sponsored by
Ministry of MSME,
Government of India

CERTIFICATE

In association with
Visweswaraya Technological
University, Belagavi

This is to certify that

Mr. Ulaganathan J

Ballari Institute of Technology
& Mangement

Participated in

Five Days Workshop On

RECENT TRENDS IN AUTOMATION
TECHNOLOGIES FOR MSME DEVELOPMENT

Organized by the Department of Mechanical Engineering

From 30th January to 03rd February 2023
at The National Institute of Engineering, Mysuru

INDUSTRY PARTNERS

HYDAC   JANATICS Pneumatic   VIDYUT AUTOMATION   rexroth A Bosch Company   AUTOMATION STUDIO

XNG   FLUIDTECHNIK SOLUTIONS
Fluid Power Piping, Services & Training

Shri Akadas G	Dr. Shivakumar H R	Dr. Rohini Nagapadma
Director, MSME- DFO, Bengaluru	Regional Director, VTU - RO, Mysuru	Principal, NIE

CERTIFICATE

OF COMPLETION

Faculty Development Program

This is to Certify that

Ms. Nayana M

of "Ballari Institute of Technology and Management" has completed the Faculty Development Program on Various aspects of *"VLSI Digital/ Analog/ Mixed signal Flow"* with a practical approach as per the Latest Industry trends, Conducted from 17th September to 23rd December 2022.

18 / 01 / 2023

Date

Semionics